

## PROCEEDINGS OF 21st ANNUAL MEETING

USE OF SHORT-LIVED POSITRON EMITTING RADIOPHARMACEUTICALS FOR THE DISTRIBUTION STUDY OF EXTRAVASCULAR LUNG WATER IN THE DOG. B. Ahluwalia, D. Kanarek, T. Jones, B. Hoop Jr., G.L. Brownell, and H. Kazemi. Physics Research Laboratory and Pulmonary Unit, Massachusetts General Hospital, Boston, MA 02114

Cyclotron produced short-lived radiopharmaceuticals labeled with oxygen-15 and nitrogen-13 are used to obtain distributions of blood volume, total lung water, extravascular lung water (EVLW), perfusion and ventilation. Measurements are carried out in anesthetized dogs and isolated lung preparations before and after the induction of pulmonary edema. Positron scintigrams are obtained with a multicrystal positron camera and are processed using a multiprogrammable interactive computer system. Intravascular blood volume, and total lung volume distributions are obtained with  $C^{15}O$  labeled hemoglobin and  $H_2^{15}O$  respectively. Scintigraphic data are taken at a steady state, which is achieved by continuous infusion of radioactive labeled blood for a predetermined time. The scintigram is normalized to the specific activity in an arterial sample which is withdrawn during the time the scintigram is taken. The EVLW distribution is obtained by the subtraction of  $C^{15}O$  distribution from the  $H_2^{15}O$  distribution. Also, the regional distribution of perfusion and ventilation are obtained with nitrogen-13 molecular  $N_2$  dissolved in saline and with gaseous  $N_2$  respectively. This method provides comparative information on the distribution of EVLW and other physiological parameters at various stages of edema.

COMPARISON OF CARDIAC OUTPUT DETERMINATIONS BASED ON RADIONUCLIDE ANGIOGRAPHY AND INDICATOR DYE DILUTION. Naomi P. Alazraki, Heinrich R. Schelbert, John W. Verba, Gary W. Brock, William L. Ashburn. VA Hospital, San Diego and University of California, San Diego.

The purpose of this study was to compare cardiac outputs derived from radionuclide cardiac angiography and computer data processing to those obtained by dye dilution techniques in the cardiac catheterization laboratory.

20 patients were injected intravenously with 8 mCi  $^{99m}Tc$  albumin immediately following the green dye study and imaged in the RAO view with a scintillation camera while still in the cardiac catheterization laboratory. The data was recorded on video tape and later transferred to digital magnetic tape for processing by a mini-computer. An area-of-interest was placed over the left ventricle (LV) and a perimeter ring area was placed around the ventricle for background determination. Curves of time vs. counts were generated and cardiac output was derived by the computer based on  $E \times BV/A$ , where E was the equilibrium counts/second in the LV area-of-interest 10 minutes after injection, BV the

patient's blood volume, and A, the integration of counts under the LV curve.

Blood volume was determined using  $^{99m}Tc$ -albumin.  $^{125}I$ -albumin was also used in 6 patients to check the reliability of the  $^{99m}Tc$ -albumin determinations.

The results of this study showed a high degree of correlation between radionuclide cardiac output determinations and the green dye results ( $r = 0.95$ ;  $p < .001$ ). One important application of cardiac output may be in calculating the stroke volume: stroke volume = cardiac output/heart rate. The end diastolic volume can then be derived if the ejection fraction is known, according to the formula: end diastolic volume = stroke volume/ejection fraction.

It is concluded that accurate cardiac output determinations can be easily obtained from non-traumatic radionuclide cardiac angiography.

QUANTITATIVE ASSESSMENT OF REGIONAL VENTILATION AND PERFUSION IN HOMOZYGOUS ALPHA-1 ANTITRYPSIN DEFICIENCY. Phillip O. Alderson, Thomas Dew, and R.H. Secker-Walker, Washington University School of Medicine, St. Louis, Mo.

$^{133}Xe$  ventilation studies have been reported in patients with alpha -1 antitrypsin deficiency, but the regional lung function of these patients has not been quantitatively analyzed. A digital computer interfaced to a gamma camera has been used to assess the regional fractional exchange of air and relative regional ventilation-perfusion ratios in 8 patients with homozygous alpha -1 antitrypsin deficiency. The bases of the lung demonstrated the lowest fractional exchange of air, with a mean of 0.82% per sec. The exchange in the mid zones was well below normal at 1.36% per sec, but the upper zones had a normal mean fractional exchange of 2.46%. The whole lung mean fractional exchange of the 8 patients was 1.54% per second. The relative distribution of lung volume was not significantly different from normal, but there was a redistribution of perfusion away from the lower zones. This resulted in an abnormal lower to upper zone perfusion ratio of 1:1. The mean relative ventilation-perfusion ratio in upper zones was 1.34, while in middle zones it was 0.97. The lower zone ratio was 0.73. These values are not significantly different from normal. In addition, analog images of the relative ventilation-perfusion ratios demonstrated a fairly uniform regional distribution. Although the overall air exchange of patients with homozygous alpha -1 antitrypsin deficiency is reduced, the fractional exchange of the upper zones of the lung may remain normal. The redistribution of perfusion increases the blood supply to normally exchanging regions and results in the maintenance of nearly normal regional ventilation-perfusion ratios.

A NEW  $^{99m}Tc$  (Sn) TRACER FOR RENAL SCANNING. Jorge Alvarez, Roberto Maass, and Catalina Arriaga. Instituto Nacional de Energía Nuclear and Hospital "20 de Noviembre", Mexico City, Mexico.

Among the many radiopharmaceuticals proposed for kidney imaging, various technetium-99m compounds offer several advantages on account of its decay characteristics. Although most of these compounds have proved to be useful for kidney function studies, not all of them have been generally accepted. This communication reports on a new agent for renal scanning. The product is a complex of tin, dextrose and technetium-99m which can be prepared by mixing the components of a kit with pertechnetate in solution. The nature of the product has been studied by means of  $^{14}\text{C}$ -glucose and radioactive tin. The amount of pertechnetate in the radiopharmaceutical as determined by Sephadex filtration, has been 5-6%. A high kidney uptake was found in rats by organ distribution studies. A predominant localization of the tracer in the renal cortex was demonstrated by means of autoradiography and scintigraphy of slices of rat kidneys. This radiopharmaceutical is now being employed in our hospital for routine use in renal scanning and over 200 patients have been studied. It has been observed that part of the activity is retained by the parenchyma and part is excreted into the urine. The obtained images give at the same time, useful information about the renal parenchyma and the upper urinary tract.

**ENDOLYMPHATIC ISOTOPIC THERAPY TREATMENT OF MALIGNANT LYMPHOMAS.** Irving M. Ariel. Pack Medical Foundation, New York, N.Y.

Malignant lymphomas above the diaphragm are treated by orthodox radiation therapy  $^{131}\text{I}$  or  $^{32}\text{P}$  re-injected into the lymphatics of both feet. The procedure is both diagnostic for the presence of subdiaphragmatic lymphoma and therapeutic in as much as 50-100 thousand rads Beta are delivered to the pelvic and periaortic lymph nodes. Twenty patients have been treated with good results.

**RESOLVING TIME OF SCINTILLATION CAMERAS.** John E. Arnold, A. Sidney Johnston, Steven M. Pinsky, Michael Reese Medical Center, Chicago, Illinois.

The observed counting rate of radioactive sources was monitored under different scatter conditions and window width settings by Pho/Gamma III and HP cameras while activity was increased stepwise to high levels. As source strength rose, observed counting rate (R) increased to a maximum ( $R_{\text{max}}$ ) and then decreased. Thus the camera behaves as a paralyzable detector. Its resolving time (T) can be estimated from  $T = (eR_{\text{max}})^{-1}$  and used in equation  $R = Ne^{-NT}$  to predict observed from true counting rate (N). By use of this paralyzable instrument model T does not vary with counting rate for constant scatter and window width conditions, whereas T varies markedly with N if the paralyzable model is used. Available data from cameras of several different manufacturers was found to conform closely to the model. However, variation in window width setting or in the degree of scatter in and around the source was found to alter T by changing the photopeak fraction (F) of detectable events which fall within the pulse height analyzer window.

By replacing T with the term (K/F) where K represents the true resolving time of both photopeak and nonphotopeak events occurring in the crystal, equation  $R = Ne^{-NK/F}$  is obtained and this depicts reasonably accurately the dependence of observed counting rate on factors N, K and F. Unless F can be accurately measured during a study this model cannot be used for clinical deadtime corrections since F varies with different scatter conditions and window settings. Clinical deadtime corrections are more easily performed by monitoring either a fixed source in the field of view or pulses electronically injected into the camera. Values of F measured in patients for lung, liver, brain, and bone scans are usually between .20 and .33.

**NEW COMPLEXES OF  $^{99\text{m}}\text{Tc}$  FOR RENAL IMAGING.** R. W. Arnold, G. Subramanian, J.G. McAfee, M.E. Rosenstreich and M.E. Gebhardt, Upstate Medical Center, Syracuse, New York

Freeze-dried kits of the saccharides lactobionate, gluconate, glucoheptonate, and mannitol were formulated with stannous chloride for "instant" labeling with  $^{99\text{m}}\text{Tc}$  generator eluate.

Tissue distribution of these agents was determined by radioassay after intravenous injection at varying intervals in rabbits, and one hour after injection in dogs. Two commercial kits, glucoheptonate (NEN) and 2-3-dimercaptosuccinate (DMS) (Mediphsysics) were tested similarly. In 6 normal volunteers, urinary clearance, blood, and plasma clearances were measured at 24 hours. The agents were then used in limited clinical trials for renal imaging with a scintillation camera.

All of the agents reached a higher renal concentration than  $^{99\text{m}}\text{Tc}$  pertechnetate or DTPA complex. In both the rabbit and dog, the highest renal concentration was obtained with labeled DMS. Its concentration in the renal cortex was relatively high, and in the medulla, exceptionally low, compared to the other agents. In the dog, there was 7% of the administered dose in the kidney at 1 hour. The distribution of the other complexes resembled that of the older agent,  $^{99\text{m}}\text{Tc}$ -Iron-Ascorbate complex. In clinical studies the renal images obtained with the various agents were qualitatively similar. Unfortunately, all agents evaluated showed some concentration in the liver.

**QUANTIFICATION OF MYOCARDIAL INFARCTION BY SCINTIGRAPHY: AN AUTOPSY CORRELATION STUDY.** A.B. Ashare\*\*, D.W. Romhilt<sup>x</sup>, V.J. Sodd<sup>+</sup>, N.I. Levenson<sup>x</sup>, R.J. Adolph<sup>x</sup>, E.L. Saenger\*, and L.S. August<sup>o</sup>. NML<sup>+</sup>, BRH, FDA, DHEW, Cinti., O. Radioisotope Lab.\* and Cardiac Research Lab.<sup>x</sup> Univ. of Cinti. Medical Center, O., and Naval Research Lab.<sup>o</sup>, Washington, D.C.

Myocardial infarction can be identified and localized by scintigraphy with a high degree of accuracy. However, to be of a therapeutic benefit, information on the size of the infarcted area is needed. Myocardial infarction was induced surgically in dogs after control scintigrams were obtained with intravenously injected Cesium-129. Four views were obtained with an Anger type gamma camera with pinhole collimator. Myocardial scintigrams were obtained two days after surgical induction of infarction. The animal was later sacrificed and the size of the infarction estimated at autopsy and expressed as a percentage of the total myocardium. Without knowledge of the autopsy findings, four readers interpreted the post infarction scintigrams with comparison to the control scintigrams. Readers quantified the lesion in each view. Then a composite percentage involvement of myocardium (CPIM) was made from the four views. CPIM was analyzed using a two-way analysis of variance. Differences between readers were not found to be significant ( $F=1.337, D.F.=3,78$ ). Also, differences between readers and autopsy findings were not found to be significant ( $F=1.337, D.F.=4,104$ ). This present study indicates that we can quantify the size of the infarction from scintigrams and that this technique may be useful in quantifying the size of myocardial infarction in humans.

**NEW CYCLOTRON NUCLIDES FOR RADIOPHARMACEUTICALS: TITANIUM-45 AND LEAD-203.** H. L. Atkins, P. R. Bradley-Moore, R. M. Lambrecht, J. C. Merrill, S. Packer, and A. P. Wolf. Brookhaven National Laboratory, Upton, N. Y.

Lead and titanium are two elements that are potentially useful as radiopharmaceuticals, either as inorganic coordination compounds or in the relatively unexplored area of organometallic radiopharmaceuticals. Certain heavy metals are known to have tumor specificity. We have developed the cyclotron production parameters for obtaining high-purity, carrier-free titanium-45 ( $T_{1/2} = 3.1 \text{ hr}$ ,  $8^+$ ), and lead-203 ( $T_{1/2} = 52.1 \text{ hr}$ ,  $\gamma = 279 \text{ keV}$ , 95%). The preferred nuclear reactions are:  $^{45}\text{Sc}(p,n)^{45}\text{Ti}$ ,  $E_{\text{th}} = 12.5 \text{ MeV}$ ; and the  $^{203}\text{Tl}(d,2n)^{203}\text{Pb}$ ,  $E_D = 22.7 \text{ MeV}$ . The thick target production yields (at EOB) after chemical separation were  $3.5 \pm 0.5 \text{ mCi}/\mu\text{AH}$ , and  $241 \pm 50 \text{ } \mu\text{Ci}/\mu\text{AH}$ , respectively.

$^{45}\text{Tl}$  was prepared in the carrier-free form as  $^{45}\text{Tl}_2\text{O}_3$ ,  $^{45}\text{Tl}$ -citrate and  $^{45}\text{Tl}$ -lactate. Significant differences were noted in the tissue distribution in mice at times up to 23 hrs.; e.g. at 2 hrs. the uptake in the lung was  $146 \pm 23$ ,  $6.2 \pm 0.7$  and  $9.7 \pm 1.2\%$ /gm, respectively. By comparison, the uptake in the spleen at 2 hrs. was  $4.4 \pm 2.3$ ,  $5.2 \pm 0.5$  and  $11.7 \pm 3.4\%$ /gm, respectively. Variations in tissue specificity with chemical form are interesting, since high concentrations of titanium have been reported to be found in certain types of lymphomas.

$^{203}\text{Pb}$  was studied as the nitrate complexed with tro-methamine, in mice with adenocarcinoma of breast tumor, and in Syrian hamsters with skin and eye melanomas. The tumor uptake in mice at 24 hrs was  $4\%$  ( $2.5\%$ /gm). In the hamster model, the ratio of the uptakes for skin melanoma/normal skin was 7.2. The eye melanoma/normal eye ratio was 2.5. The choroid/lens ratio was 22.6.

The pharmacodynamic and tissue specificity results suggest that  $^{203}\text{Pb}$  may potentially be a good nuclide in tumor-localizing radiopharmaceuticals. The results with  $^{45}\text{Tl}$  illustrate the need to systematically examine the chemical form of inorganic radiopharmaceuticals.

$^{99\text{m}}\text{Tc}$ -PYRIDOXYLIDENEGLUTAMATE: A NEW RAPID CHOLESCINTIGRAPHIC AGENT. Richmond J. Baker, John C. Bellen, and Peter M. Ronal. Inst. Med. & Vet. Sci., Adelaide, South Australia.

A new radiopharmaceutical,  $^{99\text{m}}\text{Tc}$ -pyridoxylidene-glutamate, undergoes rapid biliary excretion in experimental animals and man. The complex prepared by autoclaving  $^{99\text{m}}\text{TcO}_4^-$ , pyridoxal and sodium glutamate at pH 8-9, was found to be sterile, free of pyrogens and non-toxic up to doses of 1,200 mg/kg in mice (5,000 times the human dose). In mice, the gall bladder was visualised scintigraphically 10 min after IV injection, at which time the gall bladder to liver concentration ratio was 9:1, increasing to 80:1 by 60 min.

In human controls, the hepatic parenchymal phase was seen within the first 5 min after IV injection, the common bile duct and duodenum within 10 min and the gall bladder within 15 min. The gall bladder was not visualised in patients with acute cholecystitis, cystic duct obstruction or complete obstruction of the common bile duct, or in some patients with chronic cholecystitis. Pooling of tracer in a dilated common duct and delayed excretion into the duodenum were seen in partial extrahepatic obstruction. Marked renal excretion of tracer was a feature of both severe hepatocellular disease and complete extrahepatic obstruction, but appearance of tracer in the small bowel at 15 hours after injection was found only in the former situation.

This radiopharmaceutical promises to be of real value in the diagnosis of biliary tract disorders and concentrates in the biliary tree more rapidly than previously described agents.

UPTAKE OF RADIOLABELED DIPHENYLHYDANTOIN (DPH) IN ISLET CELLS. Suppiah Balachandran, Ung Y. Ryo, William H. Beierwaltes, Michael J. Shaw, Rodney D. Ice. University of Michigan Medical Center, Ann Arbor, Mich.

Diphenylhydantoin (DPH) suppresses insulin release. We have investigated the uptake of radiolabeled DPH in islet cells with the aim of developing a gamma emitting radiolabeled medicinal that would allow preoperative detection of insulinomas. Mature toadfish (islet cells are separate from acinar cells) weighing about 1 kg were given a tracer dose of 1.3-5.0  $\mu\text{Ci}$  of  $^{14}\text{C}$  DPH into a gill arch vein via a 26-gauge needle. A minimum of 3 fish were sacrificed at each of the following intervals by a blow on the head: 10 minutes, 30 minutes, 1, 2, 6, 24, 48 and 72 hours. Radioactivity assay of 13 different tissues with a liquid scintillation counter revealed that the highest radioactivity concentration appeared in the islet cell tissue at 10 minutes after the tracer = 7.8% dose/gm of tissue. At this time, the radioactivity concentration in

islet cell tissue was 6 X > acinar tissue, 7 X > blood, 20 X > liver and 27 X > muscle. From 30 minutes to 2 hours after the dose, radioactivity concentration was highest in the brain = 6.6% dose/gm.  $^{14}\text{C}$  DPH uptake in one patient 17 minutes before a 2/3 rds. pancreatectomy delivery of tissue was similar to that in the toadfish at 30 minutes. DPH has now been labeled with  $^{125}\text{I}$  DPH at the para position (sp. act. = 100  $\mu\text{Ci}/\text{mg}$ ) and the uptake in toadfish islets and in 3 humans with insulinomas is currently being evaluated. The % dose/gm uptake in islet cells observed here, and the target:non-target ratio in islet tissue is the highest reported to date.

THYROIDAL RADIOIODIDE "TURNOVER" IN HYPERTHYROIDISM. Julian Banerji, Richard P. Spencer. Section of Nuclear Medicine (Radiology), Yale Univ. School of Medicine; New Haven, Conn.

One of the variables in treatment of hyperthyroidism by radioiodide is the rate at which the administered dose is "turned over" by the thyroid. The effective half-time of radioiodide in the gland is usually assumed to be about 6 days, based on studies reported in the 1940's and 1950's. To obtain data on this pretreatment value in hyperthyroid individuals in the present population, 100 consecutive patients about to undergo radioiodide treatment were counted at 24 and (usually) 48 hours after a drink of  $^{131}\text{I}$  Na. From the net counts at these times, the effective T 1/2 was calculated. Of the 100 hyperthyroid patients, 85 were women with a mean age of 49 years. In the 15 men, the mean age was 53 years. The effective T 1/2 for all cases was 5.0 days (close to the value reported by Blomfield in 1959). In the males it was 4.9 days and in the females 5.0 days. Eliminating 21 cases in which the T 1/2 approached that of radioiodide (little biological turnover between 24 and 48 hours), T 1/2 for women was 4.3 days and for men 4.1 days. There was no correlation between the 2 hour uptake of radioiodide and the turnover T 1/2. Similarly, there was no correlation between the 24 hour uptake and the T 1/2. Even in 10 patients with uptake values over 50% at 2 hours, there was no clear correlation between uptake and turnover. A plot of turnover T 1/2 versus surface area of the thyroid, also revealed no correlation. The turnover rate thus appears to be biologically independent of uptake and gross gland size. This is of particular interest, since present uptake values (in the normal population) are somewhat lower than those of past decades. Studies are underway on the effects of therapy on the turnover T 1/2.

IN VIVO STUDY OF THE EFFECTS OF TISSUE INFLAMMATION ON THE UPTAKE OF BONE-SEEKING RADIONUCLIDES. George Bautovich, Harry K. Genant, Paul B. Hoffer, Paul V. Harper, and K. Lathrop. The University of Chicago, Chicago, Ill.

Bone scanning is being used increasingly to detect osteomyelitis. The purpose of this study is to determine whether inflammation in soft tissues will increase radionuclide uptake in the adjacent bone and lead to the false impression of osteomyelitis.

Tissue inflammation has been produced by the I.M. injection of turpentine (0.05, 0.1, 0.2 ml) in the knee region (right) in rats. Following the I.V. administration of a radionuclide, external counting and imaging of a selected region was performed using the Nuclear Chicago Phogamma Camera with pinhole collimation. Quantitative data were recorded and retrieved using the Ohio-Nuclear 150 Data System. The uptake in the region of interest (knee) was calculated after tissue background subtraction, and a ratio between the right and left knee obtained. In vivo quantitation has been corroborated by the use of well-counting techniques and autoradiography.

Inflammation developed within 2-4 days and was confirmed by the increased uptake in the turpentine-injected limb of  $^{99\text{m}}\text{Tc}$ -pertechnetate, used to demonstrate the intravascular and extravascular fluid spaces. Preliminary results using  $^{99\text{m}}\text{Tc}$ -EHDP, 2 hours after I.V. administration, have demonstrated no significant difference in the bone uptake between the limbs. The uptake of  $^{99\text{m}}\text{Tc}$ -EHDP by the inflamed soft tissue, however, is increased when compared to the normal side. These preliminary results suggest that soft tissue inflammation, adjacent to bone, should not result in a false interpretation of osteomyelitis.

**LEFT VENTRICULAR VOLUME FROM ECG GATED COINCIDENCE IMAGES OF  $^{11}\text{CO}$ .** George Bautovich, Paul V. Harper, Bruce Mock, Nick Lembares, Helen Krizek, and Marsha Rich. University of Chicago, Chicago, Illinois.

Coincidence counting of positron annihilation radiation eliminates the effects of attenuation and scatter in tissues, thus allowing direct comparison of a source inside the body with one outside the body. Using a previously described gamma camera configuration with a parallel hole tungsten collimator looking at a coincidence detector array of seven 2" x 2" NaI(Tl) crystals 40 inches from the collimator face, preliminary measurements have been made of the heart chambers using inhaled  $^{11}\text{CO}$  as a blood pool labeling agent. Using an ECG gate, 16K digital images were collected in systole and diastole over 40 min. Numbers were integrated in regions of interest containing the left ventricle (LAO) and an external reference source of  $^{11}\text{CO}$ . These were corrected for adjacent background, as well as nonuniformity and variable tissue attenuation using a 511 keV transmission image. After about half of the counts had been collected, a blood sample was drawn and subsequently compared to the reference standard giving the equivalent number of milliliters of blood. Comparison gave the diastolic ventricle volume. Using 5-10 mCi of  $^{11}\text{CO}$  permits collection of ~1000 net counts in the ventricle region of interest. Preliminary values for end diastolic volume, ejection volume and cardiac output (assuming competent valves) were within expected range. While the effects of chance coincidences on the ratios of net counts in the regions of interest were small, additional shielding of the coincidence detector should improve performance.

**TREATMENT OF DISTANT METASTASES FROM DIFFERENTIATED THYROID CARCINOMA.** W.H. Beierwaltes, J.K. Harness, N.W. Thompson, J.C. Sisson. University of Michigan Medical Center. Ann Arbor, Mich.

A 75% mortality rate at 5 years after diagnosis is reported for patients with papillary and follicular carcinoma of the thyroid gland metastatic to lung and/or bone. Using  $^{131}\text{I}$  after surgery, our patients in this category have a mortality rate of 27.8% at 15 years after diagnosis.

In the 26 year period of 1947-1973, 333 patients with papillary and follicular carcinoma of the thyroid gland were treated with  $^{131}\text{I}$  after surgery. Six weeks after surgery and off thyroid hormone, a tracer dose of 300 uCi of  $^{131}\text{I}$  was given and neck, lung and bone scans were performed with a dual 5" crystal rectilinear scanner. 36 of 330 patients (10.9%) had metastases remote from the neck and/or mediastinal region. In 28 patients the neoplasms were classified as papillary and 8 as follicular. In addition to pulmonary metastases, 6 of 28 (21%) of patients with papillary carcinoma also had metastases to bone. One half of those with follicular carcinoma had demonstrated concomitant lung and bone metastases at the time of the first  $^{131}\text{I}$  therapy. The average follow-up period from diagnosis was 14.9 years (1-40 years). The average follow-up period from the first therapeutic-dose of  $^{131}\text{I}$  was 11.4 years, 15 years for survivors. Twenty of 28 patients with papillary carcinoma have been followed a minimum of 10 years and half of these have been followed a minimum period of 20 years.

Our use of  $^{131}\text{I}$  therapy after surgery appears to prolong life in these patients.

**SINUS IMAGING WITH VENTILATION DYNAMICS USING  $^{133}\text{Xe}$ .** Robert M. Beihn, Mary F. Reed, George Zarocostas, and Judy S. Jones. VA Hospital and University of Kentucky Medical Center, Lexington, Ky.

The purpose of this study was to visualize the paranasal sinuses and to evaluate the dynamics of sinus ventilation.

The  $^{133}\text{Xe}$  was inhaled using a modified Medipysics Xenon ventilation system. The modification included separate nasal canulas using a T connector and tygon tubing linked to the  $^{133}\text{Xe}$  source and storage bag. For data collection, an

Anger camera with the high sensitivity low energy collimator was used. The data was observed live and also stored in a computer. All subjects used in this study were in the anterior position.

Subjects were comfortably inhaling and exhaling through the mouth until the  $^{133}\text{Xe}$  was released. At this time one nasal inhalation allowed 5-10 mCi of  $^{133}\text{Xe}$  to be drawn through the nasal passage. The subjects were instructed to begin breath holding for about 10 sec in order to permit time for the static image to be taken, after which normal mouth inhalation with nasal exhalation permitted washout data to be acquired.

Results indicate visualization of the maxillary and sphenoid sinuses. Differences in patency are apparent from the static images. Normal washout  $T_{1/2}$  for each maxillary sinus has been calculated to be about 20-30 sec with a longer  $T_{1/2}$  in subjects with sinus disease.

From this preliminary study, it has been concluded that maxillary sinuses can be easily visualized. Ventilation dynamics indicate the exchange rate of  $^{133}\text{Xe}$  to be an aid in evaluating ostia patency.

**OPTIMAL TIME FOR  $^{131}\text{I}$  TOTAL BODY IMAGING TO DETECT METASTATIC THYROID CARCINOMA.** Carlos Bekerman, Alexander Gottschalk, and Paul B. Hoffer. University of Chicago, Ill.

No universal technique exists for whole-body imaging with  $^{131}\text{I}$  to detect metastases in a patient with thyroid carcinoma who has had total thyroidectomy. Many workers have advocated different optimal imaging times from 24 to 72 hours, but we are unaware of any series which compares  $^{131}\text{I}$  body images at sequential intervals. The purpose of this study was to determine the relative accuracy of detecting thyroid metastases at various imaging times. Twenty-four patients with carcinoma of the thyroid were studied. A total of 58 body images were performed following administration of 1 mCi of  $^{131}\text{I}$ . All views were obtained using a gamma camera with medium energy diverging collimator and a 5 minute exposure time. The 58 body images were obtained in a sequential mode.

Of the 58 scans performed: (a) 9 (16%) had definite lesions at 48 hours or later that were not seen at all at 24 hours. (b) 11 (20%) had definite lesions at 48 hours or later which were questionable at 24 hours. (c) 6 (11%) showed questionable activity at 24 hours which was shown to be physiologic uptake on the delayed (48-72 hours) scans. (d) None of the scans demonstrated an area of abnormal uptake at 24 hours that was not seen at 48 or 72 hours. (e) 48 cases had both 48- and 72-hour scans. The 72-hour scan detected 5 more lesions than the 48-hour scan. (f) 8 cases had both 72- and 96-hour scans. No new lesions were seen at 96 hours.

From these data we conclude that a potential error rate of 36% of metastases might have been missed if only the 24-hour scan was employed. In addition, 11% of our cases had physiologic uptake which might have been erroneously over-diagnosed at 24 hours. These data indicate that 72 hours is the optimum time for whole-body imaging to detect thyroid cancer metastases.

**NORMAL CRITERIA FOR EARLY BONE DYNAMICS OF  $^{99\text{m}}\text{Tc}$ -DIPHOSPHONATE.** Gerald Berg, Frank Castronovo, Kenneth McKusick, Henry Pendergrass, Ronald Callahan, Majic Potsaid. Mass. General Hospital, Boston, MA.

The early dynamics of  $^{99\text{m}}\text{Tc}$ -diphosphonate were measured in normal patients to form a basis of comparison for similar studies in patients with bone pathology and disorders of mineral metabolism. Sequential quantification of radionuclide distribution was carried out for one hour after I.V. injection of 20mCi of  $^{99\text{m}}\text{Tc}$ -diphosphonate (0.4-0.6 mg diphosphonate carrier) utilizing an Anger camera interfaced with a HP5407A computer. Regions of interest were selected to include kidneys, lumbar spine, pelvis and background. Patients studied had normal renal function and no evident metastatic or metabolic bone disease. The bone time-activity curves were similar in all of those patients with an initial dominant peak at 15-30 seconds fol-



lowed by a later peak at 20-45 minutes. Activity declined gradually for the remainder of the 1 hour period. Blood clearance was biphasic with an initial rapid phase (26.2±5.1% remaining 5 minutes after injection) followed by a more gradual clearance (8.7±1.6% remaining at 1 hour, 2.0±1.1% remaining at 4.5 hours). Peak renal activity occurred at 20 minutes; approximately 30% of the dose was excreted in urine by 4.5 hrs. Chromatographic analysis of plasma and urine demonstrated the absence of free pertechnetate with all activity at the <sup>99m</sup>Tc diphosphonate peak. This data suggests that the early accumulation of <sup>99m</sup>Tc diphosphonate in normal bone occurs in a characteristic pattern.

**HIGH RESOLUTION SCINTIGRAPHY OF CARDIAC SYSTOLE AND DIASTOLE.** Daniel S. Berman, Gerald L. DeNardo, Antone F. Salel, Robert Zelis, Dean T. Mason, H. W. Strauss, and Hugo G. Bogren. University of California, School of Medicine, Davis, California

Radioisotopic methods of evaluating regional myocardial pump performance have been limited by poor resolution of images. A technique which provides high resolution images of the heart in systole and diastole has been developed. The results in 33 patients were compared with radiopaque left ventricular cineangiograms (LVC) obtained within 48 hours of the radioisotopic study. The following modifications of standard RAO gated blood pool imaging using the scintillation camera were made: a 15,000 hole high resolution collimator was used; 500,000 count images of systole and diastole were obtained; all margins of the left ventricle, including the aortic and mitral valve planes, were determined by simple inspection of the gated images; a phonocardiogram was employed to more accurately determine end-systole than was possible with EKG timing; in selected patients LAO images were obtained for observation of septal and posterior wall motion. Three of the patients were eliminated from statistical analysis; 2 because marked right ventricular enlargement prevented radioisotopic definition of the left ventricle, and 1 because LVC was inadequate. In the remaining 30, the correlation coefficient for the ejection fraction was .92 (p < .001); the regression equation was  $y = .82x + .12$  with SD .065. All 17 cases of regional abnormality on LVC were detected on the radioisotopic study. This radioisotopic method yields high resolution images of the heart which lead to accurate determination of regional and overall myocardial pump performance.

**NON-INVASIVE RADIOISOTOPIC DETERMINATION OF CARDIAC OUTPUT UTILIZING A SINGLE PROBE AND A COMPUTER MODEL.** Daniel S. Berman, Antone F. Salel, Gerald L. DeNardo, Dean T. Mason, and Robert Zelis. University of California, School of Medicine, Davis, California. Paul O. Scheibe, Peter E. Jackson, George B. Bell, Cupertino, California

Cardiac output (CO) was measured in 17 patients by a constant infusion radioisotopic method (CIRM) and compared to simultaneous dye dilution (16) and Fick (1) measurements. An injection over 4 minutes of In-113m was made into a peripheral vein. Activity over the great vessels was detected by a single probe and was recorded on punched paper tape for transmission over telephone lines to a digital computer. The CIRM is based upon modeling the circulation as a closed hydraulic system consisting of two in-series sets of parallel differing transit times, representing the pulmonary and extra-pulmonary vascular plexuses. Each of these sets are characterized by a frequency distribution of transit times whose global mean is the mean circulation time. CO was calculated by dividing measured blood volume by the computer estimate of mean transit time. One value was excluded from statistical consideration because it deviated 45% from the line of identity, whereas the remaining 16 were within 20% confidence intervals.

The correlation coefficient was .76 (p < .001); the paired t test was accepted at p=.60. In one case where the dye method was uninterpretable because of aortic insufficiency, comparison with simultaneous Fick measurement was 4.5 to 4.7 L/min. This case suggests a special use of the CIRM where the dye dilution method is invalid. The CIRM appears to be as accurate as the standard more invasive methods for measuring CO.

**RADIOPHARMACOKINETICS OF ANTINEOPLASTIC PLATINUM COMPOUNDS: EVALUATION OF <sup>195m</sup>Pt CIS-DICHLORO-BIS-CYCLOPENTYLAMINE-PLATINUM(II) ("A").** Jeffrey A. Berman, Francis K.V. Leh and Walter Wolf. Univ. of Southern Calif., Los Angeles, CA.

Previous work of this laboratory on the radiopharmacokinetics of cis-dichlorodiammine platinum(II) suggested an "in vivo" nuclear medicine technique that would assist in evaluating this new antineoplastic agent, now in phase II clinical studies as NSC-119875. A major problem in its utilization is its severe nephrotoxicity. Other platinum analogs are significantly less toxic; in particular the title compound "A" has a therapeutic index 200 times greater than NSC-119875. The present study was undertaken to evaluate "A" utilizing a <sup>195m</sup>Pt labeled radiopharmaceutical. Rats bearing Walker 256 carcinosarcoma were injected at 1.5, 5.0 and 100 mg/Kg and scanned serially. Excreta were collected over a 7 day period, after which the animals were sacrificed. No significant tumor localization was detectable, but significant activity was measured in kidney, liver and spleen. Because "A" is highly insoluble, it was administered I.M. None of the factors influencing mobilization of insoluble drugs (hyaluronidase, diathermia or fractionated dosage) affected the rate of mobilization to any significant extent. The most dramatic result is the fantastically high degree of kidney retention, which even after 7 days ranged from 26-60% of the total drug administered, and which does not appear to be dose dependant in the 5-100 mg/Kg range. The mobilization of the drug thus appears to be kinetic, rather than concentration, dependant. Urinary excretion has a fast phase, followed by slow, sustained release. The major excretion product is unmetabolized "A", accompanied by at least three other also poorly soluble metabolites. The present results illustrate once more that external monitoring of radiolabeled pharmaceuticals is a significant tool in their clinical evaluation. For "A", it is suggested that the extremely high renal retention severely questions its possible clinical usefulness.

**OCULAR SCINTIGRAPHY.** Paul Blanquet, Philippe Verin, Bernard Basse-Cathalinat, and Nour Safi. I.N.S.E.R.M. Unité 53, Domaine de Carreire, rue Camille Saint-Saens, 33000 Bordeaux and Hôpital St André, laboratoire des isotopes, 1 rue Jean Burguet, 33000 Bordeaux.

The technology of ocular scintigraphy has been recently improved. As previously, the detector is an Anger camera coupled with a multiparametric analysis system or a small computer which enables to obtain quickly isodose curves. At the origin, the pin-hole collimator with two stenopoeic apertures in front of each eye, presented an invariable interpupillar distance. It has been recently modified to render this distance variable, by the adaptation of two rotating Tungsten pieces with excentric apertures. In such conditions, the interpupillar distance can vary between 50 and 80 millimeters (65 ± 15 millimeters). The overall definition is now 2.5 millimeters, such a high value being due to the use of the pin-hole system and equally to the small diameter of the apertures (2.5 millimeters).

<sup>131</sup>I Diiodofluorescein is still used for the study of hypervascularisation (generally associated with the tumor), but Technecium is more advantageous because of its physical and dosimetric characteristics.

<sup>131</sup>I iodinated chloroquine has been equally employed for selective detection of malignant melanomas. Statistics concerning the results of 300 cases are presented (double scintigraphy <sup>131</sup>I Diiodofluorescein or Technecium and iodinated chloroquine).

The difficulties arisen by the interpretation of the images and the main indications of our method are discussed.

**RADIONUCLIDE IMAGING OF THE KIDNEY IN TUBEROUS SCLEROSIS.** Charles J. Blatt, David B. Hayt and Leonard M. Freeman. Fordham and Misericordia

Hospitals and Albert Einstein College of Medicine Bronx, New York.

Multiple space occupying lesions of the kidney are common in patients with tuberous sclerosis. They are angiomyolipomas with an abundant vascular supply. Commonly confused with angiomyolipomas are polycystic kidneys. These two diseases have a similar urographic appearance distinguished only with angiography. Two related patients with tuberous sclerosis were found to have space occupying kidney lesions on urography. Static scintigrams with  $^{197}\text{Hg}$  chlormerodrin demonstrated the lesions well. Subsequent vascular flow studies with intravenous  $^{99\text{m}}\text{Tc}$  pertechnetate revealed these lesions to have a rich blood supply. Because of their known high association (50-80%) with tuberous sclerosis the presumptive diagnosis was angiomyolipoma. This was confirmed at angiography. Similar radionuclide studies in patients with proven polycystic kidney disease clearly demonstrated the avascular nature of the lesions in sharp contrast to the angiomyolipomas. Radionuclide renal imaging studies are a useful diagnostic aid in evaluating space occupying kidney lesions in tuberous sclerosis. The finding of multiple vascular lesions is good evidence of angiomyolipomas. Conventional angiography is not necessary. Avascular polycystic or multiple cyst disease of the kidney also is easily documented on such scintiphotographic studies.

**A NEW METHOD FOR IMAGING MYOCARDIAL INFARCTS.**

Frederick J. Bonte, Robert W. Parkey. The University of Texas Southwestern Medical School, Dallas, Texas

Several investigators have shown that the calcium ion which enters myocardial cells in an infarct localizes in a crystalline structure which forms within mitochondria, tentatively identified as hydroxyapatite. We have utilized this phenomenon to visualize experimental infarcts in a number of 20 kg mongrel dogs using a member of the family of bone-imaging agents,  $^{99\text{m}}\text{Tc}$  stannous pyrophosphate (PYP). Imaging studies show that an experimental infarct becomes visible on scintillation camera images in from 12 to 16 hours following infarction, and in from 30 to 60 minutes after injection of  $^{99\text{m}}\text{Tc}$  PYP. Localization persists unchanged for about 4-6 days, but begins to fade thereafter and usually disappears by the fourteenth post-infarction day.

Accompanying tissue distribution studies show the establishment of a 10:1 ratio of  $^{99\text{m}}\text{Tc}$  activity of infarct to normal myocardium within 12 to 24 hours of infarction which is in accord with the results of imaging studies. Other favorable ratios include infarct/liver (6:1) and infarct/aerated lung (20:1). Anticipated high concentrations are observed in bone, but maximum bone uptake has not occurred at the optimum imaging time, 30-60 minutes after injection.

Possible adverse effects such as arrhythmias due to chelation of calcium ion by PYP have been ruled out by obtaining appropriately controlled EKG studies in 6 dogs before and after infarction, and before and after administration of repeated 5.0 mg imaging doses of PYP. Results obtained in this study indicate that bone-imaging agents such as  $^{99\text{m}}\text{Tc}$  PYP, polyphosphate, etc are probably the agents of choice for the demonstration of recent myocardial infarcts.

**THE ROLE OF NUCLEAR MEDICINE IN HUMAN LIVER TRANSPLANTATION.** S.E. Bostrom, D.W. Brown and G.L. Nelson. Denver Veterans Administration Hospital and University of Colorado Medical Center, Denver, CO

Since 1963 more than 80 human hepatic homografts have been performed at our institution. Although only 10 remain alive and the longest survivor has lived 4 1/2 years, great improvements in technique and long-term care have occurred so that recent patients, most of whom suffer from biliary atresia or post necrotic cirrhosis, are doing

relatively well. Nuclear Medicine has played an important role in the preoperative evaluation of these patients and in their long-term follow-up. This routinely involves a  $^{99\text{m}}\text{Tc}$  sulfur colloid scan in combination with a 20 minute I-131 Rose Bengal retention and 24 hour Rose Bengal abdominal scan. In general, these procedures are performed preoperatively, postoperatively and then at any time a clinical change occurs. One of the first signs of rejection is an increase in liver size and rise in Rose Bengal retention. As rejection subsides, the liver returns to its previous size. Over the years, an amazing variety and number of complications has occurred. These have included brain, lung, liver and abdominal abscesses; pulmonary embolism, pneumonia, hepatorenal syndrome, various infarctions, various types of biliary obstruction and recurrence or spread of hepatoma in cases where this was the underlying disease. In addition to liver scans; lung-liver, brain, lung, and renal scans and renograms have been used. Recently, Ga-67 abdominal scans have been used successfully in a number of cases complicated by abscesses. Complications, Nuclear Medicine procedures used, and interesting findings will be tabulated and shown.

**DOSIMETRY OF SEVERAL DTPA RADIOPHARMACEUTICALS IN CISTERNOGRAPHY.** Valerie A. Brookeman, Richard L. Morin and Lawrence T. Fitzgerald. University of Florida College of Medicine and VA Hospital, Gainesville, Fla.

Following intrathecal administration of  $^{169}\text{Yb}$ -DTPA to nine patients, spinal counts were obtained from 2 to 48 hours with a gamma camera/computer system. Utilizing computer outputs the length of the spine was divided into 6 equal segments. The counts in each segment at each time were corrected for surrounding blood background and converted to percent of administered activity by reference to a standard. Cumulated activity in each segment was determined by graphic integration of mean activity-time curves. Absorbed radiation doses were computed for cylindrical geometry utilizing appropriate reduction coefficients for the dose contribution from electrons. Maximum doses to the surfaces of the cord and nerve roots are  $31 \pm 18$  and  $46 \pm 20$  rads respectively, for 1 mCi  $^{169}\text{Yb}$ -DTPA administered. By 0.01 cm depth, the thickness of the pia, these doses decrease to the average values of  $5 \pm 3$  and  $8 \pm 3$  rads respectively. Surface and average doses to the cord and nerve roots from intrathecal administration of 0.4 mCi  $^{169}\text{Yb}$ -DTPA are about the same as those from 0.1 mCi  $^{131}\text{I}$ -IHSA. Electron dose reduction coefficients for cylindrical geometry were computed for 5 other radionuclides which also may be easily chelated:  $^{99\text{m}}\text{Tc}$ ,  $^{113\text{m}}\text{In}$ ,  $^{111}\text{In}$ ,  $^{67}\text{Ga}$ ,  $^{51}\text{Cr}$ . Absorbed radiation doses at various depths within the spinal cord and nerve roots were calculated, utilizing the biological distribution and clearance data obtained with  $^{169}\text{Yb}$ -DTPA. Doses decrease rapidly with distance from the cord surface and by about 0.01 cm reach their average values of about 0.2, 0.2, 2.5, 1.4 and 0.7 rads respectively, for 1 mCi of the DTPA radiopharmaceutical administered.

**COMPARISON BETWEEN BONE MARROW SCANS AND BIOPSIES.** D.W. Brown, M.H. Block, S.F. Wallner, J.W. Backhaus and T.W. Ryerson. Denver Veterans Administration and University of Colorado Medical Center, Denver, CO

Intravenously administered radioactive colloids are deposited in the reticuloendothelial system (RES) and in bone, this distribution generally corresponds to the presence of erythropoietic marrow (EM). Many authors have used colloidal RES scans clinically to assess changes in EM distribution. Nelp (1970), Van Dyke (1967) and others, however, have noted discrepancies between functioning RES and EM distributions in patients suffering from hematologic disorders. More recently, Lillien (1973) and others have suggested that intravenous ionic indium is transferred into the marrow reticulocytes and suggest that bone marrow images obtained with this material should reflect more faithfully the true EM distribution. We have performed iliac and trochanteric biopsies in 27 patients and compared these with  $^{99\text{m}}\text{Tc}$  sulfur colloid bone marrow scans in 8 of these patients,  $^{113\text{m}}\text{In}$  colloid scans in 11 and 24 hour ionic  $^{111}\text{In}$  marrow scans in 8. All of these patients suffered from hematologic disorders including various types of leukemia, aplastic anemia, thrombocyto-

penia and polycythemia vera. The presence or absence of EM shown by biopsy at these sites and on scanning was compared. Correlation was surprisingly poor in the colloid scans, primarily in the greater trochanters. RES uptake was present in the absence of EM in 4 trochanters and absent in 3 trochanters with increased EM. In the first 8 ionic indium patients, one patient showed only myelofibrosis in his trochanter and a patient with chronic lymphocytic leukemia (CLL) had no myeloid but 70% lymph tissue and 30% fat in his trochanter. Each showed extensive RES uptake in the trochanter area. Another patient with CLL had no trochanteric RES uptake but his biopsy contained 70-80% lymph tissue, the rest scattered myeloid cells.

A METHOD FOR THE PREPARATION OF A  $^{99m}\text{Tc}$ -HEMATOPORPHYRIN DERIVATIVE AND ITS TISSUE DISTRIBUTION PATTERNS. Andrea D. Browne and Henry N. Wellman. Indiana University Medical Center, Indianapolis, Ind.

Selective localization of the acetic acid-sulfuric acid derivative of hematoporphyrin (Hp-d) has been demonstrated in a variety of neoplasms by Hp-d fluorescence when activated by light of approximately 4,000 Å. The practical usefulness of this method has been limited by physical factors and the necessity for destructive testing.

To overcome some of the difficulties associated with the fluorescent detection techniques, a  $^{99m}\text{Tc}$  labeled Hp-d has been prepared. Electrolysis is effected in 60 seconds (1.5 Coul) with 1.5 ml of Hp-d using a tin anode and platinum cathode. Addition of  $\text{Na}^{99m}\text{TcO}_4$  (0.9% saline) after electrode removal results in labeled Hp-d of 98% radiochemical purity by chromatography (0.9% saline developer). Activity corresponds with fluorescence and the minimal free pertechnetate band is easily discerned. Precipitation tests have also indicated that  $^{99m}\text{Tc}$  is bound to the Hp-d molecule *in vitro*. Decrease in tag was demonstrated following treatment of the preparation with a dilute  $\text{H}_2\text{O}_2$  solution. *In vitro* stability is at least five hours. Normal animal distribution studies in the rat and rabbit indicate *in vivo* stability. Uptake is imaged mainly throughout the reticuloendothelial system and kidneys. Studies of localization patterns in a variety of tumor bearing animals, especially those with lymphosarcomas, are under way and will be reported.

ISOTOPE DISTRIBUTION RECONSTRUCTION FROM MULTIPLE GAMMA CAMERA VIEWS. Thomas F. Budinger, Grant T. Gullberg, James McRae, Hal O. Anger. Donner Laboratory, University of California, Berkeley, Calif.

Digital reconstruction of the distribution of isotope in patients has been made using gamma camera images taken at multiple angles. Of 13 algorithms investigated we chose 4 methods for patient and phantom comparative studies: back projection, SIRT, iterative least squares, and Fourier techniques including back projection of filtered projections. Back projection is transverse section scanning and filtered back projection techniques are attempts to deconvolute the true image from its convolution with  $1/r$ . Iterative techniques such as SIRT, least squares, and the EMI algorithm involve solving for the best estimate in a pixel A of the transverse section by minimizing the difference between the measured ray sum  $R_k(\theta)$  and the estimated projection  $R_k(\theta)$ . For our technique, after iteration n:

$$A^{n+1} = A^n + \frac{[\sum_{\theta} (R_k(\theta) - R_k^n(\theta))^2 / \sigma_k(\theta)^2]}{\sum_{\theta} (f^{\theta} / \sigma_k(\theta))^2}$$

where  $f^{\theta}$  is the attenuation coefficient  $e^{-\mu x}$  and  $\mu x$  is evaluated for each pixel relative to each projection using an algorithm that establishes the boundary of the object after a few initial iterations where  $f^{\theta}$  is given an initial value of 1.0. The patient is positioned before the scintillation camera an hour or more after injection of  $^{99m}\text{TcO}_4$ . The head is fixed by a mouthpiece bite holder. On  $64 \times 64$  frames 50,000 counts are digitized at  $10^6$  increments in 30 sec.

The filtered back projection technique is superior in speed; however, for quantitative results that take into

account both noise and attenuation, our iterative least squares method is appropriate for nuclear medicine quantitative studies. Resolution is 1.25 cm for detection of holes in 20-cm diameter objects.

MYOCARDIAL IMAGING WITH  $^{81}\text{Rb}$ . Thomas F. Budinger, James McRae, Yukio Yano, William G. Myers. Donner Laboratory, University of California, Berkeley, Calif.

For myocardial imaging with the properly collimated camera,  $^{81}\text{Rb}$  has an ideal half-life of 4.6 hrs and abundant photons: 511 keV, 67%; 446 keV, 23.5%; and 190 keV from daughter  $^{81m}\text{Kr}$  ( $T_{1/2} = 13$  sec). The reaction  $^{79}\text{Br}(\text{He}, 2n)^{81}\text{Rb}$  gives good yields of 500  $\mu\text{Ci } \mu\text{A}^{-1} \text{ hr}^{-1}$ , but about 30% contamination by  $^{82m}\text{Rb}$  (777 keV, 83%; and higher energy gammas) make other reactions such as  $^{80}\text{Kr}(d, n)^{81}\text{Rb}$  or  $^{85}\text{Rb}(p, 5n)^{81}\text{Sr} \rightarrow ^{81}\text{Rb}$  desirable if yields are reasonable.

From 3 to 6 mCi were injected I.V. into 12 patients. Five views (LPO, LA, LAO, AP, RAO) of 3-min duration with 300,000 counts were taken with a pinhole collimator having a platinum insert of 8-mm aperture. Studies included 190 keV vs. 440-511 keV energy windows; gated images of end systole and end diastole; regional sequential changes in isotope uptake and disappearance; and comparison to  $^{123}\text{Cs}$  and  $^{43}\text{K}$ . Seven patients with symptoms of angina pectoris had demonstrable lateral and inferior wall defects. One patient with 3 hospitalizations for presumptive myocardial infarction had normal uptake. Coronary angiogram in this patient was normal, and the final diagnosis was upper G.I. disease. Images with the window at 446-524 were better than at 190 keV. Gating shows myocardial movement different than expected from change in intercavity volume. Anterior and LPO views show significant amplitude of base rather than apex silhouette change. Sequential whole-body quantitative scans show initial distribution and redistribution similar to potassium. The whole-body dose is 100 mrad/mCi for pure  $^{81}\text{Rb}$  and about 200 mrad/mCi if contaminations from  $^{82m}\text{Rb}$  and  $^{83}\text{Rb}$  are included. Target-to-non-target ratios of 2:1 for the heart images require the good statistics obtainable with  $^{81}\text{Rb}$ , which can be given in amounts 6-10 times that of  $^{43}\text{K}$  and  $^{123}\text{Cs}$ . The limitation is the need for better high energy collimation than is generally available.

EVALUATION OF A NEW LYOPHILIZED  $^{99m}\text{Tc}$ -PYROPHOSPHATE KIT FOR SKELETAL IMAGING. J. A. Burdine, N. Anderton, J. Soin, and M. Calderon. Baylor College of Medicine, Houston, Tex.

$^{99m}\text{Tc}$ -labeled polyphosphates for skeletal imaging have demonstrated considerable instability both *in vitro* and *in vivo*, producing inconsistencies in labeling efficiency and image quality. This report summarizes an evaluation of  $^{99m}\text{Tc}$ -stannous pyrophosphate (PyP) which offers improved stability and easy labeling with an average of 99% efficiency.

In clinical trials, 253 patients referred for skeletal imaging received 10 mCi intravenously (5-10 mg PyP complex) with no cardiovascular, respiratory, central nervous system or other changes noted. In 15 patients monitored before and 24-48 hr after injection, no significant differences were found in CBC, alkaline phosphatase, SGPT, total bilirubin, BUN, creatinine, or urinalysis.

To investigate comparable clinical efficacy, 20 patients were scanned with  $^{85}\text{Sr}$  in addition to PyP. Fourteen of the 20 had abnormal PyP scans with 50 abnormal areas noted. Fifteen had abnormal strontium scans with a total of 32 abnormal areas. However, two of the abnormal strontium scans proved to be false positives due to gastrointestinal retention of activity. In addition, one normal strontium scan was a false negative. Overall lesion-to-bone contrast was judged to be good in 85% of the PyP scans, and 62% of the strontium scans. These results suggest that  $^{99m}\text{Tc}$ -PyP should prove to be an effective new agent for skeletal imaging.

<sup>67</sup> GA CITRATE IN CANCER DIAGNOSIS. L. Calderola, P. G. De Filippi, R. Polloni, and F. Badellino. Istituto di Oncologia, Torino, Italia

The reliability, significance and repeatability of diagnosis with i.v. 2.5 mC <sup>67</sup>Ga citrate were assessed 48-120 h after injection with a linear scanner and occasionally with a scintillation camera in 403 patients (313 with tumours).

Repeated enema and vesical catheterisation were used in examination of abdominal structures.

The window included the first three energy peaks and discarded the 4th (< 10% emitted energy). Calibration were naturally varied to fit patients with recent histories of radioisotope examination.

A 90% (lung diseases) and an approximately 84% fit with the intraoperative or autopic findings (lymph node and bone) were observed.

Results were also good (60% though on a limited series) in thyroid and G.E. cancer, but disappointing for the breast and the male and female G.U. apparatus.

Repeated examinations proved of value in the prognosis of spread by the primary tumour and metastases.

Uptake intensity also offered an indirect criterion for assessing the stage of the disease and the effectiveness of treatment.

**RESULTS WITH INTRA-ARTERIAL INJECTION OF RADIOACTIVE MICROSPHERES IN 21 ADVANCED TONGUE CANCERS.** Leonardo Calderola and Fausto Badellino. Istituto di Oncologia, Torino, Italia.

A series of 10 previously untreated and 11 recurrent cases of advanced (T3, T4) cancer of the tongue were treated by intra-arterial injection of 2.5-12 mC <sup>32</sup>P on 8-12,000 resin microspheres (diameter 30μ ± 5) over the period 1963-70. Site doses of 15-20,000 rads were delivered.

Tumour sites were 8/10 and 2/10 and 5/11 and 6/11 in the anterior two thirds and posterior one-third of the tongue respectively. Regional nodes were palpable (N0) in only 2 cases. 14/21 patients were subjected to neck dissection. Lymph node metastases were found in 4 and 6 patients respectively in the two groups.

10/10 and 6/11 regressions with mean durations of 19.9 and 4 months respectively were observed.

Mean survival in the 1st group was 2.3 yr and 2 patients are still alive after 5 and 8 yr.

Overall survival in the 2nd group was 8.5 months (10.6 months in the 6 cases where regression was obtained).

**THE LEFT UPPER ABDOMEN IN CHILDREN.**

Marcos Calderon and John A. Burdine. Baylor College of Medicine, Houston, Tex.

Space occupying lesions in the left upper abdomen occur as a result of certain pediatric diseases and trauma. Palpation is a simple, direct technique for evaluation, but has a low order of sensitivity and specificity. Plain abdominal radiographs and gastrointestinal series may provide indirect information of gross changes. Selective celiac angiography constitutes the only non-nuclear technique which may demonstrate considerable architectural detail of the liver and spleen, but this procedure is not universally available and has a known incidence of serious complications.

We have utilized several radiopharmaceuticals labeled with <sup>99m</sup>Tc and a scintillation camera to study such abdominal masses, and have found the information provided very helpful. Mass lesions of the left hepatic lobe and spleen can usually be differentiated, and displacement of the liver and spleen by renal masses may be determined. The static image pattern plus assessment of lesion vascularity with a sequential blood pool study in some instances may lead to a specific or near specific diagnosis. In the frequent case of abdominal trauma in our children's hospital, imaging of the spleen has proven to be invaluable, saving wasted hours of observation and appropriately directing surgical intervention.

We anticipate increased utilization of such techniques because of the unique and accurate information which they provide, and because of their simplicity and virtual absence of complications.

**RADIOMETRIC DETECTION OF M. TUBERCULOSIS AND M. LEPRAE-MURTIUM.** Edwalo E. Camargo, Steven M. Larson, Byron S. Tepper, Patricia Charache and Henry N. Wagner, Jr. Johns Hopkins Medical Institutions, Baltimore, Maryland.

Laboratory identification and study of important human pathogens of genus Mycobacterium is difficult because mycobacteria are slow growing, fastidious organisms. We have developed a radiometric technique based on the use of ionization chamber to measure the <sup>14</sup>C<sup>14</sup>O<sub>2</sub> produced by the bacterial metabolism of <sup>14</sup>C-substrates. We found that 5 ml. of liquid Middlebrook 7H9 (ADC additive), containing two microcuries of <sup>14</sup>C-acetate or <sup>14</sup>C-glycerol permitted detection of significant bacterial metabolism of M. tuberculosis within 18 hours (10<sup>6</sup> organisms inoculum). M. lepraemurium was also studied as a model for M. leprae (leprosy). 7x10<sup>7</sup> M. lepraemurium (Hawaiian strain), produced readily detectable <sup>14</sup>C<sup>14</sup>O<sub>2</sub> when inoculated into 10 ml. of a simple buffer medium (K-36) or a complex nutrient medium (NC-5). The (K-36) medium supported metabolism of M. lepraemurium for only 7 days with subsequent decline to undetectable <sup>14</sup>C<sup>14</sup>O<sub>2</sub> production by 27 days. The NC-5 medium with <sup>14</sup>C-acetate or with <sup>14</sup>C-glycerol allowed continued <sup>14</sup>C<sup>14</sup>O<sub>2</sub> production at peak levels until 20 days or 50 days, respectively. Although M. lepraemurium does not divide in these media, we have shown that it is metabolically active. In both media, about 7 days were required for the organisms to achieve peak metabolic activity. The metabolisms of M. tuberculosis and M. lepraemurium are similar in that <sup>14</sup>C-glycerol and <sup>14</sup>C-acetate are metabolized to <sup>14</sup>C<sup>14</sup>O<sub>2</sub> more rapidly than <sup>14</sup>C-glucose. The rate of metabolism for M. lepraemurium is much slower than for M. tuberculosis. The radiometric technique shows promise as a rapid and efficient system for detecting and determining drug sensitivities of M. tuberculosis and M. lepraemurium.

**A STUDY OF HGH SOLID PHASE RADIOIMMUNOASSAY.** Gino Cappelli, Franco Grandonico, Alessandro Brocchi. Nuclear Medicine Centre, Florence University, Italy.

Authors have tested antiserum characteristics and selected the best working dilution (1:32x10<sup>-7</sup>). They have determined which polystyrene tubes give the best results. They have demonstrated that the antiserum/tubes binding is fast even if not instantaneous, and it barely depends on temperature, achieving the maximum in 4h. at 4 as at 37C°; its decrease at 37C° is closely connected to the incubation time increase. Temperature affects antigen antibody binding being higher at 37C° than at 4C° and in 24h. achieves about 80% maximum. Blank check proves a constant value at each cold-antigen concentration. To have a high binding capacity, a recent labeled antigen preparation is important but a purification by gel filtration increases the binding capacity of a previous preparation. It has been proved that the binding capacity in the range 30-5% does not affect the reliability. The check of buffer (pH and molarity), washing solution, etc., has been proved to be important. The binding capacity of antiserum/coated tubes slowly decrease when at -20C°; the tubes may be used at least for 5-6 months. Authors propose a standardized HGH solid phase method according to the above data, and they prove, by comparison with another separation method, a high sensibility, precision, accuracy and repetibility; on these characteristics there is a reduction in time, cost and handling.

**COMPARISON OF COMPUTER AND VISUAL INTERPRETATIONS OF LIVER FLOW STUDIES.** Vicente J. Caride, Mohamed A. Antar, Richard P. Spencer. Sect. Nuclear Medicine (Radiology), Yale Univ. School of Medicine; New Haven, Conn.

To search for quantitative bases for interpreting liver flow studies, 50 consecutive patients had the procedure performed under a gamma camera which was coupled to a magnetic tape system and a minicomputer. Following intravenous injection of Tc-Sulfur colloid, data points were obtained at intervals of 2 seconds. Polaroid films were also pulled at intervals of 4 seconds, after an 8 seconds delay. From the taped data, analysis was carried out over an area on the right lateral portion of the liver and an equal area at the lower part of the heart. The time interval between peak cardiac counts and the crossing of the liver and heart activity curves was determined. When plotted on probability paper, a break occurred at 50 seconds. For the 36 patients on the first part of the line, the mean time for crossing was  $32 \pm 9$  seconds. In the next 13 cases, the crossing time was  $77 \pm 38$  seconds (and in 1 instance, the curves did not cross). The initial slope of rising hepatic activity was used to calculate the half-time for accumulation, from  $A = A_0(1 - \exp -\lambda t)$ . Resultant half-times, plotted on probability paper, showed a break at 30 seconds. For 38 cases on the first part of the line, the value was  $T_{1/2} = 19 \pm 5$  seconds. In the remaining cases it was  $45 \pm 14$  seconds. In 5 of the 50 cases, there was an early peak of activity over the liver (nearly coincident with the aortic flow), detected by the computer data. The early peak was followed by a fall, and then a steady increase in counts. The visual readings of the flow pictures showed agreement with the computer data in 81% of the interpretations. False positives were due mainly to renal activity. Computer aided detection of early flow (not seen in 9% of the visual readings) may be a useful adjunct.

**A RAPID RADIOIMMUNOASSAY FOR TRIIODOTHYRONINE IN UNEXTRACTED SERUM.** Gary W. Carpenter and Andrea S. Blum. University of California, San Francisco Medical Center, San Francisco, CA.

The method of Gharib et al. for the radioimmunoassay of triiodothyronine has been modified from 96 hours at 4°C to an overnight system combining both room and 4°C temperatures with polyethylene glycol precipitation.

Results of the overnight assay, a three day 4°C polyethylene glycol precipitation, and the Gharib method are compared. For this comparison accuracy was determined by recovery of measured amounts of triiodothyronine added to samples and by sample dilution while reproducibility was measured by within and between assay variation of selected samples.

Based on four months of clinical use in a large thyroid practice mean values for euthyroid, hypothyroid, and hyperthyroid states were 145 (S.D. 28), 77 (S.D. 12), and 602 (S.D. 323) nanogram percent respectively.

The assay has proved both accurate and reproducible in its assessment of thyroid status in the patients studied and has the distinct advantage of immediate results.

**THE USE OF I-125 FIBRINOGEN IN THE DIAGNOSIS OF DEEP VEIN THROMBOSIS.** R.F. Carretta, S.J. DeNardo, A.L. Jansholt, G.L. DeNardo, Sacramento Medical Center of the University of California School of Medicine.

The use of I-125 labeled fibrinogen as a screening procedure for deep vein thrombophlebitis in high risk patients has been delayed in the U.S. since the product has not received FDA clearance. We have purified and tested a chemically suitable, biologically active, and safe fibrinogen preparation at Sacramento Medical Center. An ongoing study is presently being conducted to determine the efficacy of this I-125 labeled fibrinogen in the early detection of deep vein thrombosis of the lower extremities, and to determine the biological stability of the labeled fibrinogen. Serial blood samples were drawn to determine disappearance curves and the amount of circulating labeled fibrinogen. Serial serum samples were evaluated for total clottable fibrinogen. At least 90% of the labeled fibrinogen was present in the clot specimen. The remaining 10% was divided between serum pro-

teins and plasma. The stability of the labeled fibrinogen was also examined, and it remained stable over a period of 4-6 days. 50 patients have received I-125 labeled fibrinogen with the following results: 44/50 patients had no clinical evidence of thrombophlebitis in the lower extremities. All 44 patients had negative I-125 fibrinogen studies. 6 of the remaining patients had convincing clinical evidence of unilateral thrombophlebitis. Six patients had positive I-125 fibrinogen tests. 5 of the six abnormalities were confirmed by venography. This preliminary data suggests that the use of labeled fibrinogen as a screening procedure for lower extremity thrombophlebitis is both feasible and clinically useful.

**STUDIES OF RENAL UPTAKE KINETICS OF TRIIODOTHYRONINE (T<sub>3</sub>) IN MAN USING A SCINTILLATION CAMERA.** Ralph R. Cavalieri, Charles Moser, Peter Martin, and Victor Perez-Mendez. VA Hospital and University of California, San Francisco, Cal.

T<sub>3</sub>, the more important of the thyroid hormones, is largely intracellular in distribution. Animal studies show high T<sub>3</sub> concentration in liver and kidneys. We have devised a method to quantitate the kinetics of renal uptake of T<sub>3</sub> in man using a scintillation camera and computer. Following a localizing dose of <sup>99m</sup>Tc-Kidney Scintigraphin (MPI), an iv infusion of <sup>131</sup>I-T<sub>3</sub> is given at rates calculated to maintain a constant plasma level of <sup>131</sup>I for 60 to 90 min. A posterior camera view of the left kidney is obtained during the infusion. Digitized data within selected areas-of-interest (AOI) are collected from tape playback. Cpm within the AOI over the entire kidney minus cpm within an equal AOI over a nearby background region yields an activity-time curve, Rnet(t), describing the equilibration of <sup>131</sup>I-T<sub>3</sub> between plasma and kidney and approximated by the function:

$$R_{net} = A(1 - e^{-kt}) + C$$

where A+C = the final asymptotic value approached by Rnet, C = the time-zero value of Rnet, in cpm, and k = the rate constant of equilibration, in min<sup>-1</sup>. The above function is fit graphically to the observed values of Rnet to obtain estimates of A and k. The extravascular renal T<sub>3</sub> space, V, in ml, = A/P x F, where P = the plasma concentration of <sup>131</sup>I-T<sub>3</sub>, in cpm/ml (a constant), and F = a calibration factor determined from phantom measurements at the proper skin-kidney distance for each subject. Unidirectional plasma-to-kidney T<sub>3</sub> clearance, Cl, in ml/min, is given by V x k. Six subjects with normal renal function and various thyroid states have been studied to-date. V varied from 110 to 360 ml, and Cl ranged from 4 to 37 ml/min (per kidney), correlating well with thyroid functional status. These results are probably the first quantitative data in humans on renal uptake of T<sub>3</sub>.

**A COMPARATIVE STUDY OF CONTRAST DACRYOCYSTOGRAM (DCG) AND NUCLEAR DCG.** Tapan K. Chaudhuri, Gerald R. Saporoff, Kenneth D. Dolan, and Tuhin K. Chaudhuri. University of Iowa Hospital, Iowa City, Iowa.

The purpose of this paper is to present a comparative study of conventional radiographic contrast DCG and radioisotope scanning of the lacrimal drainage system (henceforth called "Nuclear DCG"). A total of 17 contrast DCG and 24 nuclear DCG were performed in 12 patients. About 200 µCi of Tc-<sup>99m</sup>-pertechnetate in 0.01-0.05 ml sterile normal saline vehicle was used as eye drop followed by sequential scanning using a modified pinhole collimator which resulted in excellent resolution of canaliculi, sac and the nasolacrimal duct. Eleven studies demonstrated obstruction in the lacrimal drainage system in both contrast DCG and nuclear DCG. Three studies were normal in both techniques. Of two patients who had dacryocystorhinostomy (DCR), one demonstrated patency of DCR and the other revealed unsuccessful operation by isotope study which fitted well with fluorescein dye test. Two studies were normal in contrast DCG but abnormal in nuclear DCG. The reason for this discrepancy is that x-ray DCG is performed under manual injection pressure while the nuclear DCG is a physiological study mimicking normal state of tear drainage. With contrast DCG, normal and extreme pathological obstruction can be demonstrated. However, in functional block (e.g., abnormal "lacrimal pump" or partial stenosis of duct) where the system irrigates freely, the nuclear DCG would be abnormal whereas the contrast DCG would be normal. We, therefore, feel nu-

clear DCG is superior to contrast DCG because (a) atraumatic procedure, (b) better diagnosis of functional block, and (c) smaller radiation dose to the lens. DCR is indicated if the system does not irrigate and nuclear DCG shows evidence of obstruction. In conclusion, nuclear DCG should be a routine screening procedure to evaluate suspected lacrimial block. A postoperative nuclear DCG would also be a valuable tool in assessing the success of DCR.

**MEASUREMENT OF GASTRIC EMPTYING TIME (GET) OF SOLID MEAL USING  $^{99m}\text{Tc}$ -DTPA.** Tapan K. Chaudhuri, Robert C. Heading, Alan Greenwald, and Tuhin K. Chaudhuri. University of Iowa Hospitals, Iowa City, Iowa.

The purpose of this study is to test the suitability of  $^{99m}\text{Tc}$ -DTPA for use as an agent for determining GET of a solid meal and to determine the normal gastric emptying  $T_{1/2}$  value for a solid meal. In addition to its property of being nonabsorbable and nonadsorbable to the gastric mucosa, Tc-DTPA also has the property of fair adsorbability to solid meal, particularly corn flakes. This property was revealed by in vitro studies involving centrifugation of a mixture of cornflakes, gastric juice, milk and  $^{99m}\text{Tc}$ -DTPA, and counting the supernatant. Using a standard solid meal of 20 gm corn flakes with 15 gm sugar in 150 ml of milk containing 500 uCi of  $^{99m}\text{Tc}$ -DTPA, GET was determined in 8 normal volunteers each having three studies on three different days. None of the subjects were taking anticholinergic drugs or had undergone previous gastrointestinal surgery. The subjects were fasted overnight. Smoking was forbidden during this period. After consuming the meal (which took about 2 min), the subjects were positioned supine under the gamma camera. Sequential gastric scintiphotos were collected every minute on a magnetic tape (using a PDP-8 computer interfaced with the camera) over a period of 30-60 min. At the end of the study, a dynamic readout of the (integrated count over the flagged gastric area) was obtained. The GET curve was found to be monoexponential at least for the first 60 min. The disappearance half-time of Tc-DTPA from the stomach in this group was found to be 37±5 min. The  $T_{1/2}$  values obtained by previous investigators are 33, 70, 64, and 56 min. This difference may be explained by differences in the technique, meal composition etc. For this reason, each laboratory should set its own normal value using standard technique and then apply the same technique in patients. In conclusion,  $^{99m}\text{Tc}$ -DTPA seems to be a suitable marker for determining GET for solid meal.

**SYNTHESIS OF RADIOIODINATED TETRACYCLINES: EVALUATION AS TUMOR SCANNING AGENTS.** Depew M. Chauncey, Samuel E. Halpern, Naomi P. Alazraki. VA Hospital, San Diego, and University of California, San Diego.

Tetracycline and chlorotetracycline have been labeled with  $^{131}\text{I}$ . Unusually high tagging efficiencies have been obtained by careful control of the temperature and acidity of the reaction medium. The antibiotic was heated at 65° in acidic methanol for 2-3 hours. Upon termination of the reaction, the solution contained less than 15% inorganic iodide. Anion exchange produced a solution containing less than 5% iodide. The stability of the labeled product was determined under conditions applicable to the practical clinical situation. The chemistry and synthetic procedure will be discussed in detail.

The radiopharmaceuticals were evaluated in Buffalo rats which had been implanted with hepatomas in their thighs. Each rat was anesthetized with diethyl ether and the radiopharmaceutical injected intravenously. At varying times post injection, the animals were sacrificed. A blood sample was removed from a cardiac chamber through the chest wall and the heart rapidly excised. The hepatoma was immediately removed and samples taken from various areas of the tumor. A tissue sample was taken from the normal thigh for use as a control. The residual activity in each sample was determined and the appropriate tumor to background ratios were found to vary widely dependent upon the particular radiopharmaceutical and the time post injection at which the animal was sacrificed. The most promising of the iodinated tetracyclines appears to be  $^{131}\text{I}$ -tetracycline. Tumor tissue to normal tissue ratios of 20:1 and greater were found for this compound. Body distribution studies suggest that iodinated tetracyclines may have definite advantages as a tumor scanning agent.

**EFFICACY OF DIANABOL IN OSTEOPOROSIS AS DETERMINED BY CHANGES IN TOTAL BONE MINERAL MASS.** Charles H. Chesnut, III, Wil B. Nelp and John D. Denney. University of Washington Hospitals, Seattle, Washington

To assess the efficacy of Dianabol (methandrostenolone, a synthetic anabolic steroid) in the treatment of osteoporosis, a two year double blind study was performed utilizing 26 post menopausal osteoporotic females - each with radiographically demonstrated compression fractures and/or extensive bone demineralization. Patients were treated with either 5 mgm of Dianabol daily (treated group) or placebo (control group). Drug efficacy was assessed primarily by total body calcium (TBC) determination by neutron activation analysis (NAA), a technique extensively utilized at the University of Washington which essentially measures total bone mineral mass and bone mass change (calcium balance). NAA was performed initially and every six months; regional bone mass measurement (RBM) by photon densitometry was also performed.

Sixteen patients completed the 24 month study - six placebo and ten treated. The six placebo patients over an average 2.23 years lost an average 3.1% of their TBC (range plus 1 - minus 9%), or -26.9 mgm/day of calcium per patient. In contrast the ten Dianabol treated patients increased their TBC an average 2.0% (over an average 2.4 years) (range 0-+8%), or +17.5 mgm/day of calcium per patient. TBC changes in the treated group were significantly different from those in the placebo group, p value < .005. Changes in RBM determinations performed after initiation of therapy showed reasonable correspondence to changes in TBC measurements.

It is concluded that the use of Dianabol in osteoporosis resulted in a significant increase in total bone mineral mass as compared to a control group, an original and potentially valuable finding for the treatment of osteoporosis.

**$^{59}\text{Fe}$ -WHOLE BODY SCANNING.** James H. Christie, Tuhin K. Chaudhuri, Richard L. DeGowin, and James C. Ehrhardt, University of Iowa, Iowa City, Iowa U.S.A.

The goals of this study were to develop an  $^{59}\text{Fe}$  scanning system and to assess the usefulness of sequential erythropoietic marrow scanning as a means of evaluating the distribution and function of hemopoietic tissue in patients with hematological disorders, as well as in patients receiving radiation therapy for the treatment of lymphoma. To that end, a collimator has been built which allows whole body scanning with 10 uCi of  $^{59}\text{Fe}$  using a conventional rectilinear scanner. Modulation transfer function and line spread function of this collimator as well as some other existing collimators have been compared. Statistical fluctuations on the scan are minimized with a large gaussian spot light shaper.

The system is useful for visualizing marrow distribution, assessing hemopoietic function, determining sites of red cell sequestration and evaluating hepatic storage iron deposition. Concomitant clinical, morphologic and ferrokinetic studies confirmed the findings obtained from  $^{59}\text{Fe}$  whole body scanning. This technique distinguishes between focal and generalized hemopoietic insufficiency. Thus, normal, hemolytic anemia, hemochromatosis, myelofibrosis, extramedullary hemopoiesis and ineffective erythropoiesis can be distinguished from each other. Focal ablation of erythropoiesis in the bone marrow following radiation therapy can be easily demonstrated with  $^{59}\text{Fe}$  whole body scanning. Preliminary studies suggest that doses of irradiation commonly employed in the initial treatment of malignant lymphoma may prevent repopulation of bone marrow in radiated areas for at least 8 - 12 months.

**STUDIES USING NITROGEN-13 AMMONIUM AND GLUTAMINE AS TUMOR LOCALIZING AGENTS IN DOGS.** Thomas R. Christie, W. Gordon Monahan, Alan S. Gelbard, Laurence P. Clarke, and John S. Laughlin. Memorial Sloan-Kettering Cancer Center, New York.

Previous studies in mice have suggested that  $^{13}\text{N}$ -labeled ammonium and L-glutamine may be applicable as tumor localizing agents. Spontaneously occurring tumors in dogs provide an excellent model for their further evaluation.



Approximately 10 millicuries of  $^{13}\text{N}$ -ammonium chloride or  $^{13}\text{N}$ -labeled glutamine compounds were given intravenously under sedation but not anesthesia. 15 dogs were evaluated with the ammonium, 9 with glutamine. All dogs had histopathologically confirmed spontaneously occurring neoplasms, 20 of the 24 studies were followed by complete post-mortem examination. 4 mammary adenocarcinomas, 3 lymphosarcomas, 2 osteogenic sarcomas, 1 thyroid carcinoma, 1 thoracic mesothelioma, 1 myosarcoma, 1 rhabdomyosarcoma, 1 colonic adenocarcinoma, and 1 hemangiosarcoma were studied with the ammonium; 3 osteogenic sarcomas, 3 lymphosarcomas, 2 mammary adenocarcinomas, 1 hemangiosarcoma were scanned with glutamine. Both agents showed tumor affinity. Eleven of 15 studies with ammonium had direct correlation between scans and post-mortem or biopsy findings and 8 of the glutamine studies showed significant correlation. Some dogs were scanned with other agents for comparison. These studies support reports that  $^{13}\text{N}$ -labeled ammonium and glutamine may have applications as tumor localizing agents in certain neoplastic tissue types. Glutamine may also have potential applications to predict and monitor the effectiveness of glutaminase therapy.

PREPARATION OF IODINE-123 LABELED ROSE-BENGAL AND ITS DISTRIBUTION IN ANIMALS. Betsy Christy, Gaylord King, and William M. Smoak. Mount Sinai Medical Center, Miami Beach, Florida.

The primary photon energy of 159keV and a thirteen hour half-life with resulting low patient absorbed dose suggest that gamma camera imaging of I-123 radiopharmaceuticals may prove superior to present studies utilizing the available I-131 products. The major deterrents to the use of the I-123 nuclide have been its unavailability in diagnostic quantities for routine use and disagreement over potential image degradation due to the I-124 contaminant.

Hundred millicurie amounts of I-123 as Sodium Iodide with less than 1% of I-124 at E.O.B. (End of Bombardment) have been made available routinely at the Mount Sinai Medical Center Cyclotron using an enriched tellurium target. The separation of iodine and the recovery of the irradiated tellurium are described. With the availability of higher yields of I-123, clinical quantities of high specific activity radiopharmaceuticals were prepared.

A rapid method for the efficient incorporation of I-123 in the Rose Bengal molecule has been developed. The product has a specific activity of 1-2 mCi/mg with less than 3% iodide contamination. I-123 Rose Bengal has been tested in animals and the images obtained vividly demonstrate the benefits in anatomic detail of the liver, biliary tree and gall bladder.

$^{67}\text{Cu}$  AS A LABEL FOR BLEOMYCIN. G. Coates, N. Aspin, P.Y. Wong, and D.E. Wood. Toronto General Hospital and University of Toronto, Toronto, Canada.

Labelled Bleomycin has been proposed as a tumour localizing agent. Radionuclides used as labels include those with poor physical characteristics ( $^{57}\text{Co}$   $T_{1/2}$  270D) or  $^{111}\text{In}$ ,  $^{113}\text{mIn}$  and  $^{99\text{m}}\text{Tc}$  which are unstable in vivo. Since Bleomycin in its natural state contains copper, which is removed in purification, we have studied the use of  $^{67}\text{Cu}$  as a label for Bleomycin. The purpose of this study is to report on the labelling procedure, and the in vitro and in vivo stability of  $^{67}\text{Cu}$ -Bleomycin.

Copper-67 is produced by the reaction  $^{67}\text{Zn}(\text{np})^{67}\text{Cu}$ , and the copper extracted from the zinc by anion exchange column. Two units of bleomycin are dissolved in 1 ml. glycine-buffer pH 3.5 and tracer free  $^{67}\text{Cu}$  is added. Using thin layer, paper and Sephadex G10 column chromatography no free  $^{67}\text{Cu}$  was observed immediately after labelling or after 4 days at 40°C. Copper-67 Bleomycin was incubated with human plasma for 30 minutes at 37°C and the mixture passed through a Sephadex G-25 column. Copper-67 eluted in the bleomycin peak.

The plasma clearance of  $^{67}\text{Cu}$  Bleomycin was compared to that of  $^{111}\text{In}$ -Bleomycin after intravenous injection into 3 dogs. Radioactivity in the liver was monitored using a NaI(Tl) detector. The clearance curves were analysed using a least squares fit program. Plasma clearance of  $^{111}\text{In}$ -Bleomycin is described by a bi-exponential curve with a fast phase  $T_{1/2}$  of 9 minutes, representing 75% of the injected radioactivity and a slow phase  $T_{1/2}$  of 5 hours.  $^{67}\text{Cu}$  Bleomycin clearance is also bi-exponential with a fast  $T_{1/2}$  of 12 minutes representing 75% of the injected radioactivity the slow phase  $T_{1/2}$  is however 60-90 minutes. In this respect  $^{67}\text{Cu}$ -Bleomycin clears in an identical way to  $^{57}\text{Co}$ -bleomycin. No increase in liver activity indicating free copper was detected. We are now determining the organ distribution of  $^{67}\text{Cu}$  Bleomycin in tumour bearing mice.

ABSORBED RADIATION DOSE DUE TO RADIONUCLIDIC IMPURITIES IN Tc-99m OBTAINED BY DIFFERENT PROCEDURES. Lelio G. Colombetti and W. Earl Barnes. Loyola University Stritch School of Medicine, Maywood, Ill., and Veterans Administration Hospital, Hines, Ill.

A comparative study has been made of the radiation dose absorbed by the patient due to radionuclidic impurities present in Tc-99m produced by elution, MEK extraction, sublimation, and cyclotron bombardment.

Concentrations of radionuclidic contaminants were derived from original and published gamma-ray spectrometric measurements made with NaI(Tl) and Ge(Li) detectors. For each impurity the total body radiation dose to the patient was calculated from data in MIRDO publications assuming a homogeneous distribution of the radionuclide in the total body.

As expected, the type and concentration of radionuclidic impurities found in Tc-99m varied widely with the production method. Despite these variations, the radiation dose to patients from impurities relative to that of Tc-99m was comparable for elution, MEK extraction, and sublimation: elution (0.2%), MEK extraction (0.35%), sublimation (0.1%). In the case of Tc-99m produced in the cyclotron by the proton bombardment of Mo-100, the extraneous radiation dose due to impurities was 27% that due to Tc-99m using 97% isotopically enriched Mo-100 target material. The use of a Mo-100 target isotopically enriched to over 99% would achieve a higher purity product and a greatly reduced radiation dose.

PULMONARY PERFUSION DISTRIBUTION IN TRANSPOSITION OF THE GREAT ARTERIES. James J. Conway and Alexander J. Muster. The Children's Memorial Hospital, Chicago, Illinois.

Certain congenital cardiac abnormalities may have an abnormal pulmonary perfusion distribution. Those conditions implicated include tetralogy of Fallot and valvular pulmonic stenosis. In valvular pulmonic stenosis there is a preferential distribution of blood flow to the left lung.

Pulmonary perfusion distribution has been calculated in 41 children with transposition of the great arteries using  $^{99\text{m}}\text{Tc}$  human albumin microspheres. In 52% of the studies, the distribution has been "normal". In 32% of the studies, there has been an abnormal preferential distribution to the right lung. The degree of perfusion abnormality has been graded, i.e. marked (82/18), moderate (62/38), "normal" (55/45), and reverse (50/50). The etiology for the abnormal preferential distribution to the right lung has been investigated and is thought to be due primarily to the angulation of the pulmonary artery as it arises from the "left ventricle".

Compensatory circulation to the left lung has been observed via the bronchiolar circulation which can be estimated by comparing a peripheral with a ventricular injection since the ventricular injection measures the true pulmonary distribution and the peripheral injection includes the bronchiolar contribution.

**RADIONUCLIDE DIFFERENTIATION OF A UNILATERAL FLANK MASS IN THE NEWBORN PERIOD.** James J. Conway, Susan Luck, R. Bruce Filmer, and A. Barry Belman. The Children's Memorial Hospital, Chicago, Ill.

The most common renal mass lesions presenting in the newborn period are; 1.) multicystic kidney; 2.) hydronephrosis; 3.) renal vein thrombosis; and 4.) renal hamartoma. The more frequent lesions, multicystic kidney and hydronephrosis, usually present as an incidental flank mass. Both may appear avascular during the total body opacification phase of intravenous urography. Some function may be observed on delayed roentgenograms in hydronephrosis but not always. In every instance of multicystic kidney (11) and hydronephrosis (7), the lesion has appeared avascular during the early phase of radionuclide angiography. Significant function on delayed studies with  $^{131}\text{I}$  Hippuran has been observed with hydronephrosis but not with multicystic kidney. In five instances, the removed multicystic kidney had radioactivity within the cystic fluid but this "function" has not been adequate to visualize during imaging.

Neonatal renal hamartoma is an uncommon lesion which appears vascular during radionuclide angiography but generally does not function with  $^{131}\text{I}$  Hippuran.

Radionuclide studies with  $^{99\text{m}}\text{Tc}$  DTPA and  $^{131}\text{I}$  Hippuran allows an innocuous accurate differentiation between these entities.

**THE HOLE IN THE HEAD: AN ARTIFACT OF EARLY BRAIN IMAGING.** James J. Conway. The Children's Memorial Hospital, Chicago, Ill.

Posterior brain images recorded in the supine position immediately following radionuclide angiography will occasionally demonstrate an "avascular" area or areas just above the transverse sinuses. The possibility of a cystic lesion in the posterior aspect of the cerebrum was initially considered but a "lesion" was not verified. Subsequently, it has been seen in at least twelve other patients.

It was thought to be due to decreased perfusion in that portion of the scalp pressing against the camera collimator. This was proved during two studies of "brain death" where there was documented absence of cerebral circulation. The hole in the head phenomenon was pronounced since the only circulation recorded was from external carotid perfusion of the scalp. Images recorded immediately after lifting the head several mm. from the collimator resulted in disappearance of the artifact as circulation was restored to the compressed area of the scalp.

Awareness of this artifact may prevent consternation in the interpretation of brain images.

**MULTIORGAN STUDY USING PLURIRADIOPHARMACEUTICAL LABELS.** P. Czerniak and T.S. Zwas. Baruk Institute, Tel Hashomer, Israel.

Multiorgan study is developed because of the necessity 1) To diagnose interorgan - space conditions (phrenic, mediastinal); 2) To individualize superposed or adjoining organs (liver - spleen, skull - brain); 3) To obtain a simultaneous survey of several organs; 4) To shorten the time and to reduce the exposure while more than 1 organ (system) should be examined.

The realization is possible by: 1) Exploitation of chronological and spatial changes in localizations of a given radionuclide ( $^{99\text{m}}\text{TcO}_4^-$ ,

$\text{K}^*\text{I}$ ); 2) Use of various pharmaceuticals labelled with the same radionuclide ( $\text{TcO}_4^-$ ,  $\text{Na}_2\text{H}$ ,  $^*\text{Tc DP}$ ,  $^*\text{Tc FeAA}$ ,  $^*\text{Tc MAA}$ ). 3) Simultaneous or sequential administration of more than one radiopharmaceutical with various radiation energy and for different target organs.

The performance of such studies is achieved by rectilinear, dual or total body scanners and scintiscanners. Three technical requirements should be observed: 1) Notification of anatomic-topographic points on the body and on the scintigraphic images; 2) Administration of adequately calculated doses (to avoid overexposure of one organ towards the other). 3) Establishment of physiological sequence of organ visualization.

Several combinations were performed: Diagnosis of space occupying lesions in the right or left sub or overdiaphragmatic region; Pericardo-cardio-pulmonary and mediastinal conditions established by a combined multiorgan simultaneous and sequential visualization; skeletal and soft tissue lesions. More than 10 cases in each of the 6 clinical and laboratory combinations were collected. The analysis of the cases shows the diagnostic importance of this approach.

**RADIONUCLIDE ANATOMY.** Pinchas Czerniak and Hilel Nathan. Dept. of Nuclear Medicine and Dept. of Anatomy, Tel-Aviv University, Faculty of Medicine, Sheba Medical Center, Israel.

The study of Post Mortem anatomy (PMA) is hindered by ethic or religious reasons. The developed underground, lawless or law-abiding PM dissections, sculptural, comparative, archaic, museal, embalment, experimental, filogenetic, artistical, dye-injection anatomy are unable to provide all the necessary anatomical information.

Anatomical patterns are different in livings than in corpses. The physicians treat patients of all ages, both sexes of various ethnic groups and the in vivo anatomy (IVA) is important for them with consideration of five parameters: morphology, topography and their functional, ethnographic and developmental normal variants.

IVA started with the condemned vivisection. Practised physical examination of patients, surgical and experimental anatomy constitute efficient partial IVA studies. A progress is achieved by X,  $\gamma$ -ray visualization of organs and systems. 25 years ago the roentgen anatomy began. We started 4 years ago with teaching radioisotope anatomy. The gammas of selective radiopharmaceuticals, localized in 18 organs and 4 systems, exhibit their morphology - topography and functional, ethnic and developmental normal chronological or structural variations (a total of 5 anatomical parameters).

We examined in 21,000 patients by scintiscintigraphic methods 23,500 organs and systems. 18% or 4,140 of them were normal (2,500 thyroids, 990 livers, 90 stomachs, 120 kidneys, 30 subarachnoidal spaces, 40 biliary systems etc.). The five parameters were examined and presented to the students.

Research work is engaged in finding adequate radiopharmaceuticals and methods for IVA of more organs and systems.

**TECHNETIUM  $^{99\text{m}}$  POLYPHOSPHATE BONE IMAGING IN LEGG-PERTHES DISEASE.** James A. Danigelis, Robert L. Fisher, and Maer B. Ozonoff. Newington Children's Hospital, Newington, Connecticut.

This investigation was undertaken to compare the diagnostic usefulness of radionuclide bone imaging techniques to standard radiographic methods in the study of Legg-Perthes disease. Pinhole images of satisfactory diagnostic quality were obtained of both hips in the anteroposterior

and frog lateral positions. Twenty-five patients with Legg-Perthes disease and seven others simulating it were studied.

In all Legg-Perthes patients a radionuclide uptake deficiency was observed in the proximal femoral epiphysis which we believe is related to impaired blood supply. During later disease stages reparative radionuclide activity was observed in most patients at the margins of the uptake defect. Neither size of uptake epiphyseal defect nor extent of reparative process could be accurately predicted from radiographic appearance. There were no false negative bone image findings in the seven non-Legg-Perthes cases.

Our image studies correlate well with published histopathological investigations, indicating to us that assessment of extent of pathological involvement and disease course is facilitated by this technique. Preliminary experience suggests Tc-polyphosphate bone imaging has useful clinical application in Legg-Perthes disease.

**PHARMACOKINETIC STUDIES OF RADIOIODINE LABELED ORGANIC MERCURIALS.** Harold Deckart, Hermann Herzmann, Annemarie Blottner, Horst Flentje and Klaus-Dieter Schwartz. Klinikum Berlin-Buch (GDR) and Academy of Science of GDR, Berlin-Buch and Bezirkskrankenhaus Schwerin, GDR.

Pharmacokinetic studies on  $^{131}\text{I}$ - and/or  $^{203}\text{Hg}$  labeled benzoic acid and benzene-sulphonic acid derivatives have been performed in comparison with  $^{203}\text{Hg}$ -Mersalyl with the aim to develop new radiopharmaceuticals for static kidney scintigraphy.

Because of their high affinity for the kidneys organic mercury compounds are used as radiopharmaceuticals for static kidney and brain scintigraphy. The disadvantages of such compounds are limited storage and low gamma-energy in the case of  $^{197}\text{Hg}$ -compounds, a high radiation dose in the case of  $^{203}\text{Hg}$ . The kinetic behaviour of these mercury compounds is preserved when they are labeled with radioiodine. The similar chemical and pharmacological behaviour of compounds containing stable mercury and radioiodine makes it possible to label mercury compounds with the more advantageous radioisotopes of iodine.

Examples of such benzoic acid and benzene-sulphonic acid derivatives are discussed:  $^{203}\text{Hg}$ -3-chlormercuri-4-hydroxy-5-iodine-benzoic acid,  $^{131}\text{I}$ -3-chlormercuri-4-hydroxy-5-iodine-benzoic acid, 3- $^{131}\text{I}$ -4-hydroxy-benzoic acid,  $^{203}\text{Hg}$ -3-chlormercuri-4-hydroxy-benzoic acid. In the same manner four benzene-sulphonic acid compounds were labeled and their kinetic properties were examined.

It is shown that the absence of mercury in the aromatic ring leads to changed kinetic behaviour. It is also shown that an affinity for the kidneys results not only, as in the already known aliphatic mercury compounds (chlormerdrin, mersalyl for example), from an aminopropyl-mercury group but also from a chlor-mercury group in the aromatic ring. Even in these radiopharmaceuticals we observed a partial in vivo instability of the mercury bound.

**COMPETITIVE RADIOMETRIC ENZYMATIC ANALYSIS OF OXALIC ACID IN URINE AND PLASMA,** Frank H. DeLand and Robert Tilden, Veterans Administration Hospital, Gainesville, Florida.

Unlike previous enzymatic analysis of oxalic acid, this procedure takes advantage of competitive inhibition under conditions of saturation kinetics. Oxalic acid competes with  $^{14}\text{C}$ -labeled oxalic acid for a limited number of available sites on a saturated decarboxylase enzyme. The  $^{14}\text{CO}_2$  released is thereby inversely related to known concentrations of oxalic acid. Quantitation is achieved by means of a calibration curve. Evolution of  $\text{CO}_2$  gas is favored by a buffered pH 3.0 medium. The enzyme, oxalic

acid decarboxylase (derived from *Collybia velutipes*) is stable and stoichiometrically reactive under these same conditions. Both liquid scintillation spectroscopy, and gas ionization have been adapted for quantitation of  $^{14}\text{CO}_2$ . Oxalic acid concentrations in both plasma and urine have been determined with this methodology. Plasma has been analysed directly for oxalic acid with appropriate controls and internal standards for validation. Oxalic acid is removed from urine by calcium precipitation prior to analysis. Recovery of oxalic acid standards has been found to be 100% in water and 90-95% in urine. Specificity and technical simplicity of this radiometric method for quantitating oxalic acid make it useful for both screening and routine analysis. Cost of the procedure is appreciably less than the standard chemical analysis which requires two days to complete.

**DIAGNOSTIC CRITERIA IN CISTERNOGRAPHY.** Frank H. DeLand, University of Florida and Veterans Administration Hospital, Gainesville, Florida.

In the evaluation of cerebral atrophy, NPH, and probability of results from shunting procedures interpretations of cisternograms have been generally based on arbitrarily defined patterns which has left in doubt a large indecisive grey zone. The purpose of this study was: (1) correlate abnormal CSF circulatory patterns with known physiologic principles and inferred applications of these principles, (2) compare cisternograms with results of shunting procedures, and (3) define abnormal cisternograms in terms of circulation, physiology, and clinical evidence. Factors affecting CSF circulation, i.e., transport and dialysis, spatial differentials in CSF pressure, and temporal factors in transmitted pressure pulses were defined in terms of normal and abnormal patterns. Fluid pressure and anatomy were correlated with radionuclide penetration of lateral ventricles. The abnormal physiology found in atrophy and NPH was correlated with changes in CSF flow rates, distribution of radionuclides, penetration of ventricles, and status of compensatory absorption. On the basis of this data, four categories of cisternographic interpretation were defined: (1) atrophy, primary or final stage of NPH, (2) well compensated NPH, (3) partially NPH, and (4) non-compensated NPH. Forty-seven patients who had had CSF shunts were analyzed for: (1) CSF flow as indicated by cisternography, (2) clinical history, and (3) results of shunting. The cisternograms could not be primarily classified in the categories as defined. The temporal relationship in the clinical history was found to be the final factor in determining the category of the cisternogram. The combination of the cisternogram and history correlated well with the results of shunting.

**RADIOMETRIC XYLOSE TOLERANCE TEST.** Frank H. DeLand, University of Florida and Veterans Administration Hospital, Gainesville, Florida.

The xylose tolerance test estimates the absorption of pentose by the small intestine after oral ingestion. Approximately 25% to 40% of the d-xylose is excreted in the urine, 50% to 20% is expired as  $\text{CO}_2$ , and the remainder enters metabolic cycles, particularly in the liver. We have developed a radiometric procedure that measures the excretion of  $^{14}\text{C}$ -u-d-xylose after oral absorption. The patient ingests 20  $\mu\text{Ci}$  of uniformly labeled carbon-14 d-xylose in 500 ml of water. Urine is collected and pooled for 5 hours and total urine volume is measured. A 10 ml aliquot of urine adjusted to pH 7 is added to 10 ml of TSB culture media in a vial designed for use in the Bactec instrument. One ml of  $10^8$  concentration of *E. coli* ATCC 25922 is added to the vial. The culture is placed in the instrument and the atmosphere over the culture is sampled hourly for the decarboxylation of  $^{14}\text{CO}_2$  and measured in an ion chamber. The amount of  $^{14}\text{CO}_2$  detected in the specimens is compared to control cultures with serial quantities of  $^{14}\text{C}$ -u-d-xylose added. The relationship between the urine content of  $^{14}\text{C}$ -u-xylose and the  $^{14}\text{CO}_2$  detected in the ion chamber is linear. Since the pH of urine may vary commonly from 5.0 to 7.5, the affect of pH on decarboxylation was evaluated. Slightly greater decarboxylation was found with acidic urines. However a standard pH of 7 for the culture media was established with appropriate buffers. Results

in patients of the decarboxylation technique with the standard spectrophotometric method using p-bromaniline as a color developer have shown significant correlation. This investigation has illustrated a new application for the radiometric bacteriologic procedure.

**CLINICAL ASSESSMENT OF HEPATIC DISEASE BY DUAL DYNAMIC RADIOISOTOPIC ANALYSIS.** S.J. DeNardo, G.B. Bell, G.L. DeNardo, P.O. Schiebe, P.E. Jackson, R.F. Carretta, Univ. of Cal. School of Medicine, Davis, Cal.

Although methods have been developed to assess hepatic and splenic blood flow and function in previous investigations, these have generally not proven to have significant clinical applicability. Despite a large number of available techniques, the differential diagnosis of jaundice remains a difficult problem. We have developed a method for assessing the kinetic movement of radioactive colloid and rose bengal in such a manner that hepatic and splenic blood flow, hepatic excretion and re-gurgitation of rose bengal, gall bladder and intestinal accumulations, as well as renal excretion can be quantitated. Radioactivity in the abdominal organs and gut was detected by a scintillation camera with a region of interest. Heart and bladder were monitored by external probes. This data was processed by a computer in accordance with a special mathematical model. Scintigraphs were also obtained; where these revealed a focal defect, this region was flagged and processed as a separate "organ". 8 normals and 12 patients with liver disease have been studied. Different patterns were found in normals, intrahepatic obstruction, extrahepatic obstruction, cirrhosis and neoplasm. Intrahepatic obstruction was associated with a decrease in hepatic perfusion and excretion, while extrahepatic obstruction was associated with asymmetry of hepatic blood flow, excretion and intestinal uptake. Neoplasm demonstrated early increased blood flow and decreased rose bengal uptake. This technique appears to be useful in the differential diagnosis of jaundice, intrahepatic and extrahepatic obstruction, and space-occupying lesions of the liver.

**<sup>123</sup>I FIBRINOGEN IMAGING OF THROMBI IN DOGS.** Sally J. DeNardo, Gerald L. DeNardo, Timothy O'Brien, Neal F. Peek, Florian W. Zielinski, John A. Jungerman, University of California School of Medicine, Davis, California

Only 25% of patients with pulmonary embolic disease have clinical evidence of venous thrombosis. Previous investigators have demonstrated by counting techniques that fibrinogen labeled with radioiodine concentrates in evolving clots. This study was performed to evaluate <sup>123</sup>I fibrinogen as a useful agent for clinical imaging of thrombi. Using the iodine monochloride method fibrinogen was labeled with <sup>123</sup>I produced with our cyclotron. Labeling yields of 50% were obtained while limiting the iodination to 1-2 atoms per molecule of fibrinogen. Labeled and unlabeled fibrinogen were indistinguishable by clottability (90%), column chromatography, cellulose acetate and polyacrylamide gel electrophoresis. Thrombi were induced in the femoral vein of 8 dogs using the method described by Wessler. The femoral vein was occluded after the administration of <sup>123</sup>I dog fibrinogen and activated serum. Thrombi in the occluded femoral vein were demonstrated by radiopaque venography. Scintigraphs were performed serially during the next 24 hours. Within several hours increased concentration of radioactivity was visualized in the area of the thrombi. Both femoral veins were removed and counted in a well detector. The occluded vein containing the antemortem clots had greater than 100 times the radioactivity of the contralateral vein. These studies indicate that <sup>123</sup>I fibrinogen is incorporated in active clots to a degree that may permit diagnostic imaging with this radionuclide, and thus may serve as a sensitive means of visualizing venous or arterial thrombi.

**DETERMINATION OF BONE MINERAL CONTENT BY FUNCTIONAL IMAGING.** G. DePuey, V. Alagarsamy, W. Thompson, M. Calderon, N. Kutka, J.A. Burdine. Baylor Coll. Med., Houston, Tex.

Measurement of relative bone mineral content can be accomplished by photon absorptiometry using <sup>241</sup>Am and a scintillation camera with digital data processor. This report describes clinical application of the technique and a new method for displaying the results as quantitative functional images in addition to calculation of a mineral index.

Relative photon transmission through the os calcis immersed in water (I) and through water alone (I\*) during 4 min exposure to a 25 mCi planar source of <sup>241</sup>Am is recorded in a 64 x 64 matrix of an on-line PDP8/E computer interfaced to the scintillation camera. Bone mineral content is proportional to the log of the ratio of activity transmitted through water and through bone (Mineral Index = ln I\*/I). After data smoothing, mineral index for each of 4096 cells is calculated and displayed in 7 colors on a raster-type monitor, with each color representing a quantitative level of bone density. To derive the mineral index of the os calcis, the bone is outlined by a light pen, and the numerical value within these limits is printed out by the computer. In sequential studies of the same patient, the mineral index indicates the degree of change while the functional image demonstrates any mineral redistribution within the bone.

In 3 volunteers, the S.D. in 6 periodic measurements was 1.4%. The mineral index in patients with demineralizing diseases has been monitored at 4-8 week intervals. Results indicate that changes in bone mineral content of about 2% can be detected.

**LYMPH NODE SCINTIGRAPHY WITH <sup>67</sup>Ga-PHYTATE, <sup>99m</sup>Tc-PHYTATE AND <sup>67</sup>Ga(OH)<sub>3</sub>, Fe(OH)<sub>3</sub> COLLOID.** Mrinal K. Dewanjee, Paul C. Kahn, Alice Carmel and Urmila Dewanjee, Tufts-New England Medical Center, Boston, MA.

<sup>67</sup>Ga-phytate was synthesized on the premise that the precipitate of <sup>67</sup>Ga-Ca-phytate formed with the intralymphatic Ca<sup>2+</sup> ion, after S.C. administration will be useful for lymph node imaging. A comparative study of <sup>67</sup>Ga-, <sup>99m</sup>Tc-phytate, <sup>99m</sup>Tc<sub>2</sub>S<sub>7</sub> sulfur colloid and <sup>67</sup>Ga(OH)<sub>3</sub>, Fe(OH)<sub>3</sub> colloid was made. Phytic acid was added to <sup>67</sup>GaCl<sub>4</sub> complex in 0.1NHCl solution and neutralized with dilute NaOH solution to a pH of 6.2-6.5. The final concentration was adjusted to 5mg/ml. The solution was sterilized by membrane filtration (0.22µ). A R<sub>f</sub> value of zero was obtained by paper chromatography in 85% methanol. <sup>67</sup>Ga(OH)<sub>3</sub>, Fe(OH)<sub>3</sub> colloid was prepared by adding 10µg of FeCl<sub>3</sub> and 50mg of gelatin to 4-5ml of <sup>67</sup>GaCl<sub>4</sub> complex in 0.1NHCl solution and neutralized with phosphate buffer to a pH of 6.0. <sup>99m</sup>Tc-phytate was prepared with the Sn-phytate kit (NEN). The agents were administered (S.C.; 1ml in each foot of the rabbit) and imaged at 6, 24, 48, and 72 hours; optimum time was 5-6 hours after injection. Organ distribution in rats and rabbits was performed at similar time periods. (1.5-2.0)% of the S.C. dose of <sup>99m</sup>Tc- and <sup>67</sup>Ga-phytate accumulate in the popliteal and axillary lymph nodes at 6 hours; at 72 hours (60-70)% remains in the whole body, with (25-35)% retention in bone and bone marrow. (20\*5)% of S.C. dose remains at the site of injection at (6-72) hours. On the other hand, (30-50)% of <sup>67</sup>Ga(OH)<sub>3</sub>, Fe(OH)<sub>3</sub> colloid and (80-90)% of Tc<sub>2</sub>S<sub>7</sub> sulfur colloid were locally retained. (85\*5)% of I.V. dose accumulates in the RE system. Thus <sup>99m</sup>Tc- and <sup>67</sup>Ga-phytate appear promising for lympho scintigraphy.

**THE BINDING OF TECHNETIUM ION WITH HEMOGLOBIN.** Mrinal K. Dewanjee and Paul C. Kahn, New England Medical Center, Tufts Medical School, Boston, Mass.

In this investigation, the nature of binding of <sup>99m</sup>Tc-ion to hemoglobin, specifically the specific activity of <sup>99m</sup>Tc-ion bound to heme and globin as

well as  $\alpha$  and  $\beta$  chains had been determined. The washed red cell pellet had been labelled with the stannous-citrate kit method, recently developed in the laboratory. The labelled cells were lysed with water-toluene mixture. The  $^{99m}\text{Tc}$ -hemoglobin filtrate was purified from  $^{99m}\text{Tc}$ -citrate,  $^{99m}\text{TcO}_4^-$  ion, etc., by gel filtration with Sephadex G-25 column equilibrated with phosphate buffer. The pure  $^{99m}\text{Tc}$ -hemoglobin fraction was treated with cold hydrochloric acid/acetone mixture containing a few drops of mercaptoethanol solution. The heme precipitate was washed 4-5 times with cold acetone and the activity in the heme and globin fractions had been determined. The results indicate that (79±4)% of activity in  $^{99m}\text{Tc}$ -hemoglobin is associated with globin. The  $\alpha$  and  $\beta$  chains were then split by treatment of one ml aliquot with 1% parachloro-mercuribenzoate in 0.07M NaOH solution. The solution was stored at 4°C for 36 hours. Using a sodium ion gradient, the  $\alpha$  and  $\beta$  chains were separated on a DE-52 column equilibrated with 0.01M phosphate buffer. The  $^{99m}\text{Tc}$ -activities as well as optical densities at 280, 400, and 540  $\mu$  were determined with a gamma well detector and Carl-Zeiss spectrophotometer respectively. Similarities in the labelling of  $\text{Cr}^{3+}$  and  $\text{Tc}^{3+}$  or  $\text{Tc}^{4+}$  as well as their preferential binding with the  $\beta$  chain of the hemoglobin had been observed.

**DIFFERENCES IN LUNG RETENTION OF  $^{114m}\text{In}$ - AND  $^{59}\text{Fe}$ -LABELED FERRIC HYDROXIDE MACROAGGREGATES.** Carol I. Diamanti and David A. Goodwin. Veterans Administration Hospital, Palo Alto, CA.

Large differences in the lung clearance half-times of ferric hydroxide macroaggregates have been described. We have undertaken a long-term experiment in mice to more accurately define the biological half-life of these particles, with special reference to the slow component of the curve.

The labeled macroaggregates were prepared using a modification of the original procedure of Stern, et al. Two groups of 51 female Swiss Webster mice were injected in the tail vein with 0.2 ml of either  $^{114m}\text{In-Fe}(\text{OH})_3$  macroaggregates (1.1  $\mu\text{Ci}/0.2$  ml) or  $^{59}\text{Fe-Fe}(\text{OH})_3$  macroaggregates (0.83  $\mu\text{Ci}/0.2$  ml). Three mice from each group were sacrificed at times ranging from 5 minutes to 147 days after injection. Blood, lungs, and liver were assayed for  $^{114m}\text{In}$  or  $^{59}\text{Fe}$  activity. Lung samples were obtained from mice sacrificed at 56, 63, and 147 days after injection. Histological examination was undertaken and sections examined for the presence of iron using a Prussian Blue stain.

At 147 days after injection there was 15% retention of  $^{59}\text{Fe-Fe}(\text{OH})_3$  macroaggregates in the lungs and only 3% retention of  $^{114m}\text{In-Fe}(\text{OH})_3$  macroaggregates. Iron particles were identified in the lungs as late as 147 days after injection but no pathological changes were seen.

The biological half-life of the slow component was accurately defined using  $^{114m}\text{In-Fe}(\text{OH})_3$  macroaggregates as 54 days. The difference in  $^{114m}\text{In-Fe}(\text{OH})_3$  and  $^{59}\text{Fe-Fe}(\text{OH})_3$  macroaggregate retention was apparently due to high blood levels of  $^{59}\text{Fe}$  which prevented accurate half-life determination of  $^{59}\text{Fe-Fe}(\text{OH})_3$  macroaggregates.

**BRAIN SCANS AND MICROANGIOGRAPHY IN THE EVOLUTION OF STROKE.** Giovanni Di Chiro, Eugene L. Timms, A. Eric Jones, Gerald S. Johnston, Mary K. Hammock, and Sybil J. Swann. National Institutes of Health, Bethesda, Md.

Following cerebrovascular thrombosis time-related changes occur in serial brain scans. This study compares the degree of radionuclide localization in the infarcted area of brain with evolving changes in its vascularity. The right middle cerebral artery was clipped in 12 Rhesus monkeys using a transorbital approach. This avoided a craniotomy scar which could hinder subsequent scan evaluations. Anterior and lateral serial static  $^{99m}\text{TcO}_4$  brain scans were obtained using a gamma camera with a 4.5 mm pinhole collimator which permitted magnification of the monkey's head. Sequential scan interval did not exceed 10 days. Serial microangiography was

obtained by perfusing microtized barium via carotid arteries. Microangiographic findings were related to scans last obtained before sacrifice. Progression of scans from negative through fully positive to regression to normal was elucidated. The positive area on scan corresponded to the expected region of infarct i.e. the lateral basal ganglia and insular region. The scans in a majority of animals became positive by 2 weeks regressed toward negative by 4 to 6 weeks after ligation of the middle cerebral artery. Increased radioisotope uptake in the affected area is clearly related to neovascularization around the area of infarct as shown by the microangiograms. Decreased vascularity, peripheral gliosis, and central cavity formation are the main factors determining diminution of radionuclide penetration in the involved area at later stages.

**MINI COLUMN CHROMATOGRAPHIC APPROACH FOR RAPID QUALITY CONTROL TESTING OF  $^{99m}\text{Tc}$ -RADIOPHARMACEUTICALS.** Norbert S. Domek and Merle K. Loken. Division of Nuclear Medicine, University of Minnesota Hospitals, Minneapolis, Minn.

The use of small chromatographic columns is being investigated as a means for rapid quality control testing of  $^{99m}\text{Tc}$ -radiopharmaceuticals, where separation of labeled compounds can be accomplished by taking advantage of specific binding capacities of column adsorbent/solvent systems.

Of several adsorbents examined, alumina columns (0.5 x 3 cm.) were found versatile, in that, depending on the solvent system used,  $^{99m}\text{Tc}$ -labeled-Sn-containing compounds such as DTPA, polyphosphate, diphosphonate, pyrophosphate and tetracycline, and  $^{99m}\text{Tc}$ -albumin (electrolytic tagging), could be retained by the adsorbent while unreacted  $\text{TcO}_4^-$  could be eluted with 3 ml. of eluent.

For  $^{99m}\text{Tc}$ -DTPA and  $^{99m}\text{Tc}$ -diphosphonate, mini columns of Sephadex/saline were used to bind any hydrolyzed-reduced technetium in test samples. These columns, when used in conjunction with alumina, afford a means of rapidly analyzing products for parent compound,  $\text{TcO}_4^-$  and hydrolyzed-reduced technetium. For the other radiopharmaceuticals, Sephadex columns were found to retain amounts of radioactivity in excess of what was expected, which suggest artifact formation. Other column/solvents are being investigated.

The mini column approach is attractive because only small columns, small volumes of eluent, and microliter size test samples are required. As a consequence, a significant reduction in analyses time can be achieved.

**MEASUREMENT OF TOTAL AND REGIONAL OCULAR BLOOD FLOW AND THE CHANGES ACCOMPANYING ALTERATION OF INTRAOCULAR PRESSURE.** Monique S. Dupuy and Thomas G. Mitchell. The Johns Hopkins Medical Institutions, Baltimore, Md.

The purpose of this study was to validate a method for measuring total and regional ocular flow with radioactive labeled microspheres.

An intra-arterial polyethylene catheter was placed into the left ventricle. Serial injections were made with  $^{85}\text{Sr}$  or  $^{141}\text{Ce}$  labeled 15 $\mu$  spheres. A femoral artery blood sample was taken from the moment of injection for 15-45 sec. Systemic arterial pressure in each dog was constant throughout. Seven experiments under basal conditions provided controls. The eyes were dissected, weighed and their activity determined. The percent of injected spheres in each eye, the retina, sclera, choroid, ciliary body and iris was calculated. Regional blood flow was calculated from the product of measured cardiac output and the fraction of injected spheres trapped in the different ocular tissues. Nine experiments were done in which intraocular pressure was changed in one eye following the baseline injection. The other eye served as a control. Increased pressure was maintained with a scleral vacuum cup and measured with a calibrated applanatic tonometer.

Total blood flow to 2.2 ml/min  $\pm$  0.6 was distributed within the eye as follows: 80% to the choroid, 18% to the

ciliary body and iris, 0.7% to the retina and 1.3% to the sclera. In any one dog the basal results were consistent when either both eyes or serial injections in one eye were compared. The results showed that an increase in intraocular pressure produced a decrease in total eye blood flow and a decrease in flow to the ciliary body, iris and choroid whereas in the retina, flow was maintained constant throughout the pressure rise. An increase in retinal blood flow also occurred when the intraocular pressure was decreased.

**EARLY DETECTION OF MAMMARY CARCINOMA WITH RADIO-LABELED BLEOMYCIN.** W.C. Eckelman, R.C. Reba, H. Kubota, and J. Stevenson. Washington Hospital Center, Washington, D.C. and AFRRI, Bethesda, Md.

Breast cancer is the most prevalent malignancy in women; there has been no change in the related death rate over the last 40 years. We compared  $TcO_4$  &  $^{67}Ga$  citrate with various radiopharmaceuticals in rats with implanted mammary adenocarcinoma to determine the relative diagnostic sensitivity of the new compounds in the hope that early diagnosis will lower the death rate. Tumor bearing rats were sacrificed at 2 and 24 hrs after injection of the radiochemically pure compound. Since an early scanning time is clinically the most useful, the 2 hr study is presented. The  $^{57}Co$  bleomycin is far superior to the other agents; the tumor : blood (T/B) and tumor : fat (T/F) ratios are 13 and 3 times larger than those for the other compounds.

	T/B	T/F	T/Muscle
$^{57}Co$ bleomycin	16.8	12.8	2.68
$^{64}Cu$ bleomycin	1.30	1.19	1.83
$^{125}I$ estradiol	1.02	0.19	0.17
$^{125}I$ digitoxigenin	0.71	1.57	1.97
$^{125}I$ prolactin	0.62	3.06	4.29
$^{99m}Tc$ pyrophosphate	0.75	4.08	1.26
$^{67}Ga$ citrate	0.87	5.10	4.66
$^{99m}TcO_4$	0.46	2.28	3.08

These data indicate that  $^{57}Co$  bleomycin may be a sensitive agent for detection of mammary carcinoma.

**COMPARISON OF INTRA-ARTICULAR  $^{99m}Tc$  PERTECHNETATE AND RADIOGRAPHIC KNEE ARTHROGRAPHY.** David A. Emmerson, Michael J. Pitt, Robert E. O'Mara, James D. VanAntwerp and Eric P. Gall. University of Arizona College of Medicine, Tucson, Ariz.

Intra-articular  $^{99m}Tc$  pertechnetate arthroscintigraphy has not been reported to date. This study compares intra-articular  $^{99m}Tc$  pertechnetate arthroscintigraphy with radiographic contrast arthrography of the knee in the evaluation of patients with symptomatology compatible with either thrombophlebitis or an expanding or ruptured popliteal cyst.

5 mCi  $^{99m}Tc$  pertechnetate and 6-10 cc. of Renografin-76 were injected concomitantly in the patellar-femoral joint space, from either a lateral or medial approach. Routine radiographic views were followed immediately by gamma camera imaging in multiple views.

All bursal cysts were identified as well with arthroscintigraphy as with radioarthrography. Radiopertechnetate persisted in the joint space considerably longer than contrast material, long enough that scintiphotos can be taken in a reasonable period of time 4-6 hours post-injection. This would prove helpful in the occasional patient with intermittent communication between the joint space and a bursal cyst.

Radiopertechnetate knee arthroscintigraphy compares favorably with contrast arthrography in the identification of bursal cysts. The delayed imaging capability (4-6 hrs) may prove to be valuable in identifying cysts with intermittent

communication. This method is also a valuable alternative in the patient with iodine sensitivity.

**AUTOMATED BRAIN BOLUS ANALYSIS AND SIGNIFICANCE OF VARIOUS EXTRACTED PARAMETERS.** Jon J. Erickson, A. B. Brill, Dennis D. Patton, Horace Williams, and Ronald R. Price. Vanderbilt University, Nashville, Tn.

For the past six months an automated analysis program for the reduction of data obtained in routine clinical brain bolus studies has been used. The bolus data are obtained from an anterior view and are stored on magnetic tape in quarter second frames for 40 seconds immediately following the injection.

The entire analysis is performed on a DEC PDP-9 computer with no operator intervention. This includes location of the edges and midline of the head, subdivision of each half of the image into eight R.O.I. and generation of an activity-versus-time curve for each of the total sixteen regions of interest. After the curves are generated, they are normalized to unit area and printed on the line printer. The curves are analyzed by the program, and six curve parameters are tabulated. Based on the curves from the region of the superior sagittal sinus, three cumulative images are formed which approximate the arterial, capillary and venous phases of the bolus flow image. The printer output and three photographic images are returned to the clinician for interpretation.

Several parameters appear to be significant in identifying abnormal flow patterns. Among these are the difference in time to peak between corresponding areas on the right and left as well as the relative magnitude of the curves. In abnormal studies the right-to-left disparity usually appears in several adjacent areas.

We are currently in the process of performing a statistical evaluation of the automated analysis in an attempt to determine the range of parameters in normal and abnormal states and to assess the relative information content of these different measures. Methods will be presented, along with examples of the results obtained to date.

**A COMPARISON OF  $^{111}InCl_3$ ,  $^{67}Ga$  AND  $^{197}HgCl_2$  IN TUMOR-BEARING MICE.** Paul A. Farrer and Gopal B. Saha. Dept. of Nuclear Medicine, McGill University, Royal Victoria Hospital, Montreal, Quebec.

The objective of these investigations was to determine and compare the tissue distribution and tumor uptake of  $^{111}InCl_3$ ,  $^{67}Ga$  citrate and  $^{197}HgCl_2$  in male Swiss mice bearing transplanted Ehrlich ascites-cell carcinoma.

All experiments were performed starting 6-8 days after the intraperitoneal implantation of an ascites-cell carcinoma suspension into recipient mice. Two  $\mu Ci$  of  $^{111}InCl_3$ ,  $^{67}Ga$  citrate and  $^{197}HgCl_2$  were injected separately by the intravenous route into groups of mice. The animals were sacrificed by exsanguination at 1, 2, 4, 24, 48, 72 and 96 hours post injection; 4-6 mice were used for each time point and each radionuclide. The total ascitic fluid was removed and radioassayed; the tumor cells and supernatant fluid separated by centrifugation and counted. A sample of blood and the liver, spleen, kidneys, lungs myocardium, voluntary muscle and gastrointestinal tract (plus contents) were removed, weighed and counted.

Tumor uptake of  $^{111}In$ ,  $^{67}Ga$  and  $^{197}Hg$  increased progressively with time, the highest tumor-to-supernatant ratio at 96 hours being observed with  $^{197}HgCl_2$  ( $7.2 \pm 3.2$ ). The ratios of  $^{111}In$  and  $^{67}Ga$ , also at 96 hours, were  $1.85 \pm 0.78$  and  $0.70 \pm 0.19$  respectively, indicating a relatively greater affinity of  $^{111}In$  for tumor. A similar trend of progressively increasing tumor-to-blood ratio was evident with all three radiopharmaceuticals.

$^{197}HgCl_2$  shows the maximum affinity for Ehrlich ascites cell carcinoma of mice.  $^{111}In$  whilst showing lesser affinity for this tumor, is nevertheless superior to  $^{67}Ga$ . Cell fractionation techniques demonstrated that about 70-90% of  $^{111}In$ ,  $^{67}Ga$  and  $^{197}Hg$  was associated with the nucleus-containing fraction of malignant cells.

**DIAGNOSTIC RADIONUCLIDE PROCEDURES IN RENAL TRANSPLANT PATIENTS.** P.A. Farrer, R.D. Guttman, J.G. Beaudoin, D.D. Morehouse and J. Knaack. Royal Victoria Hospital and McGill University, Montreal, P.Q.



Oliguria or anuria frequently develop after renal transplantation surgery. The early detection of renal damage and identification of the specific cause is imperative since, of the several underlying causes, any one might be operative and treatment of each is different.

Over 200 patients with cadaveric renal homotransplants have been studied serially by  $^{131}\text{I}$ -radiohippuran renography with sequential gamma camera scintiphography and  $^{99\text{m}}\text{Tc}$  pertechnetate rapid transit perfusion imaging. The findings have been correlated with the clinical course, laboratory investigations and histopathologic data from biopsy and surgical samples.

In 20 patients with histologically proven acute tubular necrosis, the hippuran study (renogram plus serial scintiphography) was abnormal in every instance;  $^{99\text{m}}\text{Tc}$  perfusion was diffusely reduced in 8 patients (40%). In 34 patients with biopsy proven rejection, the hippuran study was abnormal in 91% and the perfusion study was abnormal in 74% of cases; diffuse and focal reductions in flow were found in 65% and 9%, respectively. The results of radionuclide studies were accurate and pathognomonic in all instances of renal vascular thrombosis and urinary extravasation.

Serial renography is a simple and valuable test and of useful prognostic significance. Of course, the renographic changes are non-specific.  $^{131}\text{I}$  hippuran sequential renal scintiphography is of value in detecting improvement or progressive renal deterioration and in visualizing urinary extravasation and obstruction.  $^{99\text{m}}\text{Tc}$ -pertechnetate gamma camera rapid transit perfusion studies enable the further assessment of transplant viability and are of particular help in diagnosing vascular thrombosis.

**RADIONUCLIDE IMAGING OF INTRATHORACIC MASS-LESIONS USING  $^{197}\text{HgCl}_2$  AND  $^{99\text{m}}\text{Tc}$ -MACROAGGREGATED HUMAN SERUM ALBUMIN.**  
Paul A. Farrer, Gopal B. Saha, D.D. Munro, R.E. Dollfuss, J.F. Meakins and L.D. MacLean. Dept. of Nuclear Medicine McGill University, Royal Victoria Hospital, Montreal, P.Q.

The present study was designed to critically evaluate the use of  $^{197}\text{HgCl}_2$  in the differential diagnosis of intrathoracic mass-lesions and in distinguishing malignant from benign lesions. Another objective was to assess the role of  $^{99\text{m}}\text{Tc}$ -macroaggregated human serum albumin ( $^{99\text{m}}\text{Tc}$ -MAA) radionuclide angiocardiology and perfusion lung imaging in this situation.

A total of 81 patients comprise the present series and pathologic confirmation was obtained in every case. 47 of 55 lung cancers (85%) exhibited clearly discernible selective uptake of  $^{197}\text{HgCl}_2$ . Mediastinal lymph node involvement was associated with selective uptake of the radionuclide in the midline. Only 7 of 26 benign lesions (27%) showed increased radionuclide uptake and comprise cases of lung abscess and pneumonitis. Two patients showed transient high uptake in the midline and neck within 72-96 hours of mediastinoscopy and scalene node biopsy. In vitro radioassay of resected tissue samples revealed that the specific activity of cancers was 1.5 to 3.4 times greater than that of normal lung.

$^{99\text{m}}\text{Tc}$ -MAA lung images demonstrated regional perfusion defects in 52 of 55 cancers (95%) and in 40% of the cases, the size of the perfusion defect was considerably greater than the roentgenographic lesion. Partial compression of the SVC was corroborated in four cancer patients.

$^{197}\text{HgCl}_2$  scanning was particularly useful in detecting lymphangitic spread and the presence of cancer in mediastinal lymph nodes.  $^{99\text{m}}\text{Tc}$ -MAA imaging provided valuable additional information concerning the extent of pulmonary arterial perfusion defect of importance in the evaluation of patients prior to lung resection.

**DETECTION OF OSTEOMYELITIS BY BONE MARROW SCANNING.**

David S. Feigin, H. William Strauss and A. Everette James. The Johns Hopkins Medical Institutions, Baltimore, Maryland

Osteomyelitis causes inflammatory reaction within the bone marrow early in its course suggesting that bone marrow imaging with technetium-sulfur-colloid could be used for the early detection of osteomyelitis. We investigated this possibility in 15 rabbits, 11 of whom were infected by injection of *Staphylococcus aureus*. Seven of 11 were adult animals injected in the marrow cavity of the midshaft or distal femur, and 4 of 11 were young rabbits injected into the distal epiphyseal plate of the femur. Four additional

control rabbits underwent sham experiments. Serial scans and radiographs were made on all animals.

Of the 11 experimental animals, 3 died of sepsis, 2 failed to develop any signs of infection and the remaining 6 rabbits developed osteomyelitis 13 to 25 days after inoculation documented by radiographic changes. All 6 showed marked decrease RES function in the area of infection as compared with the opposite uninfected limb at least 4 days prior to definitive radiological changes. One demonstrated a mild osteomyelitis which healed spontaneously and both the bone marrow scan and x-ray returned to normal.

None of the control animals showed any evidence of infection. The RES scans were normal in 3. One control animal did show a persistent area of decreased uptake in the marrow despite no infection. This was attributed to bone injury.

These results suggest that the bone marrow scan may be a clinically useful study to perform for the early diagnosis of osteomyelitis.

**INCREASED BRAIN SCAN SPECIFICITY BY THE USE OF  $^{99\text{m}}\text{Tc}$ -DIPHOSPHONATE.** Keith C. Fischer, Henry P. Pendergrass, Kenneth A. McKusick, Majic S. Pottsaid. Mass. General Hospital, Boston, Mass.

Certain intracerebral lesions accumulate  $^{99\text{m}}\text{Tc}$  diphosphonate (Tc-D). To study the possibility of increasing the specificity of brain scanning by the use of that radiopharmaceutical, Tc-pertechnetate (Tc-P) (15-20mCi) and Tc-D (20mCi) brain scans were done within 48 hours of each other and qualitatively compared. Diagnosis was confirmed histologically for neoplasms and angiographically and/or by computerized axial tomography for cerebrovascular lesions. In 3 of 4 cerebral infarctions, the target to background (T/B) ratio of activity was greater with Tc-D compared to Tc-P and equal in the remaining case. In 8 cases of suspected CVA's neither radionuclide demonstrated the lesion. In 4 of 6 meningiomas, the T/B ratio was greater with Tc-D; in one case equal, and in one case was only visualized by Tc-D. The T/B ratio with Tc-D was less than that with Tc-P in one astrocytoma. Bony changes and tumoral calcification may account for the increased radionuclide accumulation in some meningiomas. It is uncertain why some cerebrovascular lesions accumulate diphosphonate as intensely as demonstrated in these several cases. These results suggest that Tc-D may accumulate to a greater degree than Tc-P in some cerebrovascular lesions and meningiomas but not in other cerebral tumors.

**CARDIAC OUTPUT AND CORONARY BLOOD FLOW BY MEANS OF CESIUM 131 INFUSION.** Roger Floyrac, Roland Itti, Thérèse Planiol. Centre Hospitalo-Universitaire. 37033 - TOURS - CEDEX - FRANCE.

Injection at a constant rate of a radiocesium solution has been used to determine cardiac output by measuring the difference between arterial and venous concentrations. One can get an instantaneous data by taking the two blood samples at the same time. But continuous survey is possible following insertion in the vessels of two catheters with coils, in order to record radioactive concentrations using two probes, a peristaltic pump and a dual-channel chart recorder. This technique is very similar to the one which implies the measurement of oxygen consumptions but it shows, relatively to the latter several improvements. Tracer input control is easier. Cardiac output is known at any time making possible effort tests and pharmaceutical trials.

Simultaneously, coronary blood flow has been assessed with the help of a precordial probe. Owing to the particularity of this circulation which is fully and permanently in the detector field one can measure cesium uptake by myocardium without subtracting the radioactivity of the cardiac cavities. This point has been the object of a straightforward theoretical demonstration.

**BONE SCINTIGRAPHY IN BREAST CARCINOMA.** Robert S. Frankel, Steven D. Richman, Stanley M. Levenson, Robert L. Nelson, James N. Ingle, Douglass C. Torney, A. Eric Jones, and Gerald S. Johnston. National Institutes of Health, Bethesda, Md.

Bone scintigraphy has been shown to be a valuable means for the detection of skeletal metastases. In breast carcinoma, bone is one of the most frequent sites for metastasis. We have evaluated 70 patients with breast carcinoma using <sup>99m</sup>Tc polyphosphate bone scintigraphy, radiologic survey, and bone pain. The skeleton was divided into 12 anatomic regions. Abnormal localization on bone scan was considered metastasis if trauma, surgery, and benign bone disease were ruled out both radiologically and clinically. There were scan and x-ray abnormalities with pain in 134 sites. Seventy-four sites had scan and x-ray evidence of metastatic disease without pain. Ninety-two sites were abnormal on bone scan but normal on x-ray with no pain. Thirteen of these sites later became abnormal on x-ray. In 30 of 33 reevaluated sites, bone scan abnormality persisted without x-ray changes or pain. Of these 92 sites, 82 occurred in patients with multiple abnormalities thus increasing the likelihood that they indeed represented metastases. Only ten sites were abnormal on x-ray with a normal scan and no pain. Two of these sites became abnormal on scan later.

In breast carcinoma, bone scintigraphy is the most sensitive diagnostic modality and the means by which the earliest detection of skeletal metastases can be accomplished. Therefore, bone scintigraphy should be an integral part of the initial diagnostic evaluation and follow-up in patients with breast carcinoma.

**RENAL LOCALIZATION OF GALLIUM-67 CITRATE.** Robert S. Frankel, Steven D. Richman, Louis G. Gelrud, and Gerald S. Johnston. National Institutes of Health, Bethesda, Md.

Gallium-67 citrate is now well established as a tumor scanning agent. Renal excretion of the radiopharmaceutical occurs predominantly during the first 24 hours following administration. By 48-72 hours gallium localization in the kidneys, visualized on scintiscan, is unusual and should be considered abnormal.

Twenty-two patients with bilateral renal visualization on 48 hr. gallium scintigrams were reviewed. All patients had known malignancies. There were nine with leukemia, five with lymphoma, five with melanoma, two with Hodgkin's disease, and one with breast carcinoma. Ten patients have died, and nine have had autopsies. Five patients had tumor in the kidneys at autopsy, two had an inflammatory process, and two had no tumor or inflammation. Of the 12 patients who are still living, one had x-ray and laboratory evidence of renal involvement; two, only x-ray evidence; three, only laboratory evidence; and six had no other evidence of renal disease. Of these six, one had a repeat gallium scan showing no uptake in the kidneys. In the interim, he had been given intensive chemotherapy. Only two cases in this series were proven to be without tumor or inflammation. In the six patients with no x-ray or lab evidence of renal disease, it is possible that gallium scanning was the first evidence for renal involvement. Follow-up studies are underway to determine this. It may be concluded that gallium localization in the kidneys at 48 hrs. or later should prompt further investigations to rule out the presence of active tumor or inflammation.

**GA-67 LOCALIZATION OF POST OPERATIVE ABDOMINAL ABSCESSSES.** Melvin J. Fratkin, Jerry I. Hirsch, and Alton R. Sharpe. Medical College of Virginia, Richmond, Va.

Following abdominal surgery, a prolonged febrile course suggests intra-abdominal sepsis that may progress to ab-

cess formation despite appropriate antibiotic treatment. The purpose of this paper is to determine the value of Ga-67 scanning in localizing the presence of abscess formation in patients with post operative abdominal sepsis. Twenty-eight patients who had had abdominal surgery for various reasons were studied. All were clinically septic in the post operative period. Each patient received I.V. 40 uCi Ga-67/kg and were scanned with a rectilinear scanner 48 hours later, following cleansing of the bowel with laxatives and enemas. In three patients abscess material and blood were obtained at the time of surgery, 3-5 days following Ga-67 administration.

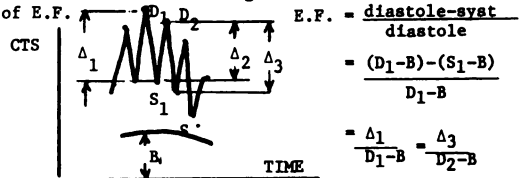
Of the 28 patients studied, 15 had positive scans and abscess formation was confirmed in each at subsequent surgical exploration. An additional four patients had positive scans, were not explored, but improved with prolonged antibiotic treatment. Of the 9 patients with normal scans, 7 improved rapidly with antibiotic treatment; 2 did not and each were later found to have a subphrenic abscess.

Radioactivity was demonstrable in the abscess wall, supernatant, and pus cells. When compared to equivalent amounts of plasma or blood, the abscess wall had the highest specific activity even though the Ga-67 uptake by the abscess pus cells and peripheral wbc's was similar.

Conclusions: (1) Ga-67 offers a non-invasive means of localizing post operative abdominal abscesses. (2) The positive scan results, most likely, from Ga-67 uptake in the abscess wall by the vast number of inflammatory cells.

**EXPRESSION OF THE CARDIAC EJECTION FRACTION WITH REDUCED BACKGROUND DEPENDENCE.** Gerald S. Freedman and Andrew Dwyer, Yale Univ. Sch. of Med. and St. Raphael's Hosp., New Haven, Ct.

Attempts to utilize the radiocardiogram to determine cardiac ejection fraction (E.F.) have been frustrated by background activity. Methods to determine and correct for this extra-ventricular activity have been relatively complex or costly. A mathematical expression for E.F. has been derived which assumes that the E.F. is constant over each cardiac cycle and that background changes are small during two successive cardiac cycles. This expression of E.F. reduces the effect of background counts on the calculation of E.F.



From the above the E.F. can be expressed in terms of the differences between systole and diastole ( $\Delta_1, \Delta_2, \Delta_3$ ) which are relatively insensitive to background as compared to  $D_1, D_2$  and  $S_1, S_2$ . The constant "B" representing background cancels from the equation leaving:

$$E.F. = \frac{\Delta_3 - \Delta_1}{\Delta_2 - \Delta_1}$$

The radiocardiographic data can be obtained with a single probe-strip chart recorder or gamma camera with area of interest capability. Evaluation of patients by this method and radiographic angiography are underway to validate this approach.

**BREAST UPTAKE OF <sup>99m</sup>Tc HEDSPA (DIPHOSPHONATE): AN INDICATOR OF BREAST CARCINOMA.** Barry H. Friedman, Michael E. Siegel, and Henry N. Wagner, Jr. The Johns Hopkins Medical Institutions, Baltimore, Maryland.

Uptake of <sup>99m</sup>Tc HEDSPA (diphosphonate) in the breasts of female patients was correlated with the presence or absence of breast carcinoma.

The population consisted of fifty consecutively studied female patients referred to our department for routine bone scans. The scans were performed in the routine manner as follows: three hours after an intravenous injection of 15-20 mCi of <sup>99m</sup>Tc HEDSPA an anterior and posterior whole body scan using a dual 5 inch scanner with 1:5 magnification was obtained. In addition lateral and oblique views of the chest using a scintillation camera were taken.

Of the 11 patients who had bilateral accumulation of the radiopharmaceutical 9 of these were subsequently proven

to have carcinoma of one breast. The remaining 2 patients had biopsy proven fibrocystic disease. In the group of sixteen patients with no increased uptake of the agent in either breast only one had carcinoma of the breast. If the remaining 23 patients who had previous mastectomies for carcinoma of breast are considered then 24 of the 33 patients who had carcinoma of the breast had uptake in the clinically normal breast. In no patients with two clinically normal breasts was there increased accumulation of the agent noted in either breast. In the patients who had increased activity in the clinically normal breast 93% had breast carcinoma.

The findings suggest that increased accumulation of  $^{99m}\text{Tc}$  HEDSPA (diphosphonate) in the breasts may be a sensitive indicator of breast disease, particularly that predisposing to breast carcinoma.

**BONE SCANNING WITH A CADMIUM-TELLURIDE PROBE.**  
Daniel Garcia, Gerald Entine, and Donald E. Tow.  
Veterans Administration Hospital, West Roxbury and Tyco Laboratories Inc., Waltham, Mass.

CdTe semiconductor nuclear detectors provide much higher stopping power and energy resolution than silicon detectors for moderate energy gamma rays. A CdTe probe, being developed for inter-cavitary use, performed well in detecting increased  $\text{Tc}^{99m}$ -PP uptake in tooth abscesses in dogs.

Twelve abscesses were induced in molars of the right jaw among 4 dogs. The dogs were probed and radiographed at weekly intervals after infection.  $\text{Tc}^{99m}$  counts were made 3 hours after 2 mCi/kg doses. Measurements were made with the probe hand held against the gum overlying the root tips of infected teeth and the data compared to that of the same areas on the left or normal jaw.

Count rates from individual root tips ranged from 2 to  $5 \times 10^3$  cpm/mCi/kg, 3 hours after injection. Significant increases in the ratios of right to left root tip counts were observed in 10 of 12 infected teeth 1 week, and the remainder, 2 weeks after infection. The ratios ranged from 1.2 to 2.0 over a 6 week period, showing progressive increases during the first 4 weeks. Repeated measurements of normal teeth in a given dog were reproducible by  $\pm 12\%$ . In contrast to this, the earliest radiographic evidence of periapical pathology was not visible until the fourth week.

The capability to detect incipient bone lesions prior to their radiographic appearance suggests the potential usefulness of CdTe detection systems in nuclear medicine. The reproducibility of measurements and high detector efficiency under clinical conditions make the system a promising diagnostic tool.

**INFANTILE OBSTRUCTIVE AIRWAY DISEASE DUE TO OXYGEN TOXICITY.** Gary F. Gates, Earl K. Dore, Marguerite Markarian, Jean Takenaka. Memorial Hospital, Long Beach, Calif.

Assisted ventilation with prolonged high oxygen therapy is sometimes necessary to treat severe neonatal respiratory distress. However, oxygen toxicity may occur resulting in cystic, fibrotic, emphysematous lungs. A series of infants with these lung complications were studied with radio-aerosol inhalation and perfusion lung scintiscans. Severe respiratory distress was present clinically with the major difficulty during expiration. Chest radiography including cinebronchography revealed expiratory collapse of major airways plus severe emphysematous changes. Radioaerosol inhalation scintiscans showed deposition of nuclide above the carina but not beyond indicating severe major airway obstruction. One infant, restudied 5 months later when free of airway obstruction, had alveolar deposition of radioaerosol. The perfusion scintiscans showed irregularities of perfusion similar to those found in adult obstructive emphysema. The tissue effects of oxygen toxicity include free radical formation with auto oxidative reactions and subsequent cellular damage. This apparently produces fibrotic, emphysematous, pulmonary changes with high peripheral airway resistance. With heightened expiratory effort, the

increased intrathoracic pressure results in collapse of the trachea and bronchi. These children were effectively treated with respirators using positive expiratory airway pressure which maintained airway patency. Radionuclide scintiscanning is a simple method of evaluating airway patency and lung perfusion in neonatal respiratory distress.

**THE HYPERPERFUSED LUNG IN CONGENITAL HEART DISEASE.** Gary F. Gates, Harry W. Orme, Earl K. Dore. Memorial Hospital, Long Beach, California

The detection of grossly unequal arterial flow to right and left lungs is crucial in evaluating congenital heart disease especially if surgery is planned. As chest radiography and angiography may not detect such flow imbalance, 35 children with congenital heart disease were studied after intravenous injection of  $^{99m}\text{Tc}$  macroaggregated albumin. Lung scintigrams were obtained with a gamma camera. Nuclide accumulation in right and left lungs is determined separately and reflects division of pulmonary arterial flow. 21 patients showed maldistribution of pulmonary flow (i.e. at least 30% hyperperfusion of one lung relative to the opposite). 5 were detected with chest radiograms, 11 by angiograms. Four of 8 tetralogies of Fallot had perfusion imbalances: 3 with branch stenosis of pulmonary arteries and 1 with blood jetting into the right pulmonary artery. Three ventricular septal defects had right lung hyperperfusion due to jetting. Six patients with branch pulmonary artery stenosis and 1 with branch atresia showed proportionately diminished flow on the affected side. Three malfunctioning Waterston shunts were discovered which resulted in imbalanced pulmonary flow. Review of chest radiograms together with radionuclide scintigrams of the lungs revealed that consistent detection of flow imbalance by inspection of chest radiograms was possible only when one lung received  $2\frac{1}{2}$  times the blood flow of the opposite side.  $1\frac{1}{2}$  times hyperperfusion was sufficient for angiographic detection. The radionuclide method is distinctly more sensitive in detecting pulmonary flow imbalances than radiography.

**ENZYMATIC SYNTHESIS AND EVALUATION OF  $^{13}\text{N}$  LABELED AMINO ACIDS AS MYOCARDIAL SCANNING AGENTS.**  
Alan S. Gelbard, Laurence P. Clarke, Joseph M. McDonald and John S. Laughlin. Memorial Sloan-Kettering Cancer Center, New York, N.Y.

Several amino acids labeled with  $^{13}\text{N}$  have been enzymatically synthesized and the absolute in-vivo distribution of radioactivity in various organs of the dog have been determined using our high energy gamma-ray scanner.  $^{13}\text{N}$ -glutamine and  $^{13}\text{N}$ -glutamic acid have been synthesized in yields of 30-60 mCi for a conversion of 70-90 per cent of  $^{13}\text{NH}_3$  to the labeled amino acid. 3-5 mCi of  $^{13}\text{N}$  asparagine were synthesized for a yield of 10-15 per cent.

Whole body scans of dogs were performed 10-50 min. after injection of the labeled amino acid.  $^{13}\text{N}$  asparagine was incorporated in the myocardium with a concentration three times greater than for the usual myocardial scanning agents. Activity could also be seen in the liver, brain and salivary glands.

There was little myocardial uptake of  $^{13}\text{N}$  glutamine or  $^{13}\text{N}$  glutamic acid although inhibitor studies by other investigators have indirectly implicated glutamine as the metabolite to which  $^{13}\text{NH}_3$  is converted in the heart. A high percentage of glutamine is incorporated into the liver. Glutamic acid has a different distribution.

These results demonstrate that there is a different pattern of distribution of radioactivity for the three amino acids. The high uptake of  $^{13}\text{N}$  asparagine in the heart indicates that this compound may be a good myocardial scanning agent.

**IN VIVO STUDY OF FACTORS INFLUENCING SKELETAL UPTAKE OF BONE-SEEKING RADIONUCLIDES.** Harry K. Genant, George J. Bautovich, Katherine A. Lathrop and Paul V. Harper. The University of Chicago, Chicago, Ill.

The factors governing skeletal uptake of the  $^{99m}\text{Tc}$ -Sn-compounds of polyphosphate (PP) and diphosphonate (EHDP) in vivo have not been previously defined. This study was undertaken to obtain basic information regarding the effects of alteration in blood flow (thermal-induced) and alteration in osteogenesis (rickets-induced) on skeletal uptake of these agents in rats and to compare them with the conventional agents,  $^{18}\text{F}$  and  $^{85}\text{Sr}$ .

An in vivo quantitative technique using pinhole collimation and an Anger Camera was developed so that serial studies could be performed on a single animal and laboratory procedures could be adapted for clinical use. Quantitative data were recorded and retrieved using a data acquisition system. The activities for a skeletal region and for an administered dose were determined under identical geometry which permitted calculation of the percent uptake in a region of interest (rat knee). The reproducibility of the measurement was within 3%, and the coefficient of variation in controls was less than 10% for each agent used. In vivo quantitative results were corroborated by autoradiographic and well-counting techniques. The effect of experimental design on blood flow was confirmed by measuring the distribution of  $^{99m}\text{Tc}$  labeled microspheres following intracardiac injection.

Our results in rats indicate that the short-term uptake of  $^{99m}\text{TcPP}$  and  $^{99m}\text{TcEHDP}$ , like  $^{18}\text{F}$  and  $^{85}\text{Sr}$ , is closely correlated with blood flow, and is independent of the rate of osteogenesis.

**DUAL WINDOW SPATIAL FILTERING.** S. Genna, S. Pang, S. Zimmerman, B. Burrows. V.A. Hospital and Boston University School of Medicine, Boston, Mass.

Improvement of image fidelity can be obtained through linear superposition of the image (count density distribution) produced by two or more gamma-ray energy discriminating windows. [phys.Med. Biol.14(1969, Medical Radiation Scintigraphy, 113-154, IAEA (1972)]. In addition, data processing (filtering) to transform one or more of the component images before combination can be used to produce a new image having more favorable characteristics (higher image signal to noise ratio). If we denote this transformation by the operator  $\hat{O}_i$ , the new image is given by

$$I = \sum w_i \hat{O}_i I_i$$

where  $w_i$  is the weighting factor of each image component  $I_i$ .

Application of dual window image filtering to  $^{99m}\text{Tc}$  and  $^{113m}\text{In}$  images are demonstrated separately in terms of their respective spread functions, phantom images and liver images. For each nuclide the photopeak is combined with a filtered image of a pulse height window below the photopeak. Subtraction of the filtered image from the photopeak image produces a sharper image spread function with high statistical reliability. For both nuclides the final spread functions have unaltered spatial characteristics and no loss of statistical reliability in the central regions (radial distance from the point source less than one FWHM), while in more distal regions ( $r > \text{FWHM}$ ) the spread functions are significantly sharper and their tails are reduced. The associated increase in statistical uncertainty is minimal and primarily associated with reduction in count density in the tail regions of the spread functions. Images produced by phantoms or liver activity are noticeably sharper with voids showing higher contrast.

**FIRST TRANSIT HEPATIC DEPOSIT OF  $^{99m}\text{Tc}$  SULFUR COLLOID (TSC) - AN INDICATOR OF HEPATIC WEDGE PRESSURE?** E.A. George, J.B. Shields, E.C. Cabal, F.K. Herbig, R.M. Donati. St. Louis VA Hospital and St. Louis University School of Medicine, St. Louis, Mo.

Sequential scintiphotographic uptake of TSC by the liver was evaluated as an index of portal circulation utilizing visual evaluative criteria in 154 patients. Diminished or absent accumulation of

TSC in the liver during the portal phase of hepatic circulation correlated with cirrhosis and/or portal hypertension. This led to the subsequent evaluation of time activity curves representing the first hepatic circulatory transit of TSC, celiac arteriograms, hepatic venograms, and hepatic wedge pressure determinations in 6 patients. The scintillation camera detector, fitted with a low energy diverging collimator, was placed over the liver and spleen. Data were recorded for 1 min following the I.V. injection of 3 mCi of TSC. Time activity curves were generated from electronic windows over the hepatic and splenic areas. Hepatic arterial and portal curve components were separated utilizing slope changes in the curve and the spleen as an arterial signal, assuming that virtually 100% of the TSC was extracted during the first hepatic arterio-portal transit and that subsequent arterial delivery was negligible. The ratio of the portal component to the hepatic arterial component (P/A index) was calculated from comparison of areas under the respective curves. The P/A index compared favorably with the hepatic wedge pressure in 5 of the 6 patients. Additional patients are presently under study to establish whether the P/A index is a reliable indicator of hepatic wedge pressure and portal pressure.

**VISUALIZATION OF REJECTING RENAL TRANSPLANTS WITH  $^{99m}\text{Tc}$  SULFUR COLLOID (TSC).** E.A. George, J.E. Codd, W.T. Newton, R.E. Henry, F.K. Herbig and R.M. Donati. St. Louis VA Hospital and St. Louis Univ., St. Louis, Mo.

Scintiphotographic visualization of renal transplants due to accumulation of TSC was evaluated with 54 examinations in 28 patients. All patients were examined with a scintillation camera 15-30 minutes following I.V. administration of 1.0 mCi of TSC. Transplant visualization was compared to the bone marrow and graded as: absent, slight, or marked. At the time of examination the diagnosis of acute or chronic rejection, acute tubular necrosis, nephrotic syndrome or normal transplant function was established by clinical criteria, and in selected instances by biopsy and/or selective arteriography. Marked visualization occurred in chronic rejection while slight visualization was observed with acute rejection. No visualization occurred in acute tubular necrosis or normal transplant function. To explore the mechanism of TSC accumulation, the kinetics of TSC was investigated daily for 5 days in 6 immunologically unmodified mongrel dogs following renal allograft transplantation. Transplant visualization occurred during acute rejection 3-4 days following grafting. Rate constant analysis of the time activity curves indicated transplant retention of TSC during rejection. Gross radioautography of the resected transplant demonstrated activity within the renal vasculature. Prominent vasculitis, endothelial proliferation and thrombosis, compatible with acute rejection was observed microscopically. These results suggest that TSC accumulation occurs in the transplanted kidney during rejection secondary to renal vasculitis and fibrin thrombosis.

**THE SENSITIVITY AND SPECIFICITY OF THE LIVER SCAN IN DIFFUSE HEPATOCELLULAR DISEASE.** George E. Geallen, Steven M. Pinsky, Roy K. Poth, and Merrill C. Johnson. Walter Reed Hospital, Washington, D.C.

Whereas  $^{99m}\text{Tc}$ -sulfur colloid liver scans have been found to be highly sensitive in the detection of space occupying lesions, their detection of diffuse hepatocellular disease has been described as relatively insensitive and nonspecific. In order to determine scan sensitivity and specificity and define scan patterns produced by diffuse hepatocellular disease, 108 consecutive histologically proven liver-spleen scan cases were reviewed by two independent unbiased observers. In all liver scans five criteria (hepatomegaly, splenomegaly, nonhomogenous liver uptake, bone marrow uptake, and liver to spleen uptake ratio), were graded on a scale of normal, 0; minimal, 1; moderate, 2; and severe, 3. These findings were tabulated for each disease.

Fifty-four of the liver-spleen scans were on patients with diffuse hepatocellular disease (cirrhosis, 9; fatty metamorphosis, 22; hepatitis, 18; portal fibrosis, 5). The sensitivity of detection in this group was 83% (45/54) and by individual disease was: cirrhosis, 100%; fatty metamorphosis, 86%; hepatitis, 78% and portal fibrosis, 60%. Three scan findings; diffuse nonhomogenous liver uptake; bone marrow uptake and reversal of the liver to spleen uptake ratio, when present simultaneously and increased significantly (Grade 2 or 3) were specific for cirrhosis. This pattern was present in 67% (6/9) of the patients with cirrhosis. It was not present in any case of hepatitis or portal fibrosis. No distinctive finding or pattern was found for the other forms of diffuse hepatocellular disease in this series.

In summary, the liver scan is highly sensitive for detecting hepatocellular disease. Scan pattern specificity for diffuse hepatocellular disease is limited to cirrhosis.

**DIAGNOSIS OF OBSCURE CHILDHOOD OSTEOID OSTEOMAS WITH THE BONE SCAN.** David L. Gilday, The Hospital for Sick Children, Toronto, Ont.

Usually osteoid osteomas are readily diagnosed by their clinical and radiologic appearance. However, occasionally they are missed due to their location or lack of typical symptoms. We have begun using Technetium - 99 m methylene diphosphonate bone scans to aid in diagnosing unusual osteoid osteomas. The most valuable scan diagnoses were made in 3 spinal lesions which had caused symptoms for at least 2 years and resulted in: a laminectomy and psychiatric consultation, incarceration of an athletic 16 year old in a whole body cast for 2 years, the labelling of a 12 year old ex-athletic as a malingerer. 3 of 5 peripheral osteoid osteomas had atypical clinical findings but all 5 had abnormal bone scans. All of the osteoid osteomas had a well localized very marked increase in radioactivity at the site. In all but one case further radiological studies, using the scan findings as a guide, demonstrated an abnormality. Six have been treated surgically and 2 are being followed. Currently the orthopedic surgeons in our hospital are convinced that any child with unexplained bone pain, even in the face of normal radiographs, should have a bone scan.

**PEDIATRIC CYSTIC BRAIN TUMORS - THE USE OF IMMEDIATE AND DELAYED BRAIN SCANS AND THEIR DIAGNOSIS.** David L. Gilday, The Hospital for Sick Children, Toronto, Ont.

In cystic astrocytomas in children we have found an unusual discrepancy between blood pool brain images and the delayed static ones. Our usual brain scan technique consists of a posterior or radionuclide angiogram, an immediate and delayed 2-4 hour brain scan. By comparing the scans and the neurosurgical findings we concluded that the abnormality seen on the blood pool images corresponded to the solid vascular portion of the tumor, whereas the additional abnormality in the delayed images represented the cystic component. The addition of an immediate post injection scan to the usual delayed scan helped in detecting those tumors which had a cystic component. The finding of a change in radionuclide tumor uptake is highly suggestive of a cystic tumor.

**THE DIFFERENTIATION OF OSTEOMYELITIS AND CELLULITIS IN CHILDREN USING A COMBINED BLOOD POOL AND BONE SCAN.** David L. Gilday, and Donald J. Paul, The Hospital for Sick Children, Toronto, Ont.

In children the differentiation of acute osteomyelitis from cellulitis is possible

using a blood pool scan and a bone scan. In patients suspected of having osteomyelitis we currently perform gamma camera images of the suspected area with a high resolution collimator immediately after the injection of Technetium - 99m methylene diphosphonate and follow this by images at one hour. In acute osteomyelitis the bone scan findings are a focal area increased radioactivity occasionally superimposed on a generalized bone uptake. This is due mainly to the reparative process. However, in most cases there is also an increase in the same location in the blood pool study which should represent hyperemia, but is always less pronounced than in the bone scan. In cellulitis the increased radioactivity is diffuse without a focal component and similar to that found in the blood pool study. The osteomyelitic changes are present before the classical radiological ones because the reparative process occurs before the destruction becomes evident. Because of our good experience in diagnosing osteomyelitis we feel that this study should be used when osteomyelitis is suspected and the normal clinical criteria are absent especially when the symptoms are in the axial skeleton.

**KINETICS OF  $^{111}\text{In}$  AS SHOWN BY BONE MARROW SCANS USING  $^{111}\text{In}$ -CITRATE.** Dieter M.H. Glaubitt and Klaus U.R. Haberland, Institut für Nuklearmedizin und Medizinische Klinik, Städtische Krankenanstalten, D-415 Krefeld, West-Germany

Scans performed for bone marrow imaging after intravenous administration of  $^{111}\text{In}$ -citrate supply remarkable information about the distribution of radioindium also in organs other than bone marrow. We carried out scans after intravenous injection of 3-5 mCi of  $^{111}\text{In}$ -citrate (carrier-free) in 11 patients suffering from end-stage renal failure treated by hemodialysis. The field of scanning covered the pelvis, the lumbar spine, and the proximal half of the femur. Scanning was performed in the first day 2-5 times and in the following days daily or in intervals of 1-3 days.

During the first hours after administration of  $^{111}\text{In}$  in the large blood vessels in the pelvis could be seen. Later on, there was an increasing uptake of radioindium in the region of the sacrum which normally shows the highest values among the pelvic organs. Unexpectedly we observed considerable radioactivity in the pudendal region of male patients; mainly the area of the penis was affected. This finding was observed from the first hour to several days after the injection of  $^{111}\text{In}$ -citrate. We saw distinctly less accumulation of radioindium in the pudendal region of female patients; our method of scanning gave no information about an uptake in the ovaries.

$^{111}\text{In}$ -citrate appears to be superior to  $^{99\text{m}}\text{Tc}$  sulfur rhenium colloid in delineating the extension and morphological details of the bone marrow. Nevertheless our results raise the question whether the long-continued  $^{111}\text{In}$  uptake in the pudendal region might be ascribed to an accumulation of radioindium in the testes, at least partly.

**IMAGING OF EXPERIMENTAL MYOCARDIAL CONTUSION WITH Tc-99m-Sn-POLYPHOSPHATE.** Raymundo T. Go, Ching L. Chiu, Donald B. Doty, Hsieh-Fu Cheng and James H. Christie, University of Iowa, Iowa City, Iowa.

Myocardial contusion is a clinical diagnosis and changes in EKG and serum enzymes are often nonspecific. In order to obtain a more accurate method of diagnosis of cardiac injury associated with closed chest trauma Tc-99m-Sn-Polyphosphate was studied to image experimental myocardial contusion.

Studies were done in 5 dogs (18-22kg.) under general anesthesia in the scintillation camera 1-2 hours after the intravenous injection of 5mCi of Tc-99m-Sn-Polyphosphate before and after contusion produced using the impact of a captive-bolt handgun to the chest wall. Follow-up scans were done when possible. All dogs were autopsied.

The scans showed no activity in the normal heart but showed increased activity in injured myocardium. This is corroborated by gross pathologic findings in 4 dogs and tissue distribution studies in 2 showing an injured to normal myocardium ratio of 4:1 and 14:1 in 2 dogs. Scans were positive early at 2-3 hours after injury in all dogs; persisted to 48 hours in 3, and up to 96 hours in one which was negative at the 8th day. High rib activity presents some problem. The mechanism of localization is under investigation.

This study shows good localization of Tc-99m-Sn-Polyphosphate in contused myocardium, and is presently undergoing clinical evaluation.

**THE "PHOTON DEFICIENT" AREA: A NEW CONCEPT IN BONE SCANNING.** T. Goergen, S. Halpern, N. Alazraki, V. Heath, R. Taketa, and W. Ashburn. University Hospital of San Diego County, San Diego, CA. and Veterans Administration Hospital, La Jolla, CA.

It is generally recognized that a positive bone scan consists visually of an area of increased photon accumulation over the affected area. It is not well appreciated that the opposite can be the case. In the past year, 8 patients with 4 disease processes involving bone (5 metastatic carcinoma, 1 sickle C disease, 1 aseptic necrosis, and 1 osteomyelitis) were studied in our community, in which the involved area of bone did not incorporate as much radiopharmaceutical as the surrounding bone and thereby presented as a "photon deficient" area on the scintiphoto. All of the malignancies were of pulmonary origin, either squamous cell or adenocarcinoma. Bone x-rays were normal or "lytic" in nature. The patient with sickle cell disease had a presumed bone infarct. The aseptic necrosis case was secondary to the trauma of an intramedullary nail and the osteomyelitis was acute and secondary to a staphylococcal infection. All bone scans were performed with  $^{99m}\text{Tc}$  polyphosphates ( $^{99m}\text{Tc}$  PP0) compounds, and in 2 cases repeat studies were performed with  $^{18}\text{F}$ . Repeat  $^{99m}\text{Tc}$  PP0 bone scans were also performed in several cases. Bone marrow scans using  $^{111}\text{In}$   $\text{Cl}$  were performed in 2 cases. Light microscopy of the lesions were available in 3 cases. The possibility exists that a spectrum of changes ranging from decreased to increased uptake may be present on bone scanning in a variety of diseases.

**BIFUNCTIONAL CHELATES FOR RADIOPHARMACEUTICAL LABELING.** David A. Goodwin, Claude F. Meares, Carol I. Diamanti, and Michael W. Sundberg, Stanford University, Palo Alto Veterans Administration Hospital and University of California at Davis.

It is difficult to use metal ions such as  $^{111}\text{In}^{3+}$  as labels for biologically interesting molecules because of their limited ability to form stable organometallic compounds under physiological conditions. In an effort to broaden the labeling capabilities of radioactive metals to include organic compounds other than chelates, a method using a covalent label based on metal chelate has recently been developed<sup>1</sup>. This bifunctional chelate utilizes the covalent metal binding molecule 1(p-benzenediazonium)-ethylene diamene-N, N', N'-tetraacetic acid (azo-EDTA). With this compound a ligand is formed between the EDTA-metal chelate and proteins or polypeptides by means of a diazo bond to tyrosine, histidine or lysine. We have used human serum albumin (HSA), Bovine fibrinogen, and bleomycin labeled with  $^{111}\text{In}$  in this way for studies of their distribution and metabolism in normal and tumor bearing mice, and for scintiphotos in dogs. The biological half life of  $^{111}\text{In}$  HSA agreed closely with control  $^{131}\text{I}$  HSA in white mice ( $T_{1/2}=28$  hours). The absolute tumor uptake of both  $^{111}\text{In}$  labeled albumin and fibrinogen was high;  $7.28 \pm .78\%$  per gm and  $7.75 \pm .17\%$  per gm;  $^{111}\text{In}$  bleomycin uptake was  $2.9\%$ /gm. In contrast, the control group, injected with azo-EDTA labeled with  $^{111}\text{In}$  had very little concentration of activity in any of the organs except the kidney, by which route it is rapidly excreted. These compounds show promise for

tumor imaging in humans. The technique represents an extension of general radioactive tagging which allows nearly any protein or polypeptide to be labeled with any metal strongly chelated by EDTA.

1. Sundberg, M. W.: Bifunctional EDTA analogues with applications for the labeling of biological molecules, Ph.D. Dissertation. Stanford Univ., Stanford, CA, 1973, 212 pp.

**SIMPLE MODIFICATIONS OF THE ANGER POSITRON CAMERA FOR ANGULAR CORRELATION MEASUREMENTS.** David A. Goodwin, Carol I. Diamanti, Claude F. Meares, and Michael W. Sundberg. Veterans Administration Hospital and Stanford University, Palo Alto, CA.

When a radionuclide decays by gamma-gamma cascade, and the two gamma rays are detected with a coincidence spectrometer, the counting rate may depend strongly on the angle between their directions of propagation. Using  $^{111}\text{In}$  as a label such measurements can determine the degree of binding by a macromolecule in vitro or in vivo, (e.g.: transferrin or antibody). The following modifications enable use of the positron system with either positron emitters or  $^{111}\text{In}$ .

A potentiometer was added to allow the 247 keV gamma<sub>2</sub> to fall within the window of the positron detector, while the gamma analyzer was adjusted to accept the 173 keV gamma<sub>1</sub>. The coincidence resolving time was lengthened to 200 nanoseconds and the input pulse from the positron detector was shortened to 50 nanoseconds. The two detectors were operated at both 90° and 180° to one another, with a source to detector distance of ten inches, using the shadow shield on the gamma detector.

Using  $^{111}\text{InCl}_3$  and  $^{111}\text{InPO}_4$  sources, each containing 15  $\mu\text{Ci}$  in 0.8 ml, the following values were obtained: for  $\text{InCl}_3$ : Anisotropy,  $A = 0.194$  ( $G_{22} = 1.01 \pm 0.05$ ), for  $\text{InPO}_4$ : Anisotropy,  $A = 0.051$  ( $G_{22} = 0.25 \pm 0.06$ ).

These values show conclusively that angular correlation measurements may be made quickly with a high degree of accuracy using a modified Anger Positron System.

**THE DIAGNOSTIC ACCURACY OF K-43 SCANS IN CARDIAC PATIENTS.** Ralph J. Gorten, Akira Nishimura, and John F. Williams, Jr. University of Texas Medical Branch, Galveston, TX

Early trials in man have suggested K-43 as a suitable myocardial scan agent. In order to challenge the actual value of this new diagnostic procedure in clinical situations, 2 cardiologists selected 85 patients for myocardial scans without providing any clinical information to the nuclear medicine staff. Rectilinear scans in anterior, left lateral, and right and left anterior oblique positions were performed shortly after intravenous doses (0.6-1.5 mCi) of  $^{43}\text{KCl}$ . Scan interpretations describing the presence and location of abnormal areas of decreased tracer concentration were recorded. The cardiologists determined the cardiac diagnoses based on all information except scan results.

In 48 patients with myocardial infarcts 36 hours to 11 years previously, scans were abnormal in 43 (88% correct). In 16 persons with acute infarcts there were 15 abnormal scan results (94% correct). Serial ECGs were diagnostic in 15 and serial blood enzymes in 14, though neither approached this accuracy with a single observation.

Normal scans were recorded in 25 of 28 persons without infarcts (89% correct). Of these, 12 had coronary artery disease with angina and 16 had other diseases. In 9 patients who possibly had myocardial infarcts, scans were abnormal in 3 and normal in 6. Coronary arteriographic findings correlated poorly with scan results. For instance 12 patients demonstrated normal scans and hemodynamically significant arteriographic abnormalities.

In conclusion, myocardial scanning with K-43 is sufficiently accurate for clinical use in detecting the presence and location of myocardial infarcts although acute and chronic stages cannot be distinguished. Coronary arterial narrowing does not directly cause K-43 scan abnormalities. Static imaging abnormalities depend on the presence of focal ischemic necrosis or fibrous tissue replacement.

**ALTERED RETICULO-ENDOTHELIAL (RE) FUNCTION IN HEMATOLOGIC DISEASES.** F. Goswitz, C. Morris, K. Kim, and M. Hansard. Oak Ridge Associated Universities, Oak Ridge, Tenn.



Useful dynamic function data were obtained after i.v. injection of two different radio-colloids (0.25 mCi <sup>198</sup>Au; 0.25 mCi <sup>99m</sup>TcS) and measurement of count rates over liver, sacrum, spleen, and thigh or heart. The counting system consisted of four scintillation detectors and a spectrometer interfaced to an IBM-1800 computer.

In 36 cancer patients, with and without hematologic disease, the <sup>99m</sup>TcS colloid prepared by the sodium sulfate method has a quicker uptake by the liver and an earlier plateau there (presumably because of its larger particles) and disappears rapidly from the blood. Usually more radioactivity is concentrated in the spleen with <sup>99m</sup>TcS colloid than with <sup>198</sup>Au, but at a relatively slower rate.

In polycythemia vera (PV) the peak sacral activity is attained very quickly and the liver-sacrum ratio is less than normal. In chronic granulocytic leukemia (CGL) the spleen to heart ratios at 25 min after injection are greater than PV and the spleen has a slow rate of <sup>99m</sup>TcS uptake. In chronic lymphocytic leukemia and lymphocytic lymphoma the splenic uptake is higher, but not necessarily faster, than the controls. Patients with Hodgkin's and histiocytic lymphoma have lower splenic uptakes than those with acute granulocytic leukemia but similar increased rates of uptake by the liver, with rapid blood clearance.

Hematologic disorders have altered RE uptake of radiocolloids and differences were noted between <sup>198</sup>Au and <sup>99m</sup>TcS colloids. Temporal patterns of uptake by RE organs for selected disorders appear to have significance.

**RADIOCOLLOID SPLEEN SCANNING IN LYMPHOMA AND CHRONIC LYMPHOCYTIC LEUKEMIA.** F. Goswitz, Oak Ridge Associated Universities, Oak Ridge, Tenn.

Radiocolloid scans with <sup>99m</sup>Tc (1 mCi i.v.) or <sup>198</sup>Au (0.2 mCi i.v.) were done to determine a size or focal abnormality of the spleen. Their clinical value was assessed by relating the scan's interpretation to the organ's histology after splenectomy in 36 patients with Hodgkin's (HD) or non-Hodgkin's (NHL) lymphoma and three patients with chronic lymphocytic leukemia (CLL) and hypersplenism.

The spleen, in the adult, was considered enlarged if its area on the posterior scan exceeded 100 cm<sup>2</sup> or if its length exceeded 13 cm. In all 20 HD patients splenectomy was part of a routine management plan. In the other two groups a specific indication (hypersplenism mostly) was responsible for the splenectomy although in 8 of the NHL group, it was a prophylactic procedure.

Results are summarized as follows:

Patients in study	20	16	3
Diagnosis	HD	NHL	CLL
Splenomegaly (with tumor)	15(11)	13(9)	2(1)
Normal-size spleen (with tumor)	5(2)	3(1)	1(1)

One false positive and five false negative scans were reported in our estimation of splenomegaly, i.e., weight of organ more than 175 g. No scans showed any focal defects.

When splenomegaly existed in patients with HD or NHL and those with CLL and hypersplenism, the chance of disease involvement of the spleen was 73%. This finding strengthens the argument that such patients should undergo laparotomy and splenectomy if other problems do not preclude it. The scans were useful in showing splenomegaly, often when the organ was not palpable, but missed some cases of borderline enlargement.

**ADVANCED LIVER IMAGING.** A. Gottschalk, B.E. Oppenheim, C. Beckerman and P.B. Holler. The Franklin McLean Memorial Research Institute.

This review of liver scanning will concentrate on four aspects of colloid liver imaging.

The first will consist of a discussion of normal hepatic anatomy, and common and uncommon anatomic variants.

Secondly, a variety of imaging artifacts will be illustrated. These include interpretation of metal-

lic objects between the liver and the detector; artifacts from overlying soft tissue such as breast; and problems posed by poorly prepared colloid preparations.

Thirdly, the characteristic appearance of common (and some unusual) hepatic lesions will be shown.

Finally a variety of adjuncts will be illustrated that have proved useful. For example, transmission images, and inspiration-expiration comparisons are quick, simple, and informative.

Although designed as a basic discussion of hepatic imaging, some of our own approaches to this topic may be useful to the more experienced.

**DOSIMETRY OF SKELETAL-SEEKING RADIOPHARMACEUTICALS.** L.S. Graham and G.T. Krishnamurthy, and B.H. Blahd, UCLA School of Medicine and Veterans Administration, Wadsworth Hospital Center; Los Angeles, California.

Human kinetic data for technetium-labeled polyphosphate (Tc-POLY), technetium-labeled diphosphate (Tc-DIP), technetium-labeled pyrophosphate (Tc-PYRO), and fluorine 18 (F 18) were used in calculating the absorbed radiation dose to the skeleton, blood, bladder, total body, and ovaries by the MIRD technique. After intravenous injection, all four agents clear from blood in a bi-exponential fashion. The rapid clearance phase was taken to represent uptake by bone; slow clearance was taken to represent renal excretion. For Tc-POLY, Tc-DIP, Tc-PYRO, and F 18 the biological clearance half-time of the first exponential was 30, 18, 14, and 24 min., respectively. For the second or late phase, the half-time was 294, 168, 380, and 198, respectively.

A three compartment model (blood, skeleton, and bladder) was used to calculate the cumulative activities for those organs. For the bladder compartment it was assumed that complete voiding occurred at 3.0 hours, then every 4.8 hrs. thereafter. The reciprocity theorem was used to calculate the radiation absorbed dose to the ovaries. The following table summarizes the dose to the patient on a rad/mCi and total dose basis (15 mCi of technetium labeled compounds; 4 mCi of F 18):

	Blood		Skeleton		Bladder		Total Body		Ovaries	
	Rad	Rad	Rad	Rad	Rad	Rad	Rad	Rad	Rad	Rad
	mCi	mCi	mCi	mCi	mCi	mCi	mCi	mCi	mCi	mCi
<sup>99m</sup> Tc-POLY	.020	.30	.066	.99	.203	3.04	.016	.24	.028	.42
<sup>99m</sup> Tc-DIP	.018	.27	.068	1.02	.229	3.44	.016	.24	.030	.45
<sup>99m</sup> Tc-PYRO	.018	.27	.068	1.02	.230	3.45	.016	.24	.030	.45
<sup>18</sup> F	.086	.34	.178	.71	1.36	5.44	.045	.18	.087	.35

Under the assumptions stated and for the agents tested, our calculations reveal that radiation absorbed dose to the patient probably does not constitute a valid criterion for choosing a skeletal seeking radiopharmaceutical in man.

**RADIATION ABSORBED DOSE IN PATHOLOGICAL RETENTION VS. COST AND QUALITY CONTROL FOR CISTERNOGRAPHIC AGENTS.** Thomas A. Graham, Jack N. Hall, and Robert E. O'Mara. University of Arizona Medical Center, Tucson, Ariz.

Absorbed dose rate calculations were performed for <sup>131</sup>I, <sup>111</sup>In, <sup>169</sup>Yb, and <sup>203</sup>Pb to compare the radiation effects due to pathologic retention of radiopharmaceuticals with these labels.

Dose rates contrasting with values given by Goodwin, et al., and Hosain, et al., show the relative significance of non-penetrating radiation in cisternography using <sup>131</sup>I-HSA, <sup>111</sup>In-DTPA, <sup>169</sup>Yb-DTPA and <sup>203</sup>Pb-EDTA. Decay schemes were examined for improved estimates of non-penetrating radiation. Absorbed fractions for an appropriate volume were used for penetrating emissions in 10 grams of tissue. Total absorbed dose was computed for infinite retention in the small volume.

The problems of incomplete sterility testing, and possible chemical meningitis are discussed. Separate considerations of local concentration, retention of the radioactive label, and comparative cost is indicated for each agent.

The agent of choice for cisternography is <sup>203</sup>Pb-EDTA considering cost and risk. <sup>169</sup>Yb-DTPA may be preferred for protracted studies, but the possibility of absorbed doses over 1000 rads is shown.

**VALUE OF RADIOGALLIUM STUDIES IN CHEST DISEASE.**  
S.F. Grebe, J.K. Siemsen, D. Wentz and E.N. Sargent. University of Giessen, Germany and University of Southern California, Los Angeles, Calif.

Gallium-67 accumulation in benign as well as malignant lesions requires re-evaluation of its significance. Scans on 459 patients with various definitely diagnosed chest diseases were selected for "blind" re-interpretation. Negativity was defined as body-background equal to activity in an abdominal area free of bowel concentration; all other scans were classified as positive. All scans were done with single- or double-headed 5" crystal rectilinear scanners, with at least anterior and posterior projections. Findings were tabulated as follows:

	Pos.	Neg.		Pos.	Neg.
Normal Controls		90	Sarcoidosis	15	5
Carcinoma	103	11	Silicosis	24	
Hodgkins	47	7	Asbestosis	8	
Tuberculosis			Chronic		
Active	93	2	Pneumonia	3	9
Inactive		21	Abscess	4	
Tuberculoma		6	Fibrosis		11

All patients were untreated at the time of their first scan. After appropriate therapy, gallium concentration disappeared or decreased greatly in all of 52 cases of tuberculosis and all of 4 cases of sarcoidosis. The malignant lesions escaping detection were 2 neurinomas, 6 hilar lesions smaller than 2 cm in diameter, and 3 bronchial carcinomas which for unknown reasons failed to concentrate <sup>67</sup>Ga.

The results support the concept that gallium accumulation indicates high cellular and metabolic activity of a given lesion rather than any specific diagnosis.

**AN ECG-GATED SCINTIGRAPHIC IMAGING PROCEDURE FOR STUDYING VENTRICULAR FUNCTION.**  
Michael V. Green, Harold G. Ostrow, Margaret A. Douglas, Richard N. Scott, Richard W. Myers, James J. Balley, and Gerald S. Johnston. National Institutes of Health, Bethesda, Md.

An ECG-gated, computer-based, scintigraphic imaging procedure is described that produces a sequence of consecutive 10-millisecond images to represent a single, complete, average cardiac cycle. Repetitive projection of this image sequence as a scintigraphic cineangiogram permits visualization of the dynamic behavior of the entire heart and associated vasculature during both systole and diastole and can reveal defects such as myocardial akinesis.

The picture sequence can also be investigated quantitatively to directly yield ejection duration and to estimate ejection fraction. Relative (and potentially absolute) measures of instantaneous ventricular volume and maximum instantaneous flow can also be made.

Limitations to the quantitative aspects of the procedure include those imposed by variable R-R interval lengths, uncertainties in the calculation of ventricular background and various physical and subject-detector geometry considerations.

The procedure offers several advantages over other techniques for assessing ventricular function. It is non-invasive, repeatable, may be performed by technical personnel and can yield information not readily obtained by other methods.

**A COOPERATIVE GROUP TO STUDY LOCALIZATION OF RADIOPHARMACEUTICALS.** Robert H. Greenlaw, Marshfield Clinic, Marshfield, Wis.

A group of physicians has organized to cooperate on studies prescribed by protocol to evaluate new radiopharmaceuticals as tumor localizing agents. The elements of mounting this cooperative project will be discussed.

The Oak Ridge Associated Universities functions as sponsor and secretariat for the group.

Activities by participants in the group are guided by Constitution and By-Laws adopted by the membership. Protocol studies with radiogallium have been funded and pursued. Details have been established which lead to standardized use of rectilinear scanners by members of the group. Reporting forms have been generated which standardize data collection and storage. The ORAU computer is used for storing the data collected and for its retrieval to permit detailed analysis.

Studies of gallium scans on more than 2500 patients have been recorded. The disease entities having the largest numbers of patients investigated are the malignant lymphomas and the lung cancers. A wide variety of other categories of neoplasm has been studied but with smaller numbers per category. Relative frequency of diagnostic localization of tumor by scanning will be presented in summary.

The evaluation of new radiopharmaceuticals is feasible with a group of investigators, cooperating, using standardized methods. Large numbers of patient studies may be pooled so as to enhance validity of observations. New protocols are being pursued for comparing other radiopharmaceuticals with studies using radiogallium.

**A COMPARATIVE STUDY OF CONVENTIONAL SALINE LOAD TEST AND ISOTOPIC METHOD FOR MEASURING GASTRIC EMPTYING TIME (GET) IN MAN.** Alan J. Greenwald, Tapan K. Chaudhuri, Robert C. Heading, and Tuhin K. Chaudhuri. University of Iowa Hospitals, Iowa City, Iowa.

<sup>99m</sup>Tc-DTPA has been found to be an ideal agent for measuring GET because it is nonabsorbable, nonadsorbable and homogeneously distributed in a liquid meal. The purpose of this paper is to present a comparative study of the conventional saline load test and the more recently introduced isotopic method for the measurement of gastric emptying rate. A group of 10 normal male volunteers between the ages of 24 and 30 years underwent at least three studies by each of the two methods, namely, (a) aspiration method of Goldstein and Boyle incorporating our modification, and (b) an isotopic method employing a gamma camera with a computer and using a meal of isotonic saline mixed with 1 mCi of <sup>99m</sup>Tc-DTPA. After positioning supine under the gamma camera face, the subjects consumed the test material and sequential gastric scintiphotos were collected every minute on a magnetic tape (with a PDP-8 computer) over a period of 20-30 minutes. At the end of the study, a dynamic readout of the computer data was obtained and the T<sub>1/2</sub> value was determined from a semilog plot. When one deduces the saline load test value in terms of T<sub>1/2</sub> (8.8±3.5 min), it appears to be faster than the isotopic method (12±3 min) probably due to incomplete aspiration of the gastric fluid in the former method giving rise to a false faster emptying time. Moreover, variations in T<sub>1/2</sub> value in the same individual was much more in the aspiration method than in the isotopic method. Estimated absorbed radiation dose to the small intestine is about 0.029 r/mCi, assuming 100% retention of the test material in the gut. Because of its simplicity, non-invasiveness, minimal radiation dose and better accuracy, the isotopic method of measuring GET is superior to the conventional aspiration method.

**ATTENUATION CORRECTION FOR THREE-DIMENSIONAL IMAGING.** Grant T. Gullberg and Thomas F. Budinger. Lawrence Berkeley Laboratory, University of California, Berkeley, Calif.

Quantitative three-dimensional reconstruction of the distribution of emission sources used in nuclear medicine requires compensation for photon attenuation. The iterative least squares technique can be adapted to include the effects of attenuation and noise. This method determines the best estimate A, which minimizes the least square function

$$R(A) = \sum_{k,\theta} \frac{(P_{k\theta} - R_{k\theta})^2}{P_{k\theta}}$$

where

$$R_{k\theta} = \sum_{i,j}^0 A(i,j) \quad (i,j) \in \text{ray}(k,\theta)$$

A(i,j) represents the value for the picture element, f<sub>ij</sub><sup>0</sup> is the attenuation factor, and the measured projection P<sub>kθ</sub> for the angle θ is assumed to be the variance for the measured

error. Thirty-six views at 10° increments are taken by rotating the patient before the gamma camera. In order to calculate the value for  $f_{ij}^0$ , we first set  $f_{ij}^0 = 1$  and form 18 geometric means by taking the square root of the product of conjugate views. After a few iterations, we use a search routine to determine the boundary of the object and then evaluate  $f_{ij}^0 = \exp(-\mu L_{ij}^0)$  assuming that  $\mu$  is a constant attenuation coefficient and  $L_{ij}^0$  is the distance from the pixel to the boundary. Using the calculated  $f_{ij}^0$ , which requires a buffer size of 76K and all 36 views for  ${}^{111}\text{In}$ , we then iterate another 8 to 10 times.

Results of three-dimensional reconstructions with and without attenuation correction for simulated projections, actual phantoms, and patient brain scans show quantitative reconstruction if the attenuation coefficient is constant. For variable attenuation coefficients, a transmission study is done to determine  $f_{ij}^0$ .

**A NEW KIT FOR RBC LABELING AND SPLEEN SCANNING: Tc-99m STANNOUS GLUCOHEPTONATE.** R. F. Gutkowski and H. J. Dworkin. William Beaumont Hospital, Royal Oak, Mich.

${}^{99m}\text{Tc}$  sulfur colloid is inadequate for visualizing the spleen when the liver is enlarged or overlaps the splenic area of interest (ectopic spleen). The  ${}^{51}\text{Cr}$  tagged autologous heat damaged red blood cell (HD-RBC) method is radiation dose and photon limited and not ideal for the Anger camera. Previous tagging methods employing  ${}^{99m}\text{Tc}$  require special expertise and may give a loose  ${}^{99m}\text{Tc}$ -RBC bond. The stannous glucoheptonate (Sn-G) kit proposed gives an adequate  ${}^{99m}\text{Tc}$ -RBC bond and is no more complex than the  ${}^{51}\text{Cr}$  HD-RBC method.

**Method:** To a Unitag bag containing 10 ml of heparinized blood and 2 ml of ACD solution, add the contents of Sn-G vial (200 mg Na Glucoheptonate; 0.1 mg Sn  $\text{Cl}_2$ ) in 1 ml of 0.9% saline. Mix and incubate for 5 min. Wash RBC by adding 1 ml of 5% EDTA solution, centrifuge and remove supernate. Repeat wash using 0.9% saline. Add Na  ${}^{99m}\text{TcO}_4$  to cellular fraction and labeling is complete (>96%) in 10 min. These RBC may be used for RBC volume determination or if heat damaged, (49°C, 15 min) for spleen imaging.

**Results:** Autologous  ${}^{51}\text{Cr}$  and  ${}^{99m}\text{Tc}$  labeled RBC given simultaneously yielded similar RBC volumes and blood disappearance curves to 30 min. post-dose in dog and man.

Labeled rat HD-RBC gave similar spleen/liver ratios (radioactivity/gm) of 12 to 25 for  ${}^{99m}\text{Tc}$  and  ${}^{51}\text{Cr}$  out to 120 min. post-dose.

In 4 patients  $T_{1/2}$  blood disappearance of  ${}^{99m}\text{Tc}$  HD-RBC was 10 min. with maximum plateau activity in spleen reached by 30 min. By external detection the spleen/liver ratios were > 5.2. Spleen images are of good diagnostic quality.

**Conclusion:** The  ${}^{99m}\text{Tc}$  Sn-G kit for labeling RBC is simple, rapid and reproducible. Good quality spleen images may be recorded 30 min. post-dose using 1 to 10  $\mu\text{Ci}$   ${}^{99m}\text{Tc}$  HD-RBC.

**${}^{67}\text{Cu}$ -BLEOMYCIN: A TUMOR LOCALIZING AGENT.** Jack N. Hall, Robert E. O'Mara. University of Arizona College of Medicine, Tucson, Ariz. and Philip Cruz. University of Arizona College of Pharmacy, Tucson, Ariz.

The anti-neoplastic antibiotic, bleomycin, has been labeled with several radionuclides. Each of these agents presents some drawback. It has been well known that bleomycin chelates readily with cupric ion. However, a suitable radioisotope of copper was not available until recently.

${}^{67}\text{Cu}$  was obtained from Oak Ridge National Laboratory. It decays with a 58 hour half-life by beta emission and emits two main gamma rays at 92 keV (23%) and 184 keV (40%). The  ${}^{67}\text{Cu}$  was chelated with the bleomycin by a simple method and radiopharmaceutical purity was checked by radiochromatography. Biological distribution studies were performed by means of sequential radionuclide scintigrams and tissue distribution studies in normal and tumor-bearing animals.

The descending order of tissue distribution with respect to the  ${}^{67}\text{Cu}$ -Bleomycin level was kidney, liver, tumor, gut, lungs, muscle and brain. The tumors were visualized at 15 minutes post-injection, but better scintigrams were obtained at 24 hours. The tumor to non-tumor (muscle) ratio of

the  ${}^{67}\text{Cu}$ -Bleomycin was approximately double that of  ${}^{111}\text{In}$ -Bleomycin in a highly vascular tumor (hepatoma).

${}^{67}\text{Cu}$ -Bleomycin appears to be an improved tumor-localizing agent when compared to  ${}^{111}\text{In}$ -Bleomycin in animal studies. Further work regarding the pharmacokinetics and toxicity of this agent are now in progress.

**203Pb: A NEW ERYTHROCYTE LABELING AGENT.** Jack N. Hall, David P. Jeffrey and Robert E. O'Mara. University of Arizona Medical Center, Tucson, Az.

The association of inorganic lead with erythrocytes has been well known for over 30 years. Recent work has suggested that lead reacts with the hemoglobin. The purpose of this study was to determine the potential use of  ${}^{203}\text{Pb}$ -Erythrocytes for blood volumes, red cell survival studies, GI blood loss, placental localizations and spleen imaging agent.

In vitro and in vivo experiments were conducted on dogs, rabbits, and humans (normal and with blood dyscrasias, i.e. hemochromatosis, polycythemia) for labeling efficiency and affinity. Incubations were performed at room temperature and at 49.5°C. in a water bath for 15 minutes. Anticoagulants used were either ACD (Strumia Formula) or Ammonium Heparin (150 u) and up to 1.5 ml. of carrier free  ${}^{203}\text{Pb}$  in the form of acetate or chloride. The labeling efficiency was greater than 97% in all human samples using Heparin as the anticoagulant but less than 10% utilizing ACD. Red cell survival studies in dogs demonstrated a multi-component curve with a varied elution rate of the  ${}^{203}\text{Pb}$  from the erythrocyte. However, the heat-denatured erythrocyte portrays an excellent spleen perfusion and scanning agent in dogs with excellent scans obtained within one hour post-injection.

When current investigations regarding toxicity and disposition of this agent are completed, a comparison study of (heat-denatured)  ${}^{203}\text{Pb}$ -Erythrocytes with current spleen scanning agents will be performed.

**BONE SCINTIGRAPHY WITH  ${}^{99m}\text{Tc}$ -PYROPHOSPHATE--ITS RELATIONSHIP TO BONE METABOLISM.** Ken Hamamoto, Itsuo Yamamoto, Rikushi Morita, Toru Mori, and Kanji Torizuka. Kyoto University Hospital, Kyoto, Japan.

Scintigraphy of bone and joint with  ${}^{99m}\text{Tc}$ -pyrophosphate (TcPyP) was performed for 134 cases with primary bone tumors, metastatic bone tumors and other diseases of bone and joint. The results were compared with the value of serum alkali-phosphatase, x-ray findings and the results of bone kinetic study with  ${}^{47}\text{Ca}$ .

All 24 cases with primary bone tumors showed positive results with exception of 2 of 5 cases with fibrous cortical defect whose results were negative. No abnormalities were noted on the x-ray films in 13 of 20 cases with metastatic bone tumors whose scintigraphies were positive. In some cases under chemotherapy, hormone therapy, or radiation therapy, metastatic bone lesions were not demonstrated on scintigrams. All 8 cases with multiple myeloma showed rather decreased accumulation of TcPyP. The grade of TcPyP uptake to bone was determined on the scintiphotos.

The kinetic studies with  ${}^{47}\text{Ca}$  were performed for normal subjects, patients with metastatic bone tumors, hyper- and hypoparathyroidism, osteoporosis, multiple myeloma and primary amyloidosis. In comparison of the calcium kinetics with TcPyP scintigraphy, increased uptake of TcPyP in the lesions was seen in cases with accelerated calcium metabolism and decreased uptake was seen in cases with decreased calcium kinetics.

It is concluded that TcPyP scintigraphy reflects the calcium metabolism of bone, and is useful in early detection of metastatic lesions of bone.

**DETECTION OF STRESS INDUCED REGIONAL MYOCARDIAL ISCHEMIA IN HUMANS BY INJECTION OF MAA AT REST AND DURING CONTRAST INDUCED CORONARY HYPEREMIA.** Glen W. Hamilton, Jim L. Ritchie, K. Lance Gould, and David Allen. VA Hospital, Seattle, Wash.

We have previously demonstrated in animals that resting coronary flow and regional distribution are normal in spite of coronary stenosis of up to 85%. However, the coronary flow response to stress and hyperemic regional distribution are both progressively impaired by stenosis exceeding 35%. 28 patients undergoing coronary arteriography were studied in the following manner. 1.5 mCi of  $^{113m}\text{In}$  MAA was injected into the right or left coronary at rest and 2-3 mCi of  $^{99m}\text{Tc}$  MAA was injected 6-10 seconds following 8 cc of Hypaque 75 M. The latter injection was timed to coincide with phase of maximal hyperemia induced by contrast material. Myocardial scintiphotos of  $^{113m}\text{In}$  and  $^{99m}\text{Tc}$  were obtained in the anterior, left anterior oblique and left lateral views using a gamma camera with a medium energy collimator.

No untoward hemodynamic responses occurred. 4 patients with no coronary disease showed normal distribution of MAA at rest and during hyperemia. 14 patients with exertional angina demonstrated regional perfusion defects during hyperemia which were not present at rest. 3 patients with infarction and single vessel disease showed defects at rest which did not change during hyperemia. 7 patients with severe 3 vessel disease demonstrated no changes between the resting and hyperemic studies. All patients (14) with new defects during coronary hyperemia had a greater than 35% stenosis of the artery supplying the area of the defect. We suspect that hyperemic distribution studies are more accurate predictors of regional myocardial ischemia than coronary arteriography.

**THE THEORETICAL BASIS FOR THE DETECTION OF STRESS INDUCED REGIONAL MYOCARDIAL ISCHEMIA BY INJECTION OF DUAL ISOTOPE MAA.** Glen W. Hamilton, K. Lance Gould, David Allen, and Jim L. Ritchie. VA Hospital, Seattle, Wash.

Resting coronary blood flow may be normal in spite of severe coronary stenosis. The relationships between coronary blood flow, degree of coronary stenosis, pressure gradient and regional distribution was determined in 22 dogs. Coronary flow was measured with single or dual electromagnetic flowmeters and regional distribution determined by quantitative analysis of scintillation images of  $^{99m}\text{Tc}$  and  $^{131}\text{I}$  MAA injected into the left atrium. Angiographic contrast material, which increases flow 4-5 times resting, was used to repeatedly induce coronary hyperemia.

Coronary stenosis of less than 35% caused no abnormalities in coronary flow or regional distribution either at rest or during coronary hyperemia. With increasing degrees of stenosis, a pressure gradient developed, but resting flow and distribution remained normal until the stenosis exceeded 85%. However, coronary flow reserve or the ability to increase flow in response to stress and regional distribution during coronary hyperemia became progressively impaired with stenosis exceeding 40% and markedly abnormal before resting flow was impaired. Impairment of coronary flow reserve was closely related to both the degree of stenosis and the pressure gradient across the stenosis. Regional flow distribution determined by imaging was uniformly related to coronary flow measured by flowmeter ( $r = 0.96$ ). The degree of coronary stenosis could thus be predicted from the regional distribution images. Likewise, defects in MAA images injected at rest detected regional infarction or severe ischemia and defects in images injected during maximal coronary hyperemia detected regional areas of stress induced ischemia.

**CLINICAL EXPERIENCE WITH  $^{99m}\text{Tc}$ -DMSA (DIMERCAPTOSUCCINIC ACID, A NEW RENAL IMAGING AGENT.** Hirsch Handmaker, Bradford W. Young, and Ray E. Stutzman

The study was performed to evaluate the clinical usefulness of a new renal imaging agent,  $^{99m}\text{Tc}$ -

Dimercaptosuccinic Acid. Following the intravenous injection of the material serial scintiphotos and delayed static scintiphotos were obtained. 25 patients with a variety of renal diseases were studied, and the information obtained compared with urographic, angiographic and/or other radionuclide renal studies.

In all patients with normal renal function the quality of the renal scintiphotos was judged excellent with virtually no pelvicalyceal interference.

In 4 of 5 patients with renal failure (BUN greater than 100 mg.%), the renal cortical detail was only fair, but size and presence of two kidneys was not apparent on any other type of study besides the DMSA scintiphotos. In one case confirmation of two kidneys proved accurate in spite of poor arteriographic visualization on one side. In 2 of 5 patients with chronic pyelonephritis the scintigraphic changes were more severe than suspected by urography.

The physical characteristics of the  $^{99m}\text{Tc}$  Technetium and the mercurial-like properties of the DMSA chelate permit high resolution images of the renal cortex in virtually all patients, and renal tissue is identifiable even in renal failure. The commercial availability of the material in a kit form makes it convenient for use in all laboratories. The low radiation exposure makes the agent suitable for use in pediatrics.

**PREOPERATIVE DIAGNOSIS OF SPLENIC ABSCESS USING SCINTIGRAPHIC TECHNIQUES.** Hirsch Handmaker and Gerald S. Freedman. Children's Hospital of San Francisco, San Francisco, Ca. and Yale New Haven Medical Center, New Haven, Conn.

This study reports the presence of an abnormal spleen scintiphoto in four patients who were later found to have splenic abscess. As the disease is rare (0.4% of all autopsies) and has a high morbidity and mortality when not treated surgically, the preoperative diagnosis of this entity in these cases, all within one year's time, justifies this report.

Patients were studied following the intravenous injection of  $^{99m}\text{Tc}$ -Sulfur Colloid, with routine views obtained with a gamma camera. In all cases the reason for the study was to detect splenic abscess.

Two patients had undergone prior surgery for ruptured appendices, and had postoperative fever and left upper quadrant pain. One patient had a dysgamma globulinemia with salmonella sepsis, the fourth patient had a rare anemia, fever, and left upper quadrant pain. All four patients were found to have defects in their splenic scintiphotos, and at surgery were found to have splenic abscess. All did well following surgery.

Literature review reveals a total of three cases of splenic abscess detected preoperatively by splenic scintigraphy. Two out of these three cases did well postoperatively.

It would appear that splenic scintigraphy can be a useful diagnostic technique in the preoperative diagnosis of this serious disease.

**RADIATION EXPOSURE TO THE FAMILY OF RADIOACTIVE PATIENTS.** John C. Harbert and Sister Nola Wells. Georgetown University Hospital, Washington, D.C.

AEC licensing regulations require that patients receiving therapeutic  $^{131}\text{I}$  and  $^{198}\text{Au}$  be hospitalized until no more than 30 mCi remains in the body except under certain well-defined conditions. Patients frequently inquire, particularly those receiving large doses, to what risks they may subject family and friends. Furthermore, recent discussions among regulatory officials have included suggestions for lowering the allowed radionuclide burden with which patients may be discharged from the hospital. To determine what radiation dose close family members might practically expect to receive from radioactive patients we provided family members with film badges for 8 days following the patient's discharge. Patients treated with moderate to large amounts of  $^{131}\text{I}$  for thyroid ablation or cancer were selected. Patients were instructed to sleep alone and to keep contact with infants at a

minimum during the 8 days. Four patients treated for thyroid cancer and discharged with burdens of 18 to 43 mCi <sup>131</sup>I had a total of 11 close relatives. No relative received greater than 80 mr during the first 8 days which extrapolates to a maximum of 130 mr assuming a 6-day biologic half life. Seven patients treated for thyroid ablation and discharged with 22.3 to 36.4 mCi had 11 relatives. No relative received more than 50 mr during the 8 days or a maximum integration of 85 mr. It was concluded from this study that: (1) The guidelines laid down in NCRP Report #37, 1970 are conservative and relatives are unlikely to receive the permissible exposure of 500 mr per year as a result of association with patients discharged with currently allowed radionuclide burdens. (2) There is no good reason from a public health standpoint to lower currently allowed radionuclide burdens, a step which would add to health care costs.

**IMAGING STUDIES WITH <sup>81</sup>Rb-<sup>81m</sup>Kr.** P. V. Harper, B. Rich, N. Lembares, and K. A. Lathrop. Franklin McLean Memorial Research Institute, University of Chicago, Chicago, Ill.

The use of 4.6 h <sup>81</sup>Rb for imaging studies has been made practical with the elimination of the <sup>82m</sup>Rb contaminant by use of ~20 MeV <sup>3</sup>He<sup>++</sup> or ~7.5 MeV <sup>2</sup>H<sup>+</sup> on an enriched <sup>80</sup>Kr target, with yields of several hundred  $\mu$ Ci/ $\mu$ Ah. The whole-body absorbed dose (~100 mrad/mCi) for <sup>81</sup>Rb alone is increased substantially by trace contamination with long-lived <sup>83</sup>Rb and <sup>84</sup>Rb. Myocardial localization gives reasonably good camera images using the 446-511 keV photopeaks of <sup>81</sup>Rb with a parallel hole <sup>44</sup>Ti tungsten collimator. Imaging with the 190 keV photopeak of the 13 sec <sup>81m</sup>Kr daughter gives ~3 times as great a count rate over the myocardium, although high-energy collimation is still required. A substantial increase in the lung background (70%) is observed from the <sup>81</sup>Kr generated elsewhere in the body and deposited in the lungs by the circulation. Estimation of tissue perfusion by quantitation of the Kr/Rb ratio gave reasonable figures for the myocardium, although precise attenuation corrections were not possible. Relative regional perfusion differences, however, should be demonstrable. Liver and kidney localization appears sufficient to allow perfusion measurements, since these organs normally have a high perfusion rate.

**ON MAXIMUM OBTAINABLE COUNT RATES FOR DYNAMIC STUDIES.** C. Craig Harris, Robert H. Jones, Jack K. Goodrich, Lynn R. Witherspoon and Bryce B. Bates. Duke University Medical Center and V.A. Hospital, Durham, N.C.

Published data (1) show that a multi-crystal camera (Baird-Atomic System 70) yielded count rates of 220,000 cps from 15 mCi Tc-99m with efficient collimation. With high-resolution collimation this count rate is reduced by about a factor of 5. These data show as expected that high sensitivity is available only at the expense of geometrical resolution. It is unfortunate these data have been used as the basis for the idea that the System-70 achieves higher count rates with less radioactivity than do Anger cameras, even within the count rate capability of the latter. With amounts of Tc-99m now used in most clinical studies single-crystal cameras achieve count rates comparable to the System-70 with collimators of comparable efficiency and high geometrical resolution. Furthermore image quality, though impaired, is maintained at count rates in excess of 40,000 cps on a Searle Pho/Gamma HP. While the System-70 has a higher count rate limit, this limit can be approached with reasonable amounts of radioactivity only with high-efficiency collimators with correspondingly compromised geometrical resolution. Anger cameras operate satisfactorily and competitively within their count rate capability (up to 45,000 cps or more) when high efficiency collimators are used. 1.) Jones, R.H. et al. Description of a new high count rate gamma camera system. IAEA Symposium on Medical Radioisotope Scintigraphy, Monte Carlo, Monaco (IAEA/SM-164/122).

**HEAVILY-IODINATED FIBRINOGEN, A LOCALIZING AGENT FOR PRE-FORMED THROMBI.** John F. Harwig, R. Edward Coleman, Sylvia S.L. Harwig, Michael J. Welch, Laurence A. Sherman, and Barry A. Siegel. Mallinckrodt Institute of Radiology, St. Louis, Mo.

As part of our study of the detection of pre-formed thrombi, we are investigating the use of heavily-iodinated fibrinogen. High thrombus-to-blood activity ratios should be attainable with such species due to increased catabolic rate but relatively unchanged clottability compared to normal fibrinogen. We have prepared fibrinogen-<sup>131</sup>I iodinated to the extent of 75, 100, 150, and 175 iodine atoms per molecule by a simple electrolytic procedure. The reaction employs I<sub>2</sub> as the iodinating species. Isotopic clottability of the product ranges from 60-70%. Hydrolytic de-iodination at 37° in pH 7.4 normal saline occurs at ~2% per day. Molecular weight profiles on a Sepharose 4B gel column reveal considerable front tailing on the fibrinogen peak, indicating that much of the labelled material has a significantly higher molecular weight than authentic fibrinogen. *In vivo* clearance in dogs occurs at a dramatically faster rate compared to normal fibrinogen, with some activity accumulating in the liver and spleen. Injection of heavily-labelled fibrinogen (100 iodine atoms per molecule) 4 hours after induction of a thrombus in the femoral vein gives a ratio of activity in the thrombus to TCA-precipitable activity in the blood 24 hours later of 50:1. Normal fibrinogen under the same conditions gives a ratio of 23:1. Injection 24 hours after thrombus induction results in a ratio of 6:1 for the heavily-iodinated material and 4:1 for normal fibrinogen. We are continuing to investigate conditions for maximum activity ratios and to further explore potential applications.

**SIGNIFICANCE OF RENAL ASYMMETRY IN BONE SCANS: EXPERIENCE IN 795 CASES.** R.S. Hattner, S.W. Miller, and D. Schimmel. University of California Medical Center, San Francisco, CA

Renal asymmetry in bone scans has been suggested in the past to be useful in inferring renal pathology. A retrospective review of 795 consecutive bone scans obtained using <sup>18</sup>F or <sup>99m</sup>Tc-pyrophosphate (POP) revealed 45 instances of renal asymmetry. Patients exhibiting this phenomenon were further investigated by reference to medical records, and to intravenous urography, if available. The results are illustrated in Table 1. The observed abnormalities included asymmetric renal function, nephrectomy, obstructive uropathy, and ectopia (transplant recipients).

Renal asymmetry in <sup>18</sup>F scans was a helpful but unreliable sign (33% false positive). In comparison the finding proved highly specific for renal abnormality in POP scans (no false positive). The overall sensitivity of renal asymmetry in bone scans as a diagnostic test cannot be assessed with the analysis employed, but POP scans were seven times as sensitive as <sup>18</sup>F scans for detecting renal abnormality, and the total incidence of renal asymmetry of 10% in the POP studies suggests that bone scans using polyphosphate analogues are a sensitive index of renal abnormality. Routine evaluation of the bone scan for renal asymmetry will add to the diagnostic information obtained from the procedure.

SCAN AGENT	TOT.	ASYM.	CONFIRMED RENAL STATUS	TRUE (+)		FALSE (+)		
				DEFINITE	PROBABLE	%	#	%
<sup>18</sup> F	536	17	12	5	3	67%	4	33%
POP	259	20	18	15	3	100%	0	0%

TABLE 1 - Note: Renal allograft recipients excluded.

**THE <sup>131</sup>I-HIPPURATE RENAL SCAN IN DIFFERENTIATION OF END-STAGE RENAL FAILURE FROM REVERSIBLE ACUTE RENAL FAILURE IN NEPHROTICS.** R.S. Hattner, H. Maltz, M. Holliday, University of California Medical Center, San Francisco, Calif.

Childhood nephrosis implies a benign prognosis in the majority of instances. However, the disease is subject to

frequent exacerbations, and a small fraction of these patients will develop end-stage renal failure ensuing parenchymal destruction from chronic nephritis and other rarer causes. Exacerbation of nephrosis with intravascular fluid depletion predisposes such patients to reversible acute renal failure, which is often clinically indistinguishable from end-stage renal failure. Differentiation of reversible acute renal failure from end-stage renal failure affords an extremely important data base for prognostic decision making in nephrotics with renal failure.

Three nephrotic children who presented with severe renal failure were studied. Although signs of intravascular fluid depletion were common, a timed sequence of  $^{131}\text{I}$ -Hippurate scintiphotos demonstrated changes typical of so-called acute tubular necrosis in each patient, and the diagnosis was confirmed by spontaneous recovery of normal renal function after appropriate intervals. The  $^{131}\text{I}$  renal scan mitigated renal biopsies in these children, and permitted appropriate prognostic decision making, notably avoiding installation of a peripheral arteriovenous shunt for dialysis.

The key scan findings are prompt, and good quantitative  $^{131}\text{I}$ -Hippurate uptake with marked prolongation in renal transit time in reversible acute renal failure, and delayed, and poor quantitative  $^{131}\text{I}$ -Hippurate uptake in end-stage renal failure.

**HOW ACCURATE ARE RADIOACTIVITY ASSAY PROCEDURES FOR IN-VIVO ADMINISTRATIONS IN NUCLEAR MEDICINE? Wolfgang Hauser. St. Mary's Hosp. and McGill Univ., Montreal, Quebec.**

The laboratories participating in this study followed a standard procedure for the preparation of chromium labelled red blood cells. The object was to measure as accurately as possible the amount of chromium-51 used. The vials with the radioactive material were then shipped to the National Bureau of Standards (NBS) for comparison with NBS working standards.

Of 33 participants, 47% obtained activity values within  $\pm 10\%$  of the activity value of NBS and 81% values within  $\pm 20\%$ . The ratios of the activity reported by the participants to the activity measured by NBS were above 1 for all users of two makes of dose calibrators and below 1 for all users of two other makes of dose calibrators. For one dose calibrator an average positive bias of 10% could definitely be established. The data were also analyzed for the activity values supplied by the radiopharmaceutical companies. Again, an average negative bias of 20% for one supplier could be confirmed.

This study thus demonstrated that at the present time the efforts of nuclear medicine laboratories to make accurate radioactivity measurements are frustrated by two variables beyond their control, namely:

- 1) differences in radioactivity assay values between radiopharmaceutical companies, and
- 2) poor calibration or instruction by manufacturers of dose calibrators.

**A COMPARISON OF THE TISSUE DISTRIBUTION OF  $^{67}\text{Ga}$  AND THE RARE EARTH RADIONUCLIDES. R. L. Hayes, D. H. Brown, B. L. Byrd, and J. E. Carlton. Medical Division, Oak Ridge Associated Universities, Oak Ridge, Tenn.**

The higher atomic number rare earth radionuclides have recently been reported to concentrate in nonosseous tumor tissues (Hisada, K. and Ando, A., J. Nucl. Med. 14, 615, 1973). It was therefore of interest to compare the tissue distribution of  $^{67}\text{Ga}$  with that of various rare earth radionuclides. High specific activity radionuclides of neodymium, samarium, gadolinium, dysprosium, erbium, thulium, and ytterbium were obtained either commercially or from the Isotopes Development Group at Oak Ridge National Laboratories.  $^{67}\text{Ga}$  and the rare earth radionuclides were administered to rats and mice (both tumor-bearing and normal) by tail vein in the citrate form (1 mg citrate/kg). When  $^{67}\text{Ga}$  and  $^{169}\text{Yb}$  were compared in 4 strains of tumor-bearing rats and mice, the two radionuclides were similar

in tumor localizing ability in three (7777 hepatoma, CA-755 adenocarcinoma, and P-1798 lymphosarcoma) types but  $^{169}\text{Yb}$  was superior in Ehrlich ascites cells. The tumor uptake of rare earth radionuclides ( $^{171}\text{Er}$ ,  $^{169}\text{Yb}$ ) is much more rapid than is that of  $^{67}\text{Ga}$ . Thulium ( $^{167}\text{Tm}$ ) showed the highest relative uptake in the 5123C hepatoma. As with  $^{67}\text{Ga}$  both sex and age have a marked effect on the distribution of rare earth radionuclides ( $^{170}\text{Tm}$ ). They ( $^{169}\text{Yb}$ ) also tend to concentrate at sites of inflammation as does  $^{67}\text{Ga}$ . Similar to  $^{67}\text{Ga}$  the administration of stable carrier with the rare earth radionuclides greatly diminished the relative affinity of rare earth radionuclides for soft tissue tumors. The subcellular distribution of rare earth radionuclides is similar to that of  $^{67}\text{Ga}$ , indicating that one of the organelles involved in tumor uptake of these radionuclides is probably lysosomal in nature.  $^{167}\text{Tm}$ ,  $^{171}\text{Er}$ , and  $^{157}\text{Dy}$  would be acceptable tumor localizing agents from a radiation standpoint.

**COMPARISON OF THE SUBCELLULAR DISTRIBUTION OF THE TUMOR-LOCALIZING AGENTS,  $^{67}\text{Ga}$ ,  $^{111}\text{In}$ ,  $^{206}\text{Bi}$ , AND  $^{167}\text{Tm}$ . R. L. Hayes, D. H. Brown, and J. E. Carlton. Medical Division, Oak Ridge Associated Universities, Oak Ridge, Tenn.**

$^{67}\text{Ga}$ ,  $^{111}\text{In}$ ,  $^{206}\text{Bi}$ , and  $^{167}\text{Tm}$  show unusual tumor-localizing properties. Recent work (Cancer Res. 33, 3265, 1973; Cancer Res. 32, 2063, 1973) has shown that  $^{67}\text{Ga}$  is intracellularly associated with lysosomal-like particles and is bound to several macromolecular species present in distilled water extracts of tumor tissues. It was of interest, therefore, to compare the subcellular distribution of  $^{111}\text{In}$ ,  $^{206}\text{Bi}$ , and  $^{167}\text{Tm}$  with that of  $^{67}\text{Ga}$ . Oak Ridge National Laboratory supplied the  $^{206}\text{Bi}$  and  $^{167}\text{Tm}$ .  $^{67}\text{Ga}$  and  $^{111}\text{In}$  were obtained commercially. The subcellular uptake profiles for  $^{111}\text{In}$  and  $^{167}\text{Tm}$  in tumor tissue were quite similar to those of  $^{67}\text{Ga}$ , the majority of the  $^{111}\text{In}$  and  $^{167}\text{Tm}$  being associated with a small particle fraction isolated by a sequential-product-recovery zonal-ultracentrifugation procedure (Arch. Biochem. Biophys. 155, 9, 1973).  $^{206}\text{Bi}$  gave quite different results. The distribution was more even in mitochondria, lysosomes, and the small particle zone, but like  $^{67}\text{Ga}$ ,  $^{111}\text{In}$ , and  $^{167}\text{Tm}$   $^{206}\text{Bi}$  was not appreciably associated with nuclei. Sephadex gel filtration studies of distilled water extracts indicated that most of the  $^{206}\text{Bi}$  activity was associated with a macromolecular species having a molecular weight in excess of 250,000.  $^{167}\text{Tm}$  did not give the same gel filtration pattern that is seen with  $^{67}\text{Ga}$  and  $^{111}\text{In}$ . Unlike  $^{67}\text{Ga}$  the macromolecular- $^{111}\text{In}$  and  $^{206}\text{Bi}$  complexes in distilled water tissue extracts were stable to heat ( $60^\circ\text{C}$ ) and alkaline pH. Both complexes were stable on storage at  $5^\circ\text{C}$  for one week. The intracellular localization of  $^{111}\text{In}$  and  $^{167}\text{Tm}$  are thus in many respects similar to that of  $^{67}\text{Ga}$ .  $^{206}\text{Bi}$  on the other hand appears to distribute in quite a different manner.

**VALUE OF  $^{99}\text{Tc}$  PERTECHNETATE IMAGING IN EVALUATION OF TESTICULAR TORSION. Larry L. Heck, Jerry L. Coles, Eugene D. Van Hove, and Thomas W. Riley. Methodist Hospital, Indianapolis, Ind.**

The differential diagnosis between torsion of the spermatic cord and epididymitis in acute, painful swelling of the scrotum is difficult. This frequently leads to belated surgical intervention in testicular torsion and unnecessary surgery in epididymitis. A method that would quickly and reliably differentiate these two entities would lead to earlier exploration of torsion and a higher salvage rate of the testis.

Ten mCi of  $^{99}\text{Tc}$ -pertechnetate is injected I. V. and either gamma camera images or rectilinear scans are begun immediately over the bladder and scrotal area. The rationale of this method is based upon the assumption that torsion of the blood supply to a testis will result in a relatively avascular testis. An inflammatory process such as epididymitis should retain a normal blood supply or in some cases have increased blood flow due to reactive hyperemia.

The preoperative scan diagnosis was correct in 11 of 12 patients with surgical proof of pathology. Seven patients had proven torsion and four



proved to have epididymitis. Three patients had their acute torsion surgically relieved and post-operative imaging demonstrated normal perfusion to the testis. Normal controls were obtained in males from ages 12-40 who were scanned after injection of  $^{99m}\text{Tc}$ -pertechnetate for brain scans.

Clinical results in 12 patients indicate that imaging of the scrotal area following I.V. pertechnetate is a simple and reliable method to differentiate between torsion and epididymitis.

**RADIONUCLIDE AORTOGRAPHY WITH  $^{99m}\text{Tc}$  ALBUMIN.**  
Robert E. Henkin, James S.T. Yao, and John J. Bergan. Northwestern Memorial Hospital. Chicago, Ill.

The diagnosis of aortic aneurysms is frequently difficult because calcification in the wall may be absent or missed on plain roentgenograms and contrast angiography is not without moderate risk in this age group.

A safe, rapid and accurate alternate screening test was developed using intravenously administered  $^{99m}\text{Tc}$  albumin and initial dynamic and 1-2 hour delayed static scintillation recording. Thirty four of 39 patients studied by plain abdominal roentgenograms and radionuclide aortography had, in addition, either conventional contrast aortography or surgery which confirmed the presence of an aneurysm. Twenty nine of 34 (85%) had positive and 5 of 34 (15%) normal radionuclide aortograms. Twelve of 34 (35%) have normal plain roentgenograms.

The delayed (1-2 hr.) scintiphotos were frequently superior to the dynamic images.

The simplicity and accuracy of this test makes it a valuable addition in the investigation of suspected intraabdominal vascular pathology.

**DEVELOPMENT OF XENON-125 FOR IN VIVO STUDIES.**  
Horace H. Hines, Jr., Neal F. Peek, and Gerald L. DeNardo. Crocker Laboratory, School of Medicine, University of California, Davis, California

Xenon-133 is presently used in ventilation and blood flow studies, but its physical properties make it less suited for in vivo studies than Xenon-125. The principle photons of Xenon-125, 188 keV (55%) and 243 keV (29%), are more intense and are in an energy range which is more advantageous for imaging with the scintillation camera than the 81 keV (35%) photons of Xenon-133. Xenon-125 was cyclotron produced by an Iodine-127 (p,3n) Xenon-125 reaction. The yield of Xenon-125 as a function of incident proton energy was determined by irradiating thin targets of naturally occurring Iodine-127. The yield curve reached a maximum at 31 MeV and had a full width at half maximum of 10 MeV. Production yields of about 18 millicuries per microampere-hour were obtained with 37 MeV protons. Phantom studies have shown that 12.7, 9.5, and 6.4 millimeter lead bars may be resolved with Xenon-125 using a 410 keV diverging collimator while only the 12.7 and 9.5 millimeter lead bars were resolved using Xenon-133 and the 410 keV or 140 keV diverging collimator. Furthermore, Xenon-125 decays by electron capture, 17.2 hour half-life, giving lower absorbed dose to the lungs from activity in the lungs than with Xenon-133. Since Xenon-125 allows better spatial resolution at lower absorbed dosage it appears better suited for in vivo ventilation and blood flow studies than Xenon-133.

**THE MECHANISM OF THE TUMOR AFFINITY OF  $^{109}\text{Yb}$ ,  $^{67}\text{Ga}$  AND  $^{111}\text{In}$ .** Kinichi Hisada, Atsushi Ando, Tatsunosuke Hiraki and Sigeru Sanada. Schools of Medicine and Paramedicine, Kanazawa University, Kanazawa, Japan.

This study was undertaken to make the difference clear on tumor affinity of  $^{109}\text{Yb}$ ,  $^{67}\text{Ga}$  and  $^{111}\text{In}$  and to

Presume the form of chemical bond in the tumor tissue. The uptake of  $^{109}\text{Yb}$ ,  $^{67}\text{Ga}$  and  $^{111}\text{In}$  into the tumor and organs was determined from 10 minutes to 72 hours after i.v. injection of  $^{109}\text{Yb}$ -,  $^{67}\text{Ga}$ -,  $^{111}\text{In}$ -citrate, using Yoshida sarcoma bearing-rats. And in order to investigate the bone affinity, adsorption of these elements to hydroxyapatite crystal and cation exchange resin was examined in the protein solution and phosphate saline buffer. In these experiments, it became clear that  $^{109}\text{Yb}$ ,  $^{67}\text{Ga}$  and  $^{111}\text{In}$  were rapidly taken up into the tumor, and these elements taken up were not excreted out of the tumor. There was no great difference of the tumor uptake rate between these three elements. And  $^{109}\text{Yb}$  was rapidly cleared from the blood and the most was taken into the bone. On the other hand, small amount of  $^{111}\text{In}$  was taken up into the bone.  $^{67}\text{Ga}$  showed the intermediate behavior between  $^{109}\text{Yb}$  and  $^{111}\text{In}$ .  $^{109}\text{Yb}$  was almost quantitatively adsorbed to hydroxyapatite crystal and cation exchange resin, but  $^{111}\text{In}$  was not adsorbed as much as  $^{109}\text{Yb}$ .  $^{67}\text{Ga}$  showed the intermediate. It might be deduced as followings. A reason of the strong affinity of  $^{109}\text{Yb}$  to the bone is attributed to the fact that  $^{109}\text{Yb}$  stays mostly as cation form in the blood, and as small amount of  $^{111}\text{In}$  stays in cation form,  $^{111}\text{In}$  shows the weak affinity to the bone, and  $^{67}\text{Ga}$  shows the intermediate. It is a well-known fact that  $^{109}\text{Yb}$ ,  $^{67}\text{Ga}$  and  $^{111}\text{In}$  are not sulfur coordinator and the weak nitrogen coordinator. Considering these facts, it is presumed theoretically that the chemical bond of these elements was not chelate ring, but ionic bond.

**THE RELEVANCE OF T<sub>3</sub> TO HORMON METABOLISM OF THE THYROID. (QUICK STEP REGULATION FOR MAINTAINING STEADY STATE).** Günter Hoffmann and Dieter Gehring. Dept. of Nuclear Medicine, University of Freiburg, Germany

Since the presence of triiodothyronine (T<sub>3</sub>) in human plasma was first reported in 1952, the source of this circulating hormone has never been clearly defined. A changing of the radioactive T<sub>3</sub>:T<sub>4</sub> ratio and the T<sub>3</sub>:T<sub>4</sub> ratio in serum is well known in many investigations. To clear up this problem some more studies were carried out in patients with and without endemic goiter, the total serum T<sub>3</sub> and T<sub>4</sub> was measured, the kinetics of labeling T<sub>3</sub> and T<sub>4</sub> with radioactive iodine was studied and also the half-time of T<sub>3</sub> and T<sub>4</sub> was determined. We found the mean value of total serum T<sub>3</sub> was 196 ng% and T<sub>4</sub> 7,6 ug%. The average of the T<sub>3</sub> half-time was 19 hours and of the T<sub>4</sub> half-time 192 hours. In the first 2 to 4 hours after treatment with the radioactive iodine the radioactive turnover rate was higher for T<sub>3</sub> than for T<sub>4</sub>. In this time T<sub>3</sub> was quicker labeled with radioactive iodine than T<sub>4</sub>. In view of the common pool (T<sub>3</sub>, T<sub>4</sub>) the T<sub>3</sub>-pool is very small and therefore little differences are already able to stimulate the feedback mechanism. In this example the mean of quick step regulation is the very quick reproducing of the relative small T<sub>3</sub> quantity in the periphery to maintain the T<sub>3</sub> steady state in view of the short half-time. On the other hand a very little changing of this concentration is able to stimulate the TSH-secretion and also to accelerate the incorporation of iodine into T<sub>3</sub>.

**COMPUTERIZING THE DOSE IN THE GYNECOLOGIC APPLICATION OF CURIETHERAPY WITH CAESIUM-137 SOURCES.** Tiberiu S. Holan, Marcel Miclutia, George Rodan, and Nicolas Toma. University Clinics, Dept. of Nuclear Medicine, Cluj, Romania.

Modern efficient radiotherapy implies rigorous dosimetry and its integration in a radiating or non-radiating therapeutical complex.

Accurate dosimetry in the gynecologic application of endocurietherapy can only be computerized since it involves a great number of mathematical operations, almost impossible to realize otherwise.

The authors discuss their experience accumulated in the use of a system of calculation of the dose applied and the methodology of detecting the radioactive sources. The Ordisk and Sievint programs are presented.

Checking the procedure by other methods gave concordant results.

**DETECTION, LOCALIZATION AND SIZING OF ACUTE MYOCARDIAL INFARCTS WITH TECHNETIUM-99m TETRACYCLINE.** B. Leonard Holman, Michael Lesch, Franklin Zweiman, John Temte, Mrinal K. Dewanjee, Bernard Lown, Richard Gorlin. Peter Bent Brigham Hospital, Boston, Mass.

Tetracycline binds to necrotic tissue; its fluorescence has been used to identify experimental acute myocardial infarcts (AMI). When tetracycline is labeled with technetium-99m (<sup>99m</sup>Tc-TC), its presence in the infarcted tissue can be imaged by external means, permitting detection, localization and sizing of the lesion. The thorax was imaged in anterior, LAO and RAO projections in 28 patients 4, 8 and 24 hours after injection of 20mCi of <sup>99m</sup>Tc-TC. Nine controls had negative scans. By clinical criteria, 14 patients sustained AMI, (10 transmural, 4 nontransmural) and in 5 the diagnosis was equivocal. The scan was positive in 14/14 and 2/5 patients, respectively. Positive scans returned to normal within 1-2 weeks in all 6 patients scanned serially. A negative scan became positive in 1 patient who developed AMI in-hospital. Scintigraphic and electrocardiographic localizations were well correlated. The size was well correlated with the peak serum CPK. The technique differs from K<sup>+</sup> analogue scanning for infarct detection because: a) <sup>99m</sup>Tc-TC produces a positive image, b) <sup>99m</sup>Tc-TC binds to acutely necrotic tissue and therefore does not image areas of old infarction or fibrosis, and c) sequential daily imaging permits temporal analysis of the course of infarction. In conclusion, <sup>99m</sup>Tc-TC permits accurate detection, localization and sizing of acutely infarcted myocardium.

**A PROPOSED MECHANISM FOR THE ALVEOLAR RETENTION OF <sup>99m</sup>Tc STANNOUS PHYTATE.** R.A. Holmes, A.T. Isitman, R. Manoli, A.M. Zimmer. Milwaukee County Medical Complex, Milwaukee, WI.

The alveolar retention of technetium-99m stannous phytate (<sup>99m</sup>Tc-Sn-Phy) appears to result from its binding to the alveolar wall or its incorporation into the surfactant that covers it. Phytate (inositol hexaphosphate) is similar structurally to phosphatidyl inositol, a principal component of alveolar surfactant and both are polar compounds with exposed phosphate radicles. To differentiate phosphate binding by alveolar receptors from competitive incorporation of the phytates cyclic molecular structure by surfactant we nebulized a non-cyclic phosphate solution, technetium-99m stannous diphosphonate (<sup>99m</sup>Tc-Sn-DiP) into several normal volunteers at tidal breathing and determined its distribution and rate of pulmonary clearance with the scintillation camera. Lung images showed uniform deposition of <sup>99m</sup>Tc-Sn-DiP qualitatively comparable to <sup>99m</sup>Tc-Sn-Phy. Similarly the clearance rate was biexponential with a more rapid first component but an identical slow late component. Blood activity suggested greater mucosal absorption of the <sup>99m</sup>Tc-Sn-DiP. Nebulization of <sup>99m</sup>Tc-Sn-Cl<sub>2</sub> solution showed a different and more rapid clearance eliminating stannous ion as a non-specific binding factor.

We therefore conclude that the alveolar retention of <sup>99m</sup>Tc-Sn-Phy is most likely due to phosphate binding to alveolar wall receptors and the superiority of <sup>99m</sup>Tc-Sn-Phy to <sup>99m</sup>Tc-Sn-DiP for inhalation imaging relates to its significantly smaller mucosal absorption and probably relates to its molecular size.

**GALLIUM-67 CITRATE TO DIAGNOSE PYELONEPHRITIS.** Sheldon R. Hurwitz, Naomi P. Alazraki, and Warren O. Kessler. University of California, San Diego, VA Hospital, San Diego.

Gallium-67 may have a role in differentiating upper from lower urinary tract infections. At a dose of 75 µC/kg, the kidneys are not normally seen on routine gallium surveys. This observation prompted a prospective study of 73 patients with pyuria. Imaging was performed in the posterior projection with a medium-energy divergent collimator. In doubtful cases, <sup>99m</sup>Tc-DTPA was also administered to confirm renal location. Visualization of the kidneys by greater gallium concentration than background was considered a "positive" study. No bowel preparation was necessary, but several cases required delayed views to permit abdominal activity to decline.

In 57 of the patients, the exact site of infection was determined with either a Fairley washout test, ureteral catheterization or renal biopsy. The <sup>67</sup>Ga scan was 84% (48/57) accurate by these criteria. Gallium differentiated pyelonephritis from simple lower tract infections without resorting to urinary catheterization, and useful results were available within 24 hours. When renal uptake was unilateral, the scan was usually correct in identifying the infected kidney. Studies became normal with response to therapy, but radioisotope uptake by the kidneys recurred with reinfection.

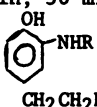
Urinary sampling cannot be done in patients with ureterostomies. In four such patients studied, <sup>67</sup>Ga proved essential in diagnosing renal parenchymal infection.

An animal model of pyelonephritis has been established in rats and rabbits. Although there is increased gallium uptake by infected kidneys in these animals, this phenomenon appears to be more impressive in patients.

In conclusion, renal imaging with gallium-67 is rapidly performed and offers a new, non-invasive means of diagnosing pyelonephritis.

**SYNTHESES AND CONCENTRATION OF DOPAMINE ANALOGS IN THE RAT.** Rodney D. Ice, Donald M. Wieland, William H. Beierwaltes and Richard G. Lawton, The University of Michigan, Ann Arbor, Mich.

A radiopharmaceutical localizing in the adrenal medulla would be useful in detection of pheochromocytomas and neuroblastomas. Labeled dopamine is known to localize in the adrenal medulla greater than any other precursors of epinephrine. We have synthesized a series of <sup>3</sup>H- and <sup>35</sup>S-sulfonanilide analogs of dopamine and compared their tissue distribution to dopamine-<sup>14</sup>C. Tissue concentrations were determined in rats at 5 min, 30 min, 1 hr, 4 hr, 6 hr and 24 hr.

	Cmpd.	R	Sp. Act.
	I	<sup>35</sup> SO <sub>2</sub> Ph-I-P	370 uCi/mg
	II	SO <sub>2</sub> Ph- <sup>3</sup> H-P	1670 uCi/mg
	III	<sup>35</sup> SO <sub>2</sub> CH <sub>3</sub>	5.1 uCi/mg

Moderate uptake of I was observed in the adrenal at short time intervals but the radioactivity was rapidly depleted; at no time interval was the adrenal/liver ratio greater than two. Arylsulfonanilide II was evaluated to determine if the iodo group caused the lack of retention of I in the adrenal. Similar distribution patterns were observed for II. Alkylsulfonanilide III showed significant uptake and retention in the adrenal with 0.66% dose/gm at 5 min and 0.27% dose/gm at 24 hr. The 24 hr target-to nontarget (T/NT) ratios for the adrenal versus liver, blood, kidney and heart were 13, 27, 30 and 60 respectively. These results compared favorably with the respective T/NT ratios of 23, 30, 8 and 15 obtained for dopamine-<sup>14</sup>C. Retention of dopamine and III may be via binding to phenethanolamine/N-methyl transferase.

**DIAGNOSIS OF GERIATRIC NUCLEAR MEDICINE: CORRELATION OF ORGAN SCINTIGRAPHY, CLINICAL SIGN AND PATHOLOGIC DIAGNOSIS.** Masahiro Iio. Tokyo Metropolitan Geriatric Medical Center, Tokyo, Japan.

Nontraumatic nature of Nuclear Medicine proved to be valuable diagnostic method to geriatric medicine, where plural and severe disorders exist

in individuals. By reading organ scintigrams of the aged patients, different criteria for diagnosis are required. Abnormal and delayed CSF circulation was found in 67 % of 55 cases over 65 y.o. Ventricular reflux of isotope was noted in 10 %. Only 15 % showed normal CSF circulation. Abnormal CSF circulation related well with the neurologic signs. Some cases were improved by V-A shunt. Sixty per cent of 345 brain scintigrams was CVD, and brain tumors were only 12 %, reflecting the high incidence of the former. Comparison with the autopsy revealed that 62 % of CVD lesions were visualized in scintigrams. Tumors and subdural hematoma remained frequently to be silent. In 109 pulmonary scintigrams, major fissure sign and decreased perfusion volume of the lower lungs were found in 60 % and 20 % respectively. Liver scintigram in the aged (510 cases) was not remarkably different from the control, however, pathologic diagnosis proved that SOL is mostly due to metastatic liver tumors (71 %) rather than primary liver tumor (16 %). High incidence (81 %) of abnormal renogram was found. Tc-99m pyrophosphate bone scan in 152 cases showed that aged people accumulated the label to the skeletal frame of the whole body, representing diffuse and negative calcium balance. Staging by bone scan of the 27 cases of prostate cancer correlated closely with the clinical sign and pathologic diagnosis, and was superior to bone survey by x-ray.

**FUNCTIONAL IMAGING OF INTRARENAL BLOOD FLOW USING SCINTILLATION CAMERA AND COMPUTER.** Yasushi Ishii, Juichi Kawamura, Takao Mukai, Masaharu Takahashi, Yasuto Onoyama, and Kanji Torizuka. Kyoto University School of Medicine, Kyoto, Japan.

In order to obtain regional flow index conforming two-dimensional distribution of a kidney contour, so-called functional imaging was attempted to construct. After a bolus injection of <sup>133</sup>Xe into a renal artery, this objective was accomplished by a digital computer processing of a sequence of scintillation camera recordings of the following washout process according to intrarenal blood flow, to be expressed in a form of disappearance rate constant. Calculation for the rate constant was done either using initial slope method or height over area method. Although the former method was thought to be suitable on theoretical ground without undue participation of background activities due to inactive part of kidney, the latter was preferred to be used because of its stable result for the image construction. Twenty-two cases with or without focal lesion of kidney were studied. By comparing the data analyzed by conventional peeling-off method with angiographic and renographic data, quantity of renal perfusion was shown to be correlated best with fractional blood supply for renal cortex. Hence, the obtained index in the image was thought to represent a degree of participation of cortical blood flow in situ, which, in the other words, to be a good visualization of a functional status within a kidney.

**AEROSOL DEPOSITION IN THE RESPIRATORY TRACT.** Harumi Itoh, Yasushi Ishii, Toru Mori, Ken Hamamoto, Toru Fuzita, Chizuko Furumatsu, Kanji Torizuka. Kyoto University School of Medicine, Kyoto, Japan. Kanji Takahashi. Atomic Energy Institute, Kyoto, Japan.

The distribution of inhaled particles and gases in the respiratory tracts has been very important problem in medicine. For example, air pollution or aerosol therapy, should be studied under the synthetic concepts of gas and particle. So aerosol scanning should be reviewed in wider aspects of aerosol science to answer various clinical requirements. First, total and regional deposition rates in human airways were calculated computationally. Next, depositions of <sup>99m</sup>technetium colloid in bronchial models and the human airways were studied by scintillation camera and whole body counter precisely. These theoretical

and experimental studies were useful in understanding normal distributions of aerosol and gas in the scintigrams. In healthy subjects, <sup>133</sup>xenon gas mainly distributed to peripheral sites. But in aerosol scanning hilar depositions were not ignored. This hilar depositions were due to impaction to several bronchial bifurcations. In peripheral airways marked deposition occurred by sedimentation. These differences in deposition mechanisms were thought quite important in considering pathogenesis of lung cancer and chronic obstructive lung disease. In aerosol scanning, generally performed, this phenomenon was usually seen, because our ultra-sonic nebulizer produced the aerosols of about 2 microns. Once airway deformity occurs, excessive regional spots and distal decrease were seen. These data showed to be careful about aerosol therapy to diseased lung.

**ACCURACY OF CARDIAC SHUNT ESTIMATES FROM RADIOCARDIOGRAPHIC MEASUREMENTS AND COMPUTER ANALYSES USING A PULSATILE FLOW MODEL.** Darko Ivancevic, Ronald R. Price, Thomas C. Rhea, Jr., Thomas P. Graham, Jr., and A. B. Brill. Vanderbilt University, Nashville, Tn.

In a cooperative effort between the University of Zagreb, Yugoslavia, and Vanderbilt University, a quantitative comparison of cardiac shunts as estimated by computer analysis using a pulsatile flow model and standard catheterization measurements was undertaken.

Each patient underwent standard catheterization procedures, and shunt magnitude was quantitated from oxygen saturation measurements. The radiocardiographic measurements were made during catheterization with the In-113 injection via catheter into the right atrium. The output of four scintillation detectors were entered into a computer where time curves were generated and analyzed.

Approximately 125 patients with various acquired or congenital heart disease were studied by means of mathematical simulations of radiocardiographic data using a pulsatile model. Of this group, 41 had right-to-left shunts, 33 had left-to-right shunts, and 51 had a normal central circulation.

Correlations between shunt estimates derived from catheter oxygen saturation measurements and shunt estimates derived from computer analyses show a correlation coefficient of 0.90 for left-to-right and 0.81 for right-to-left shunts. The technical and computational problems encountered will be discussed, and suggestions for improvement will be made. A qualitative discussion of the pulsatile model will be presented along with typical examples.

**HIGH-RESOLUTION MEASUREMENT OF REGIONAL CEREBRAL BLOOD FLOW IN MAN.** Philip M. Johnson, Sadek K. Hlail, Robert R. Sciacca, John C. M. Brust and Paul J. Cannon. College of Physicians & Surgeons, Columbia University, New York, New York.

A method was devised to measure the distribution of regional cerebral blood flow (rCBF) in gray and white matter by monitoring the washout of <sup>133</sup>Xe using the digital autoradioscope with 1.5 in. collimation. Following magnification cerebral arteriography, <sup>133</sup>Xe (20 mCi) was injected into the internal carotid artery and the desaturation of tracer was recorded for 15 minutes. Of the scintillation detector's 294 crystals ~100 overlay the brain.

Data from each crystal were corrected for differing crystal efficiencies and for instrument dead-time (22 usec) and then normalized. They were then processed by a weighted least-squares nonlinear regression technique using an IBM 360-91 computer. Each data point was weighed for its relative accuracy and an iterative technique was used to fit the sum of two exponentials to the data from each crystal. Blood flow rates of the rapid (gray) and slow (white) compartments were calculated by the Schmidt-Kety formula together with 95% confidence limits for each measurement. When arterio-venous shunting was present the desaturation curves over the abnormality were best fitted by 3 exponential curves. Printouts of compartmental flow rates were aligned on the carotid arteriogram.

Application of the method in 67 studies has disclosed both local changes in rCBF and generalized changes in the distribution of rCBF that correlated with arteriographically-demonstrated lesions including stroke, "luxury perfusion," tumor and arterio-venous malformations before and

after therapeutic embolization. The method's unique features are increased discrimination of rCBF due to simultaneous measurements at more than 100 regions, improved resolution due to greater collimation and confidence limits for each measurement.

**THIOCYANATE COMPLEXES OF TECHNETIUM.** Alun G. Jones and Michael A. Davis. Harvard Medical School, Boston, Mass.

Spectrophotometric studies of technetium solutions containing thiocyanate acting both as a reducing agent and as a coordinating ligand have been made. A standard spectrophotometric method based on the formation of the violet pentavalent thiocyanate complex has been improved so that determinations in the concentration range 0.1 to 30  $\mu\text{g/ml}$  may be made in 15 min instead of the published 3 hr. When the kinetics of this reaction are slowed, an isosbestic point is seen at 466 nm which disappears at full development. On following spectra up to 100 hr after preparation, a further isosbestic point is seen at 438 nm. Reduction of pertechnetate ions by stannous chloride in the presence of thiocyanate instantly produces a yellow complex with an absorption maximum at 403 nm. This absorption also follows Beer's Law in the range 0.5 to 30  $\mu\text{g/ml}$  and forms the basis of an alternate and simpler method of estimating the element. When a solution of  $\text{TeO}_4^-$  in 0.1 M HCl is reduced by stannous chloride in the absence of thiocyanate, a species with a strong absorption at 338 nm is formed, similar to the well-known absorption spectrum of the hexachlorotechnetate ion. Thus it may be postulated that the yellow thiocyanate complex also contains technetium in the +4 oxidation state and that the isosbestic point observed could represent the co-existence in solution of the tetravalent and pentavalent oxidation states. Furthermore, the predominant oxidation state following reduction by stannous ions in radiopharmaceutical kits may also be the tetravalent state.

**"EQUILIBRIUM" IMAGES OF SHORT-LIVED RADIOPHARMACEUTICALS FOR DYNAMIC OBSERVATIONS.** Terry Jones, Hammersmith Hospital, London, England, Gordon L. Brownell, Massachusetts General Hospital, Boston Massachusetts, Michael M. TerPogossian, Washington University, St. Louis, Mo.

The constant administration of a short-lived radiopharmaceutical permits dynamic information to be obtained from a static observation. The advantage of the use of "equilibrium" images - those obtained several half-lives following the start of constant administration - is that high-quality "static" images may be obtained of dynamic processes. Also since the radiopharmaceutical distribution does not change with time, multiple images such as those required for transverse section tomography may be obtained. The method is useful if the dynamic process has a biological half-time of the order of the physical half-life of the radionuclide.

This paper reports work commenced at Washington University and carried out using the MGH Positron Camera. Two minute  $^{150}\text{I}$  labeled to  $\text{CO}$ ,  $\text{CO}_2$  and  $\text{O}_2$  was administered by constant inhalation. Equilibrium images of the head were obtained with each of the three radiopharmaceuticals. In effect,  $\text{CO}$  labels red cells and serves as a non-diffusible indicator,  $\text{CO}_2$  labels water, and  $\text{O}_2$  labels oxyhemoglobin. The images therefore reflect respectively the major vessels, vascular and extravascular water turnover and oxygen utilization. Although the interpretation is highly tentative, the unique nature of these images suggests wider application.

**ECHOCARDIOGRAPHY AND RADIONUCLIDE ANGIO-CARDIOGRAPHY IN THE DIAGNOSIS OF PERICARDIAL EFFUSION.** Nilza Kallos, Stuart Gottlieb and August Miale, Jr., Jackson Memorial Hospital, Miami, Florida

Echocardiography (UCG) and radionuclide angiography (RAC) appear to be the most useful non-invasive methods currently available for the detection and evaluation of pericardial effusion. A retrospective comparative study of 91 consecutive patients was undertaken. Complete records and follow up data were available in 55 of 91 patients with a total 77 studies. When both UCG and RAC were positive, correlation was 95%. When both were negative, confirmation by tap was generally not obtained, but on clinical grounds the accuracy appeared to be equally high. There were twelve patients where UCG was positive and RAC negative. In 6 of these the evidence indicated that this was related to greater sensitivity of UCG for small amounts of fluid. Of the remainder, 2 were found to have no effusion and one had negative  $\text{CO}_2$  but was positive on contrast angiography. The 3 other cases of disagreement (negative RAC, positive UCG) were untapped and unexplained but had no clinical deterioration. Only one patient had RAC positive, UCG negative; diagnosis was localized hematoma. The data confirms the greater sensitivity of UCG compared to RAC when small amounts of effusion are of paramount importance for diagnostic purposes (for cytology, culture, etc.). However, in patients who present with chronic right heart failure, known or suspected malignancy or mediastinal disease, dynamic scintigraphy (RAC) of the heart and great vessels is preferred. Combined studies are more useful than either alone in patients with localized effusion and following cardiac surgery.

**AXIAL VIEW OF THE HEPATOSCINTIGRAPHY.** Masao Kaneko, Setsuro Inada\*, and Akio Inukai\*. Nagoya University Hospital and Tokai Teishin Hospital\*, Nagoya, Japan.

Conventional radioisotope imaging of the liver produces a two dimensional display. The addition of an axial view makes it possible to observe the organ in three dimensional scope.  $^{99\text{m}}\text{Tc}$ -sulphur or tin colloid was used in a dose of 3 to 5 mCi. The gamma camera head was fully elevated and the patient stands under it, bending his head forwards while keeping the upper part of his body as straight as possible. In most of 40 cases in which this method was attempted, a satisfactory axial scintigraph of the liver was obtained in 1.5 min. or so for one picture. The axial projection of the right hepatic lobe was ovoid in shape with longitudinal direction from the front to the back. This procedure was found to be most valuable to detect lesions situated in the inner portion of the right hepatic lobe, which were very difficult to show by conventional projections. The left hepatic lobe was shown in a petal shape, adjacent to the right lobe in midline. The spleen was situated on the left posteriorly with a triangular shape. When the stomach was distended by air inflation, the space between left hepatic lobe and spleen would be enlarged, if the motility of these organs and expansibility of the stomach were retained. In a case of severely impaired liver function, the image of the liver in axial view was obscured by the overlapping of bone marrow shadow. The axial view of the hepatoscintigraphy can be obtained with no special equipment and is of use to understand the spatial inter-relationship of liver, spleen, and stomach by a simple procedure.

**ECG-GATED RADIONUCLIDE DILUTION CURVES OF THE RIGHT HEART CHAMBERS.** Akira Kasahara, Hironobu Ochi, Masao Tamaki, Jun Iwasaki, and Koji Hara. Osaka City Univ. Hospital; and Toshiba Medical Inc., Osaka, Japan.

Human cardiac scintiphotos of one minute duration immediately after intravenous bolus-injection of  $^{99\text{m}}\text{Tc}$ -HSA, together with ECG, were recorded on video-tape through an analog-digital converter and on its audiotrack through a FM-modulator. While replaying this tape, selection of the area corresponding to

the right atrium or ventricle and setting of ECG-gate for P- or T-wave were performed, and the radionuclide activities from the selected area were fed into a 400-Channel Pulse Height and Wave Form Analyser (400 CH. PHA) through our module which consists of an OR-gate and an AND-gate with a time-oscillator. The former determines the channel number address among the 400 channels, concurrent with each signal of a P- or T-wave. The latter recognizes R-wave from the audiotrack by adding the definite number of pulses emitted by the time-oscillator to radionuclide activity of the output-datum, corresponding to each R-wave, and marks it on the output data. Thus, ECG-gated radionuclide dilution curves of each heart chamber were made corresponding to P- and T-waves.

Reverse relationship was clearly shown between right atrial and ventricular curves, irrespective as to whether they were obtained from P- or T-wave.

**BASIC TECHNETIUM 99M PENICILLAMINE, A NEW RENAL SCANNING AGENT.** Tim Kennedy, Ralph G. Robinson, and Allan Gubuty. University of Kansas Medical Center, Kansas City, Kansas.

The purpose of this study was to evaluate the usefulness of basic technetium-99m penicillamine as a renal scanning agent in humans.

The radiopharmaceutical was prepared as previously reported. (Invest. Rad. 8:4, 279, 1973). 30 patients have been studied to date. 10mCi of basic 99mTc Penicillamine (BTP) was administered as a bolus and dynamic flow patterns of the kidneys were obtained. Static images were obtained at varying intervals following injection to determine the optimum scanning time, and blood disappearance curves were obtained in some patients as well. Routine blood and urine chemistries were obtained before and after injection, and showed no significant alterations. Urine was also obtained from some patients for radiochromatographic analysis.

One or both kidneys were considered abnormal by scan in 19 of the 30 patients studied to date. Renal outlines could easily be discerned in patients with significant elevation of serum BUN and creatinine values, although the background was increased in these patients. Radiochromatography of the urine showed an intense activity peak with the same Rf value as the original preparation. Blood disappearance curves indicated a multicompartiment blood disappearance model. BTP lends itself to "kit-type" preparation.

The persistent renal cortical localization of the compound results in excellent renal images. BTP warrants further study as an imaging agent, especially in patients with poor renal function.

**CLINICAL APPLICATION OF A PULSATILE REGURGITANT HEART MODEL FOR ANALYSIS OF RADIONUCLIDE ANGIOCARDIOGRAMS.** Dennis L. Kirch\*, Charles E. Metz\*\*, Peter P. Steele\*, and Donald W. Brown\*. \*Veterans Administration Hospital and the University of Colorado Medical Center, Denver, Colo. \*\*The University of Chicago and the Argonne Cancer Research Hospital, Chicago, Ill.

A set of finite difference equations have been solved by Z-transform techniques to obtain closed form solutions for an atrial-ventricular model which permit accurate quantitation of cardiac valvular insufficiency. Conventional analysis of cardiac tracer dynamics has generally utilized linear differential equation concepts. Since these techniques assume constant flow rates and fixed chamber volumes, they are not totally suitable for modeling pulsatile intercardiac dynamics. The solution to the pulsatile model utilized in this study provides accurate quantitation of total, forward and regurgitant ejection fractions and end-diastolic and end-systolic volumes of both the involved atrium and ventricle. The advantages of this analytic methodology include reduced errors due to incomplete mixing and irregular cardiac contractions. An Anger camera/computer system is used to

accumulate, store, and analyze the radionuclide time-activity curves. We have applied this technique to 12 patients having mitral or aortic insufficiency. The radionuclide angiocardiograms were performed immediately following conventional contrast angiographic and indicator-dilution studies. The left ventricular end-diastolic volumes, total and regurgitant ejection fractions determined by radionuclide methods compare well with the determinations made by contrast angiographic methods ( $r > .85$  in all cases). The accuracy and safety of this method make it a useful clinical tool for quantitation of valvular insufficiency without sacrifice of diagnostic information.

**DIGITIZATION OF THE OUTPUT OF AN IMAGE INTENSIFIER CAMERA USING A SILICON DIODE ARRAY.** Dennis L. Kirch, Peter P. Steele, Richard S. Trow, Michael T. LeFree, and Donald W. Brown. Veterans Administration Hospital and the University of Colorado Medical Center, Denver, Colo.

The use of a silicon photodiode array to interface an image intensifier Gamma camera to a digital computer has resulted in a dynamic scintigraphic imaging system which has excellent performance characteristics at high count rates. The light output from the final image intensifier stage of a Harshaw Model 1070 Quantascope is lens coupled to a Reticon (MC 500) 32 x 32 element, high sensitivity, silicon diode camera. The camera has been modified for asynchronous operation and interfaced to a PDP-12 digital computer. In this mode of operation, the diode array integrates light from the image intensifier for 40 milliseconds. The analog values stored on the individual array elements are then digitized and transferred to computer memory by direct memory access. Readout time is 10 milliseconds resulting in frame rates of 20 frames per second. The resultant dynamic imaging system has been found to have the following advantageous performance characteristics. 1) The silicon diode array serves as intermediate storage or buffering for the scintigraphic image data. Dead time losses are, therefore, negligible and independent of count rate. 2) The parallel operation of the detector and image intensifier stages precludes distortion of count rate phenomenon in one portion of the detector field of view by simultaneous events detected in any other portion of the field of view. 3) The ultimate linear counting rate achieved by this system is limited only by the saturation characteristics of the image intensifier phosphors. This digital dynamic imaging system provides improved performance at high count rates compared to conventional Anger camera/computer systems.

**CORRELATION OF GAMMA CAMERA AND FLOW METER DETERMINED RENAL BLOOD FLOW MEASUREMENTS.** P.Kirchner, F.Gray, D.Short, and R.Filo. NMMC and AFRRRI, Bethesda, Md.

Gamma camera flow curves are widely used for estimating renal blood flow. We have developed a technique for analyzing renal blood flow curves that shows good correlation with simultaneously obtained electromagnetic flow meter determinations.

In six dogs an electromagnetic flow meter was attached to the left renal artery following splenectomy. During steady state renal artery flow 5 mCi of Tc-99m sulphur colloid was injected intravenously in a 0.5 ml bolus. The first transit of tracer through aorta and kidneys was recorded on magnetic tape for analysis with an on-line computer. Following hepatic clearance of the colloid from the circulation, 2nd and 3rd injections in the same dog were similarly recorded for different renal blood flow levels induced by mechanical renal artery constriction. The first transit of tracer through the kidney and through a short (constant size) section of aorta was quantitated for each injection as the integral of the respective time-activity curve or as the slope of a linear least squares fit to the curve. Internal standardization for variations in dose and injection technique was achieved by expressing renal blood flow as the ratio of quantitated renal flow curve to quantitated aortic flow curve, each reduced to unit time.

In 11 of 14 measurements the gamma camera determined renal flow quantitation produced a linear correlation with the flow meter readings for either mode of curve analysis. In each of the 3 instances of poor correlation the aortic flow curve was of poor quality.

Our results suggest that non-invasive quantitation of individual renal blood flow can be obtained from analysis of gamma camera derived renal flow curves. For us the most useful clinical application of this technique has been the evaluation of renal transplant function and viability.

APPLICATION OF THE DECAYING SOURCE METHOD TO ANGER CAMERA DEAD TIME DETERMINATION. G. F. Knoll, The University of Michigan, D. R. Strange, and W. J. O'Neill, Medical Data Systems, Ann Arbor, Mich.

We have undertaken a study of the dead time behavior of the Anger Camera using an automatic data acquisition system which monitors the activity of a decaying source. With this method the source distribution and scattering conditions can be held constant over a wide range of activities. In addition, since the interaction rate is known to decay exponentially, successive measurements of the recorded rate allow an unambiguous analysis of the count losses.

A minicomputer (MDS MODUMED) on line with an Anger Camera (NUCLEAR CHICAGO HP CAMERA) has been programmed to acquire short duration data frames at one hour intervals when using a Tc-99m source. Acquisition is generally started at the end of the day and proceeds overnight. The resulting data can be analyzed for total and regional dead time characteristics.

Preliminary results indicate that extreme caution must be used in making count loss corrections, and that very large errors can result from applying a simple non-paralyzable model using only the total counting rate from the entire field of view. Depending on the source distribution, quite different corrections may be required for different areas in the camera field. Observed count rates over an extremely hot area of the field may actually increase as the source decays, characteristic of paralyzable behavior. Since pulses falling outside of the pulse height window affect the severity of dead time loss, any method of dead time measurement must approximate as closely as possible the source geometry of clinical studies.

PSEUDORANDOM FILTERS AND CORRELATION ANALYSIS APPLIED TO GAMMA RAY IMAGING. Glenn F. Knoll, Randall S. May, and Ziya Akcasu. The University of Michigan, Ann Arbor, Mich.

A number of "coded aperture" techniques have recently gained attention as alternatives to conventional collimation for gamma ray image formation. Typical of these is the Fresnel zone plate, in which an encoded image is recorded through a stationary Fresnel filter and decoded using information from the entire detector area. We have formulated an alternative approach which substitutes a series of segmented filters for the single Fresnel plate. A sequence of successive coded images is recorded and subsequently decoded using digital correlation techniques. While requiring much greater image storage capacity, the method offers several significant advantages over prior techniques. Requirements of detector uniformity or completeness disappear and, in fact, an image can be reconstructed from data derived from a single detector resolution element. Independent images from each detector element may be combined to give tomographic effects, and artifacts observed for out-of-focus sources from stationary coded apertures do not arise.

A general definition is given for the properties required of the sequential filters, and a specific family of patterns, "pseudorandom sequences", introduced. Examples are given of these binary sequences, and specific filters of interest in gamma ray imaging are described. An analysis of the statistical advantages of the method is given together with tests of the theory using computer modeling. First experimental results using an Anger camera have been obtained by Koral, Rogers, and Beierwaltes.

QUANTITATIVE COUNT DIFFERENCE ESTIMATION BY OBSERVERS VIEWING PAIRED KIDNEYS. L.G. Knowles, K.S. Bonwit, S.E. Bonwit, L.C. Kohlenstein, and A.G. Schulz. Johns Hopkins Univ., Silver Spring, Md.

The ability of human observers to visually quantify count differences between two halves of a mal-distributed radionuclide image has been measured.

The measured response of a typical imaging instrument was incorporated into a computer program and used to produce accurate simulated images of a pair of matched kidneys. Each set was adjusted so that the number of counts in the more active kidney differed randomly from that in the less active kidney over the range 0-110%. More than 2800 total observations of 360 independent sets were made by five volunteers. Each observer was asked to estimate the probable difference by selecting one of ten difference intervals.

In clinical practice it is often sufficient to determine that the number of counts in one portion of a scan is, or is not, beyond the differential found in "normals". However, additional useful information may be gained by obtaining a reasonable estimate of the actual difference. The experimental data indicate that the average absolute error between the actual difference and the estimated difference generally follows the expression:

$Error(\%) = 5 + 0.1\delta$ ,  $\delta$  is the actual percentage difference, within the range of  $0 \leq \delta \leq 60\%$ . The estimated error was found to be  $10 \pm 2\%$  for  $60\% \leq \delta \leq 110\%$ .

Our results indicate that properly trained clinicians could be expected to be able to visually estimate differences with an average error near 5% when the difference is small; the error increases to  $10 \pm 2\%$  for differences near 100%.

DETECTION OF ASYMMETRICAL RENAL PERFUSION BY RADIOPERTECHNETATE ANGIOGRAPHY. Mordecai Koenigsberg, Ira Novich, Marc Lory, Leonard M. Freeman, and M. Donald Blafox. Albert Einstein College of Medicine, Bronx, N.Y.

Although  $^{99m}\text{Tc}$  renal angiography is commonly performed in nuclear medicine laboratories, there are little data on the sensitivity of the method.  $^{99m}\text{Tc}$ -pertechnetate was injected into the jugular vein of anesthetized dogs lying supine on the detector head of a gamma camera. Passage of radionuclide through the aorta and kidneys was recorded on digital magnetic tape through a data analysis system. Perfusion to each kidney was measured with electromagnetic flowmeters. Increasing amounts of  $^{99m}\text{TcO}_4^-$  were injected in a  $\frac{1}{2}$  ml. bolus while the difference in perfusion between the two kidneys was increased in a step-wise manner using inflatable vessel constrictors.

Areas of interest were flagged over the aorta and kidneys, and the tape was replayed generating time-activity curves of these regions for each injection. The curves were analyzed on a Sigma-9 computer. The following parameters were obtained: rate of increase in activity, activity at twice time to peak over the peak activity ( $C_2/C_1$ ), time to peak + time to  $\frac{1}{2}$  peak on the descending slope ( $T_m + T_m/2$ ) and, after curve stripping to correct for recirculation, mean transit time.

Preliminary results indicate that greater than 25% difference in flow is needed for reliable detection by this method. A difference of 40% or greater is detectable by visual inspection alone.

THE TOTAL BODY SCINTILLATION EFFECT. Mordecai Koenigsberg and Leonard M. Freeman. Albert Einstein College of Medicine, Bronx, New York.

Intravenous radionuclide angiography has proven useful in evaluating the vascularity of lesions throughout the body. At the immediate completion



of the radioangiogram radionuclide is distributed throughout the body tissues in proportion to their blood supply. We obtain cumulative static images during this period which roughly corresponds to a blood pool image. Avascular and hypovascular lesions appear "cold" in contrast to surrounding radionuclide containing structures. Lesions identified have included renal, adrenal, hepatic and ovarian cysts, hematomas, abscesses, hypovascular or necrotic neoplasms and abnormal fluid collections in various body cavities. Many such lesions have been detected incidentally in structures other than those being investigated.

To study the limitations of detecting these lesions, various sized water filled balloons were submerged to differing depths in a large vat of  $^{99m}\text{Tc}$  solution. Scintiphotos of the camera flood and of the various experimental exposures were presented to 11 physicians in random order. All tended to underestimate the size of the "lesions" "Lesions" smaller than 3 cm in diameter could not be reliably identified even at the surface. At an average depth of 10 cm most observers barely perceived a 5-6 cm "lesion". At 14 cm depth, the smallest detectable "lesion" was 10 cm in diameter. Observer experience appeared to bear no relationship to the ability to detect these lesions.

**BRAIN TUMOR SCANNING AGENTS COMPARED IN AN ANIMAL MODEL.**  
Tad Konikowski, Monroe F. Jahns, Thomas P. Haynie, and Howard J. Glenn. The University of Texas System Cancer Center, M. D. Anderson Hospital and Tumor Institute, Houston, Texas.

We have investigated 16 radiopharmaceutical preparations, using a well-established transplantable mouse brain tumor technique. In attempting to intercompare the results we appreciated the need for a rating system. The one which we will report here takes into consideration (1) the amount of radioactivity in the tumor at the time of scanning and (2) background radioactivity in brain, blood, and skin at time of scanning. Physical and radiobiological properties, including gamma energy, physical half-life, and absorbed radiation dose, and radiochemical properties such as stability and toxicology are also important, but will be considered separately in a later report.

The compounds were arranged in their order of decreasing tumor radioactivity, tumor-to-brain, tumor-to-blood, and tumor-to-skin ratios, and their ranking in the four categories added together to give a merit score. The ranking at 10 to 30 min intervals of the 16 compounds studied was as follows: (1)  $^{111}\text{In}$ -chloride (pH 1.5), (2)  $^{99m}\text{Tc}$ -iron ascorbic acid, (3)  $^{67}\text{Ga}$ -lactate, (4)  $^{197}\text{Hg}$ -chloromerodrin, (5)  $^{99m}\text{Tc}$ -Sn-DTPA, (6)  $^{111}\text{In}$ -bleomycin, (7)  $^{131}\text{I}$ -human serum albumin, (8)  $^{189}\text{Yb}$ -DTPA, (9)  $^{99m}\text{Tc}$ -iron-ascorbic acid DTPA, (10)  $^{113m}\text{In}$ -DTPA, (11)  $^{67}\text{Ga}$ -chloride, (12)  $^{67}\text{Ga}$ -citrate, (13)  $^{67}\text{Ga}$ -iron-DTPA, (14)  $^{99m}\text{Tc}$ -pertechnetate (perchlorate pre-dose), (15)  $^{197}\text{Hg}$ -chloromerodrin (meralluride pre-dose) and (16)  $^{99m}\text{Tc}$ -pertechnetate. Indium-111-chloride was also the top-rated compound at 1-2 hours, and 48 hours post-dose. At 24 hours,  $^{67}\text{Ga}$ -lactate was first and  $^{111}\text{In}$ -chloride was second.

Based on these considerations,  $^{111}\text{In}$ -chloride injected at pH 1.5 would appear as the agent of choice for brain tumor scanning.

**KINETICS OF  $^{111}\text{In}$ -BLEOMYCIN VERSUS  $^{111}\text{In}$ -CHLORIDES IN MICE.**  
T. Konikowski, T. P. Haynie, and H. J. Glenn. The University of Texas System Cancer Center, M. D. Anderson Hospital and Tumor Institute, Houston, Texas.

Indium-111 has been reported to be useful as a tumor-scanning agent both in chloride and bleomycin form. We have compared the kinetics of these compounds in mice bearing a transplantable brain sarcoma.

The pH of commercially obtained  $^{111}\text{In}$ -chloride was adjusted to 1.5 or 6.5 prior to injection. Indium-111 bleomycin at pH 6.5 was obtained commercially. Intravenous injection of  $^{111}\text{In}$ -chloride at pH 1.5 resulted in binding to transferrin. Indium-111 chloride was colloidal at pH 6.5.

The results are summarized in the following table.

Compound	Max. % dose/gm tumor	Max. ratio tumor:brain	Max. ratio tumor:blood	Renal blood clearance ml/min
$^{111}\text{In-Cl}_3$ (pH 1.5)	18.5	17.0	4.4	.0022
$^{111}\text{In}$ -bleomycin	3.0	13.5	6.8	.2535
$^{111}\text{In-Cl}_3$ (pH 6.5)	1.0	9.6	1.2	Not cleared

The maximum uptake and tumor-to-brain ratios occurred 4 hours after injection of  $^{111}\text{In}$ -chloride (pH 1.5) and 20 min after injection of  $^{111}\text{In}$ -bleomycin. Forty-eight hours after injection there was a 4% dose/gm tumor uptake with  $^{111}\text{In}$ -chloride (pH 1.5) and 0.5%/gm uptake with  $^{111}\text{In}$ -bleomycin; however, tumor-to-blood ratios were better with  $^{111}\text{In}$ -bleomycin.

Labeling bleomycin with  $^{111}\text{In}$  results in a tracer with localizing properties in this tumor model different from that obtained with  $^{111}\text{In}$ -chloride at pH 1.5 or 6.5. Although tissue ratios of  $^{111}\text{In}$ -bleomycin are higher 48 hours after injection, concentration in tumor is only one-eighth that of  $^{111}\text{In}$ -chloride at pH 1.5.

**GAMMA-RAY IMAGING WITH A TIME-MODULATED PSEUDO-RANDOM APERTURE AND AN ANGER CAMERA.** K.F. Koral, W. L. Rogers, W.R. Beierwaltes. University of Michigan, Ann Arbor, Mich.

The quest for improved signal-to-noise, higher resolution, and tomography in Nuclear Medicine has sparked an intense interest in imaging with coded apertures such as the Fresnel zone plate. Zone plate imaging, however, requires a detector resolution of 3 mm or better and use of a half-tone screen with a corresponding 50% loss in signal. Furthermore, the zone plate and other stationary apertures can give rise to image artifacts from out-of-focus sources.

May, Akcasu, and Knoll have developed a time-modulated approach to coded aperture imaging which eliminated these difficulties. Utilizing this approach we constructed a time-modulated pseudo-random aperture and tested it with an Anger camera. The aperture consists of an 121-element code distributed over a rectangular plate. A 3.3 cm square opening defines successive coded patterns. With this system we have obtained the following results. Smooth defocusing has been demonstrated for a point source. Extended sources have been imaged without a half-tone screen. Coded images of a 23 uCi thyroid phantom have been obtained in 120 seconds and the reconstructed image has been compared to images obtained under identical conditions with an equivalent pinhole. Equal resolution is obtained and the coded aperture image appears superior to the original pinhole image with respect to room background and photon statistics.

**DIAGNOSIS OF HEPATIC AMEBIASIS.** Bernadine Kovalski, Klitia Vanags, Monika Schreyer, Jorge Franco. O'Connor Hospital Medical Center, San Jose, Ca.

Amebic liver abscesses occur in less than 1% of patients with intestinal infection. However, recognition and treatment of this condition may be a medical emergency.

In this study we report the combined use of isotopic colloid scanning and a quick serologic test in the diagnosis and management of 8 patients with amebic liver abscesses.

Seven male and 1 female adults, ages 20-54, presented right upper quadrant abdominal pain and variable liver function tests. Scanning was done with the scintillation camera and  $^{99m}\text{Tc}$  sulfur colloid. Abnormalities encountered were: well-defined, multiple (3 cases), or single (5 cases) defects in the right lobe.

The serologic test consisted of a search for antibodies against HK-9E histolitic antigen in the patient's serum by means of counter-electrophoresis. Both the patient's sera and known positive and negative controls were inactivated at 56°C for 20 minutes prior to testing. Counter-electrophoresis was carried out for 30 minutes

at 40 milliamps. All patients' sera were positive. 100 control sera were negative. All 8 patients responded well to Flagyl therapy. Follow up liver scans demonstrated gradual normalization of the scan over several months. The serologic tests remained positive.

We conclude that a positive counterelectrophoresis test in a patient with defects in the liver scan is usually diagnostic of hepatic amebiasis, and that a negative test usually excludes such a diagnostic possibility.

**INSTANT LABELING HUMAN SERUM ALBUMIN MICROSPHERES.** Gary E. Krejcarek, Karen L. Bradford, and Theodore F. Bolles, Nuclear Products, 3M Co., St. Paul, Minn.

Since their introduction in 1970, technetium  $^{99m}$ -labeled HSA microspheres have become an important diagnostic radiopharmaceutical for circulatory studies.

An instant labeling microsphere kit has been developed which reliably prepares a consistent, high-quality pharmaceutical. Microspheres containing approximately 20  $\mu$ g of tin per mg of albumin and a small amount of a non-ionic detergent are contained in a pharmaceutical vial. Tagging is accomplished by simply adding the desired amount of pertechnetate to the vial and placing it in an ultrasonic bath for five minutes. No rinsing nor resuspending are necessary. The resulting labeling efficiency is greater than 98%. The technetium label does not dissociate from the microsphere *in vitro*; less than 1% free technetium is found eight hours after labeling.

The instant labeling microspheres retain all the desirable characteristics of the microspheres labeled by the current thiosulfate method; the size and swelling parameters and the LD<sub>50</sub> in mice and rats remain unchanged. The biological half life of the particles in the mouse lung is similar.

Organ distribution studies in the mouse show that more than 90% of the injected activity localizes in the lung and the lung-to-liver ratio is 65:1 five minutes after injection. Approximately 70% of the injected activity is still present in the lung two hours after injection, thereby allowing ample time for multiple views.

Clinical results indicate that high-quality lung images are consistently obtained with instant labeling HSA microspheres.

**KINETICS OF  $^{99m}$ Tc-LABELED POLYPHOSPHATE (Tc-POP) AND DIPHOSPHONATE (Tc-DIP) IN MAN.** G.T. Krishnamurthy, J.S. Endow, C.F. Walsh, V. Singhi, M. Tubis, and W.H. Bland, Veterans Administration Wadsworth Hospital Center and UCLA School of Medicine, Los Angeles, Calif.

A group of 11 patients with suspected bone lesions was studied. Studies were done following the intravenous injection of 15 mCi of Tc-POP and repeated 3 days later with 15 mCi of Tc-DIP. Blood samples were drawn at 10 and 30 min, and 1, 2, 3, and 4 hr. Radioactivity in plasma protein fractions, in red cells, and excreted in urine was determined. Skeletal images were obtained with a scintillation camera equipped with a high resolution collimator. Images of identical regions were obtained with each agent 4 hr post-injection.

Blood clearance was significantly faster with Tc-DIP ( $p < 0.01$ ). Blood clearance was also biexponential (Expo I & Expo II). Tc-DIP Expo I T/2 was 18 min and Expo II T/2 was 168 min. With Tc-POP, Expo I & II were 30 min and 294 min, respectively. Expo I represents mainly bone uptake and Expo II represents mainly renal excretion. At the end of 4 hr, 10% of the injected dose of Tc-POP was circulating in blood, 33.3 excreted in urine, and 56.7% was taken up by bone. Corresponding values with Tc-DIP were 7.0% in blood, 33.8% in urine, and 59.2% in bone. Cumulative urinary excretion was the same for both agents, 33% at the end of 4 hr, suggesting that lower blood radioactivity levels of Tc-DIP are due to increased bone uptake and not renal excretion. Protein binding was almost identical with both agents. With Tc-POP, 75.4% of plasma radioactivity was protein bound in contrast to 84.2% with Tc-DIP. The remaining radioactivity was free in plasma. RBC binding was firm with Tc-POP and loose with Tc-DIP. Skeletal images were excellent with both agents and there was evidence of more *in vivo* stability with Tc-POP. The kidneys are well visualized with both agents.

**KINETICS OF  $^{99m}$ Tc-LABELED POLYPHOSPHATE (Tc-POP) AND PYROPHOSPHATE (Tc-PYRO) IN MAN.** G.T. Krishnamurthy, R.J. Huebner, C.F. Walsh, M.D. Kehr, J.R. Taylor, M. Tubis, and W.H. Bland, Veterans Administration Wadsworth Hospital Center and UCLA School of Medicine, Los Angeles, Calif.

A clinical study was undertaken to evaluate the kinetics of Tc-POP and Tc-PYRO as bone-seeking radiopharmaceuticals. Ten patients with suspected bone lesions were injected intravenously with 15 mCi of each agent. Blood was collected at 10 and 30 min, and 1, 2, 3, and 4 hr post-injection. Radioactivity in whole blood, plasma, plasma proteins, and red blood cells was determined and expressed as percent of administered dose per liter. Urine was collected during the period of study and radioactivity excreted in urine was determined. Serum ionized calcium was determined prior to and one hour after injection. Plasma protein fraction binding of Tc-POP and Tc-PYRO was determined by microzone electrophoresis. Scintillation camera bone images of identical areas were obtained with both agents.

Blood clearance of Tc-POP and Tc-PYRO was biexponential (Expo I & Expo II). Clearance T/2 of Expo I was the same for both agents. Clearance time of Expo II was 380 min with Tc-PYRO and 512 min with Tc-POP. Expo I represents primarily bone uptake and Expo II represents urinary excretion. Total 4-hr urinary excretion was 31.7% with Tc-PYRO and 29.0% with Tc-POP. About 80% of the plasma radioactivity was protein bound with both agents. Both showed firm red blood cell binding. Four hours after injection, 12% of Tc-POP was circulating in blood, 58.5% was deposited in bone and other tissues, and 29.5% excreted in urine. With Tc-PYRO at 4 hr, 9.5% was in blood, 58.8% in bone and other tissues, and 31.7% in urine. Images obtained with Tc-PYRO were consistently better than with Tc-POP. Good renal images are obtained with both agents. There was no effect on serum ionized calcium 1 hr after injection of either agent. Both agents are stable *in vivo*.

**MEASUREMENT OF LOCAL CEREBRAL BLOOD VOLUME USING EMISSION TRANSVERSE SECTION SCANNING.** David E. Kuhl, Martin Reivich, Abass Alavi, Istvan Nyary and Muni Staum, Hospital of the University of Pennsylvania, Philadelphia, Pa.

We have developed a patient study method to determine absolute values of local cerebral blood volume (LCBV) localized throughout the brain in three dimensions and presented in cross-section picture format. Previously, absolute values of LCBV have been determined *in vivo* only by stimulated x-ray fluorescence, but these determinations have been limited to one point in the brain at a time. All other previous estimates of LCBV by external emission counting have been complicated by the significant contribution of blood in overlying scalp and cranium.

In the new method, a transverse section scan is made after an intravenous injection of  $^{99m}$ Tc-red cells. Data processing gives a point-to-point estimate of absolute radionuclide concentration, analogous to an autoradiograph. Using a known concentration of blood activity, data are converted to a two-dimensional map of LCBV representing a cross-section at a known level of the brain.

In a series of five baboons, the following equation was obtained for the regression plane relating LCBV in the center of the brain to PaCO<sub>2</sub> and mean arterial blood pressure (MABP):

$$LCBV = 2.88 + 0.049 (\text{PaCO}_2) - 0.013 (\text{MABP})$$

In patients, LCBV values ranged from 1.8 to 4.1 ml/100 gm depending on location, with higher values corresponding to regions of cerebral cortex. Differences in vascularization of focal brain lesions were quantified. In one patient, the method demonstrated reduction in LCBV surrounding a small glioma due to brain edema and showed improvement in regional circulation after treatment.

**RUBIDIUM-81 IN EVALUATION OF REGIONAL MYOCARDIAL PERFUSION.** James F. Lamb, Archie Khentigan, Gary A. Baker and H. Saul Winchell, Mediphsics, Inc., Emeryville, Calif.

Regional myocardial perfusion can be evaluated by imaging the distribution of intravenously administered  $^{81}\text{Rb}$ . Rubidium, like potassium, localizes within minutes after I. V. injection in tissues having relatively high blood perfusion rates and then clears from those tissues to equilibrate within the body's intracellular space. Because  $^{81}\text{Rb}$  decays to the short-lived inert gas daughter, 13 sec  $^{81\text{m}}\text{Kr}$ , the in vivo distribution ratio of the radiations from the decay of the daughter to the radiations from the decay of the tissue-fixed parent nuclide potentially yield a measure of instantaneous regional blood flow. Phantom studies show that the radiations emitted in the electron capture and positron decay of 4.6 hour  $^{81}\text{Rb}$ , 446 keV and 511 keV and in the isomeric transition decay of  $^{81\text{m}}\text{Kr}$ , 190 keV, are well suited to present-day imaging devices. A specially designed collimator cap for existing scintillation cameras fitted with pinhole collimators helps reduce collimator penetration and spurious edge counts which result from high-energy radiations. The calculated absorbed radiation dose for I. V. administered  $^{81}\text{Rb}$ , containing less than 33%  $^{82\text{m}}\text{Rb}$  at calibration time ( $< 0.21$  rad/mCi whole body), is about  $\frac{1}{4}$  of that associated with use of  $^{43}\text{K}$ . Satisfactory images of normal and diseased human myocardium have been obtained with  $^{81}\text{Rb}$  using both rectilinear scanners and scintillation cameras.

**DIAGNOSTIC POTENTIAL OF THE RADIOESOPHAGOGRAM.** Aldo E. Lano, Rene Dietrich, and Antonio Bosch. Puerto Rico Nuclear Center, University of Puerto Rico, Rio Piedras, P. R.

The radioesophagogram (REG) technique introduced by I. Kazem for studying esophageal dynamics through oral administration of  $^{99\text{m}}\text{Tc}$  pertechnetate has been tried after certain modifications, as an initial method for evaluating esophageal disorders, as well as for follow-up after treatment of cancer of the esophagus, and as a possible screening tool for early detection of cancer of the esophagus.

The modified method essentially consists of orally administering  $^{99\text{m}}\text{Tc}$  in a gelatin medium, and monitoring the transit of the bolus from the pharynx to the cardia with an Anger Camera on line with a Video-Tape recorder. The esophageal region is divided into two segments and the passage of radioactive bolus generates two histograms, representing the accumulation of counts for each of the segments. The transit time, together with the histograms, will indicate whether a REG is normal or not.

One-hundred and eighty normal volunteers were studied. The average value for the transit time was  $5.9 \pm 0.07$  sec.

A REG was performed on 594 subjects with esophageal symptoms, of which 121 (20%) showed an abnormal REG. Eighteen patients with proven cancer of the esophagus were studied and the REG was found abnormal in all of them. Two additional cases with abnormal REG, but with negative barium swallow, proved to have carcinoma of the esophagus on biopsy obtained during esophagoscopy. Fistulae were clearly observed and identified on the REG. Abnormal REG were also obtained in conditions such as hiatal hernia, fibrosis or stenosis due to thoracic surgery, and others.

The study takes a short time, and no special preparation is required. The irradiation is as low as 5-6 millirads; the cost is low, and the accuracy is high, all of which make the REG recommendable as a screening tool and as an aid to diagnosis and follow-up of esophageal disorders.

**INHIBITION OF THE METABOLISM OF STREPTOCOCCI AND SALMONELLA BY SPECIFIC ANTISERA.** Steven M. Larson, Patricia Charache, Marianne Chen, and Henry N. Wagner, Jr. The Johns Hopkins Medical Institutions, Baltimore, Md.

The presence of microorganisms in biologic samples can be detected radiometrically by measuring the  $^{14}\text{CO}_2$  produced by their metabolism of  $^{14}\text{C}$  labeled glucose and other substrates (DeLand & Wagner, 1969). The metabolism of streptococci and salmonella can be profoundly inhibited by specific antisera. Streptococcal and salmonella antisera inhibited carbohydrate metabolism for groups A, B, C, and D streptococci and group E salmonella. The inhibition was group specific in that, group E salmonella were inhibited only by salmonella E antisera and not anti-salmonella A or C. For streptococci, metabolism of types B and C were in-

hibited by group A antisera. However, the effect of inhibiting antibody was greatest for the specific streptococcal group. By employing different concentrations of antisera, differential identification was possible. Cross-reacting antibodies could be absorbed by incubation with either antigen, e.g., streptococcal antisera vs. heat killed salmonella. At high concentrations, the antisera were bactericidal; at more dilute concentrations, for both salmonella and streptococci carbohydrate metabolism was suppressed but subculture on chocolate agar showed abundant growth. The radiometric technique was more sensitive than either capillary flocculation or visual detection of bacterial growth for detecting the inhibition of streptococci and salmonella by specific antibodies. We conclude that these observations may provide a basis for extending the radiometric detection technique to include the rapid automated specification of bacteria.

**RADIOMETRIC SCREENING TEST OF CELL-MEDIATED IMMUNITY BASED ON PHYTOHEMAGGLUTININ(PHA) INDUCED CHANGES IN LYMPHOCYTE CARBOHYDRATE METABOLISM.** Steven M. Larson, Timothy Merz, and Henry N. Wagner, Jr. The Johns Hopkins Medical Institutions, Baltimore, Md.

The effect of phytohemagglutinin (PHA) in transforming lymphocytes into lymphoblasts is one test of the adequacy of the cellular immune system. Most tests of PHA stimulation involve either visual assessment of blast transformation at 5 to 7 days, or uptake of tritiated thymidine at 72 hours or later. These tests are relatively cumbersome, and do not lend themselves to automation. We have developed a rapid radiometric technique which is based on the measurement of  $^{14}\text{CO}_2$  produced by metabolism of  $^{14}\text{C}$ -glucose. We use an ionization chamber to quantitate the radioactivity. Lymphocytes are obtained from peripheral blood and separated by differential centrifugation. The cells are suspended in a modified Hanks buffer solution containing 1 microcurie of  $^{14}\text{C}$ -glucose. Measurements were made at one hour at  $37^\circ$  (equivalent to 0.5ml whole blood).  $1.0 \times 10^6$  lymphocytes produced sufficient  $^{14}\text{C}$  so that their basal metabolism of  $^{14}\text{C}$ -labeled glucose is easily detected. PHA induces a marked change in lymphocyte carbohydrate metabolism within one hour after addition to the test system. In a group of 20 normal adults, average PHA stimulation was 2.2 times control levels. Peak stimulation occurred within 2 hours after addition of PHA. Metabolism of  $^{14}\text{C}$ -glucose was progressively increased by increasing addition of PHA from 0-3mg of PHA. At concentrations greater than 3mg there was no further increase. The radiometric technique holds promise as an important improvement in the assessment of the response of the lymphocyte to PHA, and therefore of potential usefulness in assessing immune competence.

**A SIMPLE PROCEDURE TO MAKE  $^{99\text{m}}\text{Tc}$  ALBUMIN MACRO-AGGREGATES.** Dionisio Lasa-Perez, A. Martos and S. Perez-Modrego. Hospital Oncologico Provincial, Madrid, Spain.

We have developed a simpler, faster and more reliable method of preparing sterile and pyrogen-free  $^{99\text{m}}\text{Tc}$  M.A.A.

$^{99\text{m}}\text{Tc}$  M.A.A. using  $\text{BH}_4\text{Na}$  as reducing agent of Tc(VII) are prepared in presence of 20% H.S.A. At pH  $4.9 \pm 0.3$  and after heating in boiling water and shaking, the  $^{99\text{m}}\text{Tc}$  M.A.A. are formed.

The solutions are previously either autoclaved or filtered through a bacterial filter.

Several analytical parameters of process were studied. The size distribution of particles was controlled by microscopic examination. The  $^{99\text{m}}\text{Tc}$  M.A.A. chromatographic data showed that 96% of the activity is associated with the particles. The organ distribution of  $^{99\text{m}}\text{Tc}$  M.A.A. was performed in 15 white rats and about 86% of the dose administered was found in the lung. Over 650 patients were studied using  $^{99\text{m}}\text{Tc}$  M.A.A. prepared with this technique in an Anger camera. No secondary reactions were observed.

This method has the following advantages: It is simple and reproducible. The procedure is rapid, taking only 5 minutes and no final pH adjustment, further chemical manipulation or sterilization is required.

GENERAL APPLICATIONS OF THE PROGRAMABLE DESK TOP CALCULATOR. Michael A. Lawson, and S. R. Kiser. Letterman Army Medical Center, San Francisco, Calif.

The programable desk top calculator has been used in our clinic for a variety of administrative tasks, in vivo and in vitro procedures, and in support of the radiopharmacy. The impact of its use on accuracy, the saving of time for the physicians, technicians and secretaries, and the generation of quality hardcopy format for reporting and recording are tangible benefits of such equipment. This equipment with peripheral devices (including (1) x-y plotters, (2) typewriters, (3) thermoprinters, (4) tape cassettes, (5) paper tape readers, and a variety of soft ware) is available from a number of manufacturers. Although the capability of this equipment is not equivalent to that of a computer, the ease of operation and the reduced cost of acquisition make the programable calculator attractive for many procedures which do not require the storage capability of a true computer.

Our purpose in presentation is to demonstrate how we utilize such equipment in support of activities in our nuclear medicine clinic. Tables and the graphic examples illustrate procedures presently and routinely performed with our desk top calculator and its peripherals. These are listed in Table 1.

TABLE 1

PROCEDURES ROUTINELY PERFORMED ON DESK TOP CALCULATOR  
Nuclear Medicine Service, Letterman Army Medical Center, 1973

- General: Film badge control records, work schedules  
Radiopharmacy: Calculation of dose, continuous concentration schedules for radionuclide activity  
Radioassay Procedures: T<sub>1</sub>, T<sub>2</sub> uptake, FTI, B-12, folate, digoxin, HAA (hepatitis associated antigen)  
Hematology: Schilling test, RBC mass and blood volume with <sup>51</sup>Cr, RBC survival with <sup>51</sup>Cr

DEVELOPMENT OF <sup>97</sup>Ru AND <sup>67</sup>Cu FOR MEDICAL USE. E. Lebowitz, M. Kinsley, P. Klotz, C. Bachsmith, A. Ansari, P. Richards and H. L. Atkins. Brookhaven National Laboratory, Upton, N.Y.

The purpose of this study is to develop <sup>97</sup>Ru and <sup>67</sup>Cu, which have been suggested for use in nuclear medicine. The combination of excellent physical and chemical properties of <sup>97</sup>Ru make this isotope worth evaluating. <sup>97</sup>Ru can be produced in high yield (>5 mCi/μAh) and purity (>99.9%) using the <sup>99</sup>Tc(p,3n)<sup>97</sup>Ru reaction. The <sup>97</sup>Ru is purified by coprecipitation with Fe(OH)<sub>3</sub> which does not coprecipitate TcO<sub>4</sub><sup>-</sup>. A ruthenium radiocolloid is under development which appears advantageous for lymphangiography in animal studies, because of its rapid clearance from the injection site and rapid lymph node uptake. The possible uses of <sup>67</sup>Cu include tumor diagnosis, cancer therapy, studies of Wilson's disease and gastrointestinal protein loss. <sup>67</sup>Cu has a convenient half-life and excellent photons for imaging. Its beta emission is disadvantageous for diagnostic use. <sup>67</sup>Cu can be produced in high radioisotopic purity, high specific activity, and high chemical purity by the proton irradiation of gallium. Chemical purification is by ether extraction, then cation exchange. These results indicate a potential for producing large quantities of these isotopes in the now operating BLIP (Brookhaven Linac Isotope Producer) for wide-spread evaluation.

THE ACTA-SCANNER: A NEW TRANSVERSE AXIAL TOMOGRAPH. Robert S. Ledley, Ayub K. Ommaya, and John C. Harbert. Georgetown University Hospital, Washington, D. C.

A second generation computerized transverse axial tomograph has been developed capable of using either an X-Ray tube or radionuclide source. The instrument is capable of whole body section scanning because of a

special algorithmic program which does not require a surrounding water jacket. This program eliminates bone-tissue interface artifacts, greatly improving the resolution of para-osseous structures. In addition to the grey-white scale, a color display and 160 x 160 matrix are used to accurately delineate the numerical values of the "relative absorption coefficients" derived from the scan. A variety of scanning modalities have been provided which include stepping intervals of 1, 2 and 6 degrees and 9 and 18 - inch length scan passes. The image produced appears immediately upon completion of the scan. Examples of the display will be shown.

CORRELATION OF SCINTIGRAPHIC AND SONOGRAPHIC FINDINGS IN FOCAL LIVER DISEASE. George C. Lee, Robert L. Wilson, Alan D. Waxman and Jan K. Siemsen. LAC/USC Medical Center, Los Angeles, Calif.

Scintigraphy and sonography assess different aspects of liver disease--namely regional functional integrity and acoustic density, respectively. Their use in combination should, therefore, provide supplementary diagnostic information.

To test the practical validity of this premise, radionuclide scans (RNS) and ultrasound scans (USS) on 73 patients were analysed blindly. A definite diagnosis was available, in most cases by histology, in some amebic abscesses by immunology and prompt response to specific therapy. Selected patients (20/73) also had gallium scans.

Of 16 tumors, all were demonstrated as filling defects (FD) on RNS; 11 appeared solid on USS, 3 semicystic and 1 was obscured by ascites. 7/9 of this group had increased gallium uptake. Of 29 abscesses (23 amebic, 6 pyogenic) 8 appeared cystic and 12 semicystic on USS, but 3 were missed. One pyogenic abscess was missed on RNS. Of 11 patients with cirrhosis, only 3 showed discrete FD on RNS, the others patchy hepatomegaly. Eight had diffusely increased echos on USS, 1 was normal and 2 uninterpretable because of ascites.

Combined studies were also useful in some less common conditions.

The study supports the premise that sonography and conventional scintigraphy give complementary information and should be used concurrently as "first line" differential diagnosis tools, with additional scintigraphic techniques in selected cases.

ARGON-37 EXCRETION IN HUMANS FOLLOWING TOTAL BODY NEUTRON ACTIVATION. Thomas K. Lewellen, Wil B. Melp, H. Earl Palmer, Robert Murano, Gervys M. Hinn and Charles H. Chesnut, III. University of Washington Hospitals, Seattle, Washington and Battelle Northwest Laboratories, Richland, Washington

A technique to quantitate body calcium in humans by total body neutron irradiation utilizing the <sup>40</sup>Ca(n, α) <sup>37</sup>Ar (35 day half-life) reaction is under investigation. The quantitative excretion of <sup>37</sup>Ar in the breath could be a precise indicator of total body calcium (bone mass) and, with serial studies, of calcium balance.

As compared to the current technique, using the <sup>48</sup>Ca (n, γ) <sup>49</sup>Ca (8.8 min. half-life) reaction, the argon method has the advantages of: 1) long half-life for counting, 2) use of small proportional detectors instead of whole body counters, 3) the use of a small 14-MeV neutron generator, and 4) significant dose reduction.

To measure the excretion rate, exhaled air was collected from 6 patients at intervals up to 16 hours following irradiation at the University of Washington cyclotron. The <sup>37</sup>Ar was purified by selective absorption and final trapping on molecular sieve material at -190°C. The <sup>37</sup>Ar was then placed in a low-background proportional detector and counted for several hours.

In all subjects there is an initial rapid excretion of <sup>37</sup>Ar with a half-life of approximately 30 minutes. After 10 hours, the excretion rate is negligible, being less than 0.01 of the initial rate.

These studies confirm the  $^{37}\text{Ar}$  excretion phenomenon as suggested by animal studies (H.E. Palmer, J. Nucl. Med. 14:522, 1973) and suggest the excretion rate will be sufficiently short to undertake total body calcium studies, at very low patient doses, using a breath collection time of 4 to 8 hours. Total body neutron exposure is expected to be as little as 10 millirads.

**A CLINICAL EVALUATION OF INDIUM-BLEOMYCIN AS A TUMOR IMAGING AGENT.** David L. Lilien, Stephen E. Jones, Robert E. O'Mara, Sydney E. Salmon and Brian G. Durie. University of Arizona Medical Center and Tucson VA Hospital, Tucson, Ariz.

We have evaluated the clinical usefulness of Indium-111 Bleomycin (IB) as a tumor imaging agent in 208 patients with a variety of solid tumors. In 198 of 232 studies (84%), there was excellent correlation with known sites of disease. There were 22 false positive studies (10%) and 15 false negatives (6%). Excellent results have been seen with a wide variety of tumors including many in which reported results with other agents have been disappointing. Good correlation has been seen in 79% of 75 patients with lymphoma, 95% of 40 lung CA, 71% of 21 breast CA, 88% of 15 ovarian CA, 100% of 14 melanoma, 90% of 10 miscellaneous sarcomas, 80% of 10 colon CA, and 70% of 10 head and neck tumors. Similar results have been seen in 38 patients with a variety of other tumors. Hepatic lesions rarely contain more radioactivity than surrounding normal liver. Lesions in marrow-bearing areas of bone usually appear as negative defects. False positives have been seen with a variety of inflammatory lesions. Some false positives consist of diffuse pulmonary uptake which has invariably occurred in patients receiving chemotherapy with alkylating agents. Adverse reactions, consisting of mild fever and chills, occurred 3 times in 2 patients. Significant advantages over other available agents appear to be a broader spectrum of tumor types taking up the radiopharmaceutical as well as lack of interference from uptake in gut. IB appears to be a safe and effective new tumor-imaging agent.

**INDIUM-BLEOMYCIN IN THE EVALUATION OF LYMPHOMA.** David L. Lilien, Stephen E. Jones, and Robert E. O'Mara. University of Arizona Medical Center and Tucson VA Hospital, Tucson, Ariz.

$^{111}\text{In}$ -Bleomycin (IB) was evaluated in 75 studies in 55 patients with lymphoma. 21 were nodular in histology, 19 diffuse and 15 had Hodgkin's disease. 16 patients were studied as part of their initial staging, 21 were in clinical remission on chemotherapy, 12 were in relapse and 6 were clinically free of disease following radiation therapy. In 59 of 75 studies (79%) there was excellent correlation with known clinical status. Results were similar in all histologic subtypes of disease. 129 of 144 (90%) clinically involved sites were correctly identified. There were 15 (10%) false negative and 24 (17%) false positive sites. In 8 patients (11%), IB scanning revealed clinically unsuspected sites of disease. Soft tissue and lymphatic sites of disease both above and below the diaphragm were well identified but difficulty occasionally arose in liver and bone marrow because of "normal" activity in these sites; here disease was most frequently correlated with negative scan defects. 5 (20%) of the false positives consisted of diffuse lung uptake, which invariably occurred in patients who were being treated with alkylating agents. False positives have been seen with inflammatory lesions in other patients, but none in this series. Mild fever and chills have occurred in less than 1% of studies; no other adverse reactions have been seen. IB is a safe and effective tumor-imaging agent and promises to be of great value in the evaluation and followup of patients with lymphoma.

**$^{99\text{m}}\text{Tc}$ -DIMERCAPTOSUCCINIC ACID FOR RENAL IMAGING.** T.H. Lin, A. Khentigan, and H.S. Winchell. Medi-Physics, Inc., Emeryville, Calif.

Dimercaptosuccinic acid, 3 mM, mixed with equal parts  $\text{SnCl}_2$ , 1 mM, can be used in kit form for labeling with  $^{99\text{m}}\text{Tc}$ -pertechnetate to produce an imaging agent for the renal cortex clinically superior to  $^{203}\text{Hg}$ -Chlormerodrin. Serial whole-body scintigraphy following I.V. administration of  $^{99\text{m}}\text{Tc}$ -dimercaptosuccinate shows that plasma clearance proceeds with a  $T_{1/2}$  of approximately 45 min due almost exclusively to renal accumulation of activity. The initial distribution is approximately the plasma volume with the label bound to plasma proteins. Negligible quantities of the label are found on red blood cells. The percents of administered dose localized in rat tissues one hour after intravenous administration of  $^{99\text{m}}\text{Tc}$ -dimercaptosuccinate are: kidneys, 54.2%; urine and bladder, 7.2%; liver and spleen, 5.3%; whole blood, 19%; and remainder of body, 12.5%. The localization of the agent in the renal cortex was demonstrated by scintiphotos of slices of rat kidney. The calculated radiation dose to the renal cortex in man is 1.4 rad/mCi administered. Dimercaptosuccinate has been administered parenterally in gram quantities to humans in the treatment of heavy metal poisoning and the  $\text{LD}_{50}$  for the compound given intraperitoneally to mice, is reported as 3.2 grams/kg. Rats given 1.2 ml/kg of the  $\text{Sn}$ /dimercaptosuccinate reagent intravenously for 14 consecutive days failed to show any clinical or histological changes related to administration of the reagent. Similar results were obtained using dogs over a 17-consecutive-day period. Clinical studies have confirmed that the in vivo behavior of  $^{99\text{m}}\text{Tc}$ -dimercaptosuccinate in humans is comparable to that in test animals.

**KINETICS OF HIPPURAN IN NORMAL AND ANEPHRIC SUBJECTS.** Roberto E. Maass, Raúl E. Pérez, and Rosa María C. Montesinos. Hospital "20 de Noviembre" and Instituto Nacional de Energía Nuclear, Mexico City, Mexico.

Curves of radioactivity were obtained over the precordium and lumbar area after administration of a dose of hippuran ( $^{131}\text{I}$ ) to a group of normal, anephric and unilaterally nephrectomized individuals. Continuous sampling of blood activity was also obtained from arterio-venous shunts in the anephrics. The simultaneous tracings from each individual were standardized by equalization of the third minute ordinates with the use of digital computing techniques. Also, the blood contribution of the body tracings was subtracted, resulting in the time-concentration curves of hippuran in interstitial fluid. In anephrics, this showed a rapid increase in concentration for approximately eight minutes and then a long straight portion with a slightly upward slope. In normals we observed the same sharp initial increment, followed by an horizontal or slightly decreasing slope. These findings can not be explained with the widely accepted model of a bicompartmental open system. The shape of our curves rather suggest a valve-like mechanism allowing free diffusion towards interstitial fluid and a restricted return to the plasma. A new model is proposed with a third compartment corresponding to the lymphatic vessels which fits more closely the experimental data.

**CARBON-11 LABELED ETHANOL: SHORT TERM TISSUE DISTRIBUTIONS.** N.S. MacDonald, L.R. Bennett, J.M. Uszler, G.D. Robinson and J. Takahashi. Laboratory of Nuclear Medicine, University of California, Los Angeles, Calif.

Metabolism of ethanol in the human has been customarily investigated using alcohol labeled with Carbon-14. Substitution with 20 min. half life Carbon-11 offers the possibility of administering sufficient activity to delineate

initial movements of labeled ethanol in the body with external scintillation detectors. Labeled ethanol and methanol were prepared by reduction of the intermediate formed by carbonation of the appropriate Grignard reagent with C-11 carbon dioxide, and characterized by gas radiochromatography. Distributions of C-11 were determined in tissues removed from rats and rabbits at intervals from 10 sec. to 60 min. following injection. In vivo studies of C-11 translocations in rabbits, dogs and monkeys during the first 10 min. after injection, utilized scintillation cameras with either a lead pinhole or tungsten multi-hole collimator. Images and decay-corrected activity vs time curves for visualized organs were derived with minicomputer assistance. Activity per gm in heart muscle became about 2 times that of blood within a min. then decreased to approx. blood conc. at 30 min. Liver act/gm rose more slowly and reached nearly 3 x blood conc. at 60 min. Kidney conc. rose rapidly to 2 x blood conc. at 5 min. and remained at that level. Brain tissue act/gm reached 0.9 x blood conc. within 1 min. after which the ratio declined slowly. These organs contained more <sup>11</sup>C than could be attributed to the blood content of the tissues. Image resolution permitted estimation of gross changes of activity in whole organs but was inadequate for depicting regional detail. Although <sup>11</sup>C activity reflects ethanol conc. for only a brief time due to metabolic transformations, short-term in vivo measurements are valid. <sup>11</sup>C labeled ethanol and methanol may become useful in disclosing gross changes in kidney, liver, brain and heart tissue consequent to toxic effects of these alcohols.

**PRODUCTION OF INDIUM-111 FOR MEDICAL USE WITH A COMPACT CYCLOTRON.** N.S. MacDonald, H.H. Neely, R.A. Wood, J.M. Takahashi, S.T. Wakakusa, R.L. Birdsall. Laboratory of Nuclear Medicine, University of California, Los Angeles, Calif.

Useage of In-111 for cisternal and marrow scanning is growing and may be extended to tumor visualization in the form of bleomycin complex. Four nuclear reactions for In-111 production were studied to determine the one best suited for small, multiparticle cyclotrons currently available in a number of medical centers. These were: protons and deuterons on natural Cd and <sup>3</sup>He and alphas on natural Ag. Expensive isotopically enriched targets were excluded. A simple, remotely removeable device supported the 1" diam. target foil in the vacuum at the end of the beam line. Cold water flowing under 40 psig cooled the back surface of the thin foil. This permitted dumping excess beam energy, unwanted after traversal of the target, directly into flowing water. Thus p,2n reactions could be favored over p,n reactions by reducing target thickness. Radio indium was isolated by liquid extraction technique using di-2 ethylhexyl-phosphoric acid. Radioassay was performed with Ge-Li gamma spectrometry and chemical purity with spark emission spectrography. The <sup>109</sup>Ag(<sup>3</sup>He,n) <sup>111</sup>In reaction was least productive. The <sup>109</sup>Ag( $\alpha$ ,2n) <sup>111</sup>In reaction gave the purest product (no <sup>114m</sup>In), but low yields averaging 53  $\mu$ Ci/ $\mu$ ampere-hour at end of bombardment at our max alpha energy of 24 MeV. 4.3 hr <sup>109</sup>In contaminant required 24 hr "cooling" period before use. The <sup>111</sup>Cd(D,2n) <sup>111</sup>In yielded 117  $\mu$ Ci/ $\mu$ ampere-hour at EOB, but by-products <sup>109</sup>In and <sup>110</sup>In required 48 hr cooling period and 50 day <sup>114m</sup>In amounted to 4.7% at EOB. By far the best yields(1.0mCi/ $\mu$ ampere-hour at EOB) were with 22 MeV protons (our max) on 0.020 inch Cd. This compromise gave max <sup>111</sup>In and kept unwanted <sup>114m</sup>In below 0.6% at EOB. Despite necessary 48 hr cooling period quantities routinely supplied for use are 20-40 mCi per 3 hr run.

**<sup>18</sup>F-6-FLUORODOPAMINE AS A POTENTIAL ADRENAL SCANNING AGENT.** R. R. MacGregor, A. N. Ansari, H. L. Atkins, D. R. Christman, J. S. Fowler, and A. P. Wolf. Brookhaven National Laboratory, Upton, N. Y.

Previous work with intravenously administered <sup>14</sup>C-dopamine and <sup>11</sup>C-dopamine has shown that it is taken up and retained by the adrenal medulla. We have prepared <sup>18</sup>F-labeled dopamine to evaluate it as an agent in the diagnosis of chromaffin tissue tumors and to compare its tissue uptake with that of dopamine itself.

A rapid synthesis of 6-fluorodopamine has been developed. A protected form of this compound was labeled by pyrolyzing 3,4-dimethoxy-6-(2'-phthalimidoethyl)-phenyl diazonium fluoroborate in the presence of <sup>18</sup>F obtained from the <sup>160</sup>(<sup>3</sup>He,n)<sup>18</sup>F water target. Hydrasolysis of the phthalimide group, cleavage of the methoxy groups with HI

and elution from ion exchange resin with HCl afforded <sup>18</sup>F-labeled 6-fluorodopamine·HCl with a specific activity of 400  $\mu$ Ci/mg at the time of injection (0.4 mg produced; chemical yield 20%; radiochemical yield 1.5%). Chemical and radiochemical purity of the <sup>18</sup>F-labeled product was confirmed by tlc.

Mice were given intravenous injections of <sup>18</sup>F-fluorodopamine·HCl (1.4 mg/Kg) and the uptake by different tissues as a function of time was studied. The mice were sacrificed in groups of three at 5, 15, 30, 60, 120 and 180 minutes. The average percent uptake in the adrenals at these times were 0.037, 0.031, 0.022, 0.013, 0.013 and 0.014, respectively. The adrenal-to-kidney ratios (percent/gram) at these times were 0.49, 0.40, 0.98, 1.6, 2.7 and 2.8 respectively, while the adrenal-to-liver ratios were 0.90, 0.29, 0.87, 3.0, 4.8 and 4.6. The evaluation of this compound with different specific activities in suitable animals is presently in progress.

**COMPUTER PROCESSED DISPLAY SYSTEMS FOR COMPUTERIZED TRANSAXIAL TOMOGRAPHS (EMI SCANNER).** William J. MacIntyre, Barry Rubinson, Bruno Sufka, and Jeffrey Arnold. Cleveland Clinic Center, Cleveland, Ohio

Conventional data read-out of the Computerized Transaxial Tomograph (EMI Scanner) consists of (1) a printed copy of the EMI number digits of the relative linear attenuative coefficients at each element of the 80 x 80 matrix representing the brain cross section and (2) a Polaroid print of the oscilloscope screen showing these 6400 elements at different degrees of intensity. Since it is known from radioisotope scanning that Polaroid prints are not optimum for scan visualization, the output of the EMI Scanner has been read into a PDP-15 for further processing and formatting for various display systems.

Following the digital filtering for noise reduction the EMI Scanner output has been displayed by a line printer with contour symbols identifying various levels of the attenuation coefficients, three-dimensional displays of the matrix drawn by an x-y plotter interfaced to the computer, and a color video readout of the matrix divided into sixteen color-coded levels.

The displays thus produced have been shown both with data directly obtained from the EMI printout and following the use of various digital filters in order to ascertain if improvement of the noise level of the EMI Scanner could be accomplished.

**UNILATERAL VERSUS BILATERAL ADRENAL GLANDS DISEASES; VALUE OF <sup>131</sup>I-19 IODOCHOLESTEROL SCINTIGRAPHY.** Franco Mantero, Corrado Macri and Mario Austoni. Istituto di Semeiotica Medica, University of Padua, Italy.

To differentiate unilateral versus bilateral adrenal diseases, <sup>131</sup>I-19 iodocholesterol scintigraphy (0.7-2.0 mCi, rectilinear scanner and Anger camera) has been performed in 16 patients. In 4 cases of Cushing's syndrome due to ACTH excess, both adrenal images showed similar activity and small differences in size; in 2 patients with adenoma, only one large gland could be visualized; after removal of the adenoma, the contralateral gland became evident. Among 7 patients with primary aldosteronism, 3 had a clearly larger and more intense image on one side, and in 2 cases the suspected side was confirmed after Dexamethasone. In one patient the adrenals appeared both enlarged and a bilateral hyperplasia was suspected. In another case, after removal of the right macronodular gland, a round concentrated area at the left kidney hilum was seen. In a patient with low PRA, low aldosterone and high plasma DOC the adrenals appeared both enlarged. Finally, in 2 female patients with virilization, one



had a functional nodule on one side and low uptake in the opposite; in the other patient both glands resulted similar in size and concentration; an adrenogenital syndrome was confirmed. Scintigraphic imaging provides an excellent aid in diagnosis and localization of adrenal diseases.

**RUBIDIUM-81, A NEW AGENT FOR MYOCARDIAL PERFUSION SCANS AT REST AND EXERCISE, AND COMPARISON WITH POTASSIUM-43.** Neil D. Martin, Barry L. Zaret, Ronald L. McGowan, Harry P. Wells, and M. D. Flamm. David Grant USAF Medical Center, Travis AFB, Calif.

Although myocardial imaging with potassium-43 ( $^{43}\text{K}$ ) has been established as an effective method for evaluating regional myocardial perfusion both at rest and at exercise, undesirable production characteristics of  $^{43}\text{K}$  have motivated a search for an effective substitute radionuclide. It is the purpose of this report to detail our preliminary experience with rubidium-81 ( $^{81}\text{Rb}$ ) in the noninvasive imaging of myocardial perfusion and its favorable comparability with  $^{43}\text{K}$ . Commercial cyclotron produced  $^{81}\text{Rb}$  was utilized as a myocardial scanning agent on 14 patients with coronary artery disease and 1 normal subject at rest, exercise, or both. Rest scans were obtained in the anterior and LAO positions on a rectilinear scanner after an intravenous injection of 4 mCi of  $^{81}\text{Rb}$ , and exercise scans were obtained in a similar manner after angina or fatigue had been induced on a motorized treadmill. All patients scanned with  $^{81}\text{Rb}$  had myocardial images of diagnostic quality. The myocardial image of the normal subject was normally homogeneous throughout the left ventricular wall after exercise. Eleven patients had previous myocardial infarction, and all were seen as perfusion defects on rest scans. Seven of these also had exercise scans; four had angina pectoris and scans showed larger perfusion defects than at rest, and three without angina had scans unchanged from rest. Two of three angina patients without infarction had normal rest scans and demonstrated perfusion defects after exercise; the third had an equivocal study. Ten patients had  $^{43}\text{K}$  scans and in every case the  $^{81}\text{Rb}$  and  $^{43}\text{K}$  images were comparable. Our experience with 21 rest or exercise studies on 15 subjects has shown that diagnostic myocardial perfusion imaging can be obtained with  $^{81}\text{Rb}$  and that results are comparable to those obtained with  $^{43}\text{K}$ .

**COMPARTMENTAL ANALYSIS IN HAEMOPHILIC ARTHROPATHY SCINTIPHOTOGRAPHY.** Remo Masi, M. Rosa Voegelin, Franco Grandonico, Enrico Pesciullesi, Massimo Morfini, P. Luigi Rossi-Ferrini. Nuclear Medicine Centre, University of Florence, Department of Haematology, Santa Maria Nuova Hospital, Florence.

Authors, after an extensive clinical application of joint scintiphotography in haemophilic arthropathy have performed a dynamic study using a scintillation camera interfaced with a computer. The histograms show significant differences not only between the affected and normal joint, but also between the normal and haemophilic muscular blood pool. To quantify these differences the histograms, after a preliminary data processing, were treated according to a compartmental model based on an ion trapping by the proteins of extravascular space of inflamed joints. The processing of data according to this model, though pointing out significant differences between haemophilic and normal subjects at articular and extra-articular level, also showed systematic differences between the functions fitted according to the model and the experimental ones which proved to include two exponential functions. The processing of data on the ground of a second model based on the reversible transfer between vascular and extravascular space, gives more accurate results. These may be considered the supporting data to the interpretation of tracer accumulation in the affected joints when the experiment is carried out on a dual basis, i.e.

with  $^{99\text{m}}\text{Tc}$  pertechnetate and  $^{99\text{m}}\text{Tc}$  albumin.

**SPLenic SEQUESTRATION: AN IN VIVO TEST FOR SPLENECTOMY.** Klaus Mayer, Kenneth Cheng, Laurence Clarke, Elaine Maughan, and John Laughlin. Memorial Sloan-Kettering Institute, New York, N.Y.

Hemolytic anemias of a variety of etiologies may respond well to splenectomy in cases where the spleen plays a significant role in sequestration of red cells. Relative measurements of splenic sequestration by static probe counting over liver, spleen and heart do not provide a differential diagnosis. Absolute quantitative data are necessary.

The method developed employs 'constant resolution' collimators designed for absolute organ activity measurements. Splenic uptake, corrected for blood background, can then be determined as a percentage of the injected dose. This method was previously validated by comparison of similarly determined radioactivity in vivo with assay of the extirpated organ in vitro.

CR 51 survival studies and spleen scans were performed on 16 patients with hemolytic anemia. In the 16 patients, organ uptake ranged from 27% to 43% at a time when 50% of the circulating radioactivity was lost (T 50%). In three splenectomized patients the organ uptake was 26%, 27%, and 43% at T 50%. In all three patients, there was good clinical response to splenectomy which suggests that absolute organ quantitation can give a meaningful indication for such a procedure in hemolytic anemia.

**SCINTIGRAPHIC ANGIOGRAPHY WITH CONTINUOUSLY GENERATED KRYPTON-81m.** Lewis W. Mayton, Ervin Kaplan, W. Earl Barnes, Lelio G. Colombetti, Arnold M. Friedman and James E. Gindler. V.A. Hospital, Hines, Illinois and Argonne National Laboratories.

A method of scintigraphic angiography has been developed for the evaluation of circulatory inadequacy, based upon continuous generation and constant rate intravascular delivery of krypton-81m in 5% dextrose-and-water. This radionuclide decays with a 13 second half-life to  $^{81}\text{Kr}$ , emitting a 190 KeV monoenergetic gamma ray. It is a daughter product of rubidium-81, which has a half-life of 4.7 hours, produced by alpha bombardment of stable bromine in the 60 inch Argonne cyclotron. The target material is  $\text{Cu}^{2}\text{Br}_2$  on a copper target. A typical activation produces 50 mCi of  $^{81}\text{Rb}$  activity. A miniature  $^{81}\text{Rb}$ - $^{81\text{m}}\text{Kr}$  generator, with internal dimensions of 2.5 mm diameter and 22 mm length, retains the  $^{81}\text{Rb}$  on 80 cu. mm of Dowex 50-X8 exchange resin, layered between two plugs of inert filtering support material. A constant rate infusion pump elutes > 80% of the generated  $^{81\text{m}}\text{Kr}$  with an adjustable flow rate of 0.5 to 1.5 cc/min. A 0.28 mm I.D. polyethylene catheter will provide an on line conduit into a vein or artery. The  $^{81\text{m}}\text{Kr}$  solution, at activity levels of 6000 c/s, was virtually without  $^{81}\text{Rb}$  contamination, as the preparation was free of sodium and other exchangeable cations. During constant rate intravascular  $^{81\text{m}}\text{Kr}$  delivery, steady state conditions are rapidly achieved and maintained. Since the rapid decay is of the same order of magnitude as diffusion time into extracapillary compartments, heterogeneity of distribution of activity at equilibrium is proportional to diffusion time and may define conditions of absent or altered circulation. Many scintigraphic images of high quality have been obtained in the dog during constant intravenous and intraarterial administration. The short half-life is compatible with high photon flux and low radiation exposure.

**USE OF THE CEA TITER AS AN ADJUNCT TO THE LIVER SCAN IN THE DIAGNOSIS OF HEPATIC METASTASES.** William H. McCartney, Paul B. Hoffer, and Erika Lawrence. University of Chicago, Department of Radiology, Chicago, Ill.

The liver scan is a valuable study for the detection of hepatic metastasis, however, has a false-negative rate of between 10 and 30%. Recently, the carcinoembryonic antigen immunoassay has been introduced as a method of detection of enterodermally derived neoplasms. Clinical studies have revealed a high incidence of metastases in patients with CEA titer significantly above the "normal" range of 0 to

2.5 nanograms per ml plasma. The current study was initiated to determine if the CEA assay could be used as an adjunct to or replacement for the liver scan in the evaluation of patients for hepatic metastases.

Since September 1, 1972, all patients presenting for liver scan at our institution have had a blood specimen drawn for CEA titer. All interpretations of liver scan were performed without knowledge of the CEA titer. Currently, adequate follow-up is available on 225 of these patients. Based on retrospective analysis of the data, a CEA value of 9.0 nanograms/ml plasma or above has considered "positive" for hepatic metastases. The correlation between the results of liver scan and CEA titer were only fair:

Liver Scan	CEA	
	pos. (above 9 ngm/ml)	neg. (below 9 ngm/ml)
pos.	20	24
neg.	22	159

All 20 patients with both tests positive had hepatic metastases confirmed. Only 2 of the 159 patients with both tests negative subsequently proved to have hepatic metastases. The CEA titer failed to detect 17 hepatic metastases identified on liver scan (there were 7 false-positive liver scans) but did detect 6 hepatic metastases missed on scan.

The CEA assay was less accurate than the liver scan in detection of hepatic metastases but was sufficiently sensitive to detect 6 of 8 hepatic lesions missed by scan.

**UPTAKE OF  $^{13}\text{N}$ -GLUTAMIC ACID IN BONE AND JOINT TUMORS.** Joseph M. McDonald, Laurence P. Clarke, Thomas R. Christie, Alan S. Gelbard, and John S. Laughlin. Memorial Sloan-Kettering Cancer Center, New York, N.Y.

The use of glutamic acid, labeled with cyclotron produced  $^{13}\text{N}$ , has been investigated in this study to evaluate its potential use as a bone/joint tumor imaging agent. Dogs were used in this work with spontaneously occurring osteogenic sarcomas and synovial cell sarcoma. Quantitative and qualitative uptake imaging was performed using dual-head, rectilinear scanner and gamma-camera systems.

As a comparison with  $^{13}\text{N}$ -glutamic acid uptake, scan and gamma-camera images were also obtained using the known bone seeking agent  $^{99\text{m}}\text{Tc}$  diphosphonate. Neoplastic tissue types were determined histopathologically on tissue obtained from surgical biopsy. Scan findings were compared with Roentgenograms of the same lesions.

The uptake of  $^{13}\text{N}$ -glutamic acid by these tumors was found to compare favorably with the uptake of  $^{99\text{m}}\text{Tc}$ -diphosphonate. Clearance of the glutamic acid from the blood was rapid ( $t_{1/2} \approx 2$  min.) with a correspondingly rapid uptake in the tumor. In addition to the tumors, the glutamic acid specificity was high only for the liver and salivary glands, thereby enhancing the probability of obtaining images free from interfering uptake. These results indicate that  $^{13}\text{N}$ -glutamic acid is a potentially useful imaging agent for these specific tumor types.

**SERUM TSH AND THYROID HORMONE INTERRELATIONS FOLLOWING DEFINITIVE TREATMENT OF THYROTOXICOSIS.** S. McHardy-Young, G. Blackburn, C. Brown, and M. N. Maisey. The Central Middlesex Hospital, London, England.

53 subjects are currently being studied ten years after definitive treatment of thyrotoxicosis i.e. subtotal thyroidectomy. Clinical assessment has been combined with an analysis of thyroid antibody status and the initial histological findings and this analysis is now complete. In addition, thyroid function studies i.e. protein bound iodine (PBI), resin uptake of triiodothyronine ( $\text{T}_3\text{RU}$ ) and free thyroxine index ( $\text{FT}_4\text{I}$ ) are currently being analysed with respect to clinical status, immunological findings and the more detailed studies of thyroid function i.e. thyrotrophin (TSH) estimation and serum triiodothyronine levels.

Methods - P.B.I.,  $\text{T}_3\text{RU}$  and  $\text{FT}_4\text{I}$  were measured by conventional laboratory methods, thyroid microsomal antibodies by an immunofluorescent technique and the degree of thyroiditis assessed histologically. Radioimmunoassay of serum TSH utilized the double-antibody method and serum  $\text{T}_3$  the ANS-charcoal separation technique.

Results - 39 subjects were euthyroid on the basis of clinical examination and conventional thyroid function tests, 6 were hypothyroid (3 currently under treatment), 4 were equivocally hypothyroid and 4 were hyperthyroid.

Thyroid antibodies and a more significant degree of thyroiditis were more commonly seen in hypothyroid than euthyroid subjects.

A wide range of serum TSH values were found in the clinically euthyroid subjects; only 9 had normal levels, 20 had mildly elevated levels and 10 had markedly or grossly elevated levels. All hypothyroid and equivocally hypothyroid subjects had elevated levels except those adequately treated with thyroxine. All thyrotoxic subjects had low levels. A good inverse correlation was noted between serum thyroxine levels and TSH but no consistent or significant relationship could be demonstrated between serum cholesterol and TSH levels.

The precise relationship between serological or histological evidence of thyroiditis and serum TSH levels will be presented along with the analysis of the serum  $\text{T}_3$  measurements, particularly the relationship between TSH and  $\text{T}_3/\text{T}_4$  ratios.

These preliminary studies demonstrate the mechanism whereby a euthyroid state is maintained following thyroid damage and the relationship between thyroiditis and subsequent thyroid function, particularly serum TSH levels. Isolated elevation of serum TSH does not indicate hypothyroidism but only the degree of stimulation required to maintain a euthyroid state. The  $\text{T}_3/\text{T}_4$  ratio may also be shown to reflect this.

**IMPACT OF COMPUTERIZED AXIAL TOMOGRAPHY UPON RADIO-NUCLIDE BRAIN SCANNING IN NON-NEOPLASTIC DISEASE.** Kenneth A. McKusick, Paul F. J. New, Henry P. Pendergrass, Majic S. Potsaid, Mass. General Hospital, Boston, Mass.

Computerized Axial Tomography (CT) can resolve small variations of x-ray absorption characteristics of soft tissue within the skull. We have done 500 CT scans, of which 213 have had  $^{99\text{m}}\text{Tc}$  pertechnetate studies. The initial results of this ongoing study warrant a preliminary report. Our CT study consists of 4 scan sequences. Standard 5 view  $^{99\text{m}}\text{Tc}$  brain scans were performed 1 hour after injection. Intracerebral and cerebellar hematomas, subdural hematomas and hygromas are readily identified with the CT scan. Small clots are easily recognized within the ventricles and gray matter. Early infarction (several hours) may be recognized because of accompanying edema.  $^{99\text{m}}\text{Tc}$  scans have been diagnostic prior to the CT scan; the opposite has also been true. Strengths of CT scanning have been its capability for greater anatomical detail, differentiation of edema from hemorrhage, ease of recognition of cerebral atrophy and ventricular enlargement. Vascular anomalies such as AV malformation and aneurysms are identifiable with the CT scan after IV injection of contrast material. The CT scan will have an effect on cisternography, decreasing the numbers and increasing the selectivity of referrals. The initial results indicate that the need for  $^{99\text{m}}\text{Tc}$  brain scanning will be reduced, especially if the CT scan is positive.

**COST/BENEFIT ANALYSES IN RENOVASCULAR DISEASE.** Barbara J. McNeil, Paul D. Varady, Belton A. Burrows, and S. James Adelstein. Harvard Medical School, Boston, Mass., Cedars-Sinai Medical Center, Los Angeles, Calif. and Boston University Medical Center, Boston, Mass.

We have analyzed the role of the IVP and/or renogram in the management of renovascular disease using data from the national cooperative study and have determined preliminary cost/benefit estimates for these procedures. Forty-four percent of abnormal IVPs were associated with renovascular disease whereas 2.7% of normal IVPs were associated with renovascular disease. The analogous percentages for the renogram varied depending upon the criteria used for judging asymmetry in renal function. If the IVP and renogram had been used sequentially as screening procedures and arteriograms obtained only when both tests were abnormal, 50% of patients with renovascular disease would have been identified and characterized at a calculated cost of \$3,000 per patient. If the IVP alone had been used to select patients for arteriography, 80% of patients with renovascular disease would have been found at a cost of \$2,500 per patient. The financial costs, operative mortality, and the relative outcome of surgical versus medical therapy are being assessed in order to determine the overall cost/benefit ratio. In conclusion, it appears that when strict criteria for renography are used in conjunction with the IVP, no patients with essential hypertension need to have angiograms but fewer patients with renovascular disease are identified at a slightly greater cost per patient than when the IVP alone is used.

**BONE IMAGING WITH THE MULTIPLANE TOMOGRAPHIC SCANNER.** James McRae and H.O. Anger. Donner Laboratory, University of California, Berkeley, Ca.

In contrast to conventional scanners, which produce a single image having sharpest resolution at the geometric focal plane of the collimator, the multiplane tomographic scanner produces six image readouts from a single scan, which sharply resolve activity near six planes at six different depths. When sufficient activity is present, the resolution of these readouts exceeds that which can be obtained from the scintillation camera.

Bone surveys have been performed with the multiplane tomographic scanner in over 200 patients using  $^{99m}\text{Tc}$ -labelled polyphosphate and EHDP. The skeleton has a varied distribution of isotope at different depths, and the surrounding tissue contains a relatively low level of tracer so the tomographic effect in the readouts is quite noticeable. Much anatomical detail can be recognized, such as the spinous processes and pedicles of the vertebrae. In a number of patients the pedicles and articular processes do not have an ordered progression of labelling and one pair may appear more active than adjacent pairs. When the study is otherwise normal, we attribute the findings to increased strain on these particular joints. If these small structures are imaged with less resolution, they may be mistaken for focal abnormalities. In almost all of our clinical studies the high resolution of the six-plane tomoscans and the appreciation of depth have proved of significant value in interpreting the study.

**IMPROVED SENSITIVITY OF RIA FOR HEPATITIS ANTIGEN.** Robert C. Meade and William C. Horn. VA Hospital, Tampa, Florida

In an attempt to improve the sensitivity of the RIA for hepatitis antigen the effect of addition of protein to the buffer wash and altering the incubation temperature was studied. The Abbott Laboratories "Ausria" kit was used.

The addition of one % albumin to either or both buffer washes resulted in lower activity in the negative controls. The positive sera were not significantly affected. The net effect was to decrease the negative range and increase the separation between positive and negative sera. The zone of

questionable value was also smaller when albumin wash was used. To explain our results, it is assumed that some protein binds to the test tube during the buffer wash. One % albumin adequately completes for binding sites so that no significant amount of antigen or labeled antibody binds directly to the test tube.

By precoating the bottom of the "Ausria" test tube with as little as 0.1 ml of one % albumin, it was possible to demonstrate that additional binding sites were also available in the same area which is precoated with unlabeled antibody by the manufacturer.

Incubation was done at 25 $^{\circ}$ , 37 $^{\circ}$ , 45 $^{\circ}$  and 56 $^{\circ}$ C for periods ranging from 60 min. to 16 hours for the first and 30 to 90 minutes for the second incubation. One % albumin was used in both buffer washes. In general the length of the second incubation has greater relative significance. Incubation times of two hours and one hour respectively at 45 $^{\circ}$ C yielded higher positive values than incubation for 16 hours and 90 minutes respectively at room temperature. In addition the negative values were lower at 45 $^{\circ}$ C. This resulted in better separation of positive and negative sera. Incubation at 37 $^{\circ}$ C or 56 $^{\circ}$ C was much less effective.

The combination of one % albumin added to the buffer washes and incubation for two hours and one hour at 45 $^{\circ}$ C is a more sensitive assay than incubation periods of 16 hours and 90 minutes at room temperature.

**FACTORS ENHANCING ENTRANCE OF MANGANESE INTO THE BRAIN: IRON DEFICIENCY AND AGE.** Ismael Mena, Kazuko Horiuchi, and Gilberto Lopez. Nuclear Medicine Divisions, Harbor General Hospital, University of California, Los Angeles, Calif. and the Catholic University, Santiago, Chile.

Manganese is a neurotoxic metal and a potential atmospheric pollutant. For plasma transport Fe and Mn share transferrin. In iron deficient rats, Mn binding capacity of plasma is increased; after 24 hours equilibrium dialysis against buffer barbital, iron deficient plasma (6) retained 48%  $\pm$  9 of  $^{54}\text{MnCl}_2$  carrier free, while normal plasma (6) retained only 21%  $\pm$  6 < 0.001. This might be pertinent to the entrance of Mn into the brain. This is a slow process that reaches a maximum of 1% of injected dose at 30 days after injection.

In order to test the iron deficiency hypothesis further,  $^{54}\text{MnCl}_2$  was injected intraperitoneally to iron deficient rats and the animals were decapitated 5 days later. Specific activity of  $^{54}\text{Mn}$  was determined by measuring  $^{54}\text{Mn}$  in a well counter and  $^{55}\text{Mn}$  by neutron activation analysis. Specific activity in the brain stem was 191  $\pm$  74 cpm/ $\mu\text{g}$   $^{55}\text{Mn}$ /g in normals (6) and 360  $\pm$  58 in deficient rats (22) p < 0.001. Basal ganglia specific activity was 175  $\pm$  61 in normals and 305  $\pm$  18 in deficient animals p < 0.001, medulla 126  $\pm$  45 and 300  $\pm$  56 respectively p < 0.001.

In the deficient rat, entrance of  $^{54}\text{Mn}$  into the brain is enhanced, and appears coupled to its transport to the blood brain barrier by transferrin. It links, therefore, increased plasma Mn binding capacity to increased entrance of  $^{54}\text{Mn}$  into the CNS.

Another factor enhancing entrance of manganese into the brain is age. Newborn rats and infants younger than 18 days showed 4 times greater entrance of  $^{54}\text{MnCl}_2$  into the brain than adult rats. This latter observation is possibly linked to immaturity of the blood brain barrier.

**PREDICTING THE GEOMETRICAL COMPONENT OF MULTI-HOLE FOCUSED COLLIMATOR MTF.** Charles E. Metz, Robert N. Beck, and Benjamin Tsui. Center for Radiologic Image Research, The University of Chicago, and Franklin McLean Memorial Research Institute, Chicago, Ill.

The transfer function describing spatial resolution characteristics of a multi-hole focused collimator can be described by the weighted sum of three terms representing contributions of geometrically collimated, penetrating, and scattered radiation. The present work has shown that the geometrical component of the transfer function of a multi-hole focused collimator with round holes packed in an hexagonal array can be expressed in the form of a rather simple equation involving trigonometric functions, first-order Bessel functions, and the physical dimensions of the collimator. This expression is applicable for any collimator-to-source distance and takes into account the directional dependence of geometrical resolution due to hole packing geometry. Fourier transformation of line spread functions measured using a thin-walled line source of  $^{125}\text{I}$  in air, in

which case scatter and septal penetration can be neglected, has shown that the predicted transfer functions are accurate to within a few percent over a broad range of spatial frequencies and collimator-to-source distances. Thus the theoretical approach appears to provide a powerful tool for the designing of focused collimators.

**EVALUATION OF TECHNETIUM-LABELED PYROPHOSPHATE SCINTIGRAPHY FOR DETECTION OF BONE METASTASES FROM PROSTATIC CARCINOMA.** Makoto Miki, Toyohi Machida, and Takeshi Minami. Jikei University, School of Medicine, Tokyo, Japan.

Usefulness of bone scintigraphy with  $^{99m}\text{Tc}$ -Sn-Pyrophosphate in early detection of metastases from prostatic carcinoma was assessed.

Each of 32 cases of prostatic carcinoma was given  $^{99m}\text{Tc}$ -Sn-Pyrophosphate, and bone scintigraphy was performed. An x-ray bone survey of the whole body was obtained and serum acid phosphatase and serum alkaline phosphatase were determined. They were judged abnormal(positive) or normal(negative) respectively.

Of the 32 cases, 20 cases had an abnormal scintigram, 18 radiographic evidence of bone metastases, 17 an abnormally high acid phosphatase, and 15 an abnormally high alkaline phosphatase. Of the 20 abnormal scintigram cases, 18 had radiographic evidence of bone metastases, 12 an unusually high serum acid phosphatase, and 13 an unusually high serum alkaline phosphatase. Of 12 cases with a normal scintigram, 4 had a high acid phosphatase. Metastatic carcinomas were proved histologically in 4 of biopsied 7 cases with an abnormal scintigram. Regions with abnormal scintigrams and with normal x-rays were ribs(7 cases), sterns (5), skulls(3), cervical and thoracic vertebrae, coccyx and femur(1 respectively).

In detecting metastases from prostatic carcinoma, bone scintigraphy using  $^{99m}\text{Tc}$ -Sn-Pyrophosphate is more sensitive than x-ray bone survey, serum acid phosphatase and serum alkaline phosphatase.

**A PROTOTYPE GAMMA CAMERA SYSTEM BASED ON A STRIP-ELECTRODE, HIGH PURITY GERMANIUM DETECTOR.** D. W. Miller, P. A. Schlosser, M. S. Gerber, R. F. Redmond, The Ohio State University, Columbus, Ohio, and W. W. Hunter, Jr., Providence Hospital, Seattle, Washington.

A prototype gamma camera system has been constructed which is based on a high purity germanium detector fabricated with orthogonal-strip electrodes. In this device, position sensitivity is obtained by connecting each contact strip on the detector to a charge-dividing resistor network. Excellent energy and spatial resolution have been achieved by cooling the resistor network to 77°K and by proper selection of noise filtering parameters in the pulse shaping amplifier circuitry. The significant advantage of employing this charge-splitting detector in a semiconductor gamma camera system is its electronic readout simplicity, requiring only three amplifier channels to measure the energy and two-dimensional location of gamma ray events.

Several orthogonal strip-electrode germanium detectors have been fabricated and evaluated experimentally in our laboratory. The most recent of these measures 2 cm x 2 cm x 5 mm thick and incorporates 10 contact strips on each surface which are spaced on 2 mm centers. The measured FWHM energy and spatial resolutions were 5.5 keV and 1.66 mm, respectively. These results indicate that it is feasible to construct a semiconductor camera having sufficient field of view and sensitivity for routine clinical utilization by assembling a large-area mosaic of charge-splitting detectors.

**PULMONARY SCINTIPHOTOGRAPHY IN THE FAT EMBOLISM SYNDROME (FES).** David M. Milstein, Martin L. Nusynowitz, Stephen Stein, Robert Urban. William Beaumont Army Medical Center, El Paso, TX.

FES is a well known, potentially serious complication of major fractures. Because of the insensitivity or non-specificity of currently available laboratory tests, the diagnosis is not often entertained until the more ominous clinical features of the syndrome appear. Since FES has a significant mortality, its prompt recognition and treatment are important. Twenty consecutive patients with lower extremity fractures were studied to evaluate the incidence of FES, determine the nature and incidence of pulmonary perfusion defects in this syndrome, and correlate the scintiphotographic findings with the clinical diagnosis. A semiquantitative system employing evaluation of petechiae, urine fat, arterial oxygen tension, and vital signs was used to objectively diagnose FES, weighting each feature in accordance with its specificity. By this method, 85% of the patients had definite or suggestive evidence of the syndrome, whereas the diagnosis was considered by the ward physicians in only 30% of the patients. Abnormal pulmonary perfusion images occurred in 70% of the patients and occasionally preceded other manifestations. Perfusion defects were most often multiple and small, lending a mottled appearance to the pulmonary image; these defects cleared gradually. The scintiphoto is a relatively sensitive index of perfusion abnormalities in patients with fractures and provides an additional valuable parameter for the diagnosis of FES. The use of the semiquantitative system described in conjunction with the scintigraphic findings should greatly enhance the index of suspicion and diagnostic accuracy in this potentially fatal syndrome.

**BRAIN SCAN IN INFANTILE CEREBRAL PARALYSIS.** Fred S. Mishkin and Ivan Barrett. Martin Luther King, Jr. Hospital/Drew Postgraduate Medical School, Los Angeles, Calif.

We have performed brain scans on four patients with infantile cerebral hemiplegia. Although the clinical findings and diagnostic features of the skull roentgenogram have been well documented for many years the entity continues to be misdiagnosed and in three of the four studied cases the findings were attributed to infantile poliomyelitis. All four cases had varying degrees of spastic hemiplegia resulting from an acute episode in childhood. All four had characteristic skull roentgenographic findings of a small cerebral hemisphere with compensatory skull overgrowth. Diploic vascular channels were prominent on the affected side. Cerebral radionuclide angiograms performed with  $^{99m}\text{Tc}$  pertechnetate in three of the four patients showed decreased perfusion to the affected hemisphere. Delayed images showed in all four cases a small hemisphere, best seen on the vertex view, with increase in peripheral activity. A blood pool image with  $^{113m}\text{In}$  transferrin in one case showed a diminished blood pool of the affected hemisphere. These scan findings characterize the entity of juvenile cerebral hemiplegia. They probably result from decreased blood supply via the internal carotid artery to the atrophic hemisphere, with a relative increase in the blood supply from the external carotid system.

**DETERMINATION OF CEREBRAL DEATH BY RADIONUCLIDE ANGIOGRAPHY.** Fred S. Mishkin. Martin Luther King, Jr. Hospital/Drew Postgraduate Medical School, Los Angeles, Calif.

Since the introduction of cerebral radionuclide angiography to determine cessation of cerebral blood flow in 1969, 10 patients have been studied by this technique and followed to the post mortem examination which revealed the characteristic findings of respirator brain. These findings confirm the hypothesis that lack of activity in the cerebral hemispheres means cessation of cerebral perfusion and cerebral death in spite of the fact that medullary centers responsible for cardiovascular control may still be functioning. The radionuclide angiographic appearance is unique. During the arterial phase the carotid arteries and nasopharyngeal activity appear in the neck, the region of the scalp is then seen and delayed images over a two-minute period, the time necessary to accumulate 300,000 counts, fail to reveal any intracerebral activity including failure of delineation of the dural sinuses. Time activity histo-

grams taken from such a patient mimic the findings seen with marked slowing, but not absence, of intracranial blood flow. Thus the proposal to use probes which cannot distinguish between intracranial and extracranial circulation for the determination of cerebral death must inevitably result in occasional failure. In a field in which imaging has replaced probe techniques just because of such sources of error, it is a step backward to employ probes in such a critical decision just because they are portable. In our experience it requires little other than good coordination of resources to hand ventilate the patient during the study. The purchase of a portable gamma camera for such a procedure can be justified in terms of the increased accuracy provided over the probe method and savings in both emotional investment and investment of expensive intensive care facilities to support a patient with cerebral death.

**RADIONUCLIDE ANGIOGRAPHIC DIAGNOSIS OF TRICUSPID INSUFFICIENCY.** Fred S. Mishkin and Michael A. Prosin. Martin Luther King, Jr. Hospital/Drew Postgraduate Medical School, Los Angeles, Calif.

Review of 62 radionuclide angiocardiograms performed during the past year showed activity in the inferior vena cava or hepatic veins in 6 cases during the right heart passage of the bolus. Since injection of the bolus is made in a peripheral vein, usually the external jugular or antecubital system, activity in systemic veins other than the superior vena cava must, in the absence of superior venal caval blockage, represent regurgitation from the right atrium. Two of the six cases had hepatic pulsations corroborating the presence of tricuspid insufficiency due to mitral and aortic valve disease. In three others, although multivalvular disease was present, tricuspid insufficiency was not suspected. The last patient was a cyanotic newborn infant in whom the examination was performed because of suspected congenital heart disease, but who proved to have lung disease.

Tricuspid insufficiency is important to document since it can have a significant hemodynamic effect in the presence of involvement of the mitral and aortic valves. Radionuclide angiography provides an objective and apparently sensitive means for documenting the presence of tricuspid insufficiency. The finding is not specific since it occurs in conditions in which there is increased resistance to passage across the tricuspid valve as in the case of the infant with lung disease.

**RADIONUCLIDE IMAGING IN SCROTAL ABNORMALITIES.** Fred S. Mishkin and Dymus Lawrence. Martin Luther King, Jr. Hospital/Drew Postgraduate Medical School, Los Angeles, Calif.

Nadel et. al. introduced scrotal scanning as a means for making the preoperative diagnosis of testicular torsion (Urology 1: 489, 1973). Over the past six months we have examined 14 patients with scrotal pain and/or swelling. The scrotum is suspended in a cradle beneath an Anger camera equipped with a converging collimator and a bolus of 10 mCi  $^{99m}\text{Tc}$  as pertechnetate is injected in the antecubital vein. An image made during arrival of the bolus delineates the scrotal blood supply and, in older patients, what appears to be the prostatic plexus. An image of 300,000 counts obtained following the arrival of the bolus provides information concerning tissue distribution of pertechnetate. In the normal patient a testicular arterial supply can be seen on the angiographic phase and the testicular regions are faintly outlined. In 12 cases of inflammatory disease either acute or chronic, traumatic or infectious, involving the scrotum, epididymis or testes there was increased blood flow to the involved area. The image of the tissue distribution may show either increased or decreased activity. In both cases of traumatic orchitis a normal testicular tissue activity was noted surrounded by a rim of increased activity, a finding which mimics that reported for torsion. A case of seminoma showed increased flow and activity in the affected testicle. The technique may prove useful in separating abnormalities with increased blood flow from those with decreased blood flow.

**NON-INVASIVE STUDY OF EXTREMITY PERFUSION BY POTASSIUM 43 SCANNING.** Alan T. Miyamoto, Fred S. Mishkin and Thomas M. Maxwell. Martin Luther King, Jr. Hospital/Drew Postgraduate Medical School, Los Angeles, Calif.

Scanning after the intravenous administration of potassium 43 during claudication elicited by exercise should delineate areas of skeletal muscle ischemia in the legs. Reduction of blood flow to ischemic levels results in an arteriovenous difference of potassium with net efflux of potassium into the venous blood. Acidosis from ischemia or other causes may also result in loss of potassium from skeletal muscle cells to the extracellular fluid. These metabolic effects of ischemia plus decreased delivery of potassium 43 both should result in areas of decreased activity on the scan.

500-600 uCi potassium 43 were injected intravenously through a butterfly infusion set during exercise. Claudication was elicited by moving the legs as if pedaling a bicycle or by walking. Reactive hyperemia after elevation of the legs was also used. Immediately following injection, simultaneous anterior and posterior scans from the pelvis to the feet were obtained with a dual probe eight-inch scanner using 5:1 minification without contrast enhancement.

Interpretable scans were obtained in all patients. Demonstrated regions of ischemia in the calves and thighs correlated well with patient symptomatology, clinical findings, Doppler ultrasonically measured pressures and angiogram findings. Ischemic regions have been seen in the thigh and calves when distal pulses at the ankle were normal. Potassium 43 scan findings appear to be very similar to those obtained after the intraarterial injection of  $^{99m}\text{Tc}$  labelled albumin microspheres but the risk of arterial puncture is eliminated. The potential for studying exercise-induced ischemia is unique and its safety allows serial studies to be performed, particularly for evaluation of patients before and after vascular surgery.

**IN-VIVO ORGAN BLOOD FLOW BY FRACTIONAL DISTRIBUTION OF  $^{13}\text{N}$ -LABELLED AMMONIUM CHLORIDE.** W. Gordon Monahan†, Laurence P. Clarke and John S. Laughlin. Mount Sinai Hospital† and Memorial Sloan-Kettering Cancer Center, New York, New York.

Sapirstein (1) has shown experimentally that the fractional distribution of  $^{42}\text{KCl}$  in the dog corresponds to the fractional distribution of cardiac output. The necessary condition to maintain this relationship for a diffusible tracer is that the indicator content of an organ remains stable relative to whole body uptake. Following intravenous injection of 10-30mCi of  $^{13}\text{N}$ -labelled ammonium chloride in the dog, organ activity remains relatively constant from 1-60 minutes. Whole body scans of the  $^{13}\text{N}$  activity distribution show considerable uptake in the heart, liver and kidneys. By quantitatively determining the per cent of injected dose in these organs their blood perfusion can be determined as per cent of cardiac output.

Using a recently developed quantitative scanning technique, the absolute amount of organ activity was obtained permitting an accurate estimate of organ blood flow. Dynamic uptake studies and quantitative scans have been performed following 17 injections of  $^{13}\text{NH}_4^+$  in 5 normal dogs. Mean flow values, as a per cent of cardiac output in the major organs of the dog are: Heart  $3.6 \pm 0.5$ ; Liver  $12.0 \pm 2.0$ ; and Kidney  $8.0 \pm 3.0$ . The results compare within  $\pm 1$  standard deviation with those obtained by invasive techniques and offer the potential for sensitive non-invasive determination of organ blood flow.

(1) Sapirstein, L.A. Regional Blood Flow by Fractional Distribution of Indicators.

Am. J. of Physiol. 193 (1958) 161-168.

**CLINICAL EVALUATION OF  $^{99m}\text{Tc}$  BLEOMYCIN SCINTIGRAPHY FOR DIAGNOSIS OF THYROID CANCER.** Toru Mori, Ken Hamamoto, Rikushi Morita, and Kanji Torizuka. Kyoto University Hospital, Kyoto, Japan

Diagnostic usefulness of  $^{99m}\text{Tc}$  bleomycin (BLM\*) scintigraphy for thyroid cancer was evaluated. BLM\* was prepared as described previously. Using scintillation camera (PHO Gamma III) with 4000 hole parallel collimator, scintigraphy at 15 to 60 min. after intravenous administration of 3 to 5 mCi was performed on 56 patients with various thyroid disorders. All these cases were examined histologically by needle biopsy or after surgery. In some cases  $^{67}\text{Ga}$  scintigraphy was also performed.

All but one of 23 cases with thyroid cancer showed significant accumulation of BLM\* corresponding to the cold nodule by <sup>131</sup>I scintigraphy. Accumulation of BLM\* seemed almost identical in cancers with various cell types and even in metastatic lesions. There were found 4 positive cases whose biopsy specimen did not show malignant changes but were proved malignant lately by surgery. On the other hand, only 2 of 11 cases were positive by <sup>67</sup>Ga even though marked accumulation was observed in a case with undifferentiated cell cancer. Of 17 benign nodules, 4 gave positive results by BLM\* and one of them was confirmed as Hurthle cell adenoma by surgery. The rest were not operated yet. Two active Graves' patients and 4 follow-up cases with successfully operated thyroid cancer were all negative, however, 4 of 10 Hashimoto thyroiditis showed diffuse but faint accumulations. Accumulations of <sup>67</sup>Ga were also observed in 3 of 5 thyroiditis patients.

In conclusion, BLM\* scintigraphy was considered quite useful for differentiating thyroid cancers from benign nodules.

**THE FREQUENCY DISTRIBUTION OF THE V/Q RATIO.**  
P. H. Murphy, V. Alagarsamy, and J. A. Burdine.  
 Baylor College of Medicine, Houston, Tex.

A major goal in respiratory physiology has been to determine the frequency distribution of the ventilation-to-perfusion ratios (V/Q) in the lung since in recent years it has been postulated that an uncoupling of ventilation and perfusion is the distinguishing derangement in many forms of lung disease. The purpose of this study is to present the results of a method for both determining this distribution and for characterizing it according to disease and degree of abnormality.

Pulmonary capillary perfusion and ventilation were monitored using <sup>133</sup>Xe. Count rate data were collected in a 64 x 64 digital matrix with a dedicated mini-computer interfaced to a scintillation camera. The V/Q ratio was calculated for each cell of the matrix and the results displayed as a color-coded functional image and as a plot of the fractional lung ventilation and perfusion as a function of the V/Q.

In a normal upright individual, the V/Q ratio is best characterized by a log-normal distribution with a mean between 0.9-1.0 and a log<sub>e</sub>SD of about 0.2. In COPD the curve often has two peaks, one to either side of a V/Q of 1.0, as well as a significantly greater log<sub>e</sub>SD. The pattern in acute thromboembolism is a single peak at a relatively low V/Q and a fractional ventilation component occurring at a V/Q greater than 6.0 which reflects the magnitude of acute ischemia.

The distribution of the V/Q ratio as determined by this method follows distinct patterns in normals, COPD, and acute thromboembolism patients, and can also be used to estimate the relative severity of the disease.

**IMAGE FORMATION IN SCINTILLATING CRYSTALS.** R.C. Murry, J.E. Dowdey, and F.J. Bonte. University of Texas Health Science Center, Dallas, Texas.

The aim is to develop a detector system with adequate resolution for applications such as coded aperture imaging, with detector efficiency and light gain much higher than a film-screen combination. An analysis of light distribution within and on the surface of a scintillating crystal was undertaken and the findings suggest that a lens-coupled system offers significant resolution advantages.

A lens is focused to within the crystal, so that a point source of light scintillation event is imaged as a very small point onto an image plane (three stage image intensifier) nearly independent of crystal thickness. Early experiments were conducted with sodium and cesium iodide crystals of various sizes, thicknesses, degrees of polish, and types of backing by irradiating with x-rays and viewing the image intensifier output on television. Information about scattered and internally reflected light led to our use of a vacuum deposited mirror on one of the polished crystal faces

to form a reflected image whose position is outside the crystal. The depth of focus of the lens system is large enough so an internal point and its reflected image are superimposed as a point onto the image plane. More than 2 line pairs per millimeter were easily resolved from a Buckby-Meers resolution plate using a 1/8" thick CsI crystal. The possibilities of using a non-reflective coating opposite the mirror surface, and of optically coupling the crystal edges to an absorptive material are also under consideration. Studies with technetium-99m were conducted using fiber optics coupled film in place of the monitor. Speed is, of course, far faster than a film-screen combination and resolution has been good, but distortion is a problem at present. Effort is now directed at optimizing the image intensifier and lens system for best sensitivity with low distortion.

**IMPACT OF COMPUTERIZED AXIAL TOMOGRAPHY UPON RADIO-NUCLIDE BRAIN SCANNING FOR NEOPLASMS.** Paul New, Kenneth A. McKusick, Henry P. Pendergrass, Majic S. Potsaid, Mass General Hospital, Boston, MA

Computerized Axial Tomography (CT) is a new departure from standard x-ray technique, and can resolve small variations of x-ray absorption characteristics of soft tissues within the skull. Of the first 500 CT scans, 213 also had <sup>99m</sup>Tc pertechnetate scans. The results warrant a preliminary report of this ongoing study. The CT picture as displayed on a CRT is a computerized representation of the absorption coefficient of 6400 points in one slice of brain tissue. The head is scanned from 180 angles while two photon detectors read 160 photon transmissions through the head from each angle. Standard 5 view <sup>99m</sup>Tc scans were performed one hour after injection. Although both primary and metastatic tumors in the cerebral cortex have been identified by CT scanning in the presence of a negative <sup>99m</sup>Tc study, the opposite has not occurred. Lesions within the pituitary fossa and the cerebello-pontine angle are somewhat unfavorably situated for CT analysis, although information regarding cystic and necrotic changes, hemorrhage or edema may be obtained. The <sup>99m</sup>Tc studies have not been more sensitive in these locations. Furthermore, if the CT study is supplemented with IV injection of contrast medium, it is anticipated that vascular lesions of 1cm. will be recognizable. The results suggest that <sup>99m</sup>Tc brain scanning will have a lesser role in the diagnosis of tumors in those hospitals in which CT scanning is available.

**INTERPRETATION OF LIVER IMAGES: DO TRAINING AND EXPERIENCE MAKE A DIFFERENCE?** H. Nishiyama, J.T. Lewis, and E. L. Saenger. Nuclear Medicine Laboratory, BRH and Radioisotope Laboratory, Cincinnati General Hospital, Cincinnati, Ohio

Liver imaging imposes a variety of problems for interpretation. The purpose of this study is to determine how an individual observer interprets images in order to assess pitfalls. In turn, improved skills of interpretation can be achieved.

Forty abnormal cases with various liver diseases and 36 normal cases were presented for interpretation without clinical history. Nine readers participated in the study: 4 radiology residents, 3 fellows, and 2 full-time nuclear medicine staff. Thus, the report consists of 684 observations representing 3 groups of observers.

Higher false positive readings are more common in inexperienced observers. No difference of average percentage accuracy between residents (76%) and fellows (77%) indicates that resident training is definitely valuable. Most consistent readings were obtained by staff with average percentage accuracy of 88%. Heterogeneity is most frequently mentioned to make both correct and incorrect judgments. Cases with discrete lesions showed a high rate of correct reading. Ill-defined radionuclide distribution is the largest single source of error in



normal cases. Early stages of cirrhosis, mild hepatitis, and rare diseases such as hepatic sarcoidosis impose problems of judgment.

In conclusion, the most difficult problem is the observer's judgment of heterogeneity of an ill-defined nature. This can be minimized by categorical examination of the images in conjunction with well disciplined training and experience.

**USE OF RADIOZINC IN INVESTIGATION OF MALE INFERTILITY.** M.M. Nofal, A. El-Beheiry, A.F. El-Arini, M.N. Salama and M.G. Massoud. Alexandria University, Alexandria, Egypt.

Zinc 65 was used to evaluate spermatogenic function as a measure of fertility potential. The test was based on the suggestion that defective spermatogenesis would be associated with abnormal 65-Zn uptake due to changes in the activity or to deficiency of zinc-containing enzymes in spermatozoa.

65-Zn was injected intravenously and radioactivity recorded over each testis separately over a period of 10 days. The curve obtained in fertile persons showed a special pattern different from that observed in cases of defective spermatogenesis.

Thirty-four infertile males and 12 controls were investigated by this method. Results of the test showed good correlation with semen picture and testicular biopsy. Follow up semen analysis done on patients previously investigated showed no change in semen parameters over a period of 8 months.

In azoospermic patients, positive test was an important diagnostic measure denoting obstruction and directing the attention to surgical correction.

The test is considered a safe and reliable tool in the diagnosis and prognosis of male infertility offering more information about the dynamic activity of the testes than testicular biopsy.

**197 CHLORMERODRIN: A USEFUL SECOND APPROACH IN BRAIN SCANNING.** Nicholas G. Nolan and Frank T. Maher, Mayo Clinic and Foundation, Rochester, Minn.

We wish to suggest that 197-Hg Chlormerodrin remains a valuable agent in brain scanning, being able to identify lesions in areas not well seen on conventional pertechnetate scans. Review of our experience from 1971 to 1973 shows that 67 patients had a 99mTc brain scan which was followed by repeat examination using 197-Hg Chlormerodrin. Contradictory results were obtained in 37 instances. In 25 of these 37 cases, it was possible to reach a definite diagnosis by means of angiography, pneumoencephalography or biopsy. The chlormerodrin scan was proven correct in these latter 25 patients.

Anatomic area	Pertechnetate	Chlormerodrin
Posterior fossa	False negative 7	Abnormal 7 #
Posterior fossa	False positive 8	Normal 8 *
Choroid plexus	False negative 2	Abnormal 2 #
vicinity	False positive 3	Normal 3 *
Parasagittal region	False negative 2	Abnormal 2 #
	False positive 1	Normal 1 *
Inferior surface of brain	False negative 1	Abnormal 1 #
Periphal hemisphere	False positive 1	Normal 1 *

# Confirmed by biopsy, angiography or pneumoencephalography  
\* No evidence for abnormality on biopsy, angio or pneumo.

Because of its longer half-life, 197-Hg is scanned 18-24 hours after injection, by which time radioactivity is no longer identifiable in venous sinuses, permitting a clearer view of posterior fossa and para-sagittal regions. Secondly, Chlormerodrin is not concentrated by mucosal structures, allowing lesions in the vicinity of the Oro & naso-pharynx and choroid plexus to be more clearly seen.

**USE OF 133-XENON IN LOCALIZATION OF X-RAY - OCCULT, SPUTUM-POSITIVE LUNG CANCER.** Nicholas G. Nolan, Robert S. Fontana and David R. Sanderson, Mayo Clinic and Foundation, Rochester, Minn.

There is a small group of patients whose sputum is positive for malignant cells, but in whom chest x-rays fail to localize a tumor. We have evaluated the possible usefulness of the 133-Xenon ventilation-perfusion study\* in this situation. The technique used involves the qualitative evaluation of four parameters, namely ventilation entry and washout (Ve and Vw/o) and perfusion distribution and washout (Q distrib. and Qw/o). This study has been performed 20 times on 12 such patients. Incidence of abnormality corresponding to location of surgically resected malignancy is shown in the following table:

	Ve	Vw/o	Q Distrib	Qw/o
Abnormality corresponding to location of subsequently resected malignancy	1	8	2	10
Number of studies	20	20	20	19

The washout phases following both ventilation and perfusion yielded the highest positive correlation, showing abnormality corresponding to the documented tumor site in 40% and 53% of cases, respectively. The coexistence of C.O.P.D. may cause the appearance of one or more non-specific abnormalities in the Xenon study, commonly in either washout phase. We have nevertheless, found the procedure to be of value in this group of patients as it identifies to the bronchoscopist a limited number of high risk areas for especially close examination.

**ITERATIVE 3-DIMENSIONAL RECONSTRUCTION: A SEARCH FOR A BETTER ALGORITHM.** Bernard E. Oppenheim and Paul V. Harper, The University of Chicago, Chicago, Ill.

Computerized transverse axial tomography has found medical application in the EMI scanner of Hounsfield and the transverse section scanner of Kuhl. Both devices use algorithms closely related to Gordon's ART method of iterative 3-dimensional reconstruction. This method, however, operates as if the activity in each square sampling region were concentrated at the central point of the region, and can introduce artifacts whenever the activities in adjacent sampling regions differ by more than a small amount. To overcome this deficiency, we developed an "exact" form of ART, which operates as if the activity varies continuously throughout the entire region under reconstruction. In phantom studies carried out on a scintillation camera, the "exact" form produced more accurate reconstructions, with improved spatial resolution, compared with the usual form of ART. Computation time was not unduly increased. When attenuation was not present, the relative standard deviation ( $s_{y,x}/\bar{Y}$ ) of values about the regression line relating reconstructed activity to true activity was 5.86% for the "exact" form of ART, and 7.33% for the usual form.

Thus far, all reconstruction schemes have required that the field of view of the detector be large enough to include all of the activity in the plane under reconstruction in all views. A number of iterative algorithms were investigated to determine whether this requirement could be relaxed. It was found that algorithms based on the SIRT method of Gilbert are capable of achieving good reconstruction of the portion of the activity that remains within the field of view of the detector in all projections, even though as much as 50% of the total activity is excluded in each projection. Thus it is possible to study portions of a large region with a detector whose field of view cannot encompass the entire region.

**THE DIGITAL CEREBRAL RADIOANGIOGRAM: FURTHER DEVELOPMENTS IN AUTOMATED OFF-LINE COMPUTER ANALYSIS.** R.J. O'Reilly, P.J. Collins, and P.M. Ronai. Inst. Med. & Vet. Sci., Adelaide, South Australia.

Since our previous report to this Society, our computer program for analysis of regional cerebral perfusion data has undergone considerable further development. It now comprises the following automated sequence of operations: 1. *Filtering and smoothing.* 2. *Detector non-uniformity correction:* determines non-uniformity values for each matrix-

point, each phototube, each ROI; computes overall non-uniformity values; corrects all dynamic data for non-uniformity. 3. *ROI selection*: selects left (L) and right (R) middle cerebral and anterior (A) cerebral ROIs for each patient and draws map of head blood pool with ROIs marked. 4. *ROI area normalisation*: measures areas of L and R middle cerebral ROIs and normalises patient data to unit ROI area. 5. *Time-activity graph printout*: plots total corrected counts per unit ROI per unit time against time for each ROI, using a line printer. 6. *"Data point" statistics*: computes amplitude difference in standard deviations between L and R curves at each data point; similarly between A and L or A and R curves. 7. *"Curve section" statistics*: measures areas under defined portions of the curves and determines differences between L and R sub-areas in standard deviations from the mean L-R sub-area difference of a normal population; similarly for A-R or A-L sub-area differences. 8. *Time-activity graph X-Y plot*: plots time-activity curves for each ROI on "Calcomp" X-Y plotter, adds test identification, patient identification, date and "curve section" statistics. This forms hard copy for inclusion in report to referring physician.

COMPUTERIZED DIAGNOSIS OF THYROID DISEASES. José Ortiz-Berrocal, José R. Martínez, Maria C. Marin Luis Diez. Clinica Puerta de Hierro. Autonomous University of Madrid. Spain.

Nuclear Medicine can yield decisive information on thyroid pathology. A computer can analyze clinical and laboratory data and radionuclide examinations to automatically establish the diagnosis. We have codified 320 pieces of data and 36 different diagnosis (modified classification of the American Thyroid Association), and compiled a data bank of 2000 clinical histories of patients referred to thyroid studies.

Various procedures for computer diagnosis were compared. The "cluster method" was used to analyze the most significant quantitative data (TT4, AFT4, T<sub>3</sub><sup>125</sup>I red-cell uptake, PB<sup>127</sup>I, MBR, cholesterol, etc.) and make the initial classification of thyroid normo-, hypo-, or hyperfunction. Bayes's method of conditional probability was modified for use in the subsequent subclassification. The modification was the creation of a list of data that either excluded or established a diagnosis. The use of these data, along with an analysis of the frequency of presentation, sharpens the automatic diagnosis considerably.

THE EFFECT OF OXYGEN ON THE REDUCTION OF PERTECHNETATE ION BY STANNOUS ION. Azu Owunwanne, Larry B. Church, and Monte Blau, Roswell Park Memorial Institute and State University of New York, Buffalo, N.Y.

In the routine preparation of <sup>99m</sup>Tc labelled compounds, the reduction of TcO<sub>4</sub><sup>-</sup> requires a large excess of Sn<sup>++</sup> to overcome interference by residual oxidants. Using paper electrophoresis and carrier <sup>99</sup>TcO<sub>4</sub><sup>-</sup>, we have investigated the influence of oxygen on this reaction. At concentrations below 5.0 x 10<sup>-4</sup>N TcO<sub>4</sub><sup>-</sup>, a higher ratio of Sn<sup>++</sup> to TcO<sub>4</sub><sup>-</sup> was required for complete reduction, indicating that oxygen is effectively competing for Sn<sup>++</sup>.

If nitrogen- or oxygen-bubbled water was used to prepare solutions of the reactants, oxygen-bubbled solutions gave 10% reduced TcO<sub>4</sub><sup>-</sup> while nitrogen bubbled solutions gave 31%. When the Sn<sup>++</sup> solution was bubbled for 30 additional min. with oxygen prior to reaction with TcO<sub>4</sub><sup>-</sup>, only 2% reduction occurred while 50% reduction was obtained when the Sn<sup>++</sup> solution was bubbled with nitrogen for one additional hour.

When nitrogen or oxygen was bubbled into the solution after the addition of TcO<sub>4</sub><sup>-</sup> to Sn<sup>++</sup>, there was no effect on the observed amount of reduction. This indicates that oxygen does not re-oxidize reduced TcO<sub>4</sub><sup>-</sup> back to TcO<sub>4</sub><sup>-</sup> although it is possible that some other neutral or insoluble species is formed which is not separated from reduced pertechnetate in the paper electrophoresis.

OPTIMIZATION AND STATISTICAL LIMITATION OF SPATIAL FILTERING. S. Pang and S. Genna. Boston V.A. Hospital and University Hospital, Boston, Mass.

The limit of restoration of image fidelity by spatial filtering depends on the increase in statistical uncertainty which can be tolerated. If the system point spread function (PSF) is known and a desired spread function (DSF) is specified, then filter optimization can be carried out. The filtered spread function (FSF) equals the convolution of the optimum filter matrix with the PSF, i.e., PSF \* Filter = FSF. Optimization follows an analytical procedure which finds the filter such that the deviation, D, between the FSF and DSF is minimal for a specified increase in statistical uncertainty. Even for unlimited statistics a deviation exists because the filter matrix has a finite number of elements.

The filtering process involves the spatial redistribution and correlation of counts and, hence, the statistics of the filtered image is quite different from the original image statistics. An index E<sub>fi</sub>, which equals the ratio of the final to the initial statistical uncertainty, defines this change. Given the statistical cost, E<sub>fi</sub>, one is willing to pay and the DSF, this method yields the optimum filter matrix (minimal value of D) at this cost. Since the DSF is arbitrarily specified, this generalized approach treats smoothing and focussing operations equally.

DETECTION OF ACUTE MYOCARDIAL INFARCTION IN HUMANS USING <sup>99m</sup>Tc STANNOUS PYROPHOSPHATE (PYP).

R.W. Parkey, F.J. Bonte, S.L. Meyer, J.T. Willerson, J.M. Atkins, G.C. Curry. University of Texas Southwestern Medical School, Dallas, Texas.

We have shown that acute myocardial infarctions in dogs can be visualized using <sup>99m</sup>Tc PYP which localizes in hydroxyapatite found within the mitochondria of irreversibly damaged myocardial cells. We now report the results of myocardial imaging in 23 patients who were admitted to a medical intensive care unit with suspicion of an acute myocardial infarction. Each patient was given 15 mCi of <sup>99m</sup>Tc tagged to 5 mg of PYP I.V. All patients were on constant ECG monitoring with no patient showing any rhythm change after injection. Anterior, oblique, and lateral scintigrams of the myocardium were performed 45 to 90 minutes after injection. 22 of the patients were scanned 1-7 days post admission with the average interval being 4-5 days. The animal studies suggested 1-3 days as the best post infarct interval, but this was not feasible in the present study. Of the 22 patients, 14 had definite elevation of enzymes (CPK, HBD, SGOT) and evolution of the ECG pattern consistent with an acute myocardial infarction. 13 of the 14 had positive scintigrams. All 8 patients with negative enzymes and no evolution of the ECG pattern had negative scintigrams. Determination of location in all 13 patients with positive scintigrams correlated well with the ECG findings. One major difference between the animal and human studies was that the human infarctions were positive by scan longer with different rates of clearing. This imaging method shows promise in 1) separating old from acute infarction in patients with chest pain, 2) determining size and location of acute infarction with a high degree of accuracy, and 3) the possible detection of extension of an infarction.

A MATHEMATICAL MODEL FOR RADIOPHARMACEUTICAL KINETICS IN CISTERNOGRAPHY. C. Leon Partain, Philip O. Alderson, and Barry A. Siegel. Washington University School of Medicine, St. Louis, Mo.

The purpose of this study was to develop and test a mathematical model describing the time-dependent flow kine-

tics of the radiopharmaceutical  $^{111}\text{In}$ -DTPA, following intrathecal injection for cisternography. Cisternograms were performed on three normal volunteers. Views of the lumbar region and head were obtained every 2-4 hrs. using a gamma camera interfaced to a PDP-12 computer. Digitized images were stored on magnetic tape. Sequential counts were obtained from areas of interest over the lumbar region, the basal cisterns, and the parasagittal region. For 48 hrs. after injection all urine was collected and frequent blood samples were obtained.

Activity appeared in the basal cisterns within 45 minutes of administration. The times of peak activity in the basal cisterns and parasagittal region were similar in the three volunteers; being 4 and 14 hrs., respectively. Peak blood activity occurred within the first 4 hrs. and 86% of the dose was excreted in the first 48 hrs.

A compartmental approach was taken in developing a linear mathematical model. A system of three linear differential equations was solved in closed form, yielding a set of exponential functions. The mean values for the rate constants  $\lambda_{ij}$  (hr.<sup>-1</sup>), relating the flow out of compartment  $i$  and into compartment  $j$  for three volunteers were  $\lambda_{12} = .329$ ,  $\lambda_{23} = .203$ , and  $\lambda_{34} = .105$ ; where 1 = lumbar, 2 = basal cisterns, 3 = parasagittal, and 4 = output.

This model and experimental data, in conjunction with blood and urine activities, should prove useful in dosimetry calculations. In addition, the normal parameters may serve as an initial data base to which abnormal cisternograms may be quantitatively compared and from which more complete systems models may be developed.

**QUANTITATIVE SCANNING OF THYROIDAL IODINE POOLS FOR ASSESSMENT OF THYROID DISEASE. J.A. Patton, J. Hollifield, G.S. Lee, and A.B. Brill. Division of Nuclear Medicine, Vanderbilt University School of Medicine, Nashville, Tenn.**

The introduction of fluorescence scanning has provided a valuable tool for diagnosing thyroid disorders. The development of a new source configuration in our laboratory has resulted in significant improvements in image quality which now rivals and often surpasses emission scans. The fluorescence scanner is coupled to a computerized, digital data acquisition system so that quantitative information can be obtained. The system has been calibrated using phantoms so that milligram values can be assigned to the iodine content of the total gland or to regions of interest within the gland. Results of a study made with five cadavers showed that the thyroidal iodine content could be measured with an uncertainty of less than one milligram.

After completion of the fluorescence scan, a report is generated by our computer for the patient's chart. The report includes an explanation of the study, a computer processed image of the iodine distribution, and finally a report of the computer-determined quantitative measurements including length and width of each lobe, iodine content of each of four sections of the thyroid gland, the projected area of iodine distribution, an estimate of thyroid weight assuming a dual oblate ellipsoidal geometry, and an estimate of the specific iodine content in units of mg. of iodine per gm. of thyroid tissue. Studies on a set of eleven normals yielded an average iodine content of  $10.2 \pm 2.7$  mg. with an average gland weight of  $21.2 \pm 9.4$  gm.

The information obtained with this system is of significant benefit in the following situations: 1) Determination of gland size for planning I-131 therapy for hyperthyroid patients, 2) Mapping the anatomical size and shape of the gland in patients with flooded iodine pools, 3) Iodine content in nodules is proving to be useful in differentiating patients with malignancies from those with benign disorders.

In a group of 30 biopsied patients exhibiting cold nodules on radioisotope scans, no malignant nodule had a ratio higher than 0.58 (i.e., iodine content of nodule: normal comparison region). Benign nodule ratios were generally higher with three nodules having ratio greater than 1.00. There have been some false negatives, however

(i.e., benign nodules with ratios less than 0.58), due to hemorrhagic cysts, amyloidosis, etc. The results of this ratio study will be presented in detail along with the analytic techniques utilized in these measurements.

**THYROID SCAN IN LYMPHOCYTTIC THYROIDITIS. Barry R. Paull, Philip O. Alderson, Barry A. Siegel, Walter Bauer, Ronald G. Evens. Washington University School of Medicine, St. Louis, Mo.**

No large series describing the scan appearance of thyroiditis is available. Therefore, the thyroid scans of 51 patients who had a histologic diagnosis of Hashimoto's disease or chronic (lymphocytic) thyroiditis during the period 1963-1973 were reviewed. Two independent observers were presented with 151 thyroid scans. In order to prevent observer bias, the thyroiditis cases were randomly mixed with 32 cases previously read as normal and 68 cases with histologic proof of other thyroid diseases. The pathologic sections were reviewed in each case to assure the accuracy and uniformity of the histologic diagnosis. The most common scan findings were as follows:

	Hashimoto's Disease	Chronic Thyroiditis
Number of cases	10	41
Normal appearance	1	2
Multinodular appearance	7	20
Enlarged lobe(s)	5	13
Solitary cold nodule	5	14
Solitary warm nodule	1	5

Carcinoma was found in 4 of the 10 patients with Hashimoto's disease, but only in 2 of 42 patients with chronic thyroiditis. This difference is significant at the  $p < .01$  level. Two carcinomas in patients with Hashimoto's disease corresponded to scan cold nodules. Other carcinomas were multifocal or of small size, and did not appear as solitary cold nodules. The scan appearance of thyroiditis is variable, and there is no significant difference in the appearance of Hashimoto's disease and chronic thyroiditis. In a patient with the clinical suspicion of Hashimoto's thyroiditis, the scan appearance of a solitary cold nodule or multinodularity must raise the strong suspicion of carcinoma.

**COMPARISON OF DOSE CALIBRATORS FOR RADIOACTIVITY ASSAY. J. Thomas Payne, Merle K. Loken and Richard A. Ponto. University of Minnesota Hospitals, Minneapolis, Minn.**

In this study the accuracy, geometry dependence and linearity were determined for 11 commercial dose calibrators. Standards of  $^{99m}\text{Tc}$  were prepared using known reference standards; a  $^{133}\text{Xe}$  standard (2 mCi in a sealed ampule) was obtained from NBS.

For  $^{99m}\text{Tc}$  assay, all dose calibrators except one were accurate to within 10%. However for  $^{133}\text{Xe}$ , three calibrators read 50% low whereas two read 67% and 112% high. This range in assay of over a factor of 4 is in part due problems of source containment. The absorption of  $^{133}\text{Xe}$  X- and  $\gamma$ -radiation by a glass syringe is 20-30% and by saline 10-20%. Thus  $^{133}\text{Xe}$  gas in a thin glass ampule will assay 30-50% higher than the same activity in a glass syringe with saline. Geometry dependence (bottom vs center of well) was less than 5% for large wells and 10% for small wells. All calibrators responded linearly to within 5% from 1-200 mCi indicating recombination losses were insignificant.

In summary, the accuracy of dose calibrators for  $^{99m}\text{Tc}$  assay is about  $\pm 5\%$ , whereas  $^{133}\text{Xe}$  assay may be  $\pm 100\%$  unless suitable correction factors are used.

**$^{81}\text{Rb}$  FOR MYOCARDIAL STUDIES. Neal F. Peek, Ferenc Hegedus, Gerald L. DeNardo, and Manuel Lagunas Solar. University of California, Davis, CA.**

One of the radioactive isotopes currently used for myocardial blood flow studies is  $^{43}\text{K}$ . Unfortunately, it is expensive and its gamma emissions are excessively energetic which provide poor spatial resolution for imaging purposes. The physical and biological properties of  $^{81}\text{Rb}$  in pure form appear to be better suited for an investigation of this type than any other radionuclide thus far utilized or proposed. Approximately 80% of rubidium is extracted by the myocardium in one pass through the heart.  $^{81}\text{Rb}$  has a half life of 4.6 hours and primary gamma emissions of 190keV (65%), 446keV (24%), and 511keV (67%). The method of production of  $^{81}\text{Rb}$  has been the  $^{79}\text{Br}(\alpha,2n)^{81}\text{Rb}$  reaction. This reaction requires an expensive separated target isotope and produces fairly large amounts (~30%) of the 6.3 hour  $^{82\text{m}}\text{Rb}$  as the major contaminant, which degrades spatial resolution and adds to the radiation dose to the patient.

We have produced  $^{81}\text{Rb}$  by the  $^{85}\text{Rb}(p,5n)^{81}\text{Sr}$   $25\text{min}$   $^{81}\text{Rb}$  reaction using 65 MeV protons from the Crocker Nuclear Laboratory isochronous cyclotron. The target material is the inexpensive  $\text{RbCl}$  (naturally occurring Rb). By producing the strontium isotopes, chemically separating the Sr from the Rb target material, allowing the Sr to decay to Rb for about 1 1/2 hrs and repeating the chemical separation, we have shown that the final product is better than 99% pure  $^{81}\text{Rb}$ . (contains essentially no  $^{82\text{m}}\text{Rb}$ ). The yield for this reaction is 0.4 mCi/μahr (180 minutes after the end of the bombardment).

**DEPTH INDEPENDENT DETECTOR RESPONSE WITH POSITRON EMITTING RADIONUCLIDES.** Keith S. Pentlow and John S. Laughlin, Memorial Hospital, New York, N.Y.

Detector response which is independent of both distance from the detector and depth in an absorbing medium is required in a number of areas in nuclear medicine such as quantitative scanning, transverse section tomography and image processing. A "shift-summation technique" has been used to achieve this with positron emitting radionuclides.

With coincidence counting of annihilation radiation, plane sensitivity does not depend on depth within the absorber or on distance from the detectors, but only on the total absorber thickness and detector separation. Point sensitivity, however, does depend on the distance from each detector. To reduce this variation, detector separation is usually made large at the expense of overall sensitivity. A much higher degree of uniformity without loss of sensitivity may be achieved by a technique involving a shift of both detectors along their common axis, normally maintaining the same separation, and summing their responses at two or more positions. Acceptable point response uniformity over a region of interest may often be attained with just two positions, exact uniformity may be attained with more. Plane sensitivity remains invariant.

In contrast, for single gamma or annihilation photons, plane sensitivity does vary with depth in the absorber. Using the mean response of opposed detectors with specially designed collimators minimizes the variation in both point and plane sensitivity but the latter may still vary by ±15% throughout a typical patient thickness.

**ULTRASOUND EVALUATION OF NON-FUNCTIONING THYROID NODULES.** Gordon S. Perlmutter, Barry B. Goldberg, N. David Charkes, Jose O. Morales, and Leon S. Maimud, Temple University Health Sciences Center Hospitals, Philadelphia, Pa.

In this study 62 patients with non-functioning thyroid nodules on radionuclide scans were referred for ultrasound evaluation. Both A-mode scans utilizing low and high gain setting and B-mode scans were performed.

Pathological confirmation was obtained in 22 cases, either by surgical excision or by cyst aspiration with cytological studies. Ultrasound evaluation of these 22 cases revealed a cystic pattern in 11, a complex pattern in 7, and a solid pattern in 4. Four of the 11 cases reported

as cystic by ultrasound were subsequently proven to have some form of thyroid carcinoma or lymphoma, some of which had cystic components.

This small series suggests an appreciable incidence of carcinoma in patients with non-functioning thyroid nodules and a cystic pattern on ultrasound scans.

	Ultrasonic Pattern		
	Cyst	Complex	Solid
Benign Cyst	5	2	
Hematoma	1		
Diffuse Hyperplasia		1	
Multinodular goiter		2	2
Follicular adenoma	1	1	2
Carcinoma & lymphoma	4	1	

**DUAL ISOTOPE CARDIAC SCANNING IN 600 CASES OF MYOCARDIAL INFARCTS.** Thérèse Planiol, Mireille Brochier, André Pellois, Daniel Archambaud, Centre Hospitalo-Universitaire, 37033-TOURS-FRANCE.

$^{131}\text{Cs}$  was used in most cases, and  $^{125}\text{Cs}$  in 31. Results are similar. The latter permits left lateral scan. Most scans of cardiac blood were carried out with  $^{113}\text{mIn}$ . Both scans can be performed simultaneously when using a two channels scanner. Otherwise they are consecutive. The pictures can be separate, and or superimposed. Anterior and left anterior oblique positions are scanned. In each case scanning of cavities is coupled with the myocardial one and when possible with lungs scanning or transmission to see cardiac space.

323 out of 600 infarcts were anterior, 235 posterior. In 65% of cases with anterior lesion the scan showed a local blank. In a further 31% there was a zone of decreased activity. Not one scan was normal. The size of the abnormal area was more widespread than indicated by necrosis ECG signs. Schematically, five different aspects were observed following the ECG localizations.

In case of posterior lesions no blanks have been observed. But, except normal (10%) or heterogeneous scans (13%), all pictures have shown an hypoeactive area. This area was differently localized due to the site of the infarction. Three main patterns were distinguished. Intermediate aspects were more frequent than in the cases of anterior infarcts. Scan of blood cardiac pool permits one to appreciate size of right and left cavities, and to eliminate the influence of ventricular volume increase on an altered myocardial scan. But, above all, it is beneficial to detect cardiac insufficiency or ventricular anevrysm, specially in the acute phase of the infarct.

**SPECIFIC DIAGNOSIS OF BRAIN LESIONS BY GAMMA ANGIOENCEPHALOGRAPHY.** Thérèse Planiol, Roland Itti, Centre Hospitalo-Universitaire, 37033-TOURS-FRANCE.

Dynamic studies associated with early and late static views can supply numerous elements that can help in the diagnosis of an intracranial lesion. First stage is the methodical analysis of consecutive 2 second pictures : velocity and symmetry of the flow in the main extra and intracranial arteries, displacement of one of the same, characteristics of capillary and venous phases, abnormalities of the distribution of radioactivity. These can be either the image of an arterial obstruction and or a capillary defect, or an hyperactive area.

Data processing allows one to analyse time activity curves over whole hemispheres, arteries, cortical and deep regions, and abnormal areas (inside and around them). Each curve must be compared to the one recorded in the symmetrical region and to normal data. When there is a radioactive focus its shape, site and radioactive concentration on early and late static photos are to be compared.

Some circulatory and static criteris are well known and make easy the diagnosis of vascular malformation, meningioma, subdural hematoma and multiple metastases. But frequently difficulties are encountered in differentiating between primary malignant and solitary metastatic tumors, hematoma

and softening, and even cerebral infarction from malignant lesion. In such a case more sophisticated studies can point out the subtleties of primary concern to the diagnosis: for instance the determination of the local and hemispheric transit times, the appreciation of the regional vascular pool, and of the extra vascular diffusion.

Further change of incidence or tracer studies or pharmacological tests, could be beneficial.

**A DUAL TRACER METHOD FOR EVALUATION OF MYOCARDIAL INFARCTION.** Norman D. Poe, Gerald D. Robinson, Dennis A. Elam and Danielle J. Battaglia. Laboratory of Nuclear Medicine, University of California, Los Angeles, Calif.

Most available radiopharmaceuticals used for myocardial imaging show the ischemic area as a negative defect. From the image alone, it is impossible to determine if the observed lesion represents transient ischemia, acute or healing infarction, scar tissue or aneurysm. If a second or series of radiopharmaceuticals with a predilection for concentrating in injured, healing or scar tissue could subsequently be given, then a combined radionuclide study for infarct staging would be possible. Tetracycline, among others, has been shown to localize in or around acutely infarcted myocardium. Certain monovalent cations, including cesium, distribute in the myocardium in proportion to blood flow and infarcts appear as negative lesions.

The potential use of combined radionuclide administration was evaluated in vitro in 29 dogs after infarction produced by coronary arterial ligation. Technetium-99m tetracycline (15 mCi) and cesium-131 (200 uCi) were given IV 24 hours and 1 hour respectively before sacrifice. The hearts were removed and multiple tissue samples were counted by differential spectrometry. At 24 hours after infarction, all 9 dogs showed localized blood flow deficits ranging from 30 to over 90%. Corresponding Tc values were 2 to 8 times normal, but the lowest Cs samples did not necessarily correlate with the highest Tc counts. This inverse relationship diminished by one week (maximum Tc values 3 times normal) and was totally lost by one month.

This study demonstrates that a dual radiotracer technique is feasible for confirming the presence of acute infarction but radiopharmaceuticals with greater affinity than tetracycline (8:1 target:normal) for acutely damaged tissue must be sought for in vivo imaging as the lesions were not visualized with Tc in the intact animal.

**DELAYED RADIOAEROSOL INHALATION IMAGING IN EVALUATION OF REGIONAL PULMONARY VENTILATION.** Norman D. Poe, Earl K. Dore, Alfred Greenberg, and Marvin B. Cohen. UCLA Affiliated Hospitals, Los Angeles, Calif.

Interpretation of radioaerosol inhalation images may be confusing because the inhaled activity can deposit variably and often unpredictably in the major airways and alveoli. Presumably, tracer reaching the alveoli deposits in proportion to ventilation. If an insoluble aerosol is used, alveolar clearance will be slow (days) in relation to bronchial clearance (hours). In images where bronchial deposition is excessive and obscures the alveolar pattern, repeat imaging 4-18 hours later is necessary. With parenchymal disease the final radioaerosol image parallels the concomitant perfusion image. In vascular obstruction without parenchymal involvement, aerosol will deposit in nonperfused but ventilated regions. If a normal subject is cooperative, the initial aerosol image can be indistinguishable from a perfusion image. At present, technetium-99m sulfide is the most practical radiopharmaceutical for delayed imaging.

Alveolar deposition of aerosol as a measure of ventilation has been questioned. In a normal human subject who had relative counts determined over the lung fields after a single breath of xenon-133 followed by inhalation of ionic mercury-197 (similar photon energies), nearly identical regional distribution patterns were found. In a series of 4 dogs with ventilation to the left lung altered by permanent occlusion of the left pulmonary artery, relative aerosol deposition in the poorly perfused lung tended to be lower than corresponding gas values. This observation suggests the aerosol technique may be more sensitive in detecting poorly ventilated regions but would quantitatively overestimate the ventilation deficit.

It is concluded that immediate plus delayed studies may be required when using radioaerosol imaging to fully utilize the information potentially available.

**EVALUATION OF 16-IODO-HEXADECENOIC ACID AS AN INDICATOR OF REGIONAL MYOCARDIAL PERFUSION.** Norman D. Poe, Gerald D. Robinson, Norman S. MacDonald, Alice W. Lee, and Carl E. Selin. Laboratory of Nuclear Medicine, University of California, Los Angeles, Calif.

A number of radiopharmaceuticals are taken up by the myocardium sufficiently for imaging but most possess photon energies suboptimal for high resolution definition of perfusion defects. Fatty acids (FA) are energy sources for the heart and concentrate within myocardial cells. Early results with I-131 oleic acid gave only borderline satisfactory images. The behavior of FA iodinated across double bonds does not appear to coincide with the natural analog. Based on comparative studies with C-11 labeled FA, terminal iodination yields a compound that is metabolized by the heart very similar to the parent FA.

As FA extraction is a function of both blood flow and cell metabolism, the question arises as to its reliability as a blood flow indicator in ischemia. Previous studies showed potassium analogs to give satisfactory estimates of flow under these conditions. Therefore, a comparative study was undertaken in 20 dogs with myocardial ischemia to determine the relationship between K-43 and I-125 hexadecenoic acid. Animals were sacrificed at 4 hours, 1 day, 1 week, or 1 month post coronary arterial ligation, and multiple myocardial samples were counted to determine relative activities. With occasional exceptions, a very high correlation between the two tracers was found independent of the degree or duration of ischemia. There was a tendency for the FA values to be slightly higher than the K-43 in the ischemic samples.

I-131 FA must be dissolved in a relatively large volume of albumin for injection; rapid clearance requires imaging to be completed within about 30 minutes and the energy of I-131 has little advantage over K-43. Therefore, imaging with FA would appear to be of value clinically only if large quantities of I-123 become commercially available.

**NON-CORONARY PATTERNS IN MYOCARDIAL IMAGING.** Norman D. Poe, Leslie M. Eber, Norman S. MacDonald, Anne S. Norman, and Emory N. Terac. University of California Medical Center, Los Angeles, Calif.

Myocardial imaging with potassium analogs has been used to localize recent myocardial infarcts, but application to non-acute coronary disease, identification of variations mimicking infarction and difficulties related to quantitation of ischemia have not been well defined. With these problems in mind, 40 patients undergoing cardiac catheterization had K-43 imaging performed. After a 2 mCi dose IV four views of the heart were obtained by a scintillation camera with a pinhole collimator and a dedicated computer. Infarcts appear as discrete defects at the image periphery on two or more views. Aneurysms are indistinguishable but their presence may be suggested by the relative large size of the lesion plus evidence of increased activity (hypertrophied tissue) adjacent to the defect. Left ventricular hypertrophy invariably produces particularly distinct images due to the greater radionuclide concentration by the large muscle mass, but a defect is often noted on the left lateral projection similar to a high posterior infarct even in the presence of normal coronary angiography. Because of the increased tissue mass the usual central ventricular cavity defect is minimized or lost on the anterior view. In contrast, with a dilated heart, the cavity is accentuated. Rotation and alteration in the usual distribution patterns with mitral disease cause peripheral defects which become difficult to interpret. Severe RVH produces a double image anteriorly. Noncardiac factors, for example large breasts in female patients, also can markedly affect the myocardial image.

Because too few normal subjects have been studied, the range of normal variations has not been defined. This inadequacy plus alterations caused by noncoronary diseases pose major problems in interpretation of myocardial images using presently available techniques.

**AUTOLOGOUS 125I-LABELED FIBRINOGEN TEST: CRITERIA OF INTERPRETATION.** Erich Pollak, Milo Webber, and Winona Victory. University of California, Los Angeles, Calif.

The purpose of this communication is to report our determination of the specificity and sensitivity of the 125I-fibrinogen uptake method of diagnosing active thrombosis as

opposed to longstanding venous obstruction with emphasis on criteria of interpretation.

Three groups of approximately 15 patients each: control patients, patients with longstanding venous obstruction, and patients with active recent thrombosis were evaluated clinically, in most cases with either phlebography or with scintigraphic blood clot localization in order to determine the clinical state of each patient. <sup>125</sup>I-fibrinogen uptake tests were performed in all 45 patients serially over a period of 7-30 days. Autologous fibrinogen was isolated and radiolabeled for each patient. Three mg fibrinogen labeled with approximately 100 uCi <sup>125</sup>I was administered to each patient. Serial 1 minute profile counts were obtained at 8 positions on each leg and over the midsternum. All counts were expressed as percent of the sternal count. The criteria used in interpretation were: I. 15% increased uptake when compared with the symmetric position at the opposite leg; II. 15% increased uptake when compared with adjacent positions of the same leg; III. 15% increase in activity at the same position in subsequent days.

All but 1 control patient were negative to criteria I, II, and III; the remaining patient had positive uptake to criterion I at the level of a leg ulcer. All patients with longstanding venous thrombosis had a positive FUT. Patients in this group satisfy only criteria I, or I and II. None satisfied criterion III. All patients with recent active thrombosis had positive FUT and satisfied the third criteria of positivity as well as criteria I and II. These results, while coming from a relatively small series, are highly statistically significant (p = .0006). According to these results, criteria III is an index of active thrombosis requiring treatment.

**BRAIN SCAN SCREENING FOR ACOUSTIC NEURINOMAS.**  
Suraj Prakash and William H. Beierwaltes. University of Michigan Medical Center, Ann Arbor, Mich.

The average acoustic neurinoma removed today at our University Hospital is 3.2 cm in diameter and the tumor (or its surgical removal) is associated with loss of function of at least one cranial nerve. We report a retrospective review of the possible role of the brain scan in decreasing this morbidity.

In the period of 1967-1973, 15 patients had: 1) one or more <sup>99m</sup>Tc pertechnetate brain scans with dual 5" crystal scanners, and pantopaque cisternography, because the clinician suspected that the patient had an acoustic neurinoma or a "mass lesion" of the brain, and 2) surgical removal of the tumor. The brain scan was interpreted, without knowledge of the cisternographic studies or surgical confirmation, by two authors independently.

The mean age of the patients at diagnosis was 42 years (16-68). The most common 3 symptoms were progressive hearing deficit, unsteadiness of gait and severe headaches. The mean duration of symptoms was 4 years (2/3-15). The mean diameter of the tumors was 3.2 cm (1.5-6.0 cm). The brain scan missed 3 tumors 1.5 cm or less in diameter. One 2 cm tumor was read as "probably abnormal." The pantopaque cisternography was positive in all patients. In the 3.5-6.0 cm diameter tumors, loss of function of a minimum of 3 of the following cranial nerves was observed postoperatively (in order of decreasing frequency): VIII, VII, V, IX, III, IV, X. In tumors 3 cm or less the morbidity was significantly less, usually only the VIII and VII (occasionally V) being lost.

**DETECTION OF HYPERTHYROIDISM BY NECK UPTAKE OF PERTECHNETATE,** David F. Preston, William W. Winternitz, and James Kopp, University of Kentucky Medical Center, Lexington, Kentucky and Kansas University Medical Center, Kansas City, Kansas.

Our purpose was to evaluate the diagnostic potential of a strip chart recording of pertechnetate neck uptake in hyperthyroidism and compare results with the <sup>131</sup>I uptake.

A 10 minute strip chart recording of the neck time-activity curves of pertechnetate was recorded. The curve height at 10 minutes divided by the 1.25 minute height, (Tc10 ratio) was the parameter measured. Tc10 ratios greater than 1.15 were considered to be elevated.

304 patients were categorized into 4 proven groups.

	Number of Patients		% Agreement
	Tc10 ratio >1.15	Tc10 ratio <1.15	
Hyperthyroid			
Untreated	68	2	93
Multinodular	4	3	100
Post <sup>131</sup> I therapy	7	7	71
Euthyroid	4	209	96

The Tc10 ratio identified 97% of untreated patients with diffuse hyperthyroidism while 93% had elevated I uptake values. The Tc10 ratio properly identified 97.6% or 209/213 of all euthyroids and the <sup>131</sup>I uptake detected 96.2% or 205/213 as euthyroid.

The Tc10 ratio equalled or exceeded the <sup>131</sup>I uptake in detecting conditions of excessive trapping. The test is simple, takes 10 minutes to develop an answer, uses inexpensive materials, is relatively geometry independent and results in radiation exposure decrease from 13 Rads for 10 microcuries of <sup>131</sup>-I to .235 Rads for 1 millicurie of pertechnetate.

**MEASUREMENT OF RED CELL VOLUME BY FLUORESCENT EXCITATION ANALYSIS OF CESIUM-LABELED RED BLOOD CELLS.** David C. Price, Sammy T-C Hung, Leon Kaufman and Stephen B. Shohet, University of California School of Medicine, San Francisco, CA.

The use of <sup>51</sup>Cr for determination of the red cell volume is limited, particularly in childhood and pregnancy, by the associated radiation exposure. We have evaluated the use of fluorescent excitation analysis [FEA] and non-radioactive erythrocyte labels for measurement of the red cell volume. Stable cesium enters erythrocytes as an analogue of potassium, and its usefulness as an FEA label for red cells is now under investigation.

Initial studies have been performed in 12 rabbits. Packed red cells from 6 ml blood were incubated for 2 hours at 37°C with 2.6% cesium chloride in water. The cells were then labeled with 3 µCi <sup>51</sup>Cr by standard technique and washed 7 times with normal saline. A weighed aliquot was injected intravenously with retention of a standard, and several blood samples were drawn over the next 2 1/2 hours for cesium and <sup>51</sup>Cr assay.

FEA was performed using a 500 mCi <sup>241</sup>Am source and an 80 mm<sup>2</sup> Si(Li) detector. Comparison of the calculated cesium and <sup>51</sup>Cr dilutional red cell volumes up to 1 hour revealed an average deviation of 3.71% + 4.62% [S.D.], the cesium volumes being higher. The disappearance half-time over 72 hours in 4 rabbits was 31.5 hours for cesium and 205.6 hours for <sup>51</sup>Cr. Initial comparative studies in two humans have demonstrated comparable correlations between the two techniques, and further studies are under way.

The measurement of red cell volume by FEA of cesium-labeled erythrocytes has proven to be an effective non-radioactive technique in rabbits, with early human studies indicating equal effectiveness.

**COMBINED RADIOISOTOPE AND ULTRASOUND TECHNIQUES FOR INCREASED DIAGNOSTIC ACCURACY OF FOCAL HEPATIC LESIONS.** James H. Fritchard, Martin A. Winston, Howard G. Berger, and W.H. Bland, Veterans Administration Wadsworth Hospital Center and UCLA School of Medicine, Los Angeles, Calif.

Routine radiocolloid liver scans are one of the most sensitive means available for the detection of focal hepatic lesions. Unfortunately, the changes seen on the scan are nonspecific and can be produced by a wide variety of causes. Gallium 67 which has been shown to accumulate in a wide variety of malignant tumors and inflammatory processes can be used to further elucidate the etiology of focal hepatic lesions detected on the radiocolloid scan by comparing the concentration of <sup>67</sup>Ga in the lesion to that in the normal surrounding liver tissue.

Hepatic disease can also be detected with ultrasound B scanning. The sensitivity of ultrasonography is comparable to that of routine radiocolloid liver scans. It has two unique assets, however, that make it very useful in evaluating focal hepatic lesions; these are its ability to differentiate cystic from solid lesions, and to demonstrate the anatomy of both the liver and surrounding structures simultaneously. The latter capability is especially useful in evaluating the marked variability of the left hepatic lobe.



The purpose of this paper is to stress the complementary role of these modalities and to show that they may be combined for more reliable and accurate diagnosis of focal hepatic lesions. Illustrative clinical cases will be briefly presented.

**INDIUM-111 LABELED GAMMA GLOBULIN.** James H. Pritchard, Manuel Tubis, W. H. Bland, John S. Endow, and Norman S. MacDonald. Veterans Administration Wadsworth Hospital Center, UCLA School of Medicine, and USC School of Pharmacy, Los Angeles, Calif.

Antibodies are unique proteins capable of selecting and reacting with specific antigens in extremely small concentrations. The successful clinical application of radioiodine-labeled antibodies for the in vivo detection of specific antigens has so far been disappointing and is at least partially due to the poor physical characteristics of <sup>131</sup>I or <sup>125</sup>I and the detrimental effects of iodination itself on the antibody molecule.

We are attempting to substitute the radioiodine label with a radionuclide that is more compatible with modern nuclear medicine procedures and will permit labeling the antibody only when it is needed as is the case with "kits" that are widely used today. Several procedures are available for conjugating antibodies to various biological markers, thus allowing the identification of the Ab-Ag reaction site. We have prepared an antibody conjugate according to the procedure outlined by Auramas using glutaraldehyde as the linking molecule. In one ml of physiologic buffered saline, 2.5 mg IgG, 1.25 mg transferrin (iron free), and 0.1 ml 1% glutaraldehyde are incubated at room temperature for 2 hr. Unreacted glutaraldehyde is removed by overnight dialysis against the same buffer. This conjugate is stable for weeks at 4°C. When desired, <sup>111</sup>InCl (2mCi/cc) is added to the conjugate in a ratio of 1:10 by volume. The binding of <sup>111</sup>In is almost instantaneous and autoradiographs of electrophoretic strips show that the radioactivity is confined to the transferrin-IgG spots. When the immunoprecipitation of <sup>111</sup>In-transferrin-IgG and <sup>125</sup>I-IgG with anti-IgG antisera was compared, 60 and 85% was precipitated respectively. We feel that it will be possible to improve this result significantly and are investigating variations of the basic procedure.

**ERBIUM-165: A POSSIBLE TUMOR-LOCALIZING AGENT WITH IDEAL IMAGING PROPERTIES.** Dandamudi V. Rao and Paul N. Goodwin. Albert Einstein College of Medicine, Bronx, N.Y.

Erbium-165 may be the ideal radionuclide for imaging with multiwire proportional gamma cameras, on the basis of detector efficiency, tissue transmission and absorbed dose. Furthermore, imaging is also possible with present scintillation cameras. We have obtained reactor-produced <sup>165</sup>Er, half-life 10.3 hours, which decays by electron capture emitting K x-rays of energy 47 and 54 KeV.

When <sup>165</sup>Er-citrate was injected intraperitoneally into mice with malignant tumors, we found that the tumor to muscle ratio was about 3.5, a value similar to that obtained with <sup>67</sup>Ga-citrate. The distribution in other organs was similar to that from <sup>169</sup>Yb-citrate, with uptake primarily in bone and kidneys. Absorbed doses from <sup>165</sup>Er are less than or equal to those from <sup>99m</sup>Tc compounds.

For imaging with a pressurized multiwire proportional camera, as developed by Kaufman and others, photons of energy just above the xenon K-edge are desirable. Multiplying the percent transmission through various tissue thicknesses by the percent absorption in xenon for various photon energies shows that Erbium-165 is superior to all other available radionuclides for imaging with these promising new detectors. Furthermore, we have shown that it is also satisfactory for imaging with present scintillation cameras.

**ADRENAL SCANNING: ITS USE IN MEDICAL AND SURGICAL ROUTINE.** Ruggiero G. Kavasini, Gaetano A. Cattano, Giorgio F. Benetello, Giampiero Feltrin, Renzo C. Perelli. Radiology Department, University of Padova, Italy.

The adrenal scanning with <sup>131</sup>I-19-iodocholestergol has been performed on 18 patients: 4 presented a congenital partial deficit of 21-hydroxylase; 3 presented post-puberal hirsutism; 5 were affected with Cushing's disease; 6 presented various affections probably caused by an adrenal pathology.

On 3 patients the scanning was repeated after the inhibition with dexamethasone.

After the clinical evaluation of this method, we can state that this test gives more diagnostic data than arteriography, venography and pneumoretroperitoneum if we consider them separately. In fact this method adds functional and topographic information (ectopic adrenal tissue) to the morphologic data often reported in the usual roentgenologic examinations and moreover presents fewer hazards for the patients.

Informations offered by this research are particularly useful to the surgical ends for the choice of the type of operation and for the location of the exact seat of small aldosterone or cortisol-secreting adenoma and ectopic adrenal tissues not-detected until now with other methods.

**A COMPARISON OF CITRATE AND BLEOMYCIN COMPLEXES OF LANTHANIDES AND ACTINIDES IN S-180 TUMOR LOCALIZATION.** G.V.S. Rayudu, E.W. Fordham, P.C. Ramachandran, A.M. Friedman and J. Sullivan. Rush University Medical Center, Chicago, Ill., Argonne National Laboratory, Argonne, Ill.

Tumor localizing properties of citrate(CIT) and bleomycin(BLM) complexes of lanthanides and actinides were studied in S-180 bearing mice and the results were compared with those of <sup>67</sup>Ga citrate. <sup>239</sup>Np(IV), <sup>239</sup>Np(V), <sup>237</sup>U(VI), <sup>140</sup>La(III), <sup>153</sup>Sm(III) and <sup>169</sup>Yb(III) were chosen, in spite of sub-optimal imaging qualities; to evaluate the variation of tumor-uptake with oxidation state and atomic weight.

Citrate and bleomycin complexes were prepared by adding 8-10mg. of citric acid or BLM to high specific activity solutions and adjusting pH to 6 and incubating at 70°C for one hour. The complexes and Ga-67-citrate were injected into mice and tumor/non-target ratios were measured at 24 and 48 hours and few results are listed below:

	<sup>239</sup> Np(IV)	<sup>239</sup> Np(V)	<sup>237</sup> U(VI)			
	CIT	BLM	CIT	BLM	CIT	BLM
Tumor/Blood	49	17	10.5	3.3	9.3	5.2
Tumor/Liver	0.6	0.2	0.3	0.1	2.2	0.4
Tumor/Muscle	91	80	40.5	38.5	50.0	14.0
	<sup>140</sup> La(III)	<sup>153</sup> Sm(III)	<sup>169</sup> Yb(III)	<sup>67</sup> Ga		
	CIT	BLM	CIT	BLM	CIT	BLM
Tumor/Blood	2.7	4.8	9.6	16	38	219
Tumor/Liver	0.03	0.03	0.4	0.2	1.5	3.0
Tumor/Muscle	6.5	10.0	22.5	10.5	30	10.8

The study shows: 1) Better tumor specificity of IV oxidation state when compared to V and VI, 2) heavy lanthanides localize better than light and medium ones (3) <sup>169</sup>Yb and <sup>239</sup>Np(IV) complexes exhibit low body background than <sup>67</sup>Ga citrate.

**IN VIVO DISTRIBUTION OF <sup>134m</sup>Cs, <sup>134</sup>Cs IN EXPERIMENTAL ANIMALS.** G.V.S. Rayudu, R. Kanoor, D.A. Turner, E.W. Fordham and A.M. Friedman. Rush University Medical Center, Chicago, Ill., Argonne National Laboratory, Argonne, Ill.

Because of recent interest in <sup>134m</sup>Cs (T<sub>1/2</sub>=2.9hr, 128KeV) as a myocardial scanning agent, (J.Nucl. Med. 14:243, 1973) a study of the in vivo distribution of <sup>134m</sup>Cs, <sup>134</sup>Cs in animals was made in order to determine the optimum interval between IV injection and scanning, and to obtain tissue distribution, blood clearance, and whole body clearance data.

$^{134m}\text{Cs}$  and  $^{134}\text{Cs}$  were produced by irradiating 50-60mg of reagent grade  $\text{CsNO}_3$  at a thermal flux of  $3-5 \times 10^{13}\text{n/sec/cm}^2$ .  $^{134m}\text{Cs}$ ,  $^{134}\text{Cs}$  assay was performed with a Ge(Li) gamma spectrometer. The whole body effective  $T_{1/2}$  of Cs in mice was 3.3d. (This is considerably less than published values for humans.) In the adult dog, 85% of  $^{134m}\text{Cs}$  activity cleared from whole blood with  $T_{1/2}=8$  min., and 15% cleared with a  $T_{1/2}=80$  min. Initial heart to nontarget ratios for  $^{134m}\text{Cs}$  in mice as a function of time were:

$^{134m}\text{Cs}$ -at	0.3hr	0.5hr	1.0hr	2.0hr
Heart/Blood	17.5	19.5	20.0	17.5
Heart/Liver	3.5	2.6	4.4	2.7
Heart/Muscle	9.4	6.0	7.7	6.5

The best images of the canine heart were obtained from one half to four hours after injection. During the first hour after IV injection of  $^{134}\text{Cs}$ , the highest concentrations of the nuclide are found in kidneys (19.4%/gm), heart (16.4%/gm) and intestine (14.0%/gm). By the 72nd hour after injection, the distribution is nearly uniform throughout the body.

**PULSE: A COMPUTER CODE INCORPORATING A PULSATILE HEART MODEL TO ANALYZE RADIOCARDIOGRAPHIC DATA.** Thomas C. Rhea, Jr., Darko Ivancevic, Ronald R. Price, Thomas P. Graham, Jr., Clyde V. Smith, and A. B. Brill. Vanderbilt University, Nashville, Tn.

A computer code PULSE has been written to analyze radiocardiographic data in terms of a modified pulsatile heart model. Data are collected with four detectors (two positioned over the heart, one over a lung, one at the head) when a radioactive isotope is injected into the right atrium or a major vein through a catheter. The maximum and minimum values of the data for each cardiac cycle are selected and input to PULSE.

The pulsatile model consists of several compartments, one for each right heart chamber, 4, 6, or 8 for the lungs, one for each left heart chamber, and 2, 4, or 6 for the systemic circulation. Each compartment is considered to be in either a filled or emptied state. One compartment empties into the next during one phase and fills from the preceding one during the other phase. The phases alternate continually. Right-to-left shunts are simulated by assuming that a right heart compartment can partially empty directly into a left heart compartment. Left-to-right shunts are assumed to occur in the reverse manner. Regurgitations are simulated by allowing a compartment to empty partially into the one immediately preceding it.

PULSE uses a least squares gradient search routine to fit data and thus to derive values for shunts and insufficiencies. It is found that the program can fit data to a very acceptable accuracy and that the correlation between its results and those of the oxygen saturation method is as high as 80 - 90% for the 38 patients for which preliminary calculations have been made. Improvements are under way which will refine the calculations considerably.

**BREAST SCINTIGRAPHY WITH  $^{99m}\text{Tc}$ -PERTECHNETATE AND  $^{67}\text{Ga}$ .** Steven D. Richman, Robert S. Frankel, Douglass C. Tormey, and Gerald S. Johnston. National Institutes of Health, Bethesda, Md.

The early and accurate detection of breast carcinoma is of major importance. Breast scintigraphy with  $^{99m}\text{Tc}$ -pertechnetate ( $^{99m}\text{TcO}_4$ ) and  $^{67}\text{Ga}$  may be a valuable diagnostic adjunct. As a supplement to mammography, xerography, and thermography, the noninvasive isotope technique may enhance clinical accuracy. Patients with suspected breast tumors were given  $^{99m}\text{TcO}_4$  intravenously. Cranio-caudal, lateral, and medial gamma camera scintigraphs of the suspect breast were compared to the patient's normal breast. Next  $^{67}\text{Ga}$  was administered and 48-72 hr. gamma camera views of the breast in the lateral and medial positions were obtained. Of eight patients with breast masses and subsequent pathological proof of breast carcinoma, all showed abnormal localization of  $^{99m}\text{TcO}_4$ . There was excellent anatomic correlation with mammography. In four of these cases the lesions were detected with  $^{67}\text{Ga}$  equally as well as  $^{99m}\text{TcO}_4$ . Two cases showed less  $^{67}\text{Ga}$  uptake than with  $^{99m}\text{TcO}_4$  and in two cases there was no abnormal localization of  $^{67}\text{Ga}$ . Seven

patients had clinical and mammographic findings of either normal breasts or fibrocystic disease, and no abnormal uptake of  $^{99m}\text{TcO}_4$  or  $^{67}\text{Ga}$ . The patients with breast carcinoma studied thus far suggest excellent correlation between clinical, radiologic, and isotope methods of breast evaluation. In cases with equivocal clinical and/or radiologic findings, radionuclide scintigraphy should prove to be especially useful. It appears that  $^{99m}\text{TcO}_4$  may be more useful than  $^{67}\text{Ga}$  in the detection of breast cancer.

**SCINTIPICTOGRAPHIC EVALUATION OF PATIENTS WITH SUSPECTED LEFT VENTRICULAR ANEURYSM.** Pierre Riggo, Malcom Murray, H. William Strauss, and Bertram Pitt. The Johns Hopkins Medical Institutions, Baltimore, Md.

Gated cardiac blood pool scanning was used to evaluate 22 patients with suspected left ventricular aneurysm because of refractory congestive heart failure, angina pectoris, or arrhythmias following myocardial infarction. An attempt was made to differentiate those with localized aneurysms who are potential operative candidates, from those with diffuse left ventricular hypokinesis who are not. This technique was compared to other non-invasive techniques including routine electrocardiography and roentgenography as well as contrast left ventricular angiography. Areas of akinesis were detected on the blood pool scans by superimposing the end diastolic and end systolic gated images, and the extent of akinesis expressed as a percentage of the left ventricular circumference.

On the basis of the gated cardiac blood pool scans, 13 patients were classified as having a localized left ventricular aneurysm with an aknetic area of less than 75% and preserved function of the remaining myocardium and 9 patients as having diffuse hypokinesis, with greater than 75% akinesis and diffusely depressed function of the remaining myocardium.

These findings were confirmed by contrast angiography. There were however no significant differences between those with localized left ventricular aneurysms and diffuse hypokinesis in clinical findings, electrocardiography or standard chest roentgenography.

In conclusion, gated cardiac blood pool scanning provides a non-invasive means of evaluating patients with suspected left ventricular aneurysms and can separate those who are potential operative candidates from those who are not.

**DAMAGED RAT THIGH MUSCLE: A MODEL FOR EVALUATING MYOCARDIAL IMAGING AGENTS.** G.D. Robinson, Jr., and D.J. Battaglia. Laboratory of Nuclear Medicine, University of California, Los Angeles, Calif.

One of the major problems associated with the development of myocardial imaging agents is the lack of small animal models for evaluating test agents. We have used the rat thigh as a model to study the relative specific uptakes of several proposed myocardial scanning agents in normal and damaged muscle tissue.

Differential uptakes of  $^{43}\text{K}$ ,  $^{129}\text{Cs}$ ,  $^{131}\text{I}$ -oleic acid,  $^{131}\text{I}$ -16-iodo-9-hexadecenoic acid,  $^{131}\text{I}$ -iodide,  $^{99m}\text{Tc}$ -tetracycline,  $^{99m}\text{Tc}$ -pertechnetate and  $^{99m}\text{Tc}$  reduced by repeated "pinching" of a left rear thigh muscle with forceps. Subsequent IV administration of the test agents was followed by tissue sampling at time intervals up to 18 hr post injection. Samples taken for assay included the site of primary muscle damage and tissue immediately adjacent to the injured region. Muscle from the contralateral thigh served as control tissue.

$^{43}\text{K}$ ,  $^{129}\text{Cs}$  and  $^{131}\text{I}$ -16-iodo-9-hexadecenoic acid, which are actively concentrated in muscle, gave higher initial concentrations in undamaged regions but also washed out of those regions more rapidly.  $^{131}\text{I}$ -iodide,  $^{131}\text{I}$ -oleic acid and  $^{99m}\text{Tc}$ -pertechnetate showed qualitatively similar kinetic patterns with relatively constant damaged vs undamaged uptake ratios of  $\approx 3:1$ . Interestingly, both  $^{99m}\text{Tc}$ -tetracycline and reduced  $^{99m}\text{Tc}$  exhibited similar kinetic patterns with maximum absolute uptakes early (2 hr and 15 min, respectively) but with relatively constant subsequent absolute differences. As a result, differential uptake increased from 3:1 at 2 hr to 10:1 at 18 hr post injection. This latter observation may imply that the apparent affinity of  $^{99m}\text{Tc}$  labeled agents for damaged myocardium is specifically related to the nature of reduced  $^{99m}\text{Tc}$ .

**EVALUATION OF LEARNED "PUFFING RESPONSE" OF MONKEYS WITH IN-113m LABELED SMOKE.** G.D. Robinson, Jr., and R.K. Siegel. Laboratory of Nuclear Medicine, University of California, Los Angeles, California.

In experimental studies on the effects of psychoactive drugs administered by smoking, In-113m labeled cigarette smoke was used to determine to what extent the learned "puffing response" of trained monkeys mimics the deep inhalation of human subjects.

Lettuce leaf cigarettes were labeled with In-113m as In(OH)<sub>3</sub> by injection of neutralized generator eluate (≈ 1 mCi per cigarette) and dried under vacuum. Each of the four monkeys were placed in specially designed smoking cages where they smoked 8 to 10 labeled cigarettes over a period of 1 hour. Total drag time, total puffs, reward drag time, total rewards and total water volume (reward) were measured for each animal. Immediately following the smoking period, anterior and posterior views of the chest and a left lateral view of the head were obtained on the anesthetized animals using a gamma-ray camera.

Upon burning in air, nearly half of the radioactivity in each cigarette is volatilized, presumably as In<sub>2</sub>O<sub>3</sub>. Following smoking, In-113m was found to have been deposited in the lungs of each of the four experimental animals, with significant, variable quantities of activity also being observed in their stomachs. Significantly, relatively little radioactivity was seen in the head, indicating minimal smoke retention in the nasopharynx where mucosal absorption of psychoactive agents could be important. Although the amount of activity adsorbed in the lungs has not yet been measured quantitatively, only a small fraction of the volatilized In-113m (≈ 1-2%) is apparently retained in this region. This is consistent with the bioassays of agents such as cocaine and THC which indicate that only minute quantities of these powerful drugs are required to produce their observed psychoactive effects.

**16-IODO-9-HEXADECENOIC ACID: HIGH SPECIFIC ACTIVITY PREPARATION AND MYOCARDIAL SPECIFICITY.** G.D. Robinson, Jr., N.D. Poe, A.Y. Lee, and C.S. Selin. Laboratory of Nuclear Medicine, University of California, Los Angeles, Calif.

I-131-labeled oleic acid has been frequently proposed as an experimental agent for myocardial imaging, although the molecule itself is drastically altered during the labeling process (saturation of its double bond and addition of the bulky I and Cl atoms). Radioiodinated 16-iodo-9-hexadecenoic acid is a gamma-emitting analog of 9-heptadecenoic acid in which the iodine atom is found in the position normally occupied by the terminal methyl group in the "natural" molecule. The latter compound is readily prepared at high specific activities and offers improved myocardial uptake over radioiodinated oleic acid.

Radioiodinated 16-iodo-9-hexadecenoic acid was prepared by refluxing 16-bromo-9-hexadecenoic acid with carrier free radioiodide in acetone. Radiochemical yields of 75%, at specific activities of 2 mCi/mg, were obtained with 3 hours of refluxing. Oleic, linoleic and linolenic acid were radioiodinated by reaction with I-131-iodine monochloride in diethyl ether, and served as non-analog references.

Following intracoronary administration in 4% HSA solution, canine myocardial extractions of labeled oleic, linoleic and linolenic acid were found to be relatively low (≈ 30%). Extraction of 16-iodo-9-hexadecenoic acid was found to be comparable to that of potassium-43 (≈ 70%). Blood clearance of all agents was found to be similar.

After IV administration of 1-3 mCi of the I-131 labeled molecules (and the I-123 labeled analog) in the dog, the heart was visualized with all agents. However, the ease of preparation of the 16-iodo-analog compound, coupled with its higher myocardial extraction, indicates that this agent, labeled with I-123, may prove to be a useful alternative to K-43 of Cs-129 for myocardial imaging.

**Tc-99m-TETRACYCLINE: BIOLOGICAL DYNAMICS AND SELECTIVE UPTAKE IN DAMAGED MYOCARDIUM AND SKELETAL MUSCLE.** G.D. Robinson, Jr., D.J. Battaglia, N.D. Poe, and D.A. Elan. Laboratory of Nuclear Medicine, University of California, Los Angeles, Calif.

Many tetracyclines have been shown to localize on bone surfaces and at the interface between healthy and damaged muscle tissue. Radioiodinated tetracyclines have been proposed as agents for bone and tumor scanning, as well as for

delineating damaged myocardium. Tc-99m-tetracycline has been proposed as an agent for kidney scanning and myocardial infarct imaging. We have studied the biological dynamics of Tc-99m-tetracycline in rats and have measured the differential uptakes of this agent in damaged and healthy myocardium and skeletal muscle in animal models.

The tetracycline complex of Tc-99m is prepared by reduction of Tc-99m-pertechnetate with a Sn(II)-tetracycline complex in the presence of an excess of tetracycline. Following intravenous administration in the rat, the agent shows moderate liver uptake (≈ 10%) and substantial urinary clearance (up to 30%) during the first hour post injection. Localization in rat thigh muscle which had been damaged by repeated "pinching" with forceps was rapid, reaching a peak within 2 hr with the ratio of specific uptakes in damaged and normal muscle continuing to increase with time. At 18 hr post injection, localization in the damaged region was 7 to 9 times greater than in the contralateral, normal thigh muscle. Tc-99m-tetracycline uptake in muscle immediately adjacent to the damaged site was 2 to 3 times normal.

IV administration of Tc-99m-tetracycline in dogs 1 hr after experimentally induced myocardial infarction showed ratios of localization of 5 to 7:1 in damaged vs normal myocardium at 24 hr post injection. Although infarcted areas were visualized in several of our experimental animals, the differential uptakes do not appear to be adequate for reliable imaging of damaged myocardium in vivo.

**VENTILATORY STUDIES OF THE SINUS CAVITIES AND MIDDLE EAR WITH XENON-133.** Ralph G. Robinson, Fernando R. Kirchner, and Audrey V. Wegst. University of Kansas Medical Center, Kansas City, Kansas.

The purpose of this investigation was to study the feasibility of using Xenon-133 to study the ventilatory dynamics of the ear and paranasal sinuses.

The technique used was to inject Xenon-133 gas (5 to 10mCi) into the oral cavity with a small syringe. With the nose clamped, the subject immediately performs several valsalva maneuvers. The quantity of Xenon-133 appearing in the pneumatic spaces of the head following these maneuvers is small, but is sufficient to provide satisfactory images.

20 studies have been performed to date. The clearance of Xenon-133 from the paranasal sinuses is more rapid than from the middle ear. Clearance of Xenon-133 from the middle ear is accelerated by warming the tympanic membrane, and retarded by any obstructive process involving the eustachian tube, including otitis media and oropharyngeal tumor.

This report demonstrates the feasibility of using radioactive gases to study the ventilatory dynamics of the ears and sinuses. Quantitative clearance studies are underway, and offer great promise in providing information regarding disturbed ventilation of these cavities in a variety of otorhinolaryngeal disorders.

**RENAL FUNCTION STATUS IN THE RENAL TRANSPLANT PATIENT: A NEW QUANTITATIVE TECHNIQUE.** F. David Rollo, David M. Shames, Robert E.L. Farmer, University of California Medical Center, San Francisco, California.

A new quantitative technique has been developed to assess renal function in renal transplant patients. The working equations are derived using compartmental analysis techniques. The rate constant governing uptake of label by the kidney,  $\lambda_1$ , is shown to be proportional to  $[(dk/dt)_{t=0}/D]$ , where D is dose administered, and the numerator is the kidney-time curve slope (background corrected) when t approaches zero. The rate constant for excretion of label by the kidney,  $\lambda_2$ , is  $[B(36)/\int_{36}^{\infty} k(t)dt]$  where B(36) is a 1 minute, background corrected, bladder count at 36 minutes and the denominator is the area beneath the background corrected kidney-time curve.

In each study, scintillation camera scintiphotos of the grafted kidney and bladder were obtained at four minute intervals following iv administration of 131-I hippurate. Simultaneously, one minute frames of the kidney and bladder were recorded on disk using a gamma 11R DEC computer system

interfaced to the scintillation camera. The scintiphoto study was used to assess anatomical features of the renal transplant. The data stored on disk was used to calculate  $\lambda_1$  and  $\lambda_2$  following the determination of background corrected activity-time curves for the bladder and kidney using region of interest capabilities.

This report includes 200 studies involving 35 patients. With each patient serving as his own comparison, the results show the uptake and excretion rate constants to be sensitive and reliable indicators of hippurate transport into and out of the kidney. The indices quantitatively measure changes in uptake and excretion, thereby providing a unique method of following the course of ATN and rejection. In several cases, these indices were the first measure to demonstrate signs of rejection superimposed on ATN. There was excellent correlation between indices & lab data.

COMPARISON OF ELECTROCHEMICAL (EC) AND LACTOPEROXIDASE (LP) RADIOIODINATION OF B-TSH AND H-TSH WITH THE CHLORAMINE T (CT) METHOD. Arlen Rosenberg, Shirley Murray, and Fred W. Teare, Faculty of Pharmacy, and Women's College Hospital, University of Toronto, Toronto, Ontario, Canada.

The purpose of this study is the production of an iodinated TSH product by the mildest method possible at an optimally high specific activity (SA) for both biological and immunological assay.

The EC method employs a platinum vessel as the anode, capacity 120 ul, and a rotating mercury platinum wire cathode. The reaction proceeds at 2.5 uA and 450mV, in 50 ul composed of 2.5 ug TSH, CF, Na-125I, and normal saline buffered to pH 7.0. CT labelling has been performed using Greenwood and Hunter's method, with similar amounts of B-TSH and Na-125I. LP labelling is under investigation.

EC iodination reaches a maximum within 10-15 minutes (with SA up to 3.5 atoms I:TSH molecule) and decreases after 30 min. SA's can be varied by altering molar ratios or time of current flow. A 3 min. modified ITLC system enables label incorporation to be monitored during the reaction, hence a product of desired SA may be obtained. CT labelling yields lower SA's but reaction time is short to minimize periodate formation. EC and LP reactions are stopped physically by separation of reactants on Sephadex G-75, not chemically. The ITLC and Sephadex separation methods show excellent agreement. Currents in the mA range demonstrate denaturation of B-TSH.

Haemagglutination is performed for rapid immunoscreening; double-antibody radioimmunoassay and receptor binding studies are planned.

ACCUMULATION OF  $^{99m}\text{Tc}$ -GLUCHEPTONATE IN ACUTELY INFARCTED MYOCARDIUM. David J. Rossman, Michael E. Siegel, Barry H. Friedman, H. William Strauss and Bertram Pitt. The Johns Hopkins Medical Institutions, Baltimore, Md.

The ability of  $^{99m}\text{Tc}$ -glucuheptonate to accumulate in acutely infarcted myocardium was evaluated in animal models. Three dogs had open chest permanent coronary artery ligation producing antero-apical left ventricular infarctions. Two hours after ligation, 5 mCi of  $^{99m}\text{Tc}$ -glucuheptonate were infused over 15 minutes. Four and one half hours later, the dogs were sacrificed and the tissues counted. Maximum ratios of radioactivity per gram of infarcted:normal myocardium ranged from 32:1 to 16:1. Maximum per gram infarct:blood ratios ranged from 17:1 to 7:1. Two additional dogs were infarcted by intracoronary artery injection, under fluoroscopic guidance, of 0.1-0.2 mls of elemental mercury. Two hours after infarction, 5 mCi of the tracer was infused. In these dogs, scintillation camera images of the chest in the left lateral position were obtained at 4 and 24 hours. The areas of infarction were visualized at both times, but were best seen in the later images. Mouse tissue distribution studies revealed a T 1/2 in blood of less than 2 minutes. Maximum accumulation was noted in the kidneys, gastrointestinal tract and liver. The normal mouse heart contained less than 0.017% of the dose at 4 hours post injection. Our early studies have shown  $^{99m}\text{Tc}$ -glucuheptonate to localize in acutely

infarcted myocardium to a much greater extent than normal myocardium in the dog. Applicability of this agent as a tool in the diagnosis of acute myocardial infarction in man remains to be evaluated.

TRANSVERSE SECTION RADIONUCLIDE CISTERNOGRAPHY. Howard Rothenberg, David Kuhl, and John Devenney. Hospital of the University of Pennsylvania, Philadelphia, Pa.

Transverse section scanning was employed during cisternography in patients with dementia and hydrocephalus suspected of normal pressure hydrocephalus. Patients were studied with this technique and conventional scintiscisternography after intrathecal instillation of 0.5 to 1.0 mCi  $^{111}\text{In}$ -DTPA. Section scans at 6 and 24 hours are compared to conventional views from rectilinear scanner and gamma camera.

The anatomy of cerebral ventricles and basal cisterns is seen clearly with transverse section radionuclide cisternography. The axial orientation of the transverse section and the ability to separate overlapping areas of activity produce perspective and detail not obtainable with other radioisotopic and radiologic methods now in routine use. The section views are useful in demonstrating ventricular penetration and stasis on the delayed scans when these features may not be recognized on conventional views because of overlying convexity and dural venule activity; penetration of chelated radiopharmaceuticals into cerebral interstitium with consequent blossoming of ventricular image and loss of resolution; or when counting statistics are marginal because of faulty technique.

ARRESTED HYDROCEPHALUS: DIAGNOSIS BY COMBINED RADIONUCLIDE AND PRESSURE TESTING. Thomas G. Rudd, Darv Dismang and Patricia Hayden. University of Washington Hospitals, Seattle, Washington

The frequency of spontaneous arrest of hydrocephalus treated surgically by CSF diversionary shunt is unknown. The purpose of this paper is to describe a technique for identifying patients with arrested hydrocephalus and report the initial results in a group of hydrocephalic children.

Thirty patients with previously documented shunt-dependent hydrocephalus were studied. Twenty-five uCi of  $^{99m}\text{TcO}_4$  were injected percutaneously into the shunt reservoir, images of the shunt obtained and clearance of radioactivity observed and expressed as a clearance half-time in minutes. Simultaneous intra-shunt pressure was monitored throughout the study via a 25 gauge needle inserted percutaneously into the shunt reservoir in 26 of 30 cases.

Twenty-two patients were clinically asymptomatic. Twelve had normally functioning shunts (spontaneous and continuous clearance of radioactivity) and pressures of 200 mm (water) or less. Ten however, had non-functioning shunts; 7 of which were completely obstructed, and 3 were patent only by manual pumping of the shunt reservoir. Pressures in this group of patients were also 200 mm or less, with one exception. All of these patients have remained asymptomatic for up to 2 years.

Eight asymptomatic patients with suspected shunt malfunction were also studied. In all cases the site of obstruction was accurately predicted, and confirmed by subsequent surgical revision of the shunt.

The combined radionuclide and pressure monitoring technique is an extremely reliable method for evaluating CSF shunts. These studies indicate a significant number of asymptomatic patients who were previously shunt dependent have arrested hydrocephalus and may no longer require diversionary shunts.

OXYGEN-15 SCANNING AND GAMMA CAMERA IMAGING IN THE STEADY-STATE. Gerald A. Russ, Rodney E. Bigler, Joseph M. McDonald, Roy S. Tilbury, and John S. Laughlin. Memorial Sloan-Kettering Cancer Center, New York, N.Y.

A new concept has been developed applying the steady-state to short-lived nuclides, which

permits them to be employed effectively as agents for scanning without decay correction and for organ imaging. Oxygen-15 ( $T_{1/2} = 125$  s) as molecular oxygen has been used to demonstrate this concept, and in this case the steady state level is a function of the rate of oxygen utilization of each organ or tissue and differences in these rates provide the basis for organ imaging and assessment of tissue metabolism.

Oxygen-15 was introduced into a breathing mixture and provided to dogs continuously. NaI (Tl) probes monitored the rise to steady state and then a whole body scan was performed. Further studies were carried out using a gamma camera wherein continuous time dependent images were obtained over a number of body regions from start of 0-15 administration through to end of washout of activity. Accumulations of activity in the brain, heart, lung field and testes were well defined. Calculations of dose based upon a human whole body scan indicates less than 90 mrad exposure to the critical lung region. This technique shows promise as an in-vivo and non-invasive method of assessing tissue metabolism, in particular to allow the detection of hyperactive tissue and rapidly dividing cells or conversely to detect areas of necrosis.

**HETEROTOPIC BONE FORMATION ASSESSED BY BONE SCANNING.** Ivan T. Sakimura, John D. Hsu, E. Shannon Stauffer and Jan K. Siemsen. University of Southern California and Rancho Los Amigos Hospital, Downey, Calif.

Thirteen patients with spinal cord injuries who were suspected or known to have heterotopic bone formation around large joints were assessed by bone scanning. Correlation of the bone scan with the clinical course, x-rays and serum alkaline phosphatase levels were performed.

Rectilinear scans were performed 2 to 3 hours after intravenous administration of 10 mCi of  $^{99m}\text{Tc}$ -diphosphonate.

Cases	Signs and Symptoms	Alkaline Phosphatase	X-ray Calcification	Bone Scan
2	Atypical pain	Normal	Absent	-
2	Asymptomatic	Elevated	Absent	-
1	Soft tissue swelling	Normal	Absent	++++
4	Soft tissue swelling	Elevated	Flocculent	++++
3	Known heterotopic bone	Elevated	Mature	++
1	"	Normal	Mature	-

Bone scanning with  $^{99m}\text{Tc}$ -diphosphonate offers a sensitive and specific technique for early detection of developing heterotopic bone before calcification is detected on x-rays. The intensity of scan activity appears to correlate directly with the degree of vascularity and/or metabolic activity and inversely with the degree of maturity. Together with other parameters, bone scanning can contribute to staging the maturity of heterotopic bone and prove useful in planning the therapeutic or preventative measures.

**RE-EVALUATION OF PARATHYROID THERMOGRAPHY.** Barry I. Samuels, Richard H. Gold, and James W. Lecky. U.C.L.A. Center for the Health Sciences, Los Angeles, CA and Presbyterian-University Hospital, Pittsburgh, PA.

The purpose of this study was to evaluate the efficacy of thermography for localization of abnormal parathyroid glands.

The thermographic examination was preceded by the removal of all clothing above the upper thorax and equilibration with a room temperature of 68° for 10 minutes. Photographs of the thermographic images were obtained. Alcohol was then applied to the skin of the neck to increase the sensitivity of the examination and additional images were photographed. Thyroid scans were performed when appropriate.

Of 106 patients examined for localization of suspected abnormal parathyroid glands, the diagnosis was established in 39 by surgery and histological confirmation. There were two false negative interpretations and one false positive interpretation. Twenty-nine patients had parathyroid adenomata, nine had parathyroid hyperplasia, and one had a thyroid carcinoma.

Parathyroid adenoma was most often associated with one or two foci of increased infrared emission, or with a unilateral prominent pattern of increased venous heat. In contradistinction, parathyroid hyperplasia was usually accompanied by 3 or 4 foci of increased emission or with a generalized increase in venous heat.

Parathyroid thermography has been effective in the preoperative localization of abnormal parathyroid glands.

**DECONJUGATION OF BILE SALTS BY INTESTINAL BACTERIA IN CIRRHOTIC PATIENTS.** Y. Sasaki, K. Someya, N. Matsumoto, H. Kamada, K. Shindo, R. Yamazaki, and K. Fukushima, St. Marianna University, Tokyo Univ. and Yokohama Municipal Univ., Kawasaki, Japan.

Occurrence of deconjugation of bile salt by increased intestinal bacteria in cirrhotic patients was studied in 9 normal controls (group 1), 8 subjects with ileal bypass or bacterial overgrowth (group 2) and 31 with liver cirrhosis (group 3).

After oral administration of 5uCi glycine-1- $^{14}\text{C}$ -cholate serial breath samples were collected and  $^{14}\text{CO}_2$  specific activity measured. Cumulative specific activity in 6 hours was expressed as area under curve and used as the index of deconjugation of bile salts. Samples aspirated from the small intestine were cultured. Incubation of bacteria in the broth with ox bile causes appearance of free bile acids detected by thin layer chromatogram, indicating deconjugating ability of the bacteria.

In breath test 27 of group 3 and all of group 1 showed flat curves with the index  $1.5 \pm 0.9$  and  $3.1 \pm 1.4$ , respectively. Resembling the curves of group 2 whose index was  $29.4 \pm 24.5$ , 4 cirrhotics demonstrated significant peaks with index ranging from 8.1 to 25.6. Repeated test in 2 after antibiotics therapy revealed flat curves. Either negative culture or positive with non-deconjugating bacteria was obtained in 7 of group 3 who had flat  $^{14}\text{CO}_2$  curves as well as in 7 of group 1. Two of group 3 and 4 of group 2 who showed positive breath test gave positive culture with deconjugating bacteria.

In the present series 12.9% of cirrhotic patients showed abnormal bacterial growth in the small bowels and deconjugation of bile salts. These cases may have different prognosis from others and may need to be treated with antibiotics.

**RADIOISOTOPIC STUDIES IN UNILATERAL KIDNEY DISEASE PRODUCED BY INTRARENAL INJECTION OF MICROSPHERES IN DOGS.** Jay R. Scharoff, F. Deaver Thomas, John G. McAfee, G. Subramanian, C. Duxbury, L. Heminger and P. Vescio, Upstate Medical Center, Syracuse, New York

Graded selective reduction in the microvasculature of one kidney was produced by .5 to 5 million  $35\mu$  carbonized microspheres injected through a catheter in the renal artery in a series of dogs. This experimental model was used to assess the ability of different radioisotopic agents to detect differences in blood flow between the 2 kidneys with a scintillation camera. Serial camera images were performed after the intravenous injection of 10 mCi of various complexes of  $^{99m}\text{Tc}$  and 200-500 uCi of  $^{131}\text{I}$ -ortho-iodohippurate (Hippuran). The difference in blood flow between the two kidneys was quantitated by a left ventricular injection of  $^{85}\text{Sr}$ -labeled microspheres just prior to sacrifice. The absolute concentrations of the radioactive microspheres and the renal agents were determined in the kidneys and other organs by tissue radioassay.

Reductions in renal vasculature of the order of 37% were easily detectible with the radioactive agents. Minor degrees of unilateral reduction of renal blood flow, however, proved difficult to demonstrate consistently, even by digital com-

puter processing of the sequential camera images. Detectability with various  $^{99m}\text{Tc}$  complexes was similar to that of  $^{131}\text{I}$ -Hippuran. The absolute renal concentration of Tc-dimer-captosuccinate was higher than Tc-labeled carbohydrate compounds; however, the ability to detect unilateral damage by in vivo technics was similar for all  $^{99m}\text{Tc}$  complexes studied to date. Radioactivity in the liver interfered with the accurate comparison of the relative concentrations in the two kidneys. The tissue assay data indicated that the difference in concentration between the two kidneys with the  $^{99m}\text{Tc}$ -complexes was greater than the degree of reduction in the renal blood flow as determined by the labeled spheres.

**DETERMINATION OF LEFT VENTRICULAR EJECTION FRACTION BY RADIONUCLIDE ANGIOGRAPHY IN PATIENTS WITH CORONARY ARTERY DISEASE.** Heinrich Schelbert, Hartmut Henning, Robert O'Rourke, Allen Johnson, Frank Rose and William Ashburn. University of California, School of Medicine, La Jolla, California.

By recording the passage of a radioactive bolus through the left ventricle (LV) a time activity curve can be obtained which reflects instantaneous volume changes, allowing calculation of LV ejection fraction (EF). To assess the validity and usefulness of this method,  $^{99m}\text{Tc}$  human serum albumen was injected into the superior vena cava in 20 patients (pts) during cardiac catheterization (Group A) and  $^{99m}\text{TcO}_4$  into the jugular vein or pulmonary artery in 16 pts with acute myocardial infarction (AMI) (Group B). Precordial activity was recorded in the right anterior oblique position by an Anger camera interfaced with a small digital computer. After assigning LV and background regions-of-interest (ROI) EF was calculated automatically in time segments for the entire LV time activity curve. LVEF in Group A pts correlated well with EF obtained from biplane cineangiograms ( $r = +0.94$ ;  $p < .001$ ) but only when LV ROI was assigned properly and only when derived from the early downslope of the time activity curve in the 16 Group B pts a total of 35 studies were performed 6 to 140 hours following the onset of AMI. In pts with AMI and pulmonary congestion, the LVEF was significantly less than in those without congestion ( $0.48 \pm .07$  (SD) vs  $0.34 \pm .07$ ;  $p < .001$ ). Furthermore, LVEF in pts with elevated LV filling pressures ( $>12\text{mmHg}$ ) was considerably lower than in pts with normal pressures ( $0.46 \pm .09$  vs  $0.35 \pm .07$ ;  $p < .001$ ). In addition, EF correlated inversely with infarct size as determined by creatine phosphokinase (CPK) curve analysis. In pts with a large AMI ( $>40$  CPK -g-Eq.) EF measured  $0.35 \pm .05$  as compared to  $0.45 \pm .11$  ( $p < .05$ ) in pts with smaller AMI. These results indicate that LVEF is determined accurately by radionuclide angiography and can be used to measure LV function serially in acutely ill pts with myocardial infarction.

**THERMOGRAPHY COMPARED WITH ISOTOPIC CAROTID BLOOD FLOW STUDIES IN PATIENTS WITH PROVEN OBSTRUCTIVE DISEASE.** Monika Schreyer, Klitia Vanags, Jorge Franco, Bernadine Kovalski. O'Connor Hospital Medical Center, San Jose, Ca.

Thermography, the pictorial representation of surface temperature differences by means of infrared detectors, has been proposed as a means to detect carotid artery disease. This approach is based on the anatomical fact that the blood supply to the inner triangle of the forehead is provided by the supra-orbital artery, in fact a terminal branch of the internal carotid. Significant decreases in flow through the carotids would result in subtle but significant temperature differences in the above regions.

We studied 12 patients with angiographically proven internal carotid artery narrowing. Six patients had recent complete contralateral hemiplegia. The isotopic blood flow study was done using 15 millicuries of Tc- $^{99m}$  pertechnetate.

The carotid blood flow study was abnormal in 4, technically unsatisfactory in one, and inconclusive in another of the patients with hemiplegia. Thermography demonstrated homolateral cooling in all 6 cases.

Of the patients without hemiplegia, thermography was abnormal in 3. The isotopic blood flow study was abnormal in 3 of the patients and inconclusive in the other three.

Although a larger series of cases is needed, our preliminary conclusions are that thermography is a reliable indicator of severe internal carotid obstructive disease but that it is not more reliable than isotopic studies in the detection of lesser degrees of obstructive disease.

**IODOCHOLESTEROL ADRENAL IMAGING IN ALDOSTERONISM: OPERATIVE FINDINGS IN 30 CONSECUTIVE CASES.** J.E. Seabold, W.H. Beierwaltes, J.W. Conn, S. Balachandran, E.L. Cohen. University of Michigan, Ann Arbor, Mich.

The operative findings are compared with the iodocholesterol adrenocortical images and venography in 30 consecutive patients submitted to therapeutic surgery for aldosteronism. Baseline images were made with an Anger camera at 7-14 days after 2 mCi of  $^{131}\text{I}$ -19-iodocholesterol. Suppression images were preceded by 1 mg of dexamethasone every 6 hours, beginning 2 days before the tracer and continued through imaging repeatedly from 3-14 days after the tracer. The aldosteronomas were "lateralized" by interpretation of the images with the knowledge that aldosteronism was suspected but before venography and surgery. Twenty-two of the 25 patients with aldosteronomas had baseline images and in 17 (77%) the tumor was "lateralized" correctly. The mean maximum diameter of the tumors were 1.57 cm (0.8-3.0 cm). Seventeen of the 25 aldosteronoma patients had suppression imaging with the tumor lateralized correctly in 15 of 17 (88%). The 2 aldosteronomas that didn't image were less than 1 cm. Twenty-three of the 25 patients had venograms and the aldosteronoma was localized in 19 patients (83%). Three out of 5 patients with hyperplasia of "idiopathic" aldosteronism showed bilateral suppression of uptake on dexamethasone. Iodocholesterol imaging compares favorably with venography. Bilateral suppression of uptake in aldosteronism is strong evidence of the existence of hyperplasia.

**THYROID FUNCTION FOLLOWING RADIATION AND SURGERY IN PATIENTS WITH HEAD AND NECK CANCER.** Rex B. Shafer, Frank Q. Nuttall, Kurt Pollak, and Hans Kufak. Minneapolis V.A. Hospital, Minneapolis, Minn.

Preoperative radiation followed by surgical excision is accepted therapy for head and neck cancer. The effects of these modalities on thyroid function were evaluated in 58 patients followed prospectively with 24 hr RAI uptake, total serum thyroxine ( $T_4$ ),  $T_3$  resin sponge uptake ( $T_3$ ), thyroid stimulating hormone (TSH) and thyroid antibodies (TA).  $^{60}\text{Co}$  radiation was given preoperatively via lateral cervical portals to a total tumor dose of 5,000-6,000 rads. Location of the cancer was oral cavity in 10 (17%), pharynx in 23 (40%), and larynx in 25 (43%). Results (2-18 months follow-up) reveal 42 patients (72%) euthyroid, 5 patients (9%) with transient loss of thyroid reserve and increase in TSH, and 11 patients (19%) clinically hypothyroid. Onset of hypothyroidism was 0-4 months in 10 of 11 patients. Transient + in TSH occurred in 0-10 months. Blood urea nitrogen, serum albumin, globulin, calcium, phosphorus and alkaline phosphatase were unaffected by therapy. The presence of thyroid antibodies showed no relationship to the incidence of post-therapy hypothyroidism. A similar lack of relationship was found for serum cholesterol. In 25 patients in whom surgery included hemithyroidectomy, there was no relationship between loss of thyroid tissue and the incidence of post-therapy hypothyroidism.

These results are recognized to be preliminary and represent the initial report of an ongoing study. We are not aware of a previous report in which thyroid function has been systematically studied in patients following radiation and surgery in head and neck cancer. The high incidence of permanent hypothyroidism indicates a need for careful periodic evaluation of thyroid function in these patients for an indefinite period of time.



**RELATIVE RENAL BLOOD FLOW IN HYPERTENSIVE PATIENTS: A NEW TECHNIQUE USING THE SCINTILLATION CAMERA AND SMALL COMPUTER.** D.M. Shames, R.E.L. Farmer and F. David Rollo, University of California Medical Center, San Francisco, Calif.

Recent advances in the quantitation of the <sup>131</sup>I-hippurate renogram for detection of renal artery stenosis have generally required the use of large off-site digital computers. To surmount this problem we have developed a technique for measuring quantitatively the relative blood flow between the two kidneys using the scintillation camera and small dedicated digital computer.\*

The technique is based on first-pass kinetics of <sup>99m</sup>Tc-albumin following peripheral intravenous injection. The region of the kidneys is monitored from posterior view at one-half second time intervals for 30 seconds following injection. The computer stores the spatial-time information on disk in 64 x 64 matrices. Following completion of the study, the computer is used to extract region of interest activity-time curves over both kidney regions and then correct these curves for background activity and non-uniform crystal sensitivity. Defining the left and right kidney curves as R<sub>L</sub>(t) and R<sub>R</sub>(t) respectively, it can be shown for an intravascular indicator like <sup>99m</sup>Tc-albumin that

$$\left(\frac{F_L}{F_R}\right) = \lim_{t \rightarrow 0} \left(\frac{R_L(t)}{R_R(t)}\right)$$

where F<sub>L</sub> and F<sub>R</sub> are the renal blood flows to the left and right kidneys respectively. The computer is used to fit an n-th order polynomial in t to the curve obtained by ratioing R<sub>L</sub>(t) to R<sub>R</sub>(t) point by point. The zero-th order term of this polynomial is then the best estimate of the F<sub>L</sub>/F<sub>R</sub> which is the relative blood flow between the two kidneys.

This technique has the advantages of being quick and easy to apply to patients, quantitatively sound in terms of dye-dilution theory and readily automated using a small computer.

\*Gamma-11, Digital Equipment Corp.

**EVALUATION OF LIVER FUNCTION BY OXIDATION OF GALACTOSE-C-14 OR C-13 IN VIVO.** Walton W. Shreeve, Jon D. Shoop, Donald G. Ott and Berthus B. McInteer, State University of New York and V.A. Hospital, Northport, N.Y.; University of New Mexico, Albuquerque, N.M.; Los Alamos Scientific Lab, N.M.

A test of oxidation of carbon-labeled galactose to breath CO<sub>2</sub> is simpler to perform than the non-isotopic intravenous galactose tolerance test as well as metabolically different and possibly more sensitive and specific than present liver function tests. The authors have orally administered generally-labeled galactose-C-14 (10 to 20 microcuries) or galactose-C-13 (1.0 atoms per cent excess) in a load of 10 g. galactose/m<sup>2</sup> body surface. Breath C-14-O-2 is collected in hyamine solution for measurement by liquid scintillation counting. For C-13-O-2 analysis by a mass spectrometer the breath is collected in small evacuated glass bulbs. Times of peak C-14-O-2 or C-13-O-2 in breath are delayed an hour or more in cirrhosis. The average rates of excretion of C-14-O-2 or C-13-O-2 by cirrhotic patients (about 10) at 30, 60 and 90 minutes after ingestion are approximately 1/4, 1/3 and 1/2 of rates for normal subjects (about 10) with almost no overlap of individual values between groups. More overlap occurs for values of serum alkaline phosphatase, albumin, bilirubin, SGPT and SGOT. Average differences between groups are no greater for these other liver function tests than for galactose oxidation. Degree of abnormality in galactose oxidation correlates well with abnormality of liver scan. Besides cirrhosis, other liver disease, drug hepatotoxicity, and liver transplants can be evaluated. With C-13 the test can be applied widely without radiation exposure.

**RETICULOENDOTHELIAL(RE) SCANS IN HEMATOLOGIC DISEASES.** David P. Shreiner, VA Hospital and University of Pgh. Medical School, Pittsburgh, Pa.

RE scans were performed on 65 patients (pt) in order to determine the usefulness of this procedure in dis-

eases affecting the bone marrow. Tc-99m sulfur colloid 170μCi/kg body weight was injected I.V. Multiple areas of bone marrow were viewed with the gamma scintillation camera using pre-set time exposures of 3 minutes/view. Total counts of 300,000 and 150,000 were accumulated for liver and spleen scans, respectively. Eleven of 12 uremic, anemic pt had abnormal scans. All 6 pt with decreased RE marrow activity had a BUN > 70mg%; pt with a BUN < 70mg% had normal or increased RE activity. All 7 pt with acute or chronic leukemia had decreased central marrow activity and variable hepatosplenomegaly. In 17 pt with lymphomas the pattern of RE marrow activity was variable and could not be correlated with hematocrit, organomegaly or pretreatment with cytotoxic drugs or irradiation. However, 5 of 6 pt with focal defects on marrow scan had histologic proof of lymphoma in the marrow. Hepatosplenomegaly by scan was found in all pts with Hodgkin's disease or lymphosarcoma; organomegaly was mild or absent in reticulum cell sarcoma. All 6 pt with multiple myeloma had decreased central RE marrow activity, and 2 had focal defects on scan with normal skeletal x-rays. Pts with hemolytic or hemorrhagic anemias had increased RE marrow activity, but pts with aplastic anemia had normal marrow scans. Five of 6 pt with myelophthisic anemia or myelofibrosis had decreased central marrow activity with peripheral expansion of the marrow space. In conclusion, uremia, as well as primary bone marrow disease, may be associated with decreased RE marrow activity, possibly due to suppression of RE function. The general pattern of RE marrow activity was not helpful in staging lymphomas except when focal defects were found.

**STIMULATION BY TRIIODOTHYRONINE OF NUCLEAR AND EXTRA-NUCLEAR DNA IN T-1 HUMAN KIDNEY CELLS.** Edward Siegel and Elsie P. Siegel, Departments of Radiology and Medicine, University of Missouri, Columbia, Mo.

T-1 cells have proven useful as an *in vitro* model in investigating end-organ actions evoked by thyroxine (T<sub>4</sub>) and triiodothyronine (T<sub>3</sub>). Previous studies with T-1 cells revealed preferential localization of labelled T<sub>4</sub> by the nucleus, an organelle implicated, also, as a primary locus of hormonal interactions. To pursue these observations, the influence exerted by T<sub>3</sub> in T-1 cells was recently examined using <sup>3</sup>H-actinomycin D uptake as a specific indicator for the presence of DNA. Following stimulation for 3 days with T<sub>3</sub> (8.90x10<sup>-7</sup> M) and labelling with <sup>3</sup>H-actinomycin D, radioautographs were made of T-1 cells and of chromosomal preparations. For a representative experiment, the results of grain counting of the exposed radioautographs are as follows:

	Net average no. of grains		
	*cytoplasm	*nucleus	**chromosomes
T <sub>3</sub> treated:	1.79	7.39	2.52
Controls:	1.14	5.51	1.06

\*n = 200

\*\*n = 100

While less than 20% of the radioactivity is extra-nuclear, the relative increase elicited by T<sub>3</sub> in activity of the cytoplasm is about that of the nucleus. Evidently, T<sub>3</sub> effects marked enhancement of DNA elaboration throughout the cell.

**THE EFFECT OF SERUM ON TRIIODOTHYRONINE (T<sub>3</sub>) STIMULATION OF T<sub>3</sub> AND LEUCINE UPTAKE BY T-1 HUMAN KIDNEY CELLS.** Edward Siegel and Elsie P. Siegel, Departments of Radiology and Medicine, University of Missouri, Columbia, Mo. -

As manifested by parameters that reflect cellular proliferation, morphology, colony formation, and the metabolism of lipids, proteins, and nucleic acids, the T-1 cell line responds to thyroxine (T<sub>4</sub>) and triiodothyronine (T<sub>3</sub>). Enhanced sensitivity to and specificity for the thyroidal hormones have been unmasked by diminishing the fetal bovine serum (FBS) content

of the T-1 cell growth medium. Recent experiments utilizing radioautography indicate that uptake of  $^{125}\text{I-T}_3$  is increased, especially by T-1 cells stimulated for 1 day with  $\text{T}_3$  ( $8.90 \times 10^{-7}$  M) when FBS content is reduced from 10 to 2.5%. As demonstrated by  $^3\text{H}$ -leucine uptake, no such variation in protein synthesis with FBS content was detected either in T-1 cells stimulated for 2 days with  $\text{T}_3$  ( $8.90 \times 10^{-7}$  M) or the controls. These findings are consistent with the view that reducing serum content lowers the number of available hormonal binding sites, leaving more free  $\text{T}_3$  available for cellular localization. Since uptake of leucine does not involve binding to serum proteins, the synthetic process proceeds independently of FBS content.

**A CORRELATION OF ARTERIOGRAPHY AND PERIPHERAL PERFUSION SCANNING IN THE ASSESSMENT OF PERIPHERAL VASCULAR DISEASE.**  
Michael E. Siegel, Frank Giargiana, Robert White, Barry Friedman and Henry N. Wagner. The Johns Hopkins Medical Institutions, Baltimore, Maryland.

In patients with peripheral vascular disease the relative distribution of perfusion in the extremities, in the basal state and with the vasculature under maximal vasodilatation, was correlated with the arteriographic and clinical findings to assess the physiologic effect of the morphologic changes seen on the arteriogram.

Thirty patients with symptomatic peripheral vascular disease had perfusion scans at the time of translumbar arteriography. Fifteen minutes following the arteriogram, 5-10 mCi of  $^{99\text{m}}\text{Tc}$  microspheres were injected rapidly through the catheter. Subsequently, using full leg inflatable boots, reactive hyperemia was induced and 5-10 mCi of  $^{113\text{m}}\text{In}$  microspheres were injected rapidly, during maximal vasodilatation. The extremities are scanned anteriorly and posteriorly with a dual 5" scanner, using 1:5 minification. The arteriograms and scans were evaluated separately as to extent and location of disease and the likely clinical findings that would be expected. These results were then correlated and both studies were reviewed with the knowledge of such clinical findings as location of claudication and presence of peripheral pulses.

Only 11/28 basal scans and 12/30 reactive hyperemia scans correlated well with the arteriogram. Of the 4 basal and 6 reactive hyperemia scans which showed more abnormality than the arteriogram, all were patients with diabetes or previous sympathectomy. The reactive hyperemia scan correlated well with the patient's symptomatology in 25/30 cases, the rest scan in 18/30 and the arteriogram in 16/30. We conclude that perfusion scanning is not, in a strict sense, comparable to arteriography, but offers complementary information on the status of peripheral vascular disease.

**PERIPHERAL VASCULAR PERFUSION SCANNING: A PROGNOSTICATOR OF ULCER HEALING.** Michael E. Siegel, Frank A. Giargiana, Buck A. Rhodes and Henry N. Wagner. The Johns Hopkins Medical Institutions, Baltimore, Md.

The relative distribution of perfusion was utilized to predict the healing ability of ischemic ulcers of the lower extremity.

Peripheral vascular perfusion scans were performed on a group of 39 patients with ischemic ulcers of the lower extremities, after an intra-arterial injection of 5-10 mCi of  $^{99\text{m}}\text{Tc}$  labeled albumin microspheres. Gamma camera images of the specific ulcer region were also obtained. The study was performed both on an inpatient and outpatient basis with the microspheres administered via the femoral or translumbar approach. Contrast angiography was simultaneously performed on 18 of the patients. Particular note was taken of the presence of diabetes and of the various peripheral pulses. The maximum, clinically feasible, conservative, non amputative, course of management was afforded each patient. This period ranged from 8 days to 5 months.

The presence and degree of hyperemia in the ulcer was determined by point counting and electronic flagging of the areas of interest.

No correlation was seen between the presence or absence of diabetes or palpable pulses below the femorals, the ability to visualize at least two trifurcation vessels, as seen on the arteriogram and the ability of the lesions to

heal. We did find, however, that when the hyperemia response in the ulcer bed, expressed as counts per unit area, compared to the surrounding area, was at least 3:1 then 17 of 18 patients healed their ulcers with conservative management, while 19 of 21 patients without this hyperemia eventually required amputation because of non healing. The presence and degree of hyperemia in an ulcer bed is a clinically useful prognostic indicator of healing.

**EARLY DIAGNOSIS OF HEMATOGENOUS OSTEOMYELITIS.**  
Jan K. Siemsen and Alan D. Waxman. LAC/USC Medical Center, Los Angeles, Calif.

Hematogenous osteomyelitis (HOM) is more common than previously thought. Its early diagnosis is often difficult, since symptoms may be vague and non-specific. This study assesses the use of bone scanning for early detection of HOM.

Twenty-eight patients with suspected HOM were scanned with a dual-headed 5" crystal scanner, using 4 mCi of  $^{18}\text{F}$  or 15 mCi of  $^{99\text{m}}\text{Tc}$ -diphosphonate. The diagnosis was subsequently proven in all cases, by bone biopsy and culture in 23 patients, and by development of typical x-ray lesions associated with positive blood cultures in 5 cases.

The scans showed the focus of HOM correctly in all cases. The most common sites were the lumbar spine (20) and the sacro-iliac joint (9). Six patients had multiple foci at the time of the diagnosis. In 7/20 cases with spinal involvement the lesions were seen only or much more clearly on the anterior projection. At the time of the scan, x-rays were negative in 18 patients and equivocal in 2, while 6 had definite abnormalities. Underlying or associated conditions were IV drug abuse in 16 patients, SBE in 4, septic abortion in 3, TBC in 2 and brucellosis in one.

The study demonstrates that bone scanning is useful in the early diagnosis of HOM. The fact that many lesions in the spine were best seen on anterior views is felt to be related to the fact that the metaphyseal endplate in the anterior 2/3 of the vertebral body is richly supplied by nutrient arteries. Therefore, multiple views should be taken.

**EFFICACY OF TECHNETIUM-99m SULFUR COLLOID, ANGIOGRAPHY AND LIVER FUNCTION TESTS IN THE DIAGNOSIS OF HEPATIC DISEASE.**  
Edward B. Silberstein, University of Cincinnati Medical Center, Cincinnati, Ohio.

This study is the first to evaluate the diagnostic efficacy of hepatic scintigraphy performed solely with  $^{99\text{m}}\text{Tc}$ -sulfur colloid and compared both to hepatic angiography (HA) and routine liver function tests (LFT): serum glutamic oxaloacetic transaminase (SGOT), serum albumin concentration, serum alkaline phosphatase (SAP), and serum bilirubin.

A retrospective study was made of sixty-four patients who had received hepatic scintigraphy and angiography and liver function tests, all obtained within a 7 day period.  $^{99\text{m}}\text{Tc}$ -SC and a gamma camera (Nuclear Chicago Pho/Gam III or HP) were used in all cases. All patients had histologic confirmation of hepatic disease at laparotomy or autopsy. Results were expressed as the true and false positive and negative yield of each procedure.

The liver scintigraph was correct 89.1% of the time, the hepatic angiogram 82.8%. The liver function test with the greatest accuracy was the SAP (81.2%), followed by the SGOT (78.1%), bilirubin (68.8%) and albumin (64.0%). (Table 1). All three diagnostic modalities were simultaneously correct 62.5% of the time. The  $^{99\text{m}}\text{Tc}$ -SC study was correct when the HA was incorrect in the same patient in 14.0% of cases while the opposite was true in 9.3%. In 15.6% of cases the  $^{99\text{m}}\text{Tc}$ -SC study was correct when one or more LFT's were in error, while the LFT's were correct in confirming the presence or absence of disease in 7.8% of cases when the scintigraph reading was wrong (Table 2).

It is concluded that the liver scintigraphic study, using only  $^{99\text{m}}\text{Tc}$ -SC and a gamma camera is at least as accurate as the HA and also is correct in predicting the presence or absence of liver disease more often than the four LFT's studied.

**BASAL GANGLIA SCAN: AN EXPERIMENTAL STUDY.**  
Gregorio Skromne-Kadlubik, Francisco Diaz, and Cesar Celis. Faculty of Medicine. University of Mexico. Mexico City.

The metabolism of the basal ganglia is unique in a number of ways. The copper content of most of them is particularly high; and in Wilson's disease there is severe degeneration of the lenticular nucleus. Using Cu-64, we studied the copper distribution in basal ganglia and pericranial tissues, with the idea of obtaining a gamma image suitable for diagnosis purposes. In 20 mice injected with Cu-64, homogenized cranial and pericranial tissues were read in a "well-type" counter at 1 hr., 2 hrs., 4 hrs., 24 hrs., and 48 hrs. using the same geometry. Also in 8 rabbits injected with Cu-64 the basal ganglia were dissected and read in a "well-type" counter and compared with a standard of same dose and geometry. All this information finally was useful to take, for the first time in the world, a satisfactory gamma image of basal ganglia in 2 rabbits using 1 mCi of Cu-64 at 2 hrs. after intravenous dose. The possibility of using this method in human beings is at the present time being tested in our laboratory and will be the object of a future communication.

**A SIMPLE KIT FOR THE RAPID PREPARATION OF  $^{99m}\text{Tc}$  RED BLOOD CELLS.** Terry D. Smith, and Powell Richards. Brookhaven National Laboratory, Upton, N.Y.

A real need exists for a simple and easy-to-use vascular imaging agent particularly for cardiac function studies. And the merits of technetium-99m as the radionuclide of choice have been well established.  $^{99m}\text{Tc}$ -labeled red blood cells is the agent of choice, but until now it has not enjoyed widespread use because of the lack of a simple and reproducible, high-yielding preparative method. A simplified "kit" with an extended shelf life has now been developed. It consists of a sterile and pyrogen-free vacutainer containing both a suitable stannous reagent and an appropriate anticoagulant in freeze-dried form. The vacutainer automatically draws about 3 ml of blood from the patient. After mixing at room temp. for 5 min. to "pre-tin" the RBC's, the blood is diluted with 4 ml of sterile saline and shaken briefly. Subsequent centrifuging of the vacutainer in the inverted position causes the RBC's to settle against the stopper so that 1 ml of RBC's can be easily removed with a specially provided sterile needle and transferred to a separate sterile vial containing about 1 ml of  $^{99m}\text{TcO}_4$ . After mixing for 5 min. at room temp. the  $^{99m}\text{Tc}$ -labeled RBC's are ready for assay and injection. Yields of 97% are usual in less than 20 min. This simplified kit which requires a minimum blood volume is expected to greatly increase the use of  $^{99m}\text{Tc}$ -labeled RBC's in nuclear medicine.

**ARE RADIOPHARMACEUTICALS FOUND IN SIGNIFICANT LEVELS IN THE OHIO RIVER.** Vincent J. Sodd, Richard J. Velten, and Eugene L. Saenger. Food and Drug Administration, University of Cincinnati, and Environmental Protection Agency, Cincinnati, Oh.

Radionuclides administered to patients in the practice of nuclear medicine are usually excreted into a public sewage system. Because the medical use of radionuclides has increased greatly, concern has been shown for its possible effect on the environment. The levels of radionuclides were measured in the sewage system of a Cincinnati, Ohio, area where 14 hospitals offer nuclear medicine services. The results showed that on a given working day as much as 140 mCi

of  $^{99m}\text{Tc}$  and 40 mCi of  $^{131}\text{I}$  pass through the sewage treatment plant and are released into the Ohio River. The dilution of the activity by the river results in the downstream concentration of  $^{99m}\text{Tc}$  of  $\sim 1$  pCi/l, well below the maximum permissible concentration in water (mpc) of  $60 \mu\text{Ci/l}$ ; that of  $^{131}\text{I}$  is  $\sim 0.4$  pCi/l which can be compared to the mpc of  $2 \times 10^4$  pCi/l.  $^{99m}\text{Tc}$  decays into  $2 \times 10^5$  y half-lived  $^{99}\text{Tc}$  which emits beta particles and has been considered a potentially hazardous contaminant to the environment. Assuming a 10% increase in  $^{99m}\text{Tc}$  usage per year, the amount of  $^{99}\text{Tc}$  remaining in the environment after the next 50 years will be  $\sim 350 \mu\text{Ci}$ ; an insignificant amount when compared to the world's inventory of  $^{99}\text{Tc}$  from atmospheric weapons tests of  $5 \times 10^7$  mCi. These preliminary results indicate that the release of radiopharmaceuticals into the environment does not constitute a potential health hazard.

**COMPARATIVE BIOLOGICAL BEHAVIOR OF  $^{99m}\text{Tc}$  AND  $^{125}\text{I}$  LABELED UROKINASE.** Prantika Som and Buck A. Rhodes. The Johns Hopkins Medical Institutions, Baltimore, Md.

Radioactive compounds capable of localizing blood clots by scanning are needed radiopharmaceuticals. Streptokinase and urokinase have been under investigation for the last few years as possible clot localizing agents. The present study was designed to evaluate the biodistribution of  $^{99m}\text{Tc}$  and  $^{125}\text{I}$  labeled urokinase prepared by different methods.

Urokinase was labeled with  $^{99m}\text{Tc}$  in the presence of stannous chloride and with  $^{125}\text{I}$  in the presence of lactoperoxidase. For labeling with  $^{99m}\text{Tc}$ , 10000-20000 CTA units of urokinase in saline was taken and freshly prepared 0.25 ml of 0.1%  $\text{SnCl}_2 \cdot 2\text{H}_2\text{O}$  in weak HCl (0.001N for method-A and 0.01N for method-B) was added along with adequate amount of  $^{99m}\text{TcO}_4$ . For labeling with  $^{125}\text{I}$ , the method of Thorell and Johansson (Biochim. Biophys. Acta 251: 363, 1971) was used. The tissue distribution was determined in mice and the clearance was measured in dogs for all these preparations both with and without millipore filtration.

$^{99m}\text{Tc}$  urokinase prepared by method-B showed similar tissue distribution in mice and blood clearance in dogs compared to  $^{125}\text{I}$  urokinase. Method-A resulted in relatively greater uptake of radioactivity in the liver. Millipore filtration altered the biodistribution of all the preparations which decreased the amount of radioactivity going to the liver. The plasma clearance curves demonstrated two main components. The  $t_{1/2}$  of the slow component (about 20%) was between 2.5 and 4 hours. The total activity in the blood volume became less than 20% in 1 hour and about 50% of the dose was excreted in urine in 4 hours in dogs.  $^{99m}\text{Tc}$  urokinase has been prepared which has biologic behavior similar to  $^{125}\text{I}$  urokinase.

**CHARACTERIZATION OF DEAD-TIME OF ANGER CAMERA SYSTEMS.** James A. Sorenson. University of Utah, Salt Lake City, Utah.

Recently several analyses of Anger camera dead-time characteristics have been published in which it has been assumed that the Anger camera behaves as a simple non-paralyzable system. However, another recent report by Anger has shown that most, if not all, commercial types of Anger cameras behave as paralyzable systems, or at least as if they have both paralyzable and non-paralyzable components. The appropriate methods for measuring dead-time and calculating dead-time losses for systems with paralyzable components are quite different from those which are applicable to simple non-paralyzable systems. For example, the familiar two-source method for estimating system dead-time is not valid for paralyzable systems. Application of this method to a system with paralyzable components may give the erroneous impression that the system dead-time varies with the count rate. In this paper, the appropriate mathematics and methods for analyzing counting systems with paralyzable components will be reviewed. Data obtained from

two Nuclear Chicago cameras will be presented to show that these cameras have both paralyzable and non-paralyzable components, and that the dead-times of these components do not change with count rate over a wide range of count rates. Additional data will illustrate, however, that these dead-times do change appreciably with several other factors, including the radionuclide counted, window width and centering, and the position of the internal "time constant selector" switch found in the A-scope module of Nuclear-Chicago cameras.

<sup>99m</sup>Tc-PROTAMINE COMPLEX WITH BILIARY EXCRETION. Richard P. Spencer, Robert E. Miller, Mohamad A. Antar. Sect. Nuclear Medicine (Radiology), Yale Univ. School of Med., New Haven, Conn.

Protamine sulfate, a basically charged protein with a high arginine content, can form <sup>99m</sup>Tc-complexes. While protamine sulfate can inhibit the formation of thromboplastic activity in plasma, it is perhaps best known as an agent for counteracting heparin. When dry protamine sulfate and SnCl<sub>2</sub> are added to pertechnetate solution, an opalescent material is formed. This can also be made by using the U.S.P. solution of protamine sulfate, adding SnCl<sub>2</sub> and then the pertechnetate. On chromatography, all of the technetium stays with protein at the origin. The <sup>99m</sup>Tc-protamine complex, when injected intravenously, localizes in the lung and liver. For example, in a rabbit, letting counts per gram of tissue in the liver equal 100, results were: liver 100, lung 265, blood 7. Because of the ease of preparation, and the dual organ distribution, the <sup>99m</sup>Tc-protamine complex might have interest as a combined lung-liver scanning agent. A second type of material is formed by electrolytic complexation of pertechnetate and protamine, followed by passage through a 0.22 micron filter to eliminate larger particulates. When this material is injected intravenously in dogs, it is cleared from the blood stream by the liver and spleen. Within 2 hours, a large accumulation of radioactivity can be detected in the gallbladder. This also occurs in rabbits. The events are reminiscent of some microaggregates reported by Taplin. The <sup>99m</sup>Tc-protamine complex may be a new agent for studying interchange between the R.E. and hepatocyte systems.

SYNTHESIS AND EVALUATION OF <sup>13</sup>N-L-ALANINE FOR PANCREATIC IMAGING. Leonard Spolter, Marvin B. Cohen, Norman Macdonald, Chia Ching Chang, Joseph Takahashi, Horace Neely, Gerald Huth, Sherilyn Meyers and Darrell Bobinet. VA Hospital, Sepulveda, Calif. and UCLA, Los Angeles, Calif.

During the course of a study of the distribution of several amino acids, <sup>14</sup>C-L-alanine was found by whole-body autoradiography to concentrate in the pancreas with little hepatic uptake. The feasibility of rapidly synthesizing <sup>13</sup>N-L-alanine has been established and its use as a pancreatic imaging agent has been investigated. <sup>13</sup>NH<sub>3</sub> was produced in the UCLA Biomedical Cyclotron by irradiation of methane in a d,n reaction. This <sup>13</sup>NH<sub>3</sub> was purified on an ion exchange column and incubated with enzyme, substrate, buffer, and co-factors. <sup>13</sup>N-L-glutamic acid was synthesized from alpha-ketoglutarate and <sup>13</sup>NH<sub>4</sub><sup>+</sup> after a 3 minute incubation at 25°C with L-glutamic acid dehydrogenase. During this incubation, pyruvic acid was pre-incubated with glutamic-pyruvic transaminase. An aliquot was then added to the <sup>13</sup>N-L-glutamic acid and incubated at 38°C for an additional 7 minutes. <sup>13</sup>N-L-alanine was separated from <sup>13</sup>N-L-glutamic acid and from <sup>13</sup>NH<sub>4</sub><sup>+</sup> by ion exchange columns. Analysis of the products by thin layer chromatography revealed that 55%-60% of the <sup>13</sup>N-L-glutamic acid was converted to <sup>13</sup>N-L-alanine. Total elapsed time from receipt of <sup>13</sup>NH<sub>3</sub> to synthesis of <sup>13</sup>N-L-alanine is 15 minutes. Random preparations, passed through a 0.22 micron millipore filter, were found to be sterile and pyrogen-free. Animals were sacrificed 5 minutes after I.V. injection and aliquots of selected tissues were counted in a well counter. <sup>13</sup>N-L-alanine was found to have a significantly higher pancreas to liver ratio than was found previously with <sup>13</sup>N-L-glutamic acid. Imaging was performed on rabbits and a 9.5 Kg adult male monkey (Macacus Mulatta) with a scintillation camera. On the basis of these studies, <sup>13</sup>N-L-alanine appears to be a promising pancreatic imaging agent.

SERIAL LIVER SCANS IN PATIENTS WITH PAROXYSMAL NOCTURNAL HEMOGLOBINURIA. E. V. Staab and R. C. Hartman. University of North Carolina, Chapel Hill, N.C. and Vanderbilt University, Nashville, Tenn.

For the past five years we have had the opportunity to perform serial liver scans in 11 patients with Paroxysmal Nocturnal Hemoglobinuria (PNH). In this disease there is a generalized thrombotic tendency and more recently progressive, diffuse hepatic venous thrombosis has been emphasized as the most serious complication and frequent cause of death.

Correlation of the clinical, laboratory, radiographic and liver scan studies were performed on each patient. In four of five patients who have died, autopsy correlation was obtained. Liver scans were of great help in the establishment of the diagnosis and following the progress of the disease process.

Abnormal liver scan patterns in hepatic venous occlusion include: enlarged liver (especially the right lobe), extra-hepatic localization of the radionuclide, and large areas of decreased activity in the distribution of the involved veins.

These findings develop rapidly and in the clinical setting are very characteristic.

CLINICAL EVALUATION OF THE UTILITY OF HEPATIC SCINTIANGIOGRAPHY IN NEOPLASTIC TUMORS OF THE LIVER, R.C. Stadalnik, S. J. DeNardo, A. Raventos, G. L. DeNardo, University of California at Davis, Davis, California

Experience with more than 1000 hepatic scintiangiograms (SA) suggested the value of this method for increasing the specificity of diagnosis of space-occupying lesions of the liver. An investigation to determine its clinical utility in hepatic tumors by comparison with histologic and radiopaque angiographic (RA) diagnosis was undertaken. 92 pts. had hepatic SA, scintigraphy and histologic verification; 2 more had RA verification. 12 had RA, including 2 normal livers without histologic verification, 6 hepatomas and 4 metastases with histologic verification. In 20/23 histologically normal livers, SA was normal and the same interpretation was made in 2 more pts. who had only RA verification. 1/3 SA, which differed from the normal histology, identified a vascular extrahepatic neoplasm which encroached upon but did not invade the liver; in the remaining 2 pts. both S and SA were abnormal showing multiple focal vascular lesions. Tissue in these 2 pts. was obtained by non-operative needle biopsy, and probably these are instances of sampling error. There was complete correlation between SA and histology in 10 hepatomas. 52/59 histologically verified metastases had a corresponding interpretation on SA. Hepatogram phases of SA and RA correlated in 2/2 normal livers, 4/6 hepatomas, and 2/4 metastases. In 2/6 hepatomas and 2/4 liver metastases, SA correctly defined the vascular nature (tumor stain) of the lesion and correlated with the histology, whereas RA failed to reveal the tumor stain, although other less definitive vascular changes were noted.

In summary, the degree of vascularity of focal lesions was well defined by SA and there was good correlation with the histologic findings and greater sensitivity than RA.

EXPERIENCE IN NUCLEAR MEDICINE WITH A FREE TEXT INFORMATION STORAGE AND RETRIEVAL SYSTEM. Mark A. Stein, Ruby Okub, James Winter, and Leslie R. Bennett. University of California Medical Center, Los Angeles, Calif.

Since August 1971, the UCLA natural language information storage and retrieval system has been used to index nuclear medicine report impressions, automatically. This system, initially designed for pathology reports, is implemented on an IBM 360/50 computer.

To date, 36,915 report impressions from 14,683 examinations on 9,211 patients comprise the nuclear medicine data file. This data file is kept current by updates approximately every one and one-half months.

Natural language report impressions are entered on punch cards, encoded by an input translator, and stored sequentially on magnetic tape by patient identification number. Serial, exhaustive searches of this nuclear medicine data file and the pathology data file are performed off-line, providing the actual free text impressions as well as the patient identification. Logical (Boolean- and, or, not)

searches cross-referencing these two data files are assisted by a thesaurus that automatically expands a search request to include related terms (synonyms, subordinate terms) when desired. The structure of the nuclear medicine thesaurus is an hierarchical acyclic directed graph showing the relationships among the 3,508 encoded terms.

Thirty-one searches of the nuclear medicine data file have been conducted employing the thesaurus terms, twenty-one of these during the past nine months. This resulted in an average of 164 patients per search with a standard deviation of 253 patients and a range of 0 to 1179 patients.

Ten of the thirty-one searches were conducted on both the nuclear medicine and pathology data files. When dual searches were performed, the second search on the average eliminated 62% of the cases retrieved by the first search, indicating the increased specificity resulting from a cross-referenced search.

**IMPROVEMENT OF  $^{99m}\text{Tc}$ -STANNOUS PYROPHOSPHATE MYOCARDIAL SCINTIGRAMS USING COMPUTER PROCESSING.** Ernest M. Stokely, Robert W. Parkey, Samuel E. Lewis, and Frederick J. Bonte. University of Texas Health Science Center and Parkland Memorial Hospital, Dallas, Tex.

Results from our laboratory have recently demonstrated the usefulness of  $^{99m}\text{Tc}$ -stannous pyrophosphate as an agent for detecting myocardial infarction. While most infarcts less than 8 days old can be clearly seen on the unprocessed scintigram, others are sometimes partially obscured by  $^{99m}\text{Tc}$  pyrophosphate uptake in normal tissue or by uptake in the overlying rib structure. We have used two image processing techniques to improve the visibility of the infarct. The first is the use of simple background subtraction and contrast enhancement to emphasize the  $^{99m}\text{Tc}$  pyrophosphate uptake in the infarcted region. Figure 1 illustrates the improvement in infarct definition which can be gained by background subtraction and contrast enhancement. In this case the image modification was performed using a PDP-8I digital computer and a direct-view storage tube graphics display. A special recursive digital filtering algorithm has also been designed to remove the rib structure in the infarction. Figure 2 shows the improvement in infarct definition of a 2-day old infarction in a mongrel dog. The recursive filtering algorithm is applied to the contrast range in the image, i.e., homomorphic filtering in the logarithmic domain is used. The application of background subtraction and contrast enhancement or rib removal significantly improves the visibility of the infarct for roughly one-half of the  $^{99m}\text{Tc}$  pyrophosphate myocardial images which we have collected from cardiac patients.

**DIAGNOSIS OF SPACE OCCUPYING LESIONS OF THE ABDOMEN.** Edgar Surprenant and James Steffens. St. Mary's Medical Center, Long Beach and University of California at Los Angeles, Calif.

Records of 110 consecutive patients were reviewed to evaluate the relative usefulness of radioisotope, ultrasound, and x-ray exams in abdominal diagnosis. All had an abdominal B scan and AP x-ray. Radioisotope studies included 85 liver-spleen ( $^{99m}\text{Tc}$  colloid), 34 pancreas ( $^{75}\text{Se}$  methionine), 8 Rose Bengal, and 2  $^{67}\text{Ga}$  exams. Intervals between studies ranged from 0 to 10 days (ave. 2.7 d).

All studies were negative in  $\frac{1}{4}$  the patients. The x-ray had limited value except as an adjunct to other procedures. Radioisotope exams were most sensitive for detecting intrahepatic lesions while ultrasound was best for extrahepatic processes. Ultrasound also differentiated: a) cyst from solid, b) hepatic mass from dilated ducts, and c) abscess from other processes displacing the liver or spleen. A mass in the pancreatic area was detected in 4 of the 12 patients with an abnormal  $^{75}\text{Se}$  exam and 1 of the 22 in which it was normal. When Rose Bengal demonstrated bile duct obstruction, ultrasound determined if a mass was present and guided radiotherapy. Adenopathy was detected by ultrasound in 2 patients with equivocal  $^{67}\text{Ga}$  exams.

Ultrasound exams of the abdomen involve virtually no patient discomfort or hazard and minimal cost, yet frequently suggest the diagnosis or indicate the most appropriate radioisotope, roentgenologic, or biopsy procedure(s) that should be performed.

**REGIONAL PERFUSION AND VENTILATION ABNORMALITIES IN PATIENTS WITH MITRAL VALVE DISEASE.** Edgar L. Surprenant and Richard Spellberg. St. Mary's Medical Center, Long Beach and University of California at Los Angeles, Calif.

Regional perfusion ( $\dot{Q}_r$ )-ventilation ( $\dot{V}_r$ ) was evaluated in patients with mitral valve disease.

Adult subjects, 6 normals and 22 patients (11 MS, 3 MI, 8 Mixed), were studied excluding those with other cardiopulmonary diseases. Supine tidal volume  $\dot{Q}_r$  ( $^{99m}\text{Tc}$  MAA) and  $\dot{V}_r$  ( $^{133}\text{Xe}$ ) scintiphotos were obtained in the posterior and right lateral projections. Patients had chest x-rays and cardiac catheterization.

Reversal of the normal perfusion gradient in the right lung (relative increase in upper lobe perfusion) occurred with left atrial pressure (LAP) elevation. Reversal was noted in 10 of 12 with LAP 21 to 35 mmHg, 5 of 9 with LAP 12 to 20 mmHg and 1 of 7 with normal LAP. The ventilation gradient was reversed in 1/3 of those with reversed perfusion. Perfusion defects ( $\dot{Q}_d$ ) and ventilation defects ( $\dot{V}_d$ ) occurred in 3/4 of patients. In 1/3 of these, the  $\dot{Q}_d$  was larger (vascular obstruction); in another 1/3 the  $\dot{V}_d$  was larger (ventilatory restriction). A  $\dot{V}_d$  and  $\dot{Q}_d$  in the right middle lobe area occurred in 4. The following were noted in 1/3 of patients: gradients were modified by discreet focal defects; left lung gradients were different from the right; there was relative hypoventilation of the left lung.

Varied abnormalities of  $\dot{V}_r$  and  $\dot{Q}_r$  are common in mitral disease.

**THE M-B CARDIAC SCAN.** Edgar Surprenant, James Steffens, and Ralph Ranalli. St. Mary's Medical Center, Long Beach, and University of California at Los Angeles, Calif.

The present trend in non-invasive cardiac imaging with radioisotopes and ultrasound suggests that these may soon provide most of the anatomic and functional data necessary in the diagnoses and management of cardiac diseases. Ultrasound provides spatial resolution not possible with radioisotopes. However, the conventional time motion (M-mode) studies provide spatial resolution in only one dimension. Static B-scan and "cine" imaging are 2 dimensional but have other practical limitations.

We propose a method that combines M-mode and B-scan displays into a single static image i.e., the "M-B-scan". The transducer is placed on the precordium and a single pass is made across the heart, usually from aortic root to apex, during 5 to 40 cardiac cycles. The resultant single image has the 2 dimensional spatial accuracy of a B-scan while still demonstrating motion, since the probe was detecting different anatomic points at different points in time. A simultaneous reference EKG tracing is displayed alongside the cardiac image.

The M-B-scan is a new approach to cardiac imaging, particularly useful in identifying the exact size and location of an area of myocardial dysfunction.

**BONE SCAN ON ANEPHRICS WITH EVIDENCE OF SECONDARY HYPERPARATHYROIDISM (HPT).** Wilfrido M. Sy, and A.K. Mittal. Brooklyn-Cumberland Medical Center, Brooklyn, New York

The extent of bone disease in secondary HPT is difficult to judge since bone resorption is a late x-ray sign. Minified 5:1 anterior and posterior body scans were performed in 6 male and 8 female chronic renal failure patients on dialysis (median-43.5 mos) 3 hrs after IV injection of 15 mCi  $^{99m}\text{Tc}$ -SnPP0<sub>4</sub>. A 5" dual scanner, 3 $\frac{1}{2}$ " low energy collimators and ID of over 1000 cts/cm<sup>2</sup> were used. Calvarium, mandible, sternum, shoulders, vertebrae, pelvis and femur-tibia abnormalities

were each scored 0 to 4+. On the basis of the cumulative scores, bone involvement was considered severe in 3 patients, marked in 4, moderate in 3, mild in 2, absent in 1. Three-minute hand views were also obtained in 7 patients using 2C upgraded camera with ultrafine collimator: all showed commensurate abnormalities. Tissue proof of HPT was obtained in severe forms. Abnormal scans without x-ray changes occurred in mild and moderate forms. Strikingly abnormal scans were noted when x-ray suggested demineralization. Consistent mandibular activity appeared to be an early sign of HPT. On x-ray this has not been emphasized as such. Rib cage on one scan showed "rosary beads". Bone scan abnormalities in anephrics are described for the first time. The extent of scan abnormalities correlated well with duration of dialysis and serum alkaline phosphatase levels. Bone scanning is a sensitive technique for measuring the skeletal effects of HPT.

**LOCALIZATION OF MINUTE BRONCHOGENIC TUMOR PHANTOMS BY GATED, COMPUTERIZED CHEST SCINTIGRAPHY.** George V. Taplin and Dennis Elam. Laboratory of Nuclear Medicine, University of California, Los Angeles, Calif.

An urgent need exists to develop accurate methods for the early diagnosis and localization of bronchogenic tumors. At present, lesions smaller than 1.0 cm diameter are seldom recognized roentgenographically. By this time the lesions have usually metastasized and the 5 year mortality is approximately 90 per cent.

Radio-immunoassay methods permit detection of circulating antigen in nanogram quantities, when small (1-2 mm) lesions are dormant for several years as is the case with cervical cancer, another epidermoid carcinoma. Contemporary immunological data suggest that earlier detecting and localization of bronchogenic tumors may be accomplished through radio-immunoassay followed by computerized, gated gamma scintigraphy. The localization of 1-2 mm and larger size bronchogenic phantom tumors has been demonstrated many times in this laboratory following the I.V. injection of Indium 113m (transferrin) in amounts sufficient to give 0.2 uCi levels/ml of blood and with tumors containing 3.4 to 7.0 times this amount in minute glass spheres introduced into the major bronchi.

Visualization is readily accomplished by background subtraction and lung immobilization during expiration while breathing is slowed greatly by anesthesia and 100% oxygen breathing. Examples will be shown demonstrating 1-2 mm size phantoms localized by this technique.

**POTENTIAL VALUE AND HIGH EFFICIENCY OF DRY AEROSOLS FOR LUNG IMAGING.** G.V. Taplin, G.D. Robinson, Jr. and D.A. Elam. Laboratory of Nuclear Medicine, University of California, Los Angeles, Calif.

Wet aerosols are notoriously inefficient in terms of the amount of material nebulized versus that retained in the lung parenchyma. Dry aerosols are far more efficient and quickly administered and, when appropriately labeled, are potentially improved agents for use in lung imaging.

With micronized penicillin or aminophyllin in a dextrose or lactose base, a 60 mg dose can be administered with no more than a few breaths (tidal volume breathing). A lactose-Sn(OH)<sub>2</sub> complex can be prepared in powdered form by coprecipitation from aqueous solution by addition of acetone. The powder is subsequently labeled by suspension with <sup>99m</sup>Tc-pertechnetate in methyl ethyl ketone, the supernate removed, and the <sup>99m</sup>Tc-Sn(OH)<sub>2</sub>-lactose is dried under vacuum. Labeling yields are ≈ 50%.

In experimental studies, each of 6 dogs was placed in a closed breathing chamber where respiration was controlled by application and release of vacuum. 5mCi of <sup>99m</sup>Tc in 20 mg of Sn(OH)<sub>2</sub>-lactose were administered by insufflation through an endotracheal tube during inspiration; and anterior views of the chest, head and neck and posterior

views of the chest were obtained with a gamma-ray camera. In all cases the lungs were clearly visualized, with prominence of the trachea and central airways noted when coarse powders were used. Approximately 50% of the activity was retained by the canine subjects.

Although many practical problems are still unsolved in the development of dry aerosol "kits" for general clinical use, the dry radioaerosols appear to offer significant improvement over wet aerosols for airway studies in the lung. In addition, radioisotope bronchography may be possible with the use of dry particles of appropriate size and density for (primarily) central airway deposition.

**RADIOAEROSOL LUNG IMAGING IN EARLY CHRONIC LUNG DISEASE (ITS MAJOR APPLICATION IN MEDICINE).** G. V. Taplin, Lalitha Ramanna, D. Tashkin and Dennis Elam. Laboratory of Nuclear Medicine, University of California, Los Angeles, Calif.

Radioaerosol lung imaging is known to be a highly efficient means for the detection of early or even non-symptomatic chronic lung disease. It is also frequently positive in healed tuberculosis, in chronic pulmonary fibrosis and in asthmatic bronchitis during the asymptomatic phases. This important application has been largely overlooked because it is usually but infrequently employed mainly in cases of suspected pulmonary emboli where the existence of chronic lung disease is not appreciated because the routine chest films are usually negative and the history given the nuclear medicine people is usually incomplete or totally absent.

Examples of this type of application of the radioaerosol method and its potential value in the early detection of chronic lung disease will be emphasized. Several representative imaging studies will be presented as supplementary data and will be discussed in detail. Comparison is being made with routine lung function tests made by the lung function group at UCLA, chest films and other pertinent data will be presented and discussed covering the last several months of cooperative work.

**USE OF A MULTICRYSTAL CAMERA SYSTEM IN CENTRAL NERVOUS SYSTEM STUDIES.** Nancy Telfer, Jan K. Siemsen and David McKeel. LAC/USC Medical Center, Los Angeles, Calif.

Use of a 294 crystal scintillation camera system (S-70) has made possible improved time and space resolution of dynamic studies. Since dynamics comprise only a small percentage of clinically indicated studies, S-70 static scans and routine "flow studies" were compared with those obtained on an Anger camera-minicomputer system (AC), a Dynacamera and a dual-headed scanner. On all instruments, roughly equivalent information (300 K to 500 K counts, or 800 information density) was obtained in similar time intervals of 6-8 min./view for technetium brain scans. Using <sup>99m</sup>TcO<sub>4</sub> as well as <sup>67</sup>Ga, <sup>111</sup>In-bleomycin and <sup>113</sup>In-DTPA, images are comparable on the 4 detector systems.

"Flow studies" were compared on S-70 and AC by evaluation of images, histograms and numerical printouts. Definition of arterial, capillary and venous phases from images and histograms is similar for the 2 systems. Calculations include: rate of increase of activity (R-Inc) cps/30 μCi; maximum increase in counts (Δ Max) counts/cm<sup>2</sup>/30 mCi; minimum transit time (MTT), using first appearance in the carotid as zero-time and measuring the appearance time in the anterior cerebral artery, left and right hemisphere and pathological lesions, they gave comparable values on the 2 systems; analysis time was much longer on the AC. Criteria for the diagnosis of abnormal regional "flow" were developed using relative R-Inc, Δ Max, prolonged MTT and an abnormal arterial pattern characterized by 2 arterial components.



COMPUTER-ASSISTED QUANTITATION OF RENAL FUNCTION: A CRITICAL ANALYSIS. F.D. Thomas, C. Duxbury, P. Vesco, L. Heminger and J. Blizzard, Upstate Medical Center, Syracuse, New York

In a series of dogs, a model of unilateral kidney disease was created by selective renal artery catheterization and injection of  $35\mu$  carbonized microspheres to produce graded degrees of renal ischemia. Scintillation camera studies using Hippuran and various  $^{99m}\text{Tc}$  renal agents were recorded by both digital techniques (PDP-15 computer) to quantitate renal uptake and by conventional photographic means for subjective comparison. Prior to sacrifice, each dog was injected intravenously with various renal agents for absolute uptake measurements and by left-ventricular injection of  $^{85}\text{Sr}$  microspheres for determination of renal blood flow.

The subjectively graded photographic images and digitally quantitated images were compared to the direct organ assays. From the analysis of these data, the following observations were made:

- 1) Differentials of less than 40% in renal uptake cannot be reliably estimated by either photographic or digital techniques.
- 2) Due to inhomogeneous background distributions, great care must be taken in selecting and applying background correction.
- 3) While digital techniques provide a quantitative estimate of renal uptake, they are not more sensitive than standard photographic techniques.

BINDING CHARACTERISTICS OF CELL MEMBRANE RECEPTORS AND ANTIBODIES FOR RADIOLIGAND ASSAYS. Jan I. Thorell, Steven M. Larson, Pedro Cuatrecasas and Henry N. Wagner, Jr. The Johns Hopkins Medical Institutions, Baltimore, Md.

The kinetic characteristics of two radioligand insulin assays were compared. The binding reagents were cell membrane receptors and insulin antibodies, respectively. Both types of binding reagents were in an insoluble form so that an identical assay technique could be used. The cell membrane receptors were purified from human placentas and the antibodies, produced in rabbits were coupled with Sephadex. The binding reagents were incubated with  $^{125}\text{I}$ -insulin and with varying amounts of unlabeled insulin. After incubation, the receptors or the antibodies were isolated by centrifugation with a separating oil phase, and the bound radioactivity was measured.

In the receptor assay, equilibrium was reached rapidly: 50% binding was achieved in less than one minute. In the antibody assay, 50% binding required 18 minutes. The dissociation rates were measured after addition of excess amounts of insulin. Both systems showed a rapid and a slow component. The dissociation constants for the membrane receptors were  $1.4 \text{ min}^{-1}$  and  $2 \times 10^{-2} \text{ min}^{-1}$  and for the antibodies they were  $6 \times 10^{-2} \text{ min}^{-1}$  and  $5 \times 10^{-3} \text{ min}^{-1}$ . The average association constants ( $K_M$ ) as calculated from displacement curves were approximately  $10^9 \text{ L/M}$  for the receptors and  $10^9 \text{ L/M}$  for the antibodies. The cell membrane receptors showed binding capacities for insulin of the same order as that of the antibodies, binding up to 60% of the  $^{125}\text{I}$ -insulin. This is considerably higher than has been previously reported for cell membrane receptors.

The high association rates of the membrane receptors provides the basis for the development of more rapid radioligand assays than are possible with conventional radioimmunoassay techniques.

HYPEREMIC EFFECTS IN SKELETAL IMAGING. James H. Thrall, George E. Geslien, Nassar Ghaed, Steven M. Pinsky, and Merrill C. Johnson. Walter Reed General Hospital, Wash., D.C.

Pathological conditions which induce local or regional hyperemia may cause increased accumulation of skeletal agents in otherwise normal bone by increasing bone blood flow. To determine the incidence of hyperemic effects and their clinical significance in scan interpretation, 800 total body  $^{99m}\text{Tc}$ -Polyphosphate (Tc-PP) bone scans were reviewed.

Primary malignant bone tumors are known to be associated with hyperemia. Diffusely increased accumulation of Tc-PP was noted in the entire involved limb in 12 of 14 cases of primary bone tumor of the extremities. The increased accumulation was in both the osseous structures and the soft tissues. It occurred proximal and distal to the tumors and on opposite sides of joints. Only regional hyperemia could

account for both the extent of the increased accumulation (entire limb and limb girdle) and its pattern (bone and soft tissue). Similar effects due to regional hyperemia were also found secondary to fractures, osteomyelitis, thrombophlebitis and soft tissue sarcomas. An occasional case of metastasis demonstrated the phenomenon but to a generally lesser degree.

The diagnostic dilemma raised by the hyperemic effect is twofold. In primary osseous abnormalities (tumor, inflammation) it is often impossible to decide how far the actual lesion extends and how much of the pattern is due to hyperemia. In primary soft tissue lesions, extension or metastasis to bone may be obscured by superimposed diffuse changes.

Hyperemic effects should be anticipated in cases of primary bone tumors, fractures, osteomyelitis, thrombophlebitis and soft tissue sarcomas. Diagnostic conclusions regarding the existence and extent of skeletal lesions must be carefully qualified in the presence of regional hyperemia.

CODED APERTURE IMAGING OF LARGE EXTENDED GAMMA-RAY OBJECTS WITH AN ON-AXIS FRESNEL ZONE PLATE. M.D. Tipton and J.E. Dowdey. University of Texas Health Science Center at Dallas, Dallas, Texas.

An on-axis Fresnel zone plate aperture has been used to image extended gamma-ray distributions as large as 20 cm. This was done principally by using a dark-centered zone plate and adjusting the detecting geometry for an optimal trade-off between contrast and resolution.

It has been known for several years that an on-axis zone plate, when used as a coded aperture, is capable of imaging point sources with high contrast. However, Barrett and Horrigan (*Applied Optics* 12: 2686-2701, 1973) have pointed out that for extended objects, contrast is reduced with increasing number of object points because of the overlapping undiffracted (DC) light. For a dark-centered zone plate, this is true up to the point of zero contrast. At zero contrast the image intensity is equal to the DC light intensity. Further increase in object size increases the amount of DC light and consequently further reduces the image intensity through destructive interference. The result is a reversal in contrast, i.e., the image becomes less intense than the background. Hence, one obtains high contrast images in the negative sense.

Several isotope filled phantoms have been imaged to illustrate the technique. These phantoms were designed to give some idea of resolution, sensitivity, and signal to noise ratio. As far as possible, tests on the system were made in compliance with the agreements reached at the Engineering Foundation Conference on Coherent Radiation Systems (*Applied Optics* 13: 5-6, 1974).

Because coded apertures are capable of recording high resolution three dimensional images, much interest is being developed in these systems. On-axis zone plates seem to be a viable addition to this family of imaging devices.

COMPARISON OF ALPHA 1 - FETOPROTEIN RADIOIMMUNOASSAY METHOD AND LIVER SCANNING FOR DETECTING PRIMARY HEPATIC CELL CARCINOMA. Norihisa Tonami, Tamio Aburano and Kinichi Hisada, University of Iowa Hospital, Iowa City, Iowa and University of Kanazawa Hospital, Kanazawa, Japan.

Alpha 1-fetoprotein (AFP) radioimmunoassay method was routinely used to detect primary hepatic cell carcinoma in combination with liver scanning and the diagnostic accuracy of both methods was compared. The results of 344 patients who have been studied between October, 1971 and March, 1973 was analysed. Twenty-one of 27 cases with primary hepatic cell carcinoma including those clinically indicated showed the positive AFP titer over 200  $\mu\text{g/ml}$ . In three of these positive AFP cases, no focal defects could be found on liver scans. The presence of hepatoma in these cases, however, was suspected by the results of AFP and subsequently performed celiac angiography revealed hypervascular tumor shadows. Contrarily, four cases with negative AFP results showed focal defects clearly on liver scans. Two cases were negative in both studies. One was of diffusely disseminated small nodules and another had three small nodules of one cm. in diameter which were proven by autopsy. The results of this study indicated that although the specificity of AFP for primary hepatic cell carcinoma was not enough, the combination of AFP radioimmunoassay method and liver scanning was helpful to detect more accurately primary hepatic cell carcinoma and to evaluate the nature of focal defects on liver scans.

**DIHYDROTHIOCTIC ACID: A NEW POLYGONAL CELL IMAGING AGENT.** Allen K. Tonkin and Frank H. DeLand, V.A. Hospital and University of Florida, Gainesville, Fla.

DHTA, a lipoic acid derivative is extracted from the blood by the polygonal cells of the liver and secreted into the biliary system in a manner similar to rose bengal. This new agent, easily tagged with  $^{99m}\text{Tc}$  has been evaluated both as an imaging agent and a dynamic functional radiopharmaceutical. DHTA was compared with  $^{99m}\text{Tc}$  sulfur colloid in groups of normal patients, patients with cholecystitis and cholelithiasis, metastatic disease, diffuse parenchymal disease and biliary obstruction. Patients were given doses of the  $^{99m}\text{Tc}$ -DHTA related to their body surface area for functional appraisal with camera imaging at 30, 60 and 120 minutes. Blood samples were collected at 5, 30, 60 and 120 post injection with external surface counting over the skull and liver at identical time intervals. Visualization of concentrated activity within the gall bladder was compared with single or double dose oral cholecystographic contrast agents in most patients. In the normal patient the topography of the liver was present at 30 minutes with gall bladder activity being seen at 60-120 minutes. Extraction of DHTA from the blood demonstrated a two component curve, the first with a  $t_{1/2}$  of 15 minutes represented equilibration, and the second with a  $t_{1/2}$  of 120 minutes represented combined hepatic utilization as well as renal filtration. Good correlation was found between cholecystograms and DHTA images, in both normals and patients with gall bladder disease. DHTA was valuable for differentiating gall bladder fossa from focal defects. In diffuse parenchymal disease the images often demonstrated dramatic degeneration of liver function as compared to the colloid studies. In biliary obstruction DHTA only rarely revealed the site probably because of hepatocyte dysfunction due to the obstruction. DHTA offers better anatomical and dynamic data than I-131-rose bengal.

**ANGIOSCINTIPHOTOGRAPHY WITH  $\text{Tc}^{99m}$  IN 310 CASES OF KIDNEY OCCUPYING LESIONS.** Giulio Tori, Alberto Marabini, Roberto Franchi, and P.Giorgio Giorgetti. Department of Nuclear Medicine, City Hospitals, Verona, Italy.

Angioscintiphography with  $\text{Tc}^{99m}$  has been performed in 310 cases of kidney occupying lesions in the purpose of evaluating the diagnostic value of the kidney perfusion. In the presence of neoplasm, a more or less marked blood flow in the lesion is generally evident as hot area. This pattern does not appear in scarcely vascularized carcinoma or in Wilms' tumors. Percentage incidence of poorly vascularized carcinoma is moderate and does not invalidate the value of the method. Cystic lesions appear usually to be cold. The possibility of documenting a cold area with angioscintiphography depends upon the size of the lesion. Large cysts exhibit no uptake; on the contrary, the degree of vascularization in the small cysts is more difficult to be evaluated, as the normally supplied surrounding parenchyma overlaps the cold area caused by the cyst. In the evaluation of the angioscintiphographic picture, we must keep into account the concomitant hepatic or splenic vascularization, which may cause some doubts of interpretation through projection interferences. The renal angioscintiphography, in the light of our experience, is not only a screening test, but has a definite rule in specifying the nature of a kidney occupying lesion.

**CLINICAL VALUE OF THE BONE MARROW SCINTIGRAPHY WITH 111 INDIUM-TRANSFERRIN.** Juan J. Touya, John Byfield, Ismael Mena and Leslie R. Bennett. Nuclear Medicine Division Harbor General Hospital and Nuclear Medicine Laboratory, UCLA, Los Angeles, Cal.

In 1972 we introduced the use of 111 In labeling transferrin as a bone marrow agent and in this paper we present the results obtained after 2 years of using it as a routine diagnostic procedure.

Studies on 100 patients with adequate followup are reported. Transferrin was labeled by incubating plasma from the patient with 111 In in .05N HCl solution, in 10:1 volume ratio, for 20 min. at room temperature. If the iron serum was more than 35% of the TIBC, a ratio 20:1 was used. Scan were obtained 48 hours after injection.

A good correlation between scan image and bone marrow biopsy (29 cases) was obtained in all cases except those with localized metastatic carcinoma in bone marrow. As In-transferrin is accumulated in neoplastic tissues (as it also does in inflammatory areas) the tumor sometimes appeared with the same activity as that of the surrounding normal bone marrow.

High blood pool activity were seen when poor hematopoietic activity was present.

In-transferrin scan complemented by RE bone marrow scan was a useful procedure to differentiate aplastic anemias with marked hypoplasia from those with hyperplastic bone marrow.

In patients with Hodgkin's disease treated with segmental sequential or total lymphatic irradiation the In-transferrin was more useful than colloids to evaluate the bone marrow suppression and recovery. In these patients it also indicated when compensatory bone marrow expansion was present.

**INDIUM-TRANSFERRIN METABOLISM IN COMPARISON WITH IRON METABOLISM.** Juan J. Touya, Osvaldo E. Anselmi, William G. Figueroa, Richard F. Riley and Leslie R. Bennett. Laboratory of Nuclear Medicine, University of California, Los Angeles, California.

For a better understanding of In-transferrin and In-bleomycin scan procedures this research was made.

Similar lots of rats were injected with 111 In-transferrin and  $^{59}\text{Fe}$ -transferrin. In 12 patients with different hematological disorders both radiopharmaceuticals were injected simultaneously and activity was measured in the plasma, blood, liver, spleen, bone marrow and the heart for 14 days.

In rats 29% of the injected In-transferrin was excreted with a  $T_{1/2}$  of 40 hours and 71% with a  $T_{1/2}$  of 155 days. In patients with more than 30% of the TIBC saturated with iron some indium was very quickly cleared from the blood pool by the kidneys. This fact was not demonstrated with the iron.

Indium was not incorporated in the red cell hemoglobin. The RBC incorporation in humans was between 0.1 and 5%, and in rats was 2.29 SD 0.31 on the 4th day. Indium appeared in red cells later than iron, and it also disappeared earlier.

Indium body organ distribution was similar to the distribution of the iron labile pool and iron stores: 29% in the liver, 20% in bones, 14% in the skin, 14% in muscles, 5% in kidneys and 3% in the spleen.

In all the patients Indium bone marrow uptake during the first 72 hours after injection was parallel to their erythropoietic bone marrow activity.

It is concluded that indium behaves as iron from the non-hemoglobin orientated binding site of the transferrin and it is taken up by a nonhemoglobin protein in the tissue.

**ON THE MECHANISM OF  $^{14}\text{C}$  RELEASE FROM OXIDATION OF DOPA-CARBOXYL- $^{14}\text{C}$  IN BLOOD IN VITRO.** Ngo Tran and Etienne LeBel. Centre Hospitalier Universitaire, Sherbrooke, P.Q.

The present study concerns an evaluation of contradictory results on radiometric detection of  $^{14}\text{C}$  release from  $^{14}\text{C}$ -labeled DOPA in blood *in vitro*. An ionization chamber was used for continuous measurement of 0.12 $\mu\text{Ci}$  DOPA-carboxyl- $^{14}\text{C}$  incubated with or without 0.5-1.0mM free base L-cysteine, 0.5-1.0ml human or rat blood and plasma plus 1.0mM L-cysteine, 0.5ml rat blood plus  $10 \times 10^{-2}$ mM Iodoacetamide or 1-5  $\times 10^{-2}$ mM p-chloromercuribenzoate, in 0.1 M

phosphate buffer, pH 7.0, at 37°C, in O<sub>2</sub>, for 120 min. Results obtained show that 1) Non-enzymatic oxidation of DOPA was inhibited by 0.5-1.0mM L-cysteine (p<0.005), 0.5ml rat blood (p<0.01) or plasma (p<0.005). 2) Such an inhibition was however prevented when 1.0mM L-cysteine was added to 0.5ml human or rat blood and plasma (p<0.05-0.005). 3) The inhibition was also prevented by 10 x 10<sup>-2</sup>mM Iodoacetamide and 1-5 x 10<sup>-2</sup>mM p-chloromercuribenzoate (p<0.01-0.005), respectively. These results suggest that 1) Non-enzymatic oxidation of DOPA was inhibited by L-cysteine, blood cells, and plasma proteins; 2) Thiol compounds, i.e. L-cysteine, iodoacetamide, and p-chloromercuribenzoate were bound to free sulfhydryl groups of erythrocyte membranes and plasma proteins which subsequently prevented the inhibition of non-enzymatic oxidation of DOPA. The sulfhydryl content in blood plays, therefore, an important role on the inhibition of non-enzymatic oxidation of DOPA; 3) <sup>14</sup>CO<sub>2</sub> release from DOPA-carboxyl-<sup>14</sup>C may be considered as a sensitive index for estimating sulfhydryl content in tissues; 4) <sup>14</sup>CO<sub>2</sub> release from DOPA-<sup>14</sup>C in blood was due to a non-enzymatic oxidation of this drug in O<sub>2</sub>, but the reaction was inhibited partially by sulfhydryls of erythrocytes; 5) An automated radiometric detection of blood effects on non-enzymatic oxidation of DOPA-carboxyl-<sup>14</sup>C to <sup>14</sup>CO<sub>2</sub> for detection of rheumatoid arthritis, lupus erythematosus, and polyarthritis nodosa related to perturbations of sulfhydryl metabolism is being considered.

**RAPID RADIO-BIOASSAYS OF ENZYMATIC AND NON-ENZYMATIC OXIDATION OF DOPA IN VITRO.** Ngo Tran, Etienne LeBel, and Thomas Ntundulu. Centre Hospitalier Universitaire, Sherbrooke, P.Q.

An automated system (The Bactec) usually employed for studies on bacterial growth, leucocyte phagocytosis, and bacterial antibody titers was used, for the first time, for quantitation of enzymatic and non-enzymatic oxidation of radioactive DOPA in vitro. For enzymatic studies on DOPA oxidation, 0.5ml fresh or boiled rat liver homogenates (1mg/ml phosphate buffer) was incubated with 20ml 0.1M phosphate buffer, pH 7.0, 0.06μCi DOPA-carboxyl-<sup>14</sup>C, with or without α-methyl DOPA at 37°C, in N<sub>2</sub>, for 30 min. For non-enzymatic studies on DOPA oxidation, about 0.05-0.10ml blood or plasma was incubated with 20ml 0.1M phosphate buffer, pH 7.0, 0.06μCi DOPA-carboxyl-<sup>14</sup>C, at 37°C, in O<sub>2</sub>, for 90 min. The vial containing a mixture (Kit) was then inserted in the holder of the device, and a rapid quantitation of <sup>14</sup>CO<sub>2</sub> (80 sec.) was made on the metabolic index meter (0.14-0.21nCi/index). Results and conclusions show that 1) Approximately 7.50 ± 0.53, 0.37 ± 0.12 (p<0.01), 0.05 ± 0.03 (p<0.01), 0, and 0.13 ± 0.09 (p<0.01) of nCi were found in controls, in the presence of 0.1, 0.5, 1.0 X 10<sup>-2</sup>mM α-methyl DOPA, and boiled tissues, respectively. This shows that DOPA decarboxylation occurred in fresh tissues, but not in boiled tissues, and that DOPA decarboxylase was inhibited by α-methyl DOPA. 2) Non-enzymatic oxidation of DOPA could be measured rapidly in O<sub>2</sub> and this reaction was inhibited by 0.05-0.10ml blood (p<0.01) or 0.05-0.10ml plasma (p<0.01). Such an inhibition was probably due to free sulfhydryl groups on hemoglobin or plasma proteins. This clarifies contradictory results on erythrocytes and oxidation of radioactive DOPA in vitro. 3) The Bactec for bioassays of DOPA oxidation shows great promise for both research and clinical applications, as a radiometric Warburg apparatus. An automated radiometric detection of blood effects on non-enzymatic oxidation of DOPA-carboxyl-<sup>14</sup>C to <sup>14</sup>CO<sub>2</sub> for diagnosis of a neoplastic disease, Waldenström's macroglobulinemia, is being considered.

**DETECTION AND QUANTITATION OF LEFT TO RIGHT SHUNTS.** S Treves, D. Ahnberg, G. LaFarge, J. Askenasi, and D.L. Maltz. Children's Hospital Medical Center, Harvard Medical School, Boston, Mass.

One hundred and five patients with and without left to right shunts were studied by quantitative radionuclide angiocardiography (RAC) and by cardiac catheterization. The patients were studied supine and injected with 200μCi/kg of technetium 99m (volume 0.1 to 0.5 ml) in a peripheral vein. A gamma camera interfaced to an on-line digital computer system was used for detection, storage and analysis. The study was recorded on magnetic disc at 2 frames per second on a 64x64 matrix format. On playback, regions of interest were marked on each lung field. Addition and subtraction of frames were useful to avoid contamination from extrapulmonary activity. Time activity curves were generated and analyzed while in core using a gamma variate

fit (Circulation 47:1049-1056) results expressed as pulmonary to systemic flow ratio (Qp:Qs) were available within seconds. It is necessary to deliver a unique bolus of radioactivity for accurate results. This is determined by visual analysis of a superior vena cava histogram. Linear regression analysis between cardiac catheterization and RAC data yielded the following values: r=0.94, SEE=0.25, regression line slope=0.93, intercept=0.1 and p=0.001. This method allows precise detection and quantitation of left to right shunts with Qp:Qs between 1.12 and 3. The information generated by this technique appears to be sufficiently reliable to allow clinical management of certain patients.

**HEPATIC CIRCULATION STUDIES WITH RADIONUCLIDES.** Hideo Ueda. Central Hospital of JNR, Tokyo, Japan.

The dual blood supply of the liver in health and liver diseases has been studied using scintillation camera and data-store play back system. After injection of 99m Tc sulfur or Sn colloid in bolus, the image of hepatic scintigraphy was taken repeatedly in the first two or three minutes. The radiohepatogram(H) was taken from the area of interest and was compared with the radioaortogram(A) and radiosplenogram.

The radiohepatogram in health has usually two humps, each corresponds respectively to hepatic artery flow and portal blood flow. In liver cirrhosis, the arterial hump becomes larger and high and in liver cancer, the H looks like radioaortogram and radiosplenogram, the portal hump becomes lower or invisible. In liver cyst, both arterial and portal humps become vague.

The curve of H/A shows clearly the two humps and many kinds of hepatic circulation time. The intrasplenic injection of radionuclides induces only portal hump on radiohepatogram and stream line to the left of the liver. In portal hypertension, the intrasplenic injection can reveal the portosystemic shunt. The coeliac infusion scintigraphy shows the arterial hump only.

The digital presentation(Phosdac) of the early images of liver scintigraphy demonstrates readily the change of liver circulation, too.

In conclusion, the analysis of the early phase of radiohepatogram using scintillation camera gives many informations of hepatic circulation and contributes to the diagnosis of liver diseases.

**RADIONUCLIDE IMAGING OF THE BRAIN WITH 123-IODOANTIPYRINE.** J. Michael Uszler, Leslie R. Bennett, Norman S. MacDonald, and Ismael Mena. Nuclear Medicine Divisions, University of California and Harbor General Hospitals, Los Angeles, Calif.

Radionuclide imaging of the laboratory animal brain has been achieved using intravenously administered <sup>123</sup>I-iodoantipyrine and a scintillation camera.

Initially the rat cerebral uptake of intravenous iodoantipyrine (IAP) (labeled with I-131) was studied with 30, 60 and 300 second time samples of the whole brain. Brain uptake of intravenous 131-IAP in both dog and monkey was determined by NaI crystal probe detector. Flow images as well as uptakes were obtained with 131- and 123-IAP using a scintillation camera and computer.

Rat brain uptake data corresponded to that given in the literature, which showed that maximal value was reached 15-20 seconds after injection and declined slowly thereafter. Brain radioactivity at 30 and 60 seconds was equal to that of the surrounding blood, but dropped to half that of blood by 300 seconds.

Both dog and monkey brain uptakes by probe and by camera and computer showed a rapid brain uptake followed by slow "washout". A comparison curve obtained using technetium-99m sulfur colloid showed rapid passage of activity through the head region without any evidence of uptake or retention in the brain area.

Although there was relatively rapid brain turnover of the labeled IAP, the uptake was high enough and the retention sufficiently prolonged to make possible adequate brain images.

Human-sized head phantom studies with a variety of collimators and various-sized agar "lesions" showed that lesion visibility in the size range of the majority of human cere-

brovascular (including subdural hematoma) abnormalities is possible with I<sup>123</sup>-I-iodoantipyrine.

Dynamic and static brain imaging may play an important role in the evaluation of human cerebrovascular and central nervous system disease states.

**RADIONUCLIDE EJECTION FRACTIONS.** Eugene D. Van Hove and Larry L. Heck. Methodist Hospital, Indianapolis, Ind.

Ejection fractions obtained by a simple radionuclide technique were compared with those obtained from single plane cine left ventricular angiocardiograms to evaluate their clinical efficacy.

Patients having coronary arteriograms had isotopic studies within 24 hours of the angiogram. A multicrystal digital camera and associated equipment including a small digital computer were utilized. A bolus of 10 to 15mCi of <sup>99m</sup>Tc labeled albumin was injected in a peripheral vein. Data were stored at either 50 or 100 millisecond intervals in 20° LAO position for a total of 20 or 40 seconds. An area of interest over the left ventricular chamber was identified and histograms with associated digital printout were obtained to calculate the ejection fractions. A modification of the method of Sandler and Dodge was used to calculate the ejection fractions from cine left ventricular angiograms.

Twenty-one of 27 cases had ejection fractions that were calculable by both methods. Thirteen were in agreement to +/- .05; 20 of 21 had values within +/- .10 by the two methods.

Radionuclide ejection fractions can be done simply with acceptable accuracy. The study is reproducible, can be done serially, and results are available for the clinician almost immediately. The entire examination is done in a few minutes and is more rapidly performed than previously described radionuclide studies using gated images of systole and diastole. Results may be more accurate than angiography because the method is more physiologic.

**COMPUTERIZED PROGRAMS FOR NON-TRAUMATIC RADIOISOTOPE DETERMINATION OF LEFT VENTRICULAR EJECTION FRACTION AND CARDIAC OUTPUT CALCULATION.** John W. Verba, Heinrich R. Scheibert, Gary W. Brock, Naomi P. Alazraki, William L. Ashburn, University of California, San Diego and VA Hospital, San Diego.

In order to facilitate determination of ejection fraction (EF) and cardiac output (CO) following an injection of <sup>99m</sup>Tc HSA into the superior vena cava, computer programs were written. An Anger scintillation camera interfaced to the computer was used to accumulate time activity distributions from the left ventricular regions-of-interest (ROI). Fast (0.04 sec/point) and slower (1 sec/point) curves were generated. EF was calculated by first extracting the beat by beat information from the bolus distribution. A number of numerical techniques were explored for evaluating its sinusoidal behavior. The effects of size of ROI, framing time, background correction, and choosing various portions of the LV passage curve were studied. In addition, various approaches to normalization of the LV and background ROIs were evaluated. Those variables which produced the most reliable calculations of ejection fraction, when compared with biplane cineangiograms, were identified.

For obtaining CO, the bolus portion of the slow curve was first fit by a gamma variate. The area under the fit was compared to the counts at the time of equilibrium for the same ROI. Cardiac output was calculated by the equation: CO = counts at equilibrium/area under fit x blood volume. The effects of background corrections for the LV curve and the equilibrium counts, and choice of region of interest were studied. Results were compared to those obtained from dye-dilution measurements of CO in the cardiac catheterization laboratory.

**FURTHER OBSERVATIONS ON INDIUM-111 LABELED ELEOMYCIN FOR SCANNING TUMORS IN MAN.** Ramesh C. Verma, Juan J. Touya, and Leslie R. Bennett. University of California, Los Angeles, Calif.

The authors have previously reported preliminary results with Indium-111 Eleomycin (InElm) for tumor scintigraphy. To date over 200 patients have been scanned and the additional experience, especially the variability in the range of normals, is reported here.

A normal 48 hour scan shows considerable activity within the liver, the kidneys, and the bone marrow. Liver activity is reduced in diffuse hepatocellular disorders like cirrhosis. Further work on the role of InElm as an adjunct to the radiocolloid liver scan in diagnosis of hepatic tumors is currently in progress.

The kidneys have been visualized without fail and appear to show greater uptake of the tracer in patients with poor liver uptake. The degree of splenic visualization is more variable than the above two organs.

The bone marrow shows a definite, although highly variable accumulation which increases with time over the first few days. Irradiated marrow sites show almost no uptake and resultant hyperplastic marrow may show an intense uptake which, if focal, can be misinterpreted.

Minimal activity in parts of the colon has been observed in apparently healthy individuals; the exact significance or origin of which is not yet known. However, when the bowel is involved, the concentration of the tracer is far out of proportion to this 'normal' accumulation.

Primary bone tumors show an avid accumulation although experiences with small skeletal metastases are disappointing. Results with various other tumors and dosimetry data are favorable. As reported earlier, InElm is not specific for tumors.

Etiology of the variable accumulations noted in the genital region, the female breast, and occasionally the lungs remains to be elucidated.

**PROMINENT CHOROID PLEXUS ON Tc<sup>99m</sup>-PERTECHESTATE BRAIN SCANS — POSSIBLE ETIOPATHOLOGIC MECHANISMS.** Ramesh C. Verma and Leslie R. Bennett. University of California Center for Health Sciences, Los Angeles, California.

This study was designed to seek possible explanations for variations in different patients of choroidal accumulation of Tc <sup>99m</sup>-pertechnetate (Tc) as noted on brain scans. Choroid plexus activity as seen on lateral views of <sup>350</sup> routine Tc brain scans (without prior block with perchlorate or thiocyanate) was graded and the cases divided into three groups: 'A' (19%) constituted the prominent, 'B' (57%) the faintly visualized and 'C' (24%) the poorly visualized choroid plexuses. Hospital records of 'A' and 'C' were reviewed to determine common denominators, if any, in either of these groups. 'B' was eventually excluded from the study since it represented the grey zone between the extremes.

Various clinical, investigational and therapeutic parameters were evaluated. A Chi-square test was computed on 'A' and 'C' for each of the parameters. All the significant (at 95% confidence level) parameters showed a higher occurrence in 'A' only. The significant findings in patients with prominent choroids included: dilated ventricles, suspected adhesions, local CNS or systemic infections and elevated cerebrospinal fluid (CSF) pressure.

Choroid plexus affinity for Tc from ventricular CSF is much higher than from circulating blood. The findings of this study can be explained on the premise that the predominant source of Tc in the choroid plexus is the ventricular fluid. In a reversal of flow state, as might occur in dilated ventricles and suspected meningeal adhesions, larger volume of CSF with higher concentration of Tc is made available to the choroid plexus. Raised CSF pressure may contribute towards prominent choroids by creating a transient or permanent state of reversal of flow.

A plausible explanation for prominent choroids in infections is that there is increased permeation of Tc into the CSF because of breakdown of blood-brain barrier.

**CHANGES IN BONE MINERAL CONTENT DURING BEDREST AND WEIGHTLESSNESS MEASURED BY PHOTON ABSORPTIOMETRIC TRANSMISSION SCANNING.** John M. Vogel, Darrell Lockwood, Victor Schneider and Stephan Hulley. University of California School of Medicine, Davis, Calif. and USPHS Hospital, San Francisco, Calif.

The observation that bone mineral is lost in patients who are either immobilized or remain in bed for extended periods of time formed the basis for concern that excessive bone mineral losses may occur during long periods of weightlessness. This concern was magnified when X-ray densi-

ometry studies during the 4 to 14 day Gemini missions reported large losses. A newer more precise photon absorptometric technique was employed to measure the calcaneus, radius and ulnar mineral content in 15 subjects undergoing 30 to 36 weeks of bedrest and in the 6 astronauts of the first two SKYLAB missions. The device employed the 27.5 kev photon of <sup>125</sup>I and a scintillation detector operating in a rectilinear scanning mode. It was designed to measure multiple bone sites, not only in a single bone, but in several bones because of a unique variable axis scanning capability not available in commercial systems. Variable mineral losses were observed. Negligible losses occurred during the first 6 weeks. Calcaneus mineral losses thereafter averaged 5% per month. No losses occurred in the radius and ulna. Variability in mineral loss between subjects correlated with their initial 24 hour urinary hydroxyproline and calcaneal mineral content. Prediction terms were derived that permitted the estimation of mineral losses during bedrest. Data derived from the SKYLAB astronauts during 28 and 56 day missions fell within these prediction limits. These observations support the concept that bedrest is a reasonable simulator for bone mineral changes during weightlessness and that excessive losses have not occurred.

**HIGH RESOLUTION TRANSVERSE SECTION TOMOGRAPHY.**  
Timothy E. Walters, John W. Keyes, Jr. and William Simon. University of Rochester, Rochester, N.Y.

The ideal tomographic reconstruction technique should not introduce any image distortion or noise into the final image. Reconstruction algorithms based on Fourier mathematics are theoretically capable of such "perfect" reconstructions. We have implemented one of the alternative Fourier algorithms (the convolution technique) which approaches the theoretical capability of the technique in real application. A commercial image processing system (Medical Data Systems-Modumed Trinary System) incorporating a 20 K, 16 bit minicomputer was programmed in FORTRAN to reconstruct tomograms from data gathered with an unmodified gamma camera (Searle Radiographics-Pho/Gamma HP) and standard collimators. From 60 rotation views obtained at 6° angular increments around a 360° arc, tomograms have been reconstructed which closely approximate the spatial resolution of the gamma camera. If the number of input views is increased to 120 at 3° increments there is no discernable difference between the tomogram and a digitized original camera image. These images also show very little reconstruction "noise" and are accurately quantitative except for distortions introduced by internal absorption losses. The results demonstrate that transverse tomograms can be produced with presently available equipment in which the quantitative and spatial accuracy is limited only by the detector system used, statistical considerations and counting losses caused by internal absorption.

**COMPARISON OF REGIONAL RENOGAM AND RENAL ARTERIOGRAM.** Yen Wang. Homestead Hospital, Homestead, Pa.

The regional renogram has been reported to be a more sensitive screening test than the conventional renogram. The regional renograms are the selective evaluation of the three regions of the kidney - outer, middle and inner. In a group of 25 patients of known hypertension both regional renogram and renal arteriogram were performed and compared. The findings recorded on the regional renogram were more distinguishable and profound than the findings on the renal arteriogram. This difference is probably because the renal arteriogram has been limited to the evaluation of major renal arteries and secondary arterial structures and the condition of interlobular and arcuate arteries and even smaller arteriolar structures are not readily accessible to the arteriographic study. A direct comparison between these two tests for evaluation of renal condition in this group of hypertensive patients

showed significant difference with a good correlation and indicates that a regional renogram should be performed prior to renal arteriographic procedure.

All of the 25 patients showed unilateral abnormal middle regional renogram. 12 of them showed unilateral arterial abnormality and 3 showed bilateral changes. The remaining 10 patients showed apparently normal arterial studies. There is about 50 per cent correlation between the two studies. The remaining 10 patients had unilateral changes on the regional renogram and this probably caused by some abnormality which is not noted by the arteriogram.

**A COMBINED RADIONUCLIDE APPROACH IN THE EVALUATION OF POST CRANIOTOMY PATIENTS.** Alan D. Waxman, George Lee, Ralph S. Wolfstein and Jan K. Siemsen. LAC/USC Medical Center, Los Angeles, Calif. and Cedars-Sinai Medical Center, Los Angeles, Calif.

The postoperative assessment of intracranial tumors is a difficult problem. Technetium-99m-pertechnetate or technetium-99m-polyphosphate (TPP) studies may remain positive for years following craniotomy, rendering the detection or differentiation of underlying tumors problematic. This report deals with the use of <sup>67</sup>Ga-citrate, <sup>99m</sup>TcO<sub>4</sub><sup>-</sup> and TPP in the detection and differentiation of intracerebral pathology in post craniotomy patients.

Nineteen post craniotomy cases were evaluated using conventional four view <sup>99m</sup>TcO<sub>4</sub><sup>-</sup>, <sup>67</sup>Ga-citrate and TPP delayed brain scanning techniques on the Anger camera or dual headed scanner. All cases had documented intracerebral tumors prior to surgery. The postoperative period varied from 6 weeks to 7 years. The results are summarized in the following table:

	<sup>99m</sup> TcO <sub>4</sub> <sup>-</sup>		TPP		<sup>67</sup> Ga-citrate	
	+	-	+	-	+	-
Tumor Recurrence	7		7		7	
No Tumor Recurrence		10		10		10
Osteomyelitis	2		2		2	

The fact that gallium uptake did not occur in the craniotomy site makes the differentiation between craniotomy site and tumor possible. Inflammation or infection of the surgical site would preclude this method of evaluation. We conclude that a multinuclide approach is important in the evaluation of post craniotomy patients.

**FURTHER OBSERVATIONS OF GALLIUM-67 EVALUATION OF CEREBRAL LESIONS.** Alan D. Waxman, George Lee, Ralph S. Wolfstein and Jan K. Siemsen. LAC/USC Medical Center, Los Angeles, Calif. and Cedars-Sinai Medical Center, Los Angeles, Calif.

Previous studies of cerebral lesions using <sup>67</sup>Ga have shown promise in tumor detection and in the differentiation of infarction from tumor. This report deals with the comparison of brain scans done with <sup>99m</sup>Tc-pertechnetate and <sup>67</sup>Ga-citrate on 148 cases.

Using four view conventional brain scan technique on either a dual headed scanner or Anger camera a delayed .15 mCi <sup>99m</sup>Tc-pertechnetate study was compared with a 48-96 hr, 5 mCi <sup>67</sup>Ga-citrate study. The lesion to calvarium ratio of activity was used as the basis of comparison. The results are summarized in the following table:

Relative Gallium-Technetium Uptake In Brain Lesions

	Ga-Tc+	Ga<Tc	Ga=Tc	Ga=Tc	Ga>Tc
Neoplasm			2	50	21
Infarct (1)	31	8	2	2	
Infarct (2)	18	8	3	2	

(1) Infarct confirmed by angiography or post.  
 (2) Infarct diagnosed by clinical course with resolution of scan findings.

In the neoplasm group 21 cases clearly were seen better with <sup>67</sup>Ga. Of importance was the detection of cerebral lesions with <sup>67</sup>Ga in 8 cases in which the <sup>99m</sup>Tc study was read as normal.

We conclude that gallium brain scanning is a valuable technique in the detection and differentiation of intracerebral pathology and should be considered as complementary to conventional procedures done with  $^{99m}\text{Tc}$  radiopharmaceuticals.

**GALLIUM SCANNING OF THE GALLBLADDER.** Alan D. Waxman and Jan K. Siemsen. Los Angeles County/University of Southern California Medical Center Los Angeles, Calif.

$^{67}\text{Ga}$  is known to have an affinity for infectious or inflammatory sites. The use of gallium for detection of cholecystitis was considered both feasible and important since many cholecystitis patients present as diagnostic problems or fever of unknown etiology.

Nine patients are included in the initial series. Four patients had surgically proven cholecystitis with a nonvisualizing oral cholecystogram. Two cases were shown to have cholelithiasis by oral cholecystogram and the 3 remaining cases had normal oral cholecystogram with no gallbladder pathology found for abdominal pain or fever. Rectilinear scans were done 24 hours following intravenous administration of 5 mCi of  $^{67}\text{Ga}$ -citrate.

The 4 surgically proven cases had intense gallium accumulation in the region of the gallbladder. The remaining studies were normal with no gallbladder uptake of gallium.

Our preliminary conclusion is that gallium will prove to be a valuable aid in the detection of cholecystitis especially in patients with a nonvisualizing oral cholecystogram.

**THE CALCULATION OF RELATIVE WEIGHTS FOR NUCLEAR MEDICINE PROCEDURES.** Alan D. Waxman and Jan K. Siemsen. LAC/USC Medical Center, Los Angeles, California.

Relative weights for nuclear medicine procedures have been assigned previously on the basis of subjective estimates of resources expended. Thus, ultimate values have frequently not reflected accurately time and cost of personnel and equipment.

Based upon computerized data collected on over 8,000 patients we have tried to calculate relative weights more objectively. Five parameters were evaluated by the computer, including: 1. physician time; 2. technologist time; 3. nurse (or aide) time; 4. equipment time and depreciation; 5. radiopharmaceutical cost. An aggregate score was derived for a given procedure by rating each parameter from 0 to 9. Thus, a procedure could have a total maximum score of 45. The aggregate scores were normalized using the Schilling test as unity, as shown in the table. E.g. the relative weight of the brain scan is  $20 \div 7 = 2.86$ .

	4 View Static Brain Scan	Schilling Test
Physician	6	1
Technician	5	3
Machine	8	2
Radiopharmaceutical	1	1

The use of special equipment such as minicomputers or videotape was assigned additional aggregate points which increase relative weights from 10 to 15%. Procedures previously thought to rate low on a value schedule were found to have high relative weights when analyzed objectively.

**FEMORAL HEAD BLOOD SUPPLY DEMONSTRATED BY RADIOTRACERS.** Milo M. Webber, Joseph Wagner, Michael D. Cragin, and Winona Victory. University of California, Los Angeles, Calif.

The purpose of this study is to evaluate femoral head trauma and disease by the use of radiotracers. Hip joint diseases and injuries often manifest themselves by decreased

blood flow to the femoral head. This study describes a non-invasive method of estimating femoral head blood flow which can be accomplished by the use of radiotracers.

The use of technetium sulfur colloid for hip scanning was previously reported. In addition, the new bone scanning agents permit superior visualization of the femoral heads compared to previously used  $^{109}\text{Cd}$  and  $^{87}\text{Sr}$ . A procedure for the clinical application of both of these agents has been introduced for femoral head evaluation.

The uptake of colloid by bone marrow delineates the femoral head by virtue of phagocytoses within it. Absence of uptake is expected in avascularity. The uptake of technetium-99a diphosphonate is also diminished in avascularity. However, increased uptake is often seen in adjacent areas of reactive new bone formation. This double scan approach appears to present a more thorough and conclusive result than either alone.

Scans of the hips in 50 liver patients with no hip disease, showed that the colloid distribution was uniformly symmetrical, although 50% failed to show uptake bilaterally.

The normal pattern of radiotechnetium diphosphonate is also symmetrical with poor uptake of the diphosphonate seen in a small number of cases but most cases present a good delineation of the femoral head. In cases of avascular necrosis where colloid uptake is lacking, an intense reactive uptake of radiotechnetium diphosphonate is observed. This finding is present in very early cases where x-rays are equivocal or negative.

**PITFALLS IN ULTRASONIC DIAGNOSIS OF PSEUDOCYSTS OF THE PANCREAS.** Milo M. Webber, Francine Aguilar, and Michael D. Cragin. University of California, Los Angeles, Calif.

B-scan ultrasound section scanning of the abdomen is generally accepted to be a very useful technique in the demonstration of cysts within the abdomen. However, it is possible to obtain erroneous results using the B-scan technique, if the cyst is not filled with homogeneous clear fluid. This problem has been brought into focus, because of the findings in a patient who had a high suspicion of pseudocyst of the pancreas. A mass was noted in the left upper quadrant, the ultrasound examination was interpreted showing a solid mass in the left upper quadrant of the abdomen. Surgery revealed a pseudocyst of the pancreas containing viscous fluid. The technique used for this examination was previously found to be consistently reliable in a separation of cysts from solid masses in multiple renal and abdominal studies.

A model was constructed which would enable the simulation of abdominal abscesses containing various amounts of particulate material. Abscess material was approximated with finely ground beef uniformly suspended in gelatin. The gelatin itself was found to be echo-free at ordinary gain settings. A marked increase in echos was noted from the gelatin even with concentration of particulate debris as low as 1 mg per cc. Increasing concentration of particulate debris serves to dramatically increase the echo activity. The findings suggest that all cystic structures are not necessarily echo-free and that it is extremely likely that purulent cystic debris may cause sonographic findings similar to that seen in a solid mass. The liquid nature of the contents of such masses would appear to be undiscoverable by any method commonly used to separate cystic from solid masses ultrasonically.

**RENAL CORTICAL IMAGING: A SUPERIOR  $^{99m}\text{Tc}$  CHELATE.** Paul M. Weber and Leo V. dos Remedios. Kaiser-Permanente Medical Center, Oakland, Calif.

The kinetics and clinical use of dimercaptosuccinic acid (DMSA) complexed with  $^{99m}\text{TcO}_4^-$ , an excellent renal cortical imaging agent in animals, was studied in 35 patients. After injection of 5 mCi  $^{99m}\text{Tc}$ -DMSA, dynamic and static data were recorded by Anger camera and computer for up to 17 hr. Kidneys were imaged with the high resolution collimator and each enlarged with the 5-mm pinhole. DMSA plasma turnover, urine excretion, renal trapping, and whole body scanning were performed; IHSA plasma volume was measured.

Plasma disappearance of  $^{99m}\text{Tc}$ -DMSA in 15 of 21 patients fits a single exponential function ( $t_{1/2}$  in normals ~56 min). Initial distribution volume exceeded IHSA volume ~12.5%. Of 20 patients, 12 showed no RBC binding; in 8, 1.5-10% was bound.



Cumulative urine excretion was 4-8% in 1 hr; 26-29% in  $\geq 14$  hr. Of injected  $^{99m}\text{Tc}$ -DMSA, 50% was bound to renal tubules in 1 hr; 70% after  $\sim 15$  hr. After 15 hr, some was in the vascular space; none elsewhere. Renal extraction fraction was 4-5%.

All images were excellent. Corticomedullary structure, unseen with other agents, required learning a new normal pattern seen in 18 patients. The kidneys differed in size in 4; 1 or more cortical lesions were seen in 4; in 9, uneven or diminished cortical labeling or marked anatomic distortion was due to hydronephrosis or chronic pyelonephritis. This superior, safe agent regularly and uniquely reveals renal morphology. The 50% of dose retained by renal cortex at 1 hr is the highest for any  $^{99m}\text{Tc}$  complex reported.

**TOTAL BODY SCANNING FOR CANCER IN THE LIVER: FAILURE WITH  $^{67}\text{Ga}$  AND  $^{111}\text{In}$ .** Morton B. Weinstein and August Miale, Jr. University of Miami School of Medicine, Miami, Fla.

The major factor in the rapid demise of the patient with carcinomatosis is the presence of liver metastasis with increasing hepatic failure. Rational programs of cancer management with surgery, chemotherapy, radionuclide therapy or external beam irradiation therapy should be based upon the most reliable methods available to define the presence of liver metastasis.

Filling defects seen with  $\text{Tc-99m}$  sulfur colloid scans are notoriously nonspecific and materials that have an avidity for tumor tissue have been employed to detect neoplastic involvement. Since 1969 we have examined 350 patients' total body scanning using Indium-111 or Gallium-67. Less than 1% of the scans were prospectively or retrospectively suggestive of liver involvement. Liver involvement was proven or highly suggested in 15% of these patients by other methods.

Computer analysis of representative cases defined the low detection rate to be due to high concentration of radiopharmaceutical in normal liver. Rarely would neoplastic involvement of the liver exceed normal liver uptake. Only with primary hepatocellular carcinoma did the tumor-to-liver ratio exceed unity. The liver uptake of  $\text{Ga-67}$  and  $\text{In-111}$  was reduced to background in patients with large body burdens of nonhepatic neoplastic tissue.

**INDICATION, TECHNIQUE AND RESULTS OF ENDOLYMPHATIC RADIOTHERAPY.** Karl zum Winkel, and Thomas Newiger. Free University Berlin, Klinikum Westend.

Endolymphatic therapy was performed in more than 70 patients with  $\text{I }^{131}\text{-Lipiodol}$  since 1964 and in 132 patients with  $\text{P }^{32}$  since 1971. Different effective half-life periods in lymph nodes and lungs were measured. For the selection of patients the lymphoscintigraphy was suitable which must reveal nearly normal distribution of radiocolloid in the lymphatics after subcutaneous application. The endolymphatic radiotherapy is indicated in malignant tumors with moderate or less radiosensitivity frequently metastasizing in the lymphatic system as melanoblastoma (43 patients treated with  $\text{P }^{32}$ ) and teratoma (12 patients). Additionally to the percutaneous radiotherapy we further used it in 11 patients with bladder and 14 with prostatic cancer and in 24 patients with lymphoma. 14 cases were proved either by laparotomy, lymphadenectomy or autopsy. 11 histologically were free of metastases, 3 died of progressive metastases outside the filled lymph nodes. Before each lymphography in patients with ascertained malignant tumor it must be decided if the endolymphatic application of radionuclides is indicated or not.

**MEASUREMENT OF SALIVARY AND GASTRIC EMPTYING.** Karl zum Winkel, Lena Schmidt, and Michael Meves. Free University Berlin, Klinikum Westend.

Sequential scintigraphy and integral curves of the salivary glands using the scintillation camera and data processing system were performed in 412 patients 1 hour and more after  $\text{Pertechnetate i.v.}$  20 to 30 min after the application  $\text{Carbachol}$  was administered, which caused a rapid discharge of the radioactivity into the oral cavity. Patients with normal salivary function showed an excretion of  $67\% \pm 4\%$  in the parotid regions and  $61\% \pm 3\%$  in the submandibular regions after stimulation. Incomplete emptying was observed in acute and partly in chronic inflammation, in poor functioning sialosis and after radiotherapy. Occlusion of the salivary ducts led to refractory retention of  $\text{Pertechnetate}$  after  $\text{Carbachol}$ . In connection with the perfusion and the concentration registered before stimulation typical changes in several diseases could be seen. In order to evaluate the coherence between gastric motility and both ulcer disease and intestinal hormones we developed according to Griffith's investigations a method of measuring gastric emptying by use of a  $\text{Cr-51}$ -labelled test meal. The emptying of the meal from the stomach was measured by two scintillation probes, attached to a dual ratemeter system. 1.) In 23 healthy patients the normal half-life values were  $64 \pm 13$  min. 2.) The preoperatively accelerated gastric emptying in 40 duodenal ulcer patients ( $49 \pm 14$  min) was significantly delayed ( $145 \pm 54$  min) after vagotomy and pyloroplasty. 3.) Gastrin and pentagastrin (13 patients) distinctly delayed gastric emptying from  $21\%/20$  min to  $3\%/20$  min or  $2\%/20$  min, respectively.

**CEREBRAL DYNAMIC STUDIES FOR THE EARLY DETECTION OF RECURRENT NEOPLASM.** L.R. Witherspoon, M.S. Mahaley, J.R. Leonard, J.W. Tyson, C.C. Harris, J.K. Goodrich. Duke University Medical Center and V.A. Hospital, Durham, N.C.

The value of repeated dynamic imaging of the cerebral circulation after i.v. injection of  $^{99m}\text{Tc}$ - $\text{pertechnetate}$  in patients with anaplastic intracerebral gliomas has been evaluated. In 28 patients 148 studies were obtained at 2 month intervals for up to 40 months. Six patients stabilized after post treatment improvement; two were reoperated for tumor recurrence providing 36 opportunities to compare sensitivity of dynamic studies, static brain scans and clinical evaluation to tumor growth or regression. Cerebral dynamic studies correctly predicted progression in 12 of 30 opportunities to observe such change. In 6 of these 12, change preceded clinical deterioration by 2 months. In the other 6 patients dynamic study change preceded deterioration by 4-10 months. Eight of these twelve instances occurred in nondominant hemisphere lesions. In six patients improvement occurred without change on dynamic study. Brain scanning was insensitive as a predictor of clinical deterioration. In 6 of 36 instances scan evidence of tumor change preceded clinical change. In 7 of 36 instances clinical change preceded change on brain scan. Cerebral dynamic studies have been shown to be more sensitive predictors of clinical deterioration than brain scanning. The routine use of this technique may permit earlier therapeutic intervention in recurrent anaplastic intracerebral gliomas.

**ELECTROLYTIC LABELING OF AUTOLOGOUS HUMAN FIBRINOGEN WITH  $^{99m}\text{Tc}$ .** Dennis W. Wong and Fred S. Mishkin. Martin Luther King, Jr. Hospital/Drew Postgraduate Medical School, Los Angeles, Calif.

Exogenous fibrinogen labeled with  $^{125}\text{I}$  and  $^{131}\text{I}$  carries the risk of hepatitis infection which may be avoided using autologous fibrinogen. Using a rapid, practical electrolytic method, we have successfully labeled  $^{99m}\text{Tc}$  to exogenous fibrinogen as well as to autologous fibrinogen isolated and purified from patient's plasma. The entire labeling process requires less than one hour with good yield.

The fibrinogen, precipitated using 4 M ammonium sulfate, twice separated, and redissolved in sterile water, yields a final concentration of approximately 4-12 mg/ml. To a sterile pyrogen-free vial with zirconium electrodes are added 4 ml 0.05 N HCl, 1-2 ml  $^{99m}\text{Tc}$ -pertechnetate (20-40 mCi) and 1 ml of the fibrinogen solution. Direct current (100 mAmp at 5-6 volts) is passed through the inverted vial. Denaturation of the fibrinogen will occur if 6 volts is exceeded. After incubation at 37°C for 30 minutes, the pH is adjusted to 4 with 0.02 N NaOH. Precipitation of the labeled fibrinogen will occur if the pH exceeds the isoelectric point of 5.5. The solution, slightly cloudy with colloidal precipitates, is filtered through a 0.22  $\mu$  size Millipore filter. Radiochromatography using an 85% methanol solvent system showed in 10 trials an average binding efficiency of 66.4% (range 32-92.5%) with good reproducibility. Precipitation with thrombin showed the activity remained with the clot, indicating that the final product remains labeled and biochemically active.

The obvious advantage of  $^{99m}\text{Tc}$  labeled fibrinogen is that it allows administration of larger doses than possible with  $^{131}\text{I}$  or  $^{125}\text{I}$  labels and permits imaging. The disadvantage of the short half-life may be circumvented by using  $^{111}\text{In}$  as a label, but thus far we have achieved sporadic results using acid indium chloride.

EVALUATION OF SQUAMOUS CELL CARCINOMA OF THE CERVIX USING  $^{111}\text{In}$ -BLEOMYCIN. James M. Woolfenden, Alan D. Waxman, Philip J. DiSala and Jan K. Siensen. LAC/USC Medical Center, Los Angeles, Calif.

Bleomycin labeled with  $^{111}\text{In}$  has been proposed as a radiopharmaceutical for tumor localization, particularly for squamous cell carcinoma. The present study evaluates the correlation between scintigraphic tumor localization using  $^{111}\text{In}$ -bleomycin ( $^{111}\text{In}$ -BLM) and anatomic findings in patients with squamous cell carcinoma of the cervix.

Rectilinear torso scans using a dual probe scanner were performed in 19 patients from 2 to 7 days after intravenous administration of 5 mCi  $^{111}\text{In}$ -BLM. Staging laparotomy was performed in 9 of the patients; in the remaining 10, who had recurrence of previously treated tumor, the extent of disease was determined by physical examination, x-ray, biopsy or cytology.

Anatomically documented tumor sites showed increased  $^{111}\text{In}$ -BLM uptake in 12 patients. There were 2 apparently false positive scans; one showed increased abdominal uptake, although laparotomy showed no intra-abdominal tumor, and the other showed uptake at a recent biopsy site. In one patient the extent of pelvic disease was underestinated on scan. In 4 patients with disease confined to the uterus, including 2 with Stage I cervical tumors, no increase in uptake was seen; this finding suggests that a minimum volume of tumor is necessary for increased uptake to be demonstrated.

SCINTIGRAPHIC EVALUATION OF LIVER METASTASES FROM THYROID CARCINOMA. James M. Woolfenden, Alan D. Waxman, Ralph S. Wolfstein and Jan K. Siensen. LAC/USC Medical Center, Los Angeles, Calif. and Cedars Sinai Medical Center, Los Angeles, Calif.

Radioiodine liver scan can be combined with radiocolloid liver scan to evaluate liver metastases from thyroid carcinoma. Focal hepatic lesions on radiocolloid scan would be expected to show  $^{131}\text{I}$  uptake on radioiodine scan if the lesions represent functioning thyroid carcinoma. Failure to show  $^{131}\text{I}$  uptake would not exclude the presence of nonfunctioning thyroid metastases.

Radioiodine torso scans including the area of the liver were reviewed in 31 patients with thyroid carcinoma. Scans in all patients except 2 showed either no  $^{131}\text{I}$  uptake in liver or a diffuse pattern of  $^{131}\text{I}$  uptake presumably secondary to liver uptake of radioiodinated thyroid hormone or albumin. Scans in 2 patients with follicular

thyroid carcinoma showed focal  $^{131}\text{I}$  uptake in liver in an area which was abnormal on radiocolloid scan. In the first patient the area of  $^{131}\text{I}$  uptake coincided with a large filling defect on radiocolloid scan. In the second patient the marked increase in  $^{131}\text{I}$  uptake was more prominent than the decrease in radiocolloid uptake. Since a "hot" lesion with "cold" surrounding tissue is more readily seen than a "cold" lesion surrounded by "hot" tissue, this finding in the second patient suggests that  $^{131}\text{I}$  liver scan may be more sensitive than radiocolloid scan in detecting small functioning thyroid metastases in liver. Inclusion of radioiodine scan of liver in the evaluation of patients with thyroid carcinoma is recommended.

CARDIOVASCULAR DYNAMIC PERFUSION STUDY IN LUNG PERFUSION SCAN WITH  $^{99m}\text{Tc}$ -MAA. Chang-Sing Yang, R. Vincent Grieco, and Noel F. Bartone. The Methodist Hospital, Brooklyn, N.Y.

In our department, 75% of the patients referred for lung perfusion scans have a history of previous or current cardiac disorder; 6% have malignant disease in the lungs. Since  $^{99m}\text{Tc}$ -MAA can offer rapid direct visualization of great vessels, right cardiac chambers, and dynamic lung perfusion, we have done the so-called "dynamic cardiovascular perfusion study" in addition to the regular static lung perfusion scans in order to obtain additional information about cardiovascular status with the same single injection.

After I.V. bolus injection of 3 mCi. of  $^{99m}\text{Tc}$ -MAA into the antecubital vein, sequential scintiphotos were taken immediately via gamma camera over the anterior chest for one minute at intervals, e.g., 0-3 seconds, 3-10 seconds, 10-30 seconds, 30-60 seconds. Immediately following this, the regular static lung perfusion scans were performed.

In reviewing 264 cases of lung perfusion scans using this technique, we found the following extra information could be obtained: (1) Determination of transit time between two points along the blood circulation from arm to lung; (2) Evaluation of the caliber of the subclavian vein, innominate vein, superior vena cava, and pulmonary arteries (information which is particularly useful for those patients with pulmonary malignancy), and the chambers of the right atrium and right ventricle; (3) Differentiation of the major central or minor peripheral thromboembolic process, which could be used as a guide for surgical or medical treatment; (4) Differentiation of hilar lymphadenopathy or prominence of pulmonary arteries; (5) Determination of the location of the right-to-left shunt by direct visualization; (6) Indirect evaluation of the left atrium and left ventricle; (7) Detection of pulmonary venous hypertension.

We believe that "cardiovascular dynamic study" can and should be done as part of  $^{99m}\text{Tc}$ -MAA lung perfusion scan.

THULIUM-167: CYCLOTRON PRODUCTION, CHEMICAL SEPARATION, AND UPTAKE IN TUMOR MICE. Yukio Yano, Patricia Chu and Hal O. Anger. Donner Laboratory, University of Calif., Berkeley, California

The work of Chandra and of Hisada indicate the potential usefulness of the heavier lanthanides for bone and tumor uptake. In the present study holmium chloride,  $^{163}\text{Ho}$  (100%), was irradiated with 29-32 Mev  $^3\text{He}$  beam at the LBL 88-inch cyclotron to produce 20-30  $\mu\text{Ci}/\mu\text{Ah}$  for 2-3 hr irradiations. Thulium-167 was separated from the  $\text{HoCl}_3$  target by ion-exchange column chromatography by the method of Ketelle and Boyd (Bio-Rad AG50 x 10, -400 mesh) using 4.75% ammonium citrate at pH 3.4. The separated  $^{167}\text{Tm}$  citrate was given I.V. to tumor bearing mice to give the following distribution (%/gm) at 42 hr:

	Blood	Tumor	Femur	Tumor/Blood
Adenocar. (Ca755)	0.046	1.32	12.6	47.7
Neuroblast (Cl300)	0.058	.94	8.21	16.2
Sarcoma (S180)	0.006	1.09	17.3	182.

These preliminary results indicate good tumor to blood ratio and high bone uptake with the "carrier-free"  $^{167}\text{Tm}$ -citrate. Conventional cyclotron production methods will give low yields

and make the availability of Tm-167 difficult and expensive. However there is a possibility for lower production costs by high energy proton irradiations at BLIP or LAMPF. If  $^{167}\text{Tm}$  can be produced in quantity, it can be a useful bone and tumor scanning agent because of its 208 kev photon, 9.6 d half life and decay by electron capture.

**METABOLIC AND SCINTIGRAPHIC STUDIES OF  $^{111}\text{INDIUM BLEOMYCIN IN MAN AND TUMOR BEARING ANIMALS. Samuel D.J. Yeh, Robert E. Grando, Charles W. Young, and Richard S. Benua. Memorial Sloan-Kettering Cancer Center, Cornell Medical College, NYC$**

Successful demonstration of tumor uptake of labeled bleomycin was recently reported in a small number of patients. Detailed information is not yet available. We have studied the metabolism of  $^{111}\text{In}$  bleomycin and the images in 63 patients with known tumor. Mice with transplanted tumor and rats with experimental abscess were examined to determine the sensitivity and specificity of this tumor localizing agent. In man, total body scans with 5:1 minification and computer data were obtained from a dual head rectilinear scanner, 6 to 72 hrs after IV injection of  $^{111}\text{In}$  bleomycin (5 mCi/mg). Whenever possible, scanning with other agents such as  $^{67}\text{Ga}$  citrate,  $\text{Na }^{18}\text{F}$ , or  $^{99\text{m}}\text{Tc}$  pertechnetate was carried out. The radioactivity in the plasma and urine was measured. Our results showed that  $^{111}\text{In}$  was present primarily in the bleomycin B and A. The biological activity of labeled bleomycin was intact in the B. subtilis assay. Plasma clearance and urinary excretion were very rapid. Tumor or abscess in animals took up several-fold more bleomycin than the surrounding muscle. Increased uptake in the known tumor sites was demonstrated in a majority of patients studied. Our best results were obtained in the carcinoma of breast, cervix, malignant melanoma, and Hodgkin's disease. Gallium uptakes in lymphoma were much superior to those of bleomycin. Results in tumor from GI tract and their liver metastases were poor. All 8 patients suspected to have brain metastases showed increased bleomycin uptakes in the areas with positive conventional brain scans. Increased uptake, however, was also demonstrated in non-neoplastic conditions such as osteomyelitis in man and induced abscesses in rats. It is concluded that labeled bleomycin appears to be a useful tumor localizing agent especially for brain lesions. The early enthusiasm for bleomycin's tumor specificity is, however, questionable.

**DISTRIBUTION AND SCINTIPHOTOGRAPHY STUDIES OF A LUNG SCANNING AGENT:  $^{99\text{m}}\text{Tc(Sn)}$  MACROAGGREGATES. Shin-Hwa Yeh, Ho-Hsiu Wu, and Mu-Tien Chien. Veterans General Hospital and National Defense Medical Center, Taipei, Taiwan**

During reducing  $^{99\text{m}}\text{TcO}_4^-$  with stannous chloride, we happened to notice aggregation. This led us to the development of a fast and efficient preparation system of a lung scanning agent with a short retention time in the lungs.

$^{99\text{m}}\text{Tc(Sn)}$  macroaggregates,  $^{99\text{m}}\text{Tc(Sn)}$  MA, were prepared as follows: (1) adding  $^{99\text{m}}\text{Tc}$  eluate to a vial containing stannous chloride during stirring; (2) adjusting the mixture to pH 6-7 with 0.1 N NaOH in the presence of carboxymethylcellulose; and (3) addition of dextran as a dispersing agent. Neither heating nor centrifugation was required. The whole procedure took less than 5 min. The quantity of  $^{99\text{m}}\text{Tc}$  bound to the aggregates averaged 98%, and the particle sizes ranged from 5 to 50 microns.

The tissue distribution of  $^{99\text{m}}\text{Tc(Sn)}$  MA was performed in the rat. Intravenously injected  $^{99\text{m}}\text{Tc(Sn)}$  MA had pulmonary uptake of 96% at 5 min and less than 10% at 24 hr. The biological half-life was approximately 3 hr. The trapped particles in the lungs were progressively transposed mainly to the liver and spleen. The uptake was approximately 69% in the former, and 9% in the latter at 24 hr.

Scintiphotographic studies using an Anger scintillation camera in the rabbit confirmed the findings of the distribution studies. The lung scintiphotos of good quality could be obtained until 1 hr after injection; after that there was progressive transposition of radioactivity in the lungs to the liver and spleen. At 24 hr, the lungs were only faintly visualized. The kidneys were not delineated. Neither chemical toxicity nor hypersensitivity was observed.

The preparation of  $^{99\text{m}}\text{Tc(Sn)}$  MA is simple, rapid and efficient, eliminating centrifugation, heating and accurate

pH adjustment. Pulmonary disappearance is fast but suitable for lung scanning. Accordingly,  $^{99\text{m}}\text{Tc(Sn)}$  MA would be a useful addition to the present lung scanning agents.

**INTRAVENOUS RADIONUCLIDE HEPATOGRAPHY IN HEPATOMA. Shin-Hwa Yeh, Wei-Jen Shih, Sabu-Quinn Iiso, and Wei-Jian Chen. Veterans General Hospital, Tri-Service General Hospital, and National Defense Medical Center, Taipei, Taiwan, Republic of China**

Intravenous perfusion hepatography with  $^{113\text{m}}\text{In}$  eluate has been used by us to evaluate capillary perfusion of hepatic masses shown by  $^{99\text{m}}\text{TcS}$  colloid scintiphotography. This simple and innocuous approach has proved to be a useful screening technique for differentiating intrashepatic mass lesions. This report is to present our further results of such a study in a large series of hepatomas.

The studies were performed with an Anger scintillation camera as follows:  $^{99\text{m}}\text{TcS}$  colloid liver scintiphotography was done first to localize masses of reduced uptake, and then another scintiphoto was taken immediately after intravenous injection of 6-7 mCi of  $^{113\text{m}}\text{In}$  eluate with the same positioning of the patient and the same scintiphotographic factors except for changing the spectrometer from the  $^{99\text{m}}\text{Tc}$  "window" to the  $^{113\text{m}}\text{In}$  one. The colloidal  $^{99\text{m}}\text{Tc}$  scintiphoto was compared with the  $^{113\text{m}}\text{In}$  perfusion image, and the degree of perfusion was assigned. The examined cases were divided into three categories: (A) good perfusion; (B) poor perfusion; and (C) no perfusion of the defect.

In all cases studied, the diagnosis was proved by biopsy or postmortem examination. In 141 cases of hepatoma, the assigned degree of perfusion is shown in the table:

Degree of perfusion	no.	%
Good	111	79
Poor	30	21

Hepatomas which showed poor perfusion had central necrosis. In 117 cases of good perfusion, hepatoma occurred in 111 (94.9%), hepatic metastases in 5 (4.2%), and hemangioma in 1 (0.9%). From these results, it can be seen that hepatomas are predominantly well perfused. Especially in the countries of high prevalence of hepatoma, hepatic masses with good perfusion usually suggest the diagnosis of hepatoma.

**ENZYMATIC INHIBITION BY DIPHOSPHONATE: A PROPOSED MECHANISM OF TISSUE UPTAKE. A.M. Zimmer, A.T. Isitman, G.H. Schmitt, R.A. Holmes. Milwaukee County Medical Complex, Milwaukee, WI.**

Although "Chemisorption," the chemical bonding of diphosphonate to hydroxyapatite crystals, is the mechanism generally ascribed to the skeletal uptake of technetium- $^{99\text{m}}$  stannous diphosphonate ( $^{99\text{m}}\text{Tc-DiP}$ ), it fails to explain soft tissue uptake when ossification or calcification is not present. In normal and pathologic breast tissues that showed  $^{99\text{m}}\text{Tc-DiP}$  uptake, biopsies showed no microscopic calcification or significant stainable calcium. Histochemical stains for phosphatase showed high concentrations of acid phosphatase in the areas of  $^{99\text{m}}\text{Tc-DiP}$  uptake. Because these enzymes are normally found in high concentration in bone, we propose that enzymes bind diphosphonate and may be the mechanism of diphosphonate uptake by tissues.

To test the hypothesis, we have studied the effect of diphosphonate in varying concentrations ( $10^{-3}$  mM to  $4 \times 10^{-3}$  mM) on the activity of phosphatases in vitro. Diphosphonate added to acid phosphatase in 1, 2, and 4 micromole concentrations showed 10%, 27%, and 30% inhibition of the enzyme activity at 10 minutes. Alkaline phosphatase activity showed no appreciable inhibition at the same concentrations of diphosphonate. Non-specific inhibition was excluded when glutamic-oxalacetic transaminase (GOT) and lactate dehydrogenase (LDH) showed no inhibition with diphosphonate.

The data gives support to our hypothesis of enzyme receptor binding by diphosphonate.

**SELECTIVE UPTAKE OF  $^{99\text{m}}\text{Tc}$ -CHELATES AND  $^{67}\text{Ga}$  IN ACUTELY INFARCTED MYOCARDIUM. Franklin G. Zweiman, Augustine O'Keefe, John Idoline, Leopoldo L. Camin, B. Leonard Holman, Harvard Medical School, Boston, Mass.**

A number of  $^{99m}\text{Tc}$ -chelates including  $^{99m}\text{Tc}$ -tetracycline ( $^{99m}\text{Tc}$ -TC) and its analogs,  $^{99m}\text{Tc}$ -glucoheptonate ( $^{99m}\text{Tc}$ -GH),  $^{99m}\text{Tc}$ -diphosphonate ( $^{99m}\text{Tc}$ -DHDP) and  $^{67}\text{Ga}$  were evaluated in the dog to determine (a) concentration in infarct relative to normal myocardium and surrounding tissues including liver, blood and bone and (b) rate of clearance from the blood. Twenty dogs were experimentally embolized using a catheter guide wire system introduced into the left main coronary artery under fluoroscopic control.  $^{67}\text{Ga}$  citrate (5 mCi) was injected intravenously into 5 dogs at the time of infarction. The remaining dogs received 15-20 mCi of  $^{99m}\text{Tc}$ -TC (9),  $^{99m}\text{Tc}$ -GH (3)

and  $^{99m}\text{Tc}$ -DHDP (3) 24 hr after infarction. All animals were sacrificed 48 hr after infarction. The infarct to normal myocardium ratio was 24 with  $^{99m}\text{Tc}$ -DHDP, 11 with  $^{99m}\text{Tc}$ -GH, 6 with  $^{99m}\text{Tc}$ -TC and 1.5 with  $^{67}\text{Ga}$ . The highest infarct to liver ratio was obtained with  $^{99m}\text{Tc}$ -DHDP (8). The infarct to blood ratio was highest with  $^{99m}\text{Tc}$ -GH (6). The infarct to bone ratio was 0.6 with  $^{99m}\text{Tc}$ -DHDP. The blood clearance at 24 hr was greatest with  $^{99m}\text{Tc}$ -DHDP and  $^{99m}\text{Tc}$ -GH. The relatively high infarct concentration, the rapid clearance and its absence from the surrounding skeleton would appear to make  $^{99m}\text{Tc}$ -GH the agent of choice for myocardial infarct imaging.

## TECHNOLOGISTS' SCIENTIFIC PROGRAM

The following papers have been accepted for the Technologists' Scientific Program. Complete abstracts may be found in the June issue of the JOURNAL OF NUCLEAR MEDICINE TECHNOLOGY.

RADIOIMMUNOASSAY SHORT EFFICIENT METHODS BY POLYMERIZED ANTIBODY TABLET. Merri B. Benetazzo and Gerald H. Spirek. Sherman Hospital, Elgin, Ill.

CISTERNOGRAPHY USING  $^{111}\text{In}$ -DTPA AND A SCINTILLATION CAMERA. Mark J. Cochran and Don R. Bernier. Edward Mallinckrodt Institute of Radiology, St. Louis, Mo.

EVALUATION OF A MULTI-IMAGING SYSTEM. Rao Dasika, Robert Tokarz, Teresa DiRienzo and Theodore Stahl. St. Peter's General Hospital, New Brunswick, N.J.

TECHNOLOGIST EXPOSURE CONTROL. Charles J. Dunn. Memorial Hospital, Hollywood, Fla.

THE RES-O-MAT E.T.R. TEST FOR THE DETERMINATION OF NEO-NATAL THYROID ACTIVITY. Gary D. Gallamore, Robert C. Spagnoli, Susan Sujansky, and Janie Frank. Jersey Shore Medical Center, Neptune, N.J.

THE USE OF AN EXPERIMENTAL MODEL IN THE EVALUATION OF RADIOIODINATED AUTOLOGOUS FIBRINOGEN. Paul F. Godin, Donald E. Tow and Daniel J. O'Connell. VA Hospital, West Roxbury, Mass.

CALCULATION OF THE RADIOPHARMACEUTICAL DOSE FOR THE PEDIATRIC PATIENT. Charles A. Henry and Edward G. Bell. Crouse-Irving Memorial Hospital, Syracuse, N.Y.

RADIATION SAFETY IN NUCLEAR MEDICINE. John R. Howley, Michael V. Green, Mardalee B. Dickinson, A. Eric Jones, and Gerald S. Johnston. National Institutes of Health, Bethesda, Md.

BLOOD POOL IMAGES IN CONJUNCTION WITH BONE AND BRAIN STUDIES. Elisabeth Kilburn and David L. Gilday. The Hospital for Sick Children, Toronto, Ont.

CARDIAC SCINTIGRAPHIC IMAGING USING A PHYSIOLOGICAL SYNCHRONIZER. John J. Kozar III, Kenneth A. McKusick, Gerald M. Pohost, and Majic S. Potsaid. Massachusetts General Hospital, Boston, Mass.

CONTAMINATION AND QUALITY CONTROL OF RADIOPHARMACEUTICALS. Peter P. Lamy and Donald R. Hamilton. University of Maryland School of Pharmacy, Baltimore, Md.

A  $^{99m}\text{Tc}$ -AEROSOL INHALATION TECHNIQUE FOR LUNG SCINTIPHOTOGRAPHY. Max S. Lin, C.K. Erickson, C.L. Whiteleather, David A. Goodwin, and S.L. Kruse. VA Hospital, Palo Alto, Ca.

SMALL DIAMETER PINHOLES FOR HIGH RESOLUTION CAMERA IMAGING. E. Ling, C. Duxbury, J.G. McAfee and F.D. Thomas. Upstate Medical Center, Syracuse, N.Y.

AN "INSTANT" KIT METHOD FOR THE PREPARATION OF  $^{99m}\text{Tc}$  LABELED INULIN FOR GAMMA-CISTERNOGRAPHY. Bernard Maher and Edward G. Bell. Crouse-Irving Memorial Hospital, Syracuse, N.Y.

THE EFFICACY OF ADMINISTERING SIMULTANEOUS ORAL  $\text{NaClO}_4$  AND INTRAVENOUS  $^{99m}\text{TcO}_4^-$  FOR BRAIN SCANNING. Mary E. Maxwell and Bonnie Baggenstoss. St. Paul-Ramsey Hospital, St. Paul, Minn.

EVALUATION OF MYOCARDIAL SCANNING WITH  $^{43}\text{KCl}$ . Bonnie A. Mefferd, Richard W. Myers, and Gerald S. Johnston. National Institutes of Health, Bethesda, Md.

DUAL-RADIONUCLIDE MYOCARDIAL SCANNING USING A SCINTILLATION CAMERA. Linda L. Morrow. Ohio State University Hospital, Columbus, Ohio.

IN-VIVO DISTRIBUTION STUDIES OF TECHNETIUM-LABELED MACROAGGREGATED ALBUMIN. John H. Norris, Peter C. Stang, and Pinya Cohen. Bureau of Biologics, FDA, Bethesda, Md.

QUALITY CONTROL OF RADIOPHARMACEUTICALS IN THE COMMUNITY HOSPITAL. Walter L. Robinson. Bionuclears, Inc., Fanwood, N.J.

A RAPID RENAL SCREENING PROCEDURE USING A SINGLE DOSE OF  $^{99m}\text{Tc}$ -DTPA. Herbert D. Strauss, Eva C. Nikawitz, and Mary Jane B. Zarzycki. VA Hospital, East Orange, N.J.

SCINTIGRAPHIC ISOTOPE MAMMOGRAPHY. Sybil J. Swann, Steven D. Richman, Camille L. Boyce, and Gerald S. Johnston. National Institutes of Health, Bethesda, Md.

PANCREAS IMAGING WITH COMPUTER ENHANCEMENT. Sharon M. Thorp. University of California Medical Center, San Francisco, Ca.

QUALITY CONTROL FOR THE RADIOIMMUNOASSAY. Robert Tokarz and Theodore Stahl. Middlesex General Hospital, New Brunswick, N.J.

ORAL  $^{99m}\text{Tc}$ -PERTECHNETATE: AN AID IN THE DIFFERENTIATION OF EPIGASTRIC LESIONS. Susan Weiss and James J. Conway. The Children's Memorial Hospital, Chicago, Ill.

THE TECHNOLOGY OF IMAGING WITH  $^{67}\text{Ga}$  CITRATE. Douglas B. Wigton. Penrose Hospital, Colorado Springs, Colo.